Stockholm
University

Multicomponent Catalytic Reactions

Theoretical and Experimental Studies

Martin Pauze

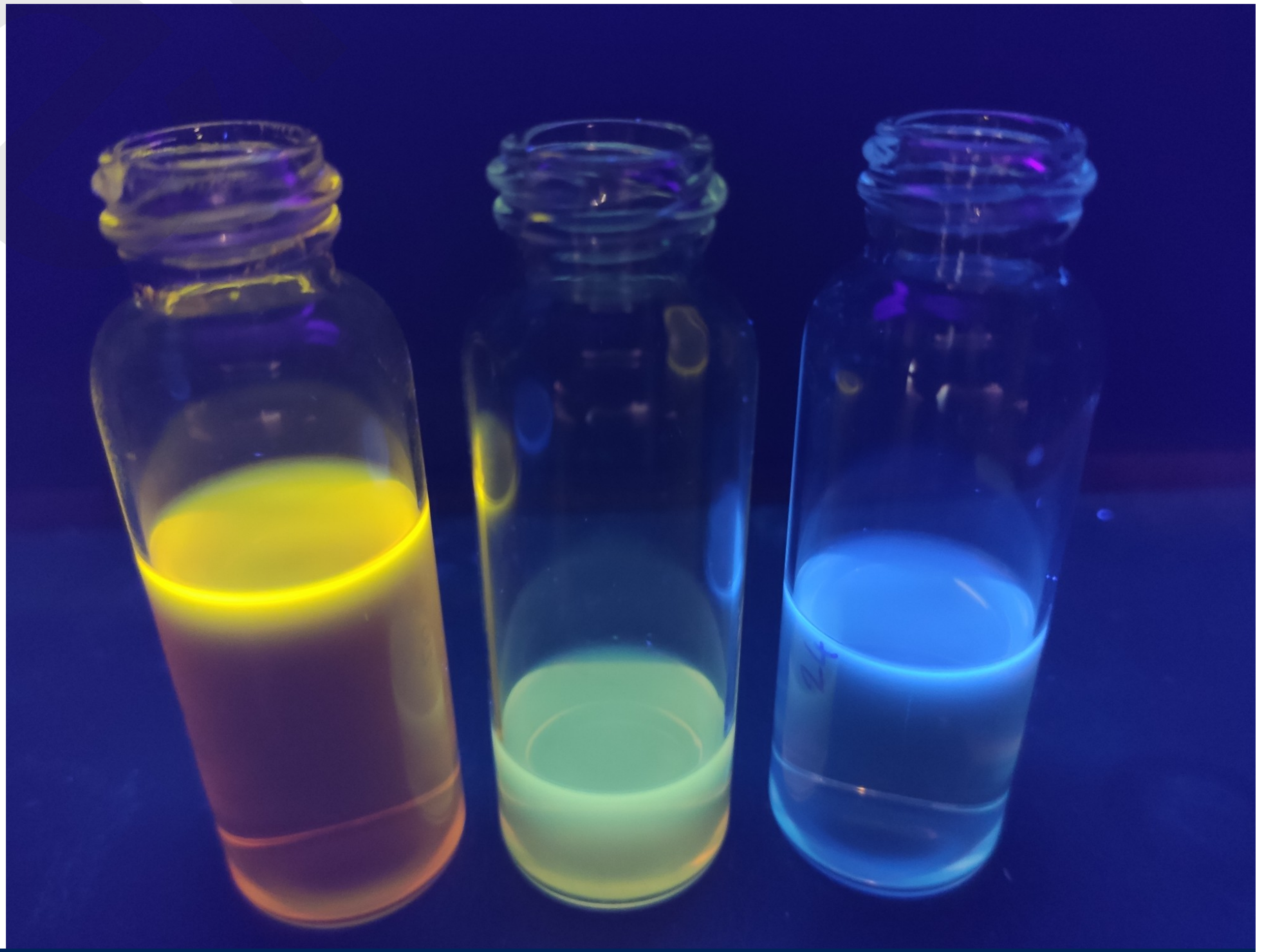

Doctoral Thesis in Organic Chemistry at Stockholm University, Sweden 2021

Martin Pauze Multicomponent Catalytic Reactions

ISBN 978-91-7911-544-9

(cc)2021 MARTIN PAUZE (cc by-nc-nd 4.0)

Department of Organic Chemistry

Stockholm
University

Korrektur

Multicomponent Catalytic Reactions

Theoretical and Experimental Studies

Martin Pauze

Academic dissertation for the Degree of Doctor of Philosophy in Organic Chemistry at Stockholm University to be publicly defended on Tuesday 28 September 2021 at 10.00 in online via Zoom, public link is available at the department website.

Abstract

In this thesis, Density Functional Theory (DFT) methods have been applied to study the mechanisms of three different multicomponent organic reactions. Also, a new synthetic procedure for the preparation of quinolinium salts is presented, and its mechanism also studied by DFT calculations. The thesis summarizes the work realized in two universities, and is divided in the following way: The first part of the thesis concerns the development of an experimentally simple, but mechanistically complex, reaction for the formation of quaternary quinolinium salts catalyzed by palladium salts. This multicomponent process uses readily available propylamine and its derivatives as starting materials. Through DFT studies a mechanism through the activation of two aliphatic C-H bonds is proposed. The second part focuses on the mechanistic investigation of a three-components reaction, namely terminal alkynes, CO_2 and allylic chlorides, mediated by an *N*-heterocyclic carbene catalyst that yields propargylic esters. By DFT calculations, the rate-limiting step was identified to be the reaction between the carboxylated catalyst and the allylic chloride. Through DFT modelling, we were also able to understand the limitations of this reaction. The mechanism of a multicomponent reaction in which allylic alcohols are transformed into α-functionalized carbonyls was also investigated. The reaction relies on an umpolung strategy that enables to react enol intermediates with different nucleophiles. By DFT studies, a mechanism *via* enolonium intermediates is proposed, which provides an understanding of the selectivity of the reaction. The final chapter of the thesis deals with another multicomponent solvent-free reaction for synthesizing propargylamines catalyzed by manganese *via* a KA^2 coupling. DFT studies were undertaken and a mechanism *via* manganese phenylacetylide species is proposed.

Keywords: *C-H Activation, Quaternary Quinolinium, Organocatalyst, Transition Metal Catalyst, Umpolung Strategy, Multi-step Reactions, Mechanistic Investigation, Density Functional Theory.*

Stockholm 2021
http://urn.kb.se/resolve?urn=urn:nbn:se:su:diva-195122

ISBN 978-91-7911-544-9
ISBN 978-91-7911-545-6

Department of Organic Chemistry

Stockholm University, 106 91 Stockholm

Korr

Korr

MULTICOMPONENT CATALYTIC REACTIONS

Martin Pauze

korr

Korr

Stockholm
University

Multicomponent Catalytic Reactions

Theoretical and Experimental Studies

Martin Pauze

Korr

©Martin Pauze, Stockholm University 2021

ISBN print 978-91-7911-544-9
ISBN PDF 978-91-7911-545-6

Printed in Sweden by Universitetsservice US-AB, Stockholm 2021

Korr

“I am among those who
think that science has
great beauty”

Marie Curie

Korr

Abstract

In this thesis, Density Functional Theory (DFT) methods have been applied to study the mechanisms of three different multicomponent organic reactions. Also, a new synthetic procedure for the preparation of quinolinium salts is presented, and its mechanism also studied by DFT calculations. The thesis summarizes the work realized in two universities, and is divided in the following way: The first part of the thesis concerns the development of an experimentally simple, but mechanistically complex, reaction for the formation of quaternary quinolinium salts catalyzed by palladium salts. This multicomponent process uses readily available propylamine and its derivatives as starting materials. Through DFT studies a mechanism through the activation of two aliphatic C‒H bonds is proposed. The second part focuses on the mechanistic investigation of a three-components reaction, namely terminal alkynes, CO_2 and allylic chlorides, mediated by an *N*-heterocyclic carbene catalyst that yields propargylic esters. By DFT calculations, the rate-limiting step was identified to be the reaction between the carboxylated catalyst and the allylic chloride. Through DFT modelling, we were also able to understand the limitations of this reaction. The mechanism of a multicomponent reaction in which allylic alcohols are transformed into α-functionalized carbonyls was also investigated. The reaction relies on an umpolung strategy that enables to react enol intermediates with different nucleophiles. By DFT studies, a mechanism *via* enolonium intermediates is proposed, which provides an understanding of the selectivity of the reaction. The final chapter of the thesis deals with another multicomponent solvent-free reaction for synthesizing propargylamines catalyzed by manganese *via* a KA^2 coupling. DFT studies were undertaken and a mechanism *via* manganese phenylacetylide species is proposed.

Keywords: C‒H Activation, Quaternary Quinolinium, Organocatalyst, Transition Metal Catalyst, Umpolung Strategy, Multi-step Reactions, Mechanistic Investigation, Density Functional Theory.

Populärvetenskaplig sammanfattning

Upptäckten av nya kemiska processer för att få tillgång till organiska molekyler är av stor betydelse för vårt samhälle. Läkemedel är oftast organiska föreningar, så även jordbrukskemikalier och andra material. En stor utmaning som organiska kemister står inför idag är dock att utveckla nya metoder som är effektiva, minimerar avfall, och följer principerna för grön kemi. För att ta itu med några av dessa utmaningar i modern organisk syntes är det viktigt att få tillgång till reaktionsmekanismer. Att förstå hur en kemisk reaktion sker ner på molekylär nivå gör det möjligt att förbättra den kemiska processen.

Denna avhandling fokuserar på användningen av teoretiska verktyg, särskilt densitetsfunktionsteori, för studier av tre nya kemiska reaktioner som ger tillgång till organiska molekyler. En viktig aspekt i denna forskning har varit förståelsen av två olika metoder som gör det möjligt att invertera den normala reaktiviteten hos vissa kemikalier, känt som *umpolung* kemi. En annan typ av kemisk reaktion som har studerats i detta arbete ger tillgång till komplexa organiska cykliska molekyler genom att uppnå en selektiv funktionalisering av kol-vätebindningar. Dessa metoder är effektiva för syntes av många funktionella föreningar och har potential att användas för framställning av mer komplexa material.

Korr

List of abbreviations

Abbreviations and acronyms are in agreement with standards in the field, following the ACS abbreviations and acronyms in the 2016 guidelines for authors (http://pubsapp.acs.org/paragonplus/submission/joceah/joceah_abbreviations.pdf). Common abbreviations in this report and other non-conventional abbreviations are listed below:

A^3	aldehyde-alkyne-amine reaction
CMD	Concerted Metalation Deprotonation
DFT	Density Functional Theory
DG	Directing Group
IRC	Intrinsic Reaction Coordinate
KA^2	ketone-alkyne-amine reaction
NHC	*N*-Heterocyclic Carbene
NMR	Nuclear Magnetic Resonance
NOE	Nuclear Overhauser Effect
SET	Single Electron Transfer
TBAF	Tetra-*n*-Butyl Ammonium Fluoride
TFE	2,2,2-Trifluoroethanol
TLC	Thin Layer Chromatography
TS	Transition State

Kor

List of publications

This thesis is based on the following publications. The authors' contribution to each publication is clarified in a contribution list in Appendix B.

I. **Cascade C–H activation for the synthesis of quaternary quinolinium salts from propylamine and its derivatives.**
Martin Pauze, Enrique Gómez-Bengoa
Manuscript in preparation.

II. **Unprecedented Multicomponent Organocatalytic Synthesis of Propargylic Esters via CO_2 Activation.**
Argyro T. Papastavrou, Martin Pauze, Enrique Gómez-Bengoa and Georgios C. Vougioukalakis
ChemCatChem **2019**, *11*, 5379

III. **An Umpolung Strategy to React Catalytic Enols with Nucleophiles**
Amparo Sanz-Marco, Samuel Martinez-Erro, Martin Pauze, Enrique Gómez-Bengoa and Belén Martín-Matute
Nature Communications **2019**, *10,* 5244

IV. **Manganese-Catalyzed Multicomponent Synthesis of Tetrasubstituted Propargylamines: System Development and Theoretical Study**
Stavros P Neofotistos, Nikolaos V Tzouras, Martin Pauze, Enrique Gómez-Bengoa, Georgios C Vougioukalakis
Advanced Synthesis & Catalysis **2020**, *362*, 3872-3885

Kor

Reprint Permissions

Permissions to reprint the following publications were obtained from their respective publishers:

II. Argyro T. Papastavrou, Martin Pauze, Enrique Gómez-Bengoa and Georgios C. Vougioukalakis. *ChemCatChem***2019**, *11*, 5379.
Copyright © 2021 *ChemCatChem* published by Wiley-VCH Verlag GmbH & Co. KGaA, Weinheim

III. Amparo Sanz-Marco, Samuel Martinez-Erro, Martin Pauze, Enrique Gómez-Bengoa and Belén Martín-Matute. *Nature Communications* **2019**, *10*, 5244.
Copyright © 2018 Nature Communications published by Springer Nature. Open access article licensed under a Creative Commons Attribution 4.0 International License.

IV. Stavros P Neofotistos, Nikolaos V Tzouras, Martin Pauze, Enrique Gómez-Bengoa, Georgios C Vougioukalakis. *Advanced Synthesis & Catalysis* **2020**, *362*, 3872-3885.
Copyright © 2021 *Advanced Synthesis & Catalysis* published by Wiley-VCH Verlag GmbH & Co. KGaA, Weinheim.

Korr

Other documents based on this work

The content of this thesis builds partly upon the author´s half-time report, presented on the 24th of November 2020. Chapters III and IV have now been updated. Chapter II and Chapter V are presented in this thesis for the first time.

This thesis summarizes the work performed at the University of Basque Country and at Stockholm University as part of the multi-partner Marie Sklodovska Curie Actions (MSCA) Innovative Training Network (ITN) European Joint Doctorate (EJD) “Catalytic Methods for Sustainable Synthesis. A Merged Experimental and Computational Approach” (CATMEC). Within this program, I aim to obtain a double PhD degree, from Stockholm University, Sweden, and from the University of Basque Country, Spain. Therefore, the content of this thesis will be used to a PhD degree from each university. The thesis at Stockholm University will be published the 07th of September 2021 and the thesis at the University of Basque Country in September 2021.

Korr

Table of Contents

Abstract i
Populärvetenskaplig sammanfattning ii
List of abbreviations iii
List of publications iv
Reprint Permissions v
Other documents based on this work vi
I Introduction 1
  I.1 Catalysis in organic chemistry 1
    I.1.1 Catalysis and catalytic reactions 1
    I.1.2 Transition metal catalysis 1
    I.1.3 NHC catalysis 2
  I.2 Umpolung reactivity 4
    I.2.1 Hypervalent Iodine 5
    I.2.2 CO_2 Activation by NHC 6
  I.3 C_{sp^2}–H and C_{sp^3}–H activations by transition metals 7
    I.3.1 Mechanisms of C–H bond activations 7
    I.3.2 Directing groups for C–H activation 8
    I.3.3 C_{sp^3}–H activation of aliphatic amines 10
  I.4 A^3 coupling and KA^2 coupling reactions 11
  I.5 Density functional theory for mechanistic investigations 13
    I.5.1 Principles of density functional theory and functionals construction 13
    I.5.2 Basis sets 14
    I.5.3 Solvation model 14
    I.5.4 Functionals and basis sets selected in the thesis 15
  I.6 Objective of the thesis 16
II Synthesis of substituted alkyl quinoliniums from propylamine and its derivatives (Paper I) 17
  II.1 Introduction 17
  II.2 Preliminary work and structure determination 19
  II.3 Optimization of the reaction conditions 23
  II.4 Scope 26
    II.4.1 Substrate scope: 26
    II.4.2 Scope of the reaction 26
    II.4.3 Propylamine substrate scope: 28
  II.5 Mechanistic investigation 30
  II.6 Conclusion 37

III NHC-catalyzed synthesis of propargylic esters with CO_2 capture (Paper II)... 38
III.1 Introduction... 38
III.2 Experimental results and scope of the reaction ... 39
III.3 Mechanistic studies... 41
III.3.1 Proposed mechanism ... 41
III.3.2 Methodology for computational investigations ... 41
III.3.3 Results and discussion ... 42
III.4 Conclusion ... 45
IV Reaction of Catalytic Enols with Nucleophiles (Paper III) ... 46
IV.1 Introduction ... 46
IV.2 Experimental results and scope of the reaction ... 47
IV.3 Mechanistic studies... 49
IV.3.1 Method and model selection... 49
IV.3.2 Intermolecular reactivity mechanism ... 50
IV.3.3 Intramolecular reactivity mechanism ... 51
IV.4 Conclusion... 52
V Theoretical study of manganese-catalyzed synthesis of propargylamines (Paper IV)... 53
V.1 Introduction... 53
V.2 Scope of reaction... 54
V.3 Mechanism study ... 55
V.4 Conclusion ... 56
VI Concluding remarks... 57
Appendix A. Author contribution:... 58
Acknowledgements... 59
References... 60

Kor

I Introduction

I.1 Catalysis in organic chemistry

I.1.1 Catalysis and catalytic reactions

The rate of a reaction depends on various chemical and physical factors (pressure, solvent, stirring conditions, etc.). When those factors are fixed, the rate of reaction relies on the concentration of the reactants and on the energy given to the system, experimentally evaluated by the temperature. Every reaction has an activation energy, which represents a barrier that needs to be overcome in order for the reaction to happen, and to obtain the product. A catalytic reaction is characterized by a lower energy of activation compared to that of the reaction in the absence of the catalyst. A catalyst is a species that increases the reaction rate by lowering the activation energy.[1] Because the energy of activation is lower with catalyst and the entities involved can be different, catalytic reactions may follow pathways that are very different from those of their uncatalyzed reactions. Other characteristic is that the catalyst is not consumed during the reaction.

Catalysis can be divided into three main categories, homogeneous, heterogeneous and bio-catalysis. In homogeneous catalysis, all the components are soluble in the reaction media. One of the main sub-groups in this category is the catalysis mediated by transition metal complexes, where the metal is usually coordinated by anions or neutral ligands.[2] An example can be the Hoveyda-Grubbs catalyst for metathesis reactions.[3] Another important sub-group in homogeneous catalysis is that involving organocatalysts, which are small organic molecules used in processes.[4] An example could be the secondary amines used in Knoevenagel reaction.[5] Heterogeneous catalysts are not soluble in the reaction media (e.g. liquid media) and the physical interactions (adsorption, diffusion, etc…) between the reagents and the catalyst play a key role. The last type of catalysts, at the frontier between organic chemistry and biochemistry, are the enzymes, which catalyse a major part of the reactions needed for life and are becoming of common use in the chemical industry.[6]

I.1.2 Transition metal catalysis

Transition metals are elements that form one or more stable cations with incomplete *d* orbitals.[1] These elements form the *d*-block of the periodic table, including groups 3 to 12 (Figure 1). Interestingly, one of the main particularities of the transition metals is the ability to exhibit a range of possible oxidation states. All of them have at least two different positive states of oxidation.

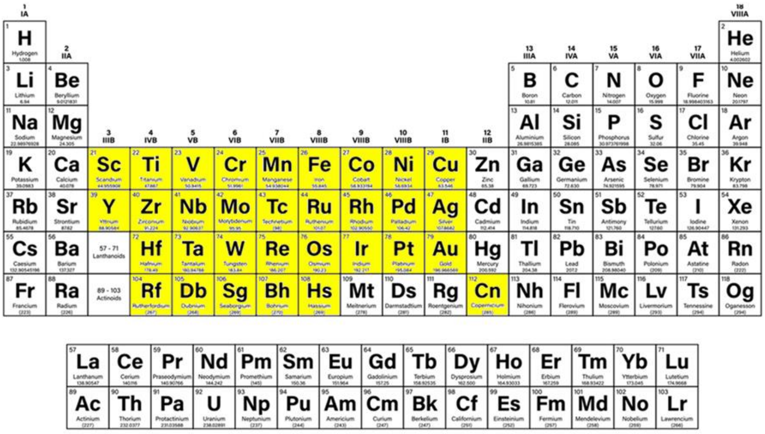

Figure 1. Transition metals (in yellow) on the periodic table

In recent years, transition metals have fulfilled an important role in the synthesis of organic compounds. Numerous organic transformations need transition metals, as it happens for example in the family of cross-coupling and related reactions. Mizoroki-Heck,[7] Suzuki-Miyaura[8] or Buchwald-Hartwig[9] coupling reactions are widely used in academia and in industry.

There are two major drawbacks for the general use of transition metals in synthetic chemistry. The first one is related to the supply chain. Noble metals are not abundant and others, like cobalt, are produced in socially and politically unstable countries. The second problem is toxicity, which can be of great concern for an industrial use.

I.1.3 NHC catalysis

N-Heterocyclic carbenes (NHCs) are organic molecules used in a wide range of applications, and they can also function as organocatalysts. The first evidence of the existence of *N*-heterocyclic carbenes was provided during the 50's, but the first stable and isolable ones were developed by Arduengo and co-workers in 1991.[10] NHCs serve as ligands for organometallic complexes[11] as well as catalysts in their own right, more prominently as nucleophilic species in umpolung chemistry,[12] but also as Brønsted bases in organic transformations.[13]

Many NHCs are readily accessible and even commercially available, mainly from imidazolonium salts upon deprotonation with a base (Scheme 1).[14,15] They allow a rapid development of new synthetic methodologies, giving access to a wide range of structures. The introduction of chirality in the carbenes has also been exploited for the asymmetric construction of organic molecules.[16]

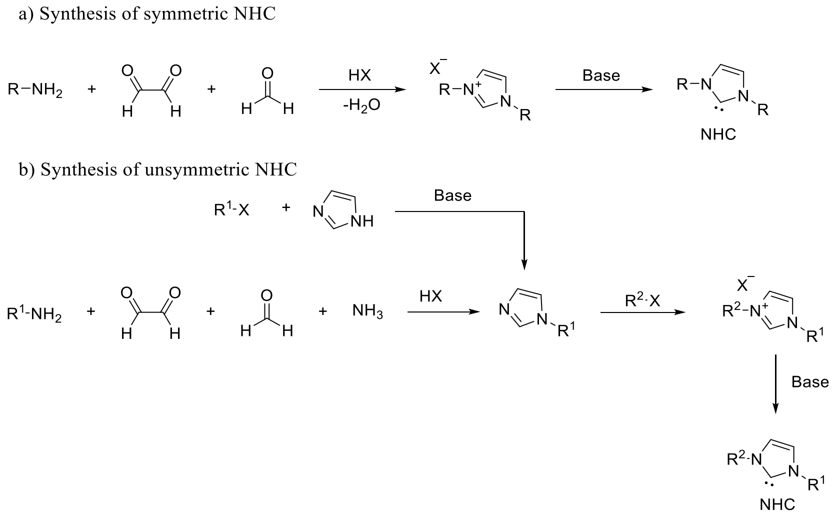
a) Synthesis of symmetric NHC
R−NH2
HX
-H2O
Base
NHC
b) Synthesis of unsymmetric NHC
R1-X
Base
R1-NH2
NH3
HX
R2-X
Base
NHC

Scheme 1. Two different strategies to synthesize NHCs

An example of a reaction involving an NHC catalyst is the benzoin condensation reaction, where two aldehydes react together to form α-hydroxy ketones (Scheme 2), important intermediates in the synthesis of bioactive molecules. These processes show in general high yields and high enantiomeric excess.[17]

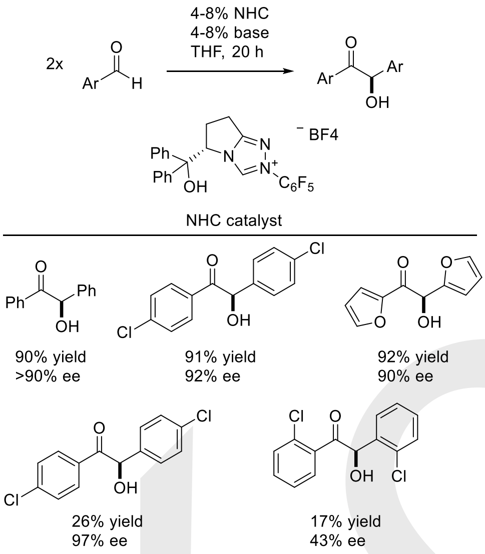
2x
4-8% NHC
4-8% base
THF, 20 h
NHC catalyst
90% yield
>90% ee
91% yield
92% ee
92% yield
90% ee
26% yield
97% ee
17% yield
43% ee

Scheme 2. Synthesis of α-hydroxy ketones in high yields and with enantiomeric excess.[18]

In addition, the use of carbenes has been expanded to other related reactions, like cross benzoin condensations, cross aza-benzoin reactions, and the Stetter reaction.[19] It has to be noticed that a base is necessary to *in situ* generate the catalyst and initiate the reaction. The base is used in the same amount as the catalyst, and its strength can vary from mild bases (such as carbonate salts and tertiary amines) to stronger ones, such as potassium *tert*-butoxide. For the last case, the scope can be limited due to the absence of orthogonality of reaction between the base and certain substituents, especially protecting groups.

The N-heterocyclic carbene family includes a sub-group called “non-classical carbenes”. Their main characteristic is that they have a significantly lower heteroatom stabilization by adjacent heteroatoms (Figure 2).[20] Those non-classical carbenes recently discovered have been used mainly for complexation with metals (palladium, nickel, rhodium), with implications for C–C formation,[21] hydrogenation[22] and metathesis reactions.[23] A characteristic of non-classical NHCs is that they have less donor ability. Their complexes are less stable than those of classical NHC, widening the scope of catalytic species.

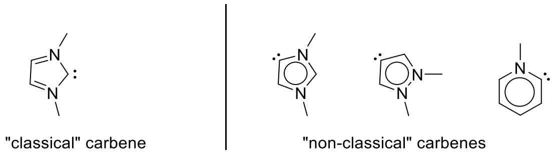

Figure 2. Examples of classical and non-classical carbenes

I.2 Umpolung reactivity

The principle of umpolung is the inversion of the natural reactivity of a synthon.[24] A major part of the reactivity in organic chemistry is based on the reaction between an electrophile and a nucleophile. According to this model, two entities with the same polarity (nucleophile-nucleophile, or electrophile-electrophile) would not react together. Umpolung is a process that allows this kind of reactivity to happen, by switching the polarity of one of the reagents. An example could be the reaction between an aldehyde and an alkyl bromide, which are both electrophilic by nature. However, reacting the aldehyde with 1,3-propanedithiol yields a thioketal, which can form a nucleophilic organolithium reagent. This species can then react with the electrophilic alkyl bromide, and after removal of the 1,3-propanedithiol, the ketone is obtained (Scheme 3).[25]

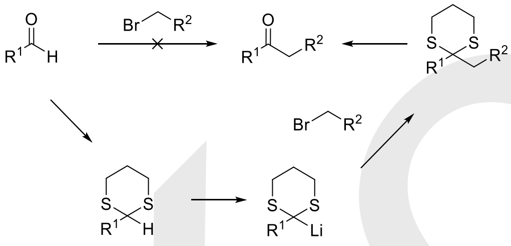

Scheme 3. Umpolung strategy to make aldehydes nucleophilic species.

I.2.1 Hypervalent Iodine

Polyvalent iodine compounds overpass the octet rule, providing specific reactivity. Those compounds are built around iodine atoms with an oxidation state of III or V, and they can be cyclic. They have three main types of applications. The first one is as oxidation reagents, such as the Dess-Martin periodinane (Scheme 4a), used for the mild oxidation of alcohols, or (diacetoxyiodo)benzene (PIDA) commonly used for reoxidizing transition metal catalysts.[26] A second usage is as reagents for organic synthesis.[27] For example, they are precursors of benzyne, which can be produced *in-situ* with fluorine donor reagents (Scheme 4b).[28] Finally, hypervalent iodine reagents can also work as umpolung reagents. The electrophilicity of the iodine atom allows access to electrophilic synthons starting from nucleophiles,[29,30] due to their capacity to induce ligand exchange, reductive eliminations or ligand couplings.[31] For example, Ochiai's group reported the α-acetylation of ketones with iodobenzene diacetate.[32] After formation of the enolate, a ligand exchange happens with the hypervalent iodine reagent, followed by either a S_N2 reaction with the acetate anion or either an intramolecular ligands exchange to form the desired product and iodobenzene, which could be then reoxidized and used in catalytic amount (Scheme 4c).

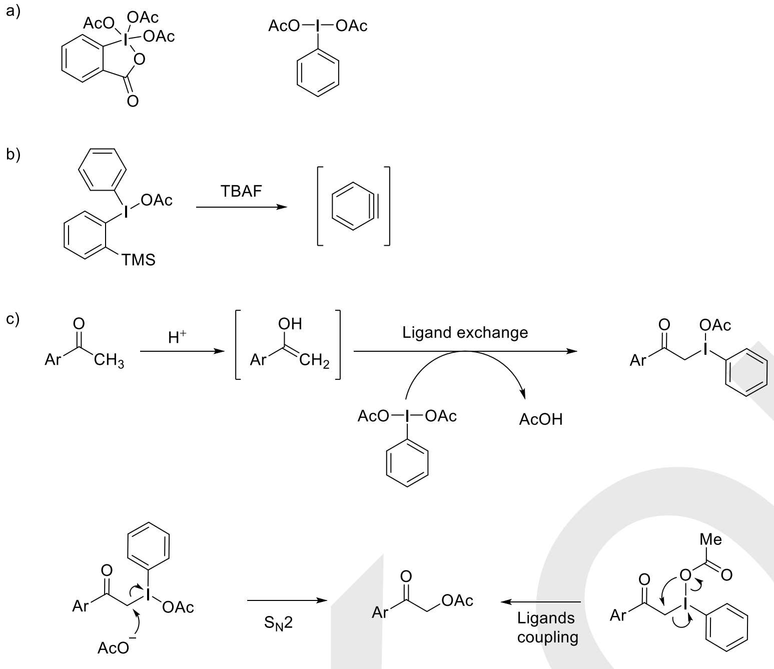

Scheme 4. a) Hypervalent reagents used as oxidants. b) Precursor of aryne. c) Example of an umpolung reaction mediated by PIDA.

I.2.2 CO_2 Activation by NHC

As previously shown, NHCs are nucleophilic entities, and are able to react with carbon dioxide to form imidazole-2-carboxylates. The first example of this adduct was reported by the Kuhn group, from a preformed NHC.[33] The NHC–CO_2 adduct has a relative low stability, because CO_2 can be released if the adduct is heated above 100 °C. The NHC-CO_2 adduct can be used as a precursor of NHCs, or it can be used as a temporary carrier of CO_2 (Scheme 5).

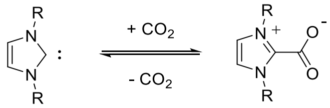

Scheme 5. Synthesis of NHC-CO_2 adduct.

The NHC-CO_2 adduct is a neutral zwitterionic species, where the carboxylate holds a formal negative charge. CO_2 is normally a kinetically stable, weak electrophile; it can react only with strong nucleophiles, like phenylmagnesium bromide, forming benzoic acid in this case. After formation of the NHC-CO_2 adduct, due to the negative charge at the oxygen atom, the CO_2 molecule can act as a nucleophile. This fact enriches and expands enormously the reactivity of carbon dioxide, like in the formation of cyclic carbonates by reaction between NHC-CO_2 adducts and propargylic alcohols.[34] The carboxylate group of the adduct attacks the alkyne, and the carbanion then deprotonates the alcohol. The catalytic cycle is closed after a cyclization step, releasing the NHC catalyst (Scheme 6).

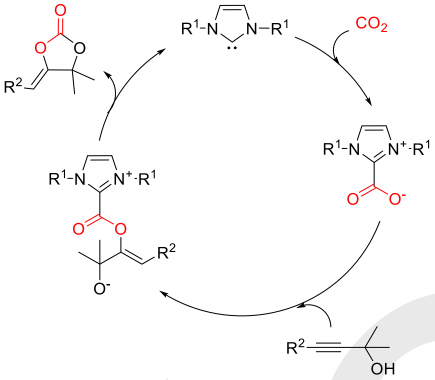

Scheme 6. Mechanism of the synthesis of cyclic carbonates *via* NHC-CO_2 adducts.[35]

Korr

I.3 C_{sp^2}–H and C_{sp^3}–H activations by transition metals

I.3.1 Mechanisms of C–H bond activations

Unrelated to any functional groups, C–H bonds have low intrinsic reactivity.[36] The energy barrier to cleave them is so high that, without harsh chemical conditions (high temperature, strong bases or acids), uncatalyzed reactions are unlikely to happen. However, some reactions as difficult as the C–H bond activation of methane to form methanol have been achieved, like in the platinum catalyzed process reported by Shilov.[37] And, in past decades, an abundant literature has been developed.[38] Due to the potential for atom economy and shorter synthetic paths, important research efforts have been dedicated to seek catalysts and potential substrates for attainable C–H activation processes.

In the case of transition metal catalyzed C–H activations, different mechanisms have been proposed. Among them, one of the fundamental variants is the oxidative addition to the C–H bond, forming a metal hydride and increasing the oxidation state of the metal atom (Scheme 8a); other mechanisms involve electrophilic aromatic substitution (S_EAr) (Scheme 7b); σ-bond metathesis (Scheme 7c); or single-electron transfer (SET) with radical intermediates (Scheme 7e).

More closely related to our work, two other approaches have recently appeared. First, the concerted metalation deprotonation (CMD), where the formation of the carbon-metal bond and the cleavage of the C–H bond are concerted. The proton departure is assisted by a base, in a single elementary step. The electropositivity of the metal, while approaching the carbon, increases the acidity of the proton. CMD is one of the most proposed mechanisms for palladium C–H activation (Scheme 7e). On the other hand, the base-assisted intramolecular electrophilic substitution (BIES), is a mechanism with two elementary steps, where the metal first coordinates with the carbon and then the proton is removed by the base (Scheme 7f). The bases involved in both mechanism are commonly carboxylates, carbonate, amide or phosphine oxide.[39,40]

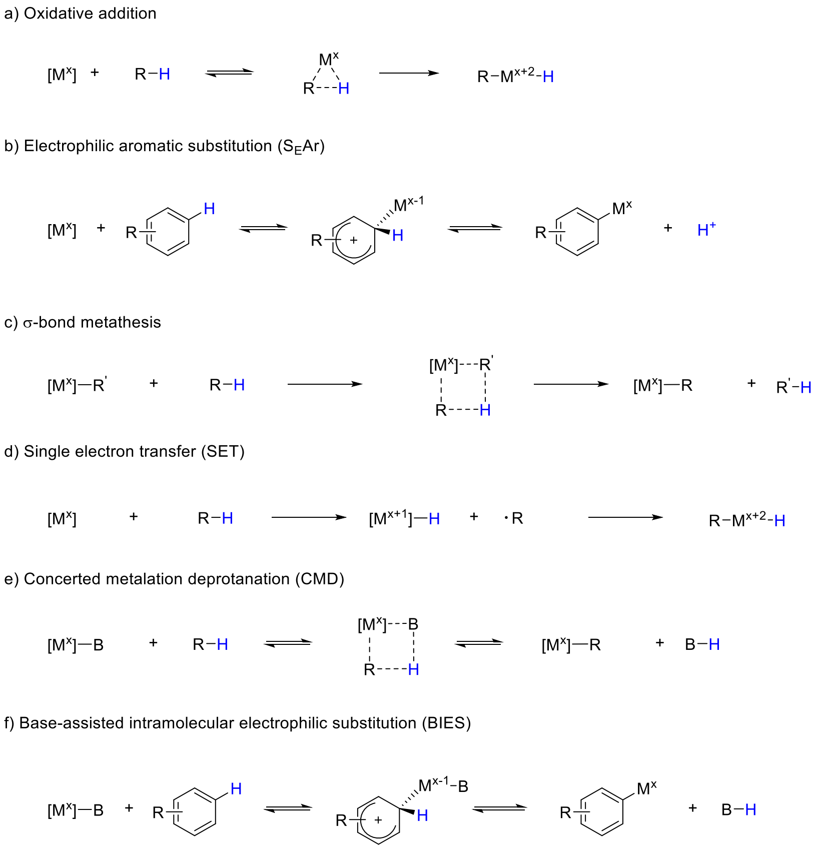
a) Oxidative addition

b) Electrophilic aromatic substitution (S_EAr)

c) σ-bond metathesis

d) Single electron transfer (SET)

e) Concerted metalation deprotanation (CMD)

f) Base-assisted intramolecular electrophilic substitution (BIES)

Scheme 7. Mechanisms of C–H activations by transition metals.

I.3.2 Directing groups for C–H activation

A great interest of C-H activation is the possibility of controlling the regioselectivity. This is achieved by the introduction of directing groups (DG). When using Pd complexes, once the C–H bond is cleaved, a palladacycle is formed. The size of the cycle may vary from three to ten atoms, although the most stable ones are the five- and six-membered rings.[41] Many of these metallacycles have been isolated.[42–44] Thus, the position of the directing group on the molecule dictates the position of the C–H bond that will be activated. For palladium, numerous types of functional groups can direct the activation. Those based on oxygen as the coordinating atom commonly include carboxylic acids (carboxylate form in the palladacycle), esters or alkoxides.[45] Among the family based on nitrogen as the coordinating group, amines, imines, oximes, amides, N-oxides and sulfamides have been reported.[46] A classification of the strength of those directing groups has been reported by Norrby and co-workers (Figure 3).[47]

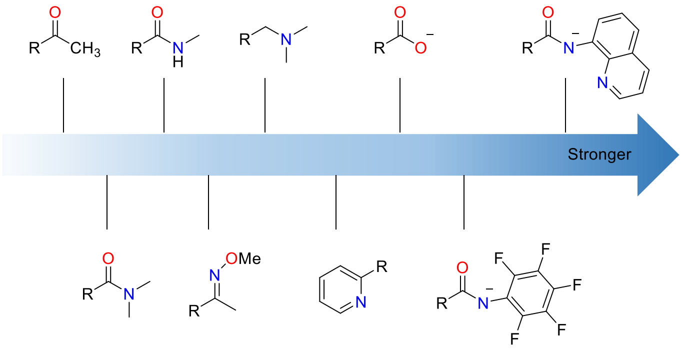

Figure 3. Qualitative scale of strength of selected directing groups.[47]

If the starting material contains a weak directing functional group, it can be modified to create a DG with the expected length. Then the metal can coordinate at the desired position and activate the desired C–H bond. Two categories exist, a functionality with a covalent link to the molecule, or with a removable link. The covalent linked one's can be, for example, of an amide made from the carboxylic acid and amines, such as 8-aminoquinoline, picolinamide[48] or sulfamide. In these cases, the substrate and the metal can proceed to the activation with harsher conditions thanks to a stable DG. This type of directing group can be challenging if the desired functional group do not have and orthogonal reactivity with the other ones (if other functional groups can react in the same reaction conditions for setting or removing the DG). On the other hand, the second category are the, so called, transient directing groups. They are incorporated in the molecule *in situ* upon reaction with a functionality already present in the molecule. As before, the aim is to generate the DG with the wanted characteristics (strong chelating ability and regioselectivity).

To have a good transient DG, the following criteria need to be fulfilled: a) the introduction of the DG has to be reversible, b) the formation should be chemo-selective, and c) they should be stable enough to allow the C–H activation and the subsequent transformations. It is also necessary that the DG do not interact with other functional groups (orthogonal reactivity) (Scheme 8).

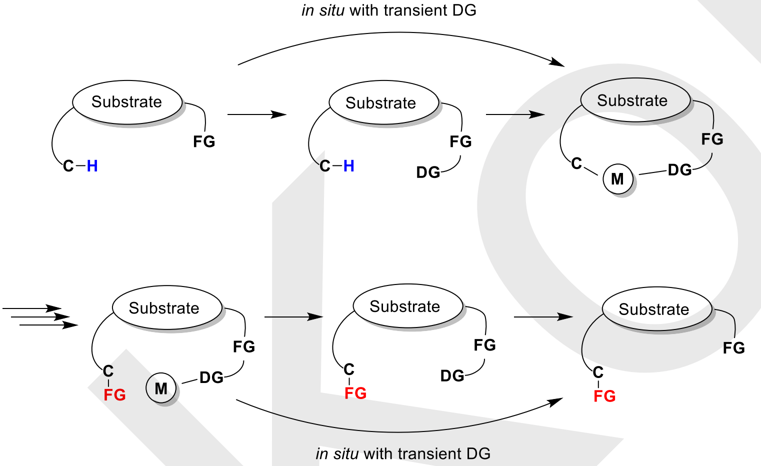

Scheme 8. Strategy for incorporation of directing group.

I.3.3 C_{sp^3}*–H activation of aliphatic amines*

C–H activation is a great synthetic strategy to reach new potential drugs. Nitrogen containing molecules are prevalent in bioactive compounds, methods towards the C–H activation of aliphatic amines have recently emerged. Those methods represent a powerful synthetic strategy, especially for late stage functionalization.[49] The number of such valuable reactions keeps continuously growing. However, universal methods for activating any position of the alkyl chains of an aliphatic amine do not exist. Therefore, inventive and convenient procedures have been developed to suit with the different constraints of the substrates for achieving the reaction.[50]

The most popular approach to reach C–H activation of amines is the use of a directing group. For example, the group of Maes reported the use of a pyridine moiety to activate the α-position of piperidines (Scheme 9a).[51] Also, the γ-position of alicyclic amines has been activated by the Sandford group with an innovative directing group (Scheme 9b).[52] The Ge group succeeded in the selective γ-functionalization of polysubstitued aliphatic amines with glyoxylic acid as transient directing group (Scheme 9c).[44] Methods with no directing group added exist, but only with secondary/tertiary amines or in the presence of protective groups on the nitrogen (Scheme 9d).[53] So far, the C–H activation of free amines, with no additional directing groups, remains a challenge.

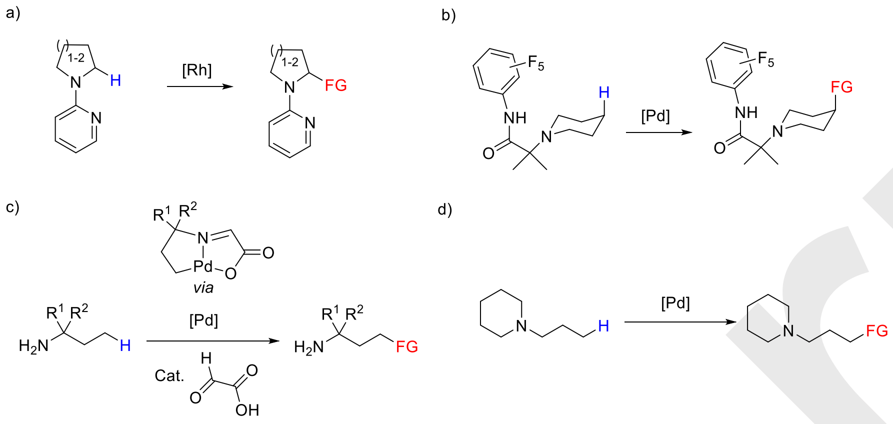

Scheme 9. Examples of functionalization of aliphatic amines through C–H activation.[44,45,52,53]

I.4 A^3 coupling and KA^2 coupling reactions

A^3 stands for Aldehyde-Alkyne-Amine reaction, a multicomponent synthesis of propargylamines (Scheme 10), with water as by-product. This denomination was first proposed by Li,[54] but the first reaction of this type was reported by Dax and co-workers.[55] The reaction needs a metal catalyst, and several transition metal complexes have been reported to mediate this transformation.[56] The most common are copper, ruthenium, gold or even silver.[57,58] Recently, more earth abundant metals are also able to catalyze the reaction, such as zinc, or iron.[59]

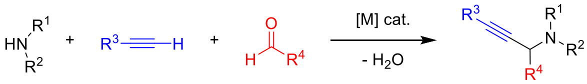

Scheme 10. General A^3 coupling reaction.

Propargylamines prepared through this method may be reacted further towards the synthesis of more complex molecules. An example is the synthesis of quinoline by Tu and co-workers.[60] They reacted the three components, aniline, aldehyde and terminal alkylne, in the presence of an iron salt. The same catalyst mediated the nucleophilic functionalization of the triple bond, resulting in a cyclization, which is followed by a final oxidation by air (Scheme 11).

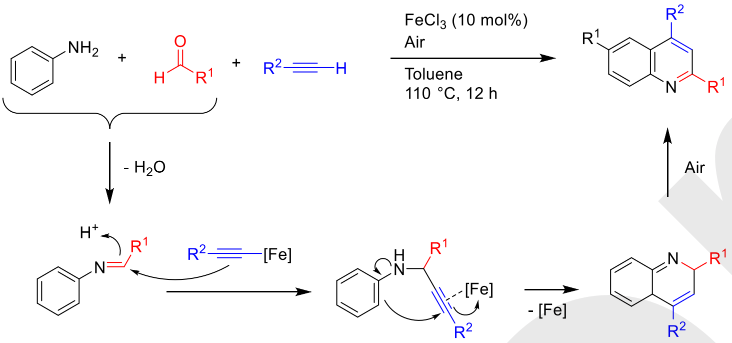

Scheme 11. Synthesis of quinolines by tandem A^3 / cyclization reaction reactions.

Another modified version was reported by Li and co-workers,[61] consisting on performing the A^3 reaction in the presence of CO_2 (1 atm), resulting in the synthesis of carbamates in a one-pot reaction. The catalyst used was CuBr (Scheme 12).

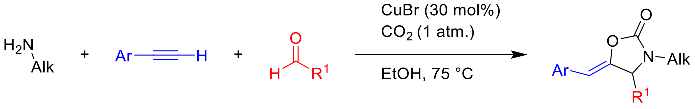
H2N
Alk
+
Ar
H
+
O
H
R1
CuBr (30 mol%)
CO2 (1 atm.)
EtOH, 75 °C
O
O
N
Alk
Ar
R1

Scheme 12. Modified A^3 coupling reaction for the synthesis of carbamates.

The KA^2 coupling stands for Ketone, Alkyne and Amine coupling, and affords fully α-substituted propargylamines.[62] Changing the aldehydes to ketones have an impact on the reaction rate, as ketimines, the intermediates formed in this instance, are less reactive than aldimines. Despite these difficulties, several examples of KA^2 couplings have been reported, also mediated by transition metal catalysts.

An example of KA^2 reaction is the one reported by Larsen and co-workers,[63] who used $CuCl_2$ as catalyst and $Ti(OEt)_4$ as Lewis acid, without solvent. The Lewis Acid is necessary to form the ketimine, and also acts as a dehydrating agent (Scheme 13a). Ji's group reported the first KA^2 catalyzed by gold ($AuBr_3$), also in neat conditions (Scheme 13b).[64] Intermolecular KA^2 reactions have also been reported. For example, Tehrani and co-workers reacted amino ketones with terminal alkynes under copper catalysis, yielding α-substituted pyrrolidines in good yield (Scheme 13d).[65]

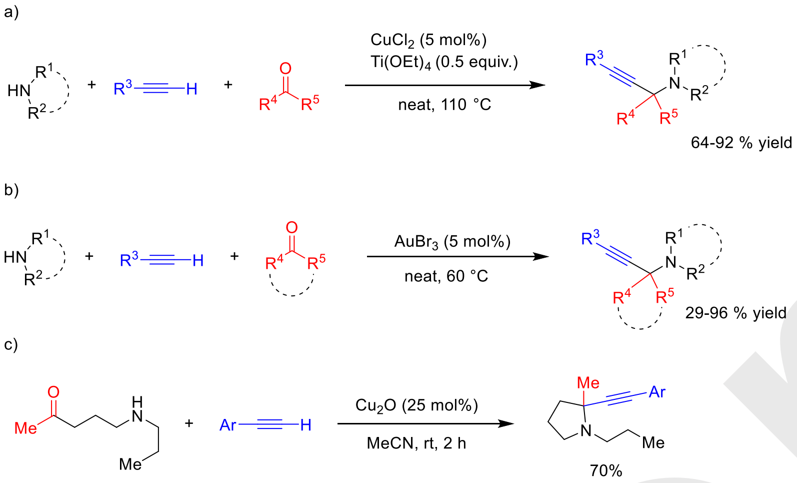
a)
HN
R1
R2
+
R3
H
+
O
R4
R5
CuCl2 (5 mol%)
Ti(OEt)4 (0.5 equiv.)
neat, 110 °C
R3
R1
N
R2
R4
R5
64-92 % yield
b)
HN
R1
R2
+
R3
H
+
O
R4
R5
AuBr3 (5 mol%)
neat, 60 °C
R3
R1
N
R2
R4
R5
29-96 % yield
c)
O
Me
H
N
Me
+
Ar
H
Cu2O (25 mol%)
MeCN, rt, 2 h
Me
Ar
N
Me
70%

Scheme 13. KA^2 coupling reactions. a) KA^2 coupling catalyzed by copper and Lewis acids. b) KA^2 reaction mediated by a gold catalyst. c) Cu-catalyzed intramolecular KA^2 reaction.

Korr

I.5 Density functional theory for mechanistic investigations

I.5.1 Principles of density functional theory and functionals construction

The Schrodinger equation (Equation 1)[66] describes the wave function of a quantum-mechanical system, where $\widehat{H}$ is the time dependant Hamiltonian operator, ψ the wave function and E the total energy of the defined system.

$$\widehat{H}\psi = E\psi$$

Equation 1. Schrodinger equation

In spite of its apparent simplicity, it is not possible to find a solution of the Schrödinger equation for systems containing two or more electrons, and some particular approximations and cases are required to describe multi-electronic systems.

Density Functional Theory (DFT) is one of the most commonly used computational approaches for the calculation of the energies and structures of complex chemical structures. The idea behind DFT is to use a different approach, describing the chemical systems based on their electron density function,[67] and not its wave function, providing an accurate answer in a reasonable time, without too much simplification.

The electron density is represented by a function, noted ρ, giving the probability of finding an electron in certain position of the space. This function ρ depends on three variables (x, y, z), while the wave function depends on 3N variables, where N is the number of electrons. This is the main advantage of DFT, to greatly reduce the complexity of the equation and the cost of computation.

Two theorems founded the grounds of DFT, and were stated by Hohenberg and Kohn[68]: 1) the ground state electronic energy can be calculated as a function of the electron density, and 2) the electron density follows the variational principle, thus the calculated electronic energy must be greater or equal to the true ground state value (Equation 2).

$$E(\rho) \geq E(\rho_{exact}) = E_{exact}$$

Equation 2. Mathematical description of the Hohenberg-Kohn theorems

From there, they showed that the energy can be calculated from the electron density functional (a mathematic object using electron density function), without explicitly giving the nature definition of the functional. Shortly after, as Kohn and Sham noticed,[69] if the system is considered with non-interacting electrons, the functional can be written as the sum of specific terms (Equation 3):

$$E(\rho) = T_{ni}(\rho) + V_{ne}(\rho) + V_{ee}(\rho) + E_{XC}(\rho)$$

$$\text{With: } E_{XC}(\rho) = \Delta T(\rho) + \Delta V_{ee}(\rho)$$

Equation 3. Composition of the total energy

$T_{ni}(\rho)$ is the kinetic energy of the non-interacting electrons, $V_{ne}(\rho)$ the potential energies due to nuclear-electron interaction and $V_{ee}(\rho)$ the term for the electron-electron repulsion. The exchange-correlation energy $E_{XC}(\rho)$ is composed by the correction to the kinetic energy due to electronic interactions $\Delta T(\rho)$ and the non-classical corrections to the electron-electron repulsion energy $\Delta V_{ee}(\rho)$. Except the exchange-correlation energy, all the terms can be classically calculated.

This last term, the exchange-correlation energy cannot be exactly calculated. Therefore, functionals have been developed with different approximations of this term.[70] They can be ranked by their type of approximation and the accuracy associated. More complex functional leads to a better accuracy, accompanied at the same time by higher computational cost.

I.5.2 Basis sets

Basis sets in DFT are necessary in order to describe the shape of the different atomic orbitals, as are linear combinations of different functions. Two different types of functions exist. The Slater Type Orbitals, STO, and the Gaussian Type Orbitals, GTO. Whilst the STO are more accurate for the description of the orbitals, the GTO are used due to their simplicity and lower computational cost.

The number of functions per orbital is free to be set. A perfect basis set would have an infinite number of functions, but this is obviously impossible from a practical point of view. If a basis set contains one function per orbital, it is called minimum basis set. However, most of the basis set used contain more than one function. A basis set with two functions per orbital will be named double-zeta, with three triple-zeta, etc.

With the idea to have a lower computational cost without a high loss of accuracy, the number of function can differ between the core orbital and the valence orbitals. As bonds formation rely on the valence orbitals, more functions are used for a better description. This is called a split valence set.

Too take into account the polarization, when electronic charges are altering the shape of the orbitals, functions can be added too.

To describe more accurately the behaviour of the electrons far from the nucleus, diffusion functions can be added to the basis set. This is needed in case of ions or radicals for example.

I.5.3 Solvation model

Most of the chemical reactions are done in a solvent media, and the solvent is an important parameter of the reaction conditions. As the components of a given reaction interact differently with different solvents, the energy associated to the system can differ accordingly.

Two main approaches exist for the description of the solute/solvent interaction. The first one is the explicitly model, where molecules of solvent are surrounding the molecule. In DFT, the cost of this approach is too high to be used on system with 50-100 atoms.[67]

The second approach is the implicit model. The most used is the Polarized Continuum Model, PCM, where the system is placed in a cavity with a suitable shape.[71] The most important parameter of the PCM is the dielectric constant, than can be known by experimental or computational means. The free energy of solvation can be then calculated (Equation 4):

$$\Delta G_{sol} = \Delta G_{cav} + \Delta G_{disp} + \Delta G_{rep} + \Delta G_{elec}$$

Equation 4. Composition of the free energy of solvation

With ΔG_{cav} is the cavitation energy, it is the energy difference with and without the cavity in the continuum. ΔG_{disp} is the dispersion energy between solute and solvent, ΔG_{rep} represents the repulsion between solute and solvent and ΔG_{elec} is the term for the electrostatic polarization caused by the charge distribution of the solute molecules in the solvent, or the opposite.

I.5.4 Functionals and basis sets selected in the thesis

In the second chapter, the B97D functional was used for optimization of the different structures. It is an adequate method for the calculation of structures containing palladium.[72] Also, the 6-311G(d,p) basis set was used, known to be cost effective and providing accurate geometries. M06/Def2TZVPP were used together for energy refinement. Considering the physical interactions between atoms, the accuracy is much higher with Def2TZVPP,[73] set although presenting the drawback of an increase in the calculation time, becoming not applicable for iterative geometry optimizations. Iodine and palladium are not defined in the Pople basis set 6-311G, but an appropriate alternative exist, known as the SDD basis set. Both atoms are defined within the Def2TZVPP basis set.

In the third chapter, M06-2X and 6-31G(d,p) were used for geometry optimization as functional and basis set, respectively. Recent literature examples also use this pair for the study or pure organic reactions,[74] and in addition, it has been demonstrated that they perform well in cases involving zwitterionic species and halogen-ions.[75]

In the fourth chapter, the study was done with using the B97D functional for the structure optimizations, together with the 6-31G(d,p) basis sets for all the atoms.

Korr

I.6 Objective of the thesis

The aims of the thesis are the development of efficient methods for the formation of complex molecules from simple and easily accessible materials. The thesis is divided into four independent projects with different inherent objectives.

The first project (Chapter II) reports a new synthetic method to produce alkylated quinoliniums, as molecules of high value, which are prepared from simple propylamine and its derivatives. In addition, the focus was put on the comprehension of the mechanism for further development.

The second project (Chapter III) focuses on the comprehension of an organocatalytic reaction that yields propargylic esters from simple reagents, as alcohols, carbon dioxide and propargyl halides. The study by DFT aims to give a clear view of the mechanism, and to try to explain certain intriguing reactivity in some cases. Also, the aim was to understand the limitation of the scope and highlight the possible incompatibilities between the different reagents.

The third project (Chapter IV) has for objective to understand how hypervalent iodine enables the reaction of two nucleophiles, an enolate and an alcohol, *via* an umpolung reaction. The enolate is generated under the reaction conditions from allylic alcohols *via* an iridium-catalyzed isomerization. A second objective is to understand the selectivity obtained when there exist two different nucleophiles that may react with the enolate produced *via* isomerization.

The last project (Chapter V), used the experimental result of a KA2 coupling reaction, in order to understand the mechanism. For the first time, manganese is used as a catalyst for this reaction, therefore, it is interesting to study his role. To proceed, DFT calculations were used.

Korr

II Synthesis of substituted alkyl quinoliniums from propylamine and its derivatives (Paper I)

II.1 Introduction

Quinoliniums and quinolines represent an important class of molecules with strategic applications in many fields of chemistry. Looking to their bioactivity, they are found in antiviral, antibacterial, analgesic, and antidepressant drugs.[76] Well-known molecules such as quinine are emblematic in organic chemistry, and its derivatives are essential for anti-malarial treatments. Quinoliniums are used as tools in biology as DNA dyes and intercalants. They are essential for studies of cells and their environment, and in flow cytometry the main known dye is thiazole orange. Other applications in chromatography have been reported (Figure 4).[77]

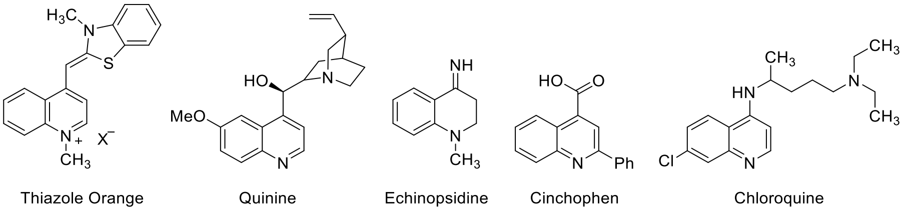

Figure 4. Examples of high-value molecules with quinoline scaffolds.

New methods for the synthesis of quinolines are continuously reported, and some of them are part of the most well-known reactions in organic chemistry. However, those syntheses, with few exceptions, need C_{sp^2}-N bond containing starting material, in the form of substituted anilines or nitrobenzenes. For example, the Combes synthesis needs anilines with 1,3-diketone and acid as catalyst to render the quinoline.[78] The drawback of this simplicity is the difficulty to reach regioselectivity. Regioselectivity can be achieved by using steric effects and kinetics, but the scope is meanwhile reduced.

To obtain the desired structure of quinoline, the development of methodologies has been prolific during the last decades.[79] However, the complexity of the starting materials needed for those transformations may be high, and incompatibilities may exist with the desired substituents on the final molecule (Scheme 14).

Kor

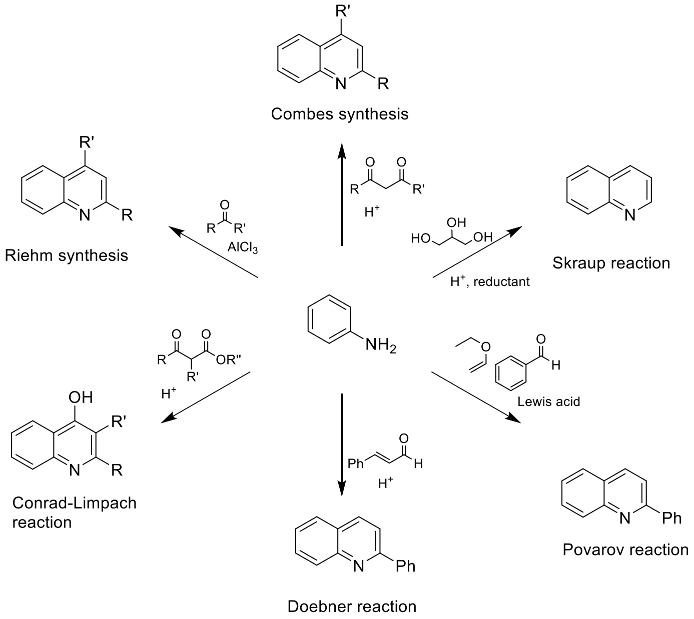
Combes synthesis
Riehm synthesis
AlCl3
Skraup reaction
H+, reductant
NH2
Lewis acid
Conrad-Limpach reaction
Povarov reaction
Doebner reaction
H+

Scheme 14. Classical synthetic routes to form quinolines from aniline

Most of the quaternary quinolinium species are synthetized from quinolines through alkylation with halogenated building blocks. For the direct preparation of quinolinium salts, only few examples are reported. One method was developed by L. Cheng *et al.*,[80] using *N*-substituted anilines, aldehydes and alkynes, in a reaction catalyzed by copper (scheme 15).

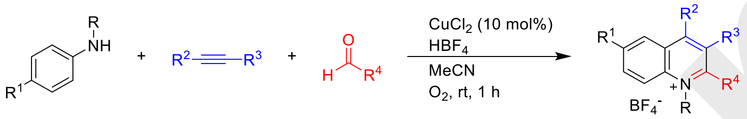
CuCl2 (10 mol%)
HBF4
MeCN
O2, rt, 1 h
BF4-

Scheme 15. Three components reaction for the synthesis of substituted quinolinium salts.

In addition to the mentioned applications of the quinolinium compounds, they can be used also as intermediates for the synthesis of complex molecules. For example, positions 2 and 4 become electrophilic, and can react with strong nucleophiles such as Grignard reagents.[81]

Quinolinium salts can also be hydrogenated to yield the tetrahydroquinoline skeleton. Further, methods have been recently developed for the formation of functionalized tetrahydro/dihydro-quinolines (Scheme 16).[82,83]

Korr

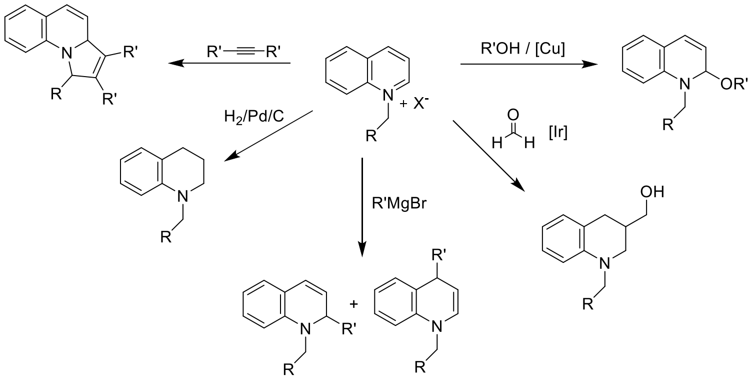
R'—≡—R'
R'OH / [Cu]
H2/Pd/C
[Ir]
R'MgBr
N+ X-
R
R'
OR'
OH
+

Scheme 16. Examples of possible reactions from quinolinium salts.

The aim of this project is to access to quinoline scaffolds from arylpropylamines, in one step. As the majority of synthetic routes to quinolines use aniline as starting material, our method offers an alternative approach to access their cyclic structure, forming the key Ar-N bond from open aliphatic amines. In addition, the control of the substitution pattern is important to provide a reliable transformation. The introduction of an alkyl quinolinium moiety offers diverse possibilities of further transformations.

II.2 Preliminary work and structure determination

Initially we reacted 3-phenylpropylamine with iodobenzene (**2a**) in the presence of a catalytic amount of palladium acetate and silver trifluoroacetate in acetic acid at 110 °C, with the intention of preparing diarylpropylamine derivatives (**4**). However, the formation of an unknown compound was observed (**3a**). A similar outcome was obtained when the reaction was run with iodotoluene (**2b**), obtaining a complex adduct (**3b**). In either case the arylated product **4** was not formed (Scheme 17).

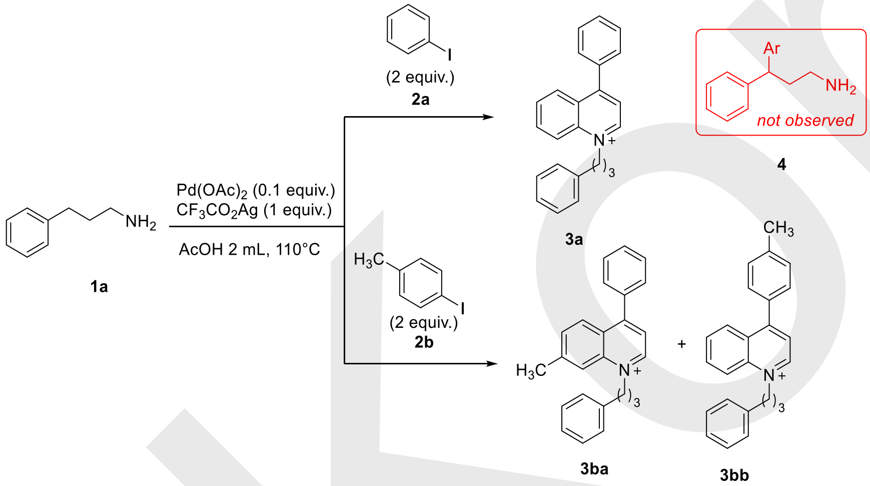
1a
Pd(OAc)2 (0.1 equiv.)
CF3CO2Ag (1 equiv.)
AcOH 2 mL, 110°C
(2 equiv.)
2a
(2 equiv.)
2b
3a
Ar
NH2
not observed
4
CH3
H3C
3ba
+
3bb

Scheme 17. Early attempts on the arylation of aliphatic amines via C–H activation.

Products **3a** and **3b** were then isolated by preparative TLC and characterized. According to the starting materials used, the assumption was made that a limited number of nitrogen and oxygen atoms can be present on products **3a** and **3b**. The exact masses were fundamental to know the molecular formula of **3a** and **3b**, which, as expected, differ in one methyl group. With a measure of 324.1745 m/z for **3a**, its molecular formula was preliminary proposed to be $C_{24}H_{22}N$. For **3b**, a mass of 338.1900 m/z was measured, corresponding to $C_{25}H_{24}N$ (Figure 5). The error of the exact masses was below 3 ppm in both instances.

These formulas provided very useful pieces of information. For example, both **3a** and **3b** contained 14.5 unsaturations, so they contained potentially a polycyclic structure. The unsaturation figure is not an integer (14.5 unsaturations), and this could come from having the M+H detection. However, by ^{1}H NMR spectroscopy, 22 + 3 protons were obtained after integration of the signals, and a highly polar compound was detected by TLC. These data suggested the presence of a positive charge on the molecule, accompanied by an acetate moiety, possibly coming from the solvent. This is supported by a signal at around 1.9 ppm on the ^{1}H NMR spectrum, and at 181 ppm on the ^{13}C NMR spectrum.

The difference of mass and formula between **3a** and **3b** was equivalent to a methyl group, being the same difference between phenyl and tolyl starting materials, so it can be deduced that only one aryl group is involved in the reaction, as mentioned before.

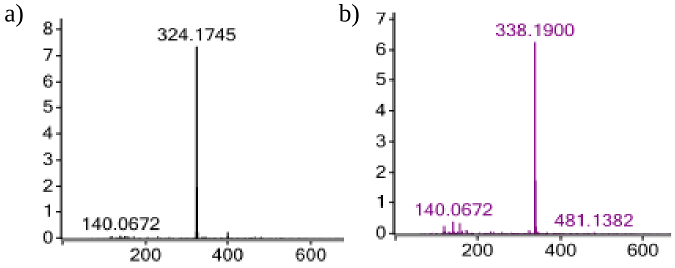

Figure 5. a) Exact mass of **3a**, b) Exact mass of **3b**.

From the ^{1}H NMR and COSY NMR spectra of compound **3a** independent coupling systems could be identified. A first one, with three signals from 2.5 to 5.0 ppm, each signal integrating for 2H, which can be assigned to a chain $R\text{-}CH_2\text{-}CH_2\text{-}CH_2\text{-}R'$, associated with the propylamine moiety. Around 7.0 ppm, a multiplet signal for 5H, typical of a benzene ring with single substitution can be noticed. The same system for 5H, around 7.5 ppm, is also associated with a benzene ring, linked to a different part of the molecule. The next system contains two protons, one at 7.6 ppm, directly coupled with another at 9 ppm. The last coupling system bears four protons system, one of them at 7.8 ppm, coupled with two H at 8.1 ppm, which are coupled themselves with one proton at 8.3 ppm (Figures 6 and 7).

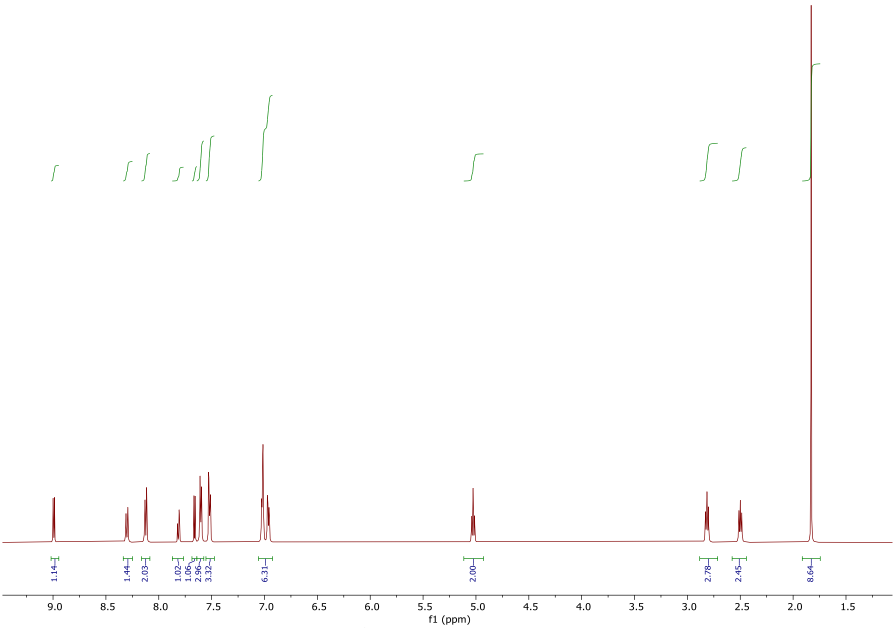

Figure 6. ^{1}H NMR in CDCl$_3$ of **3a**

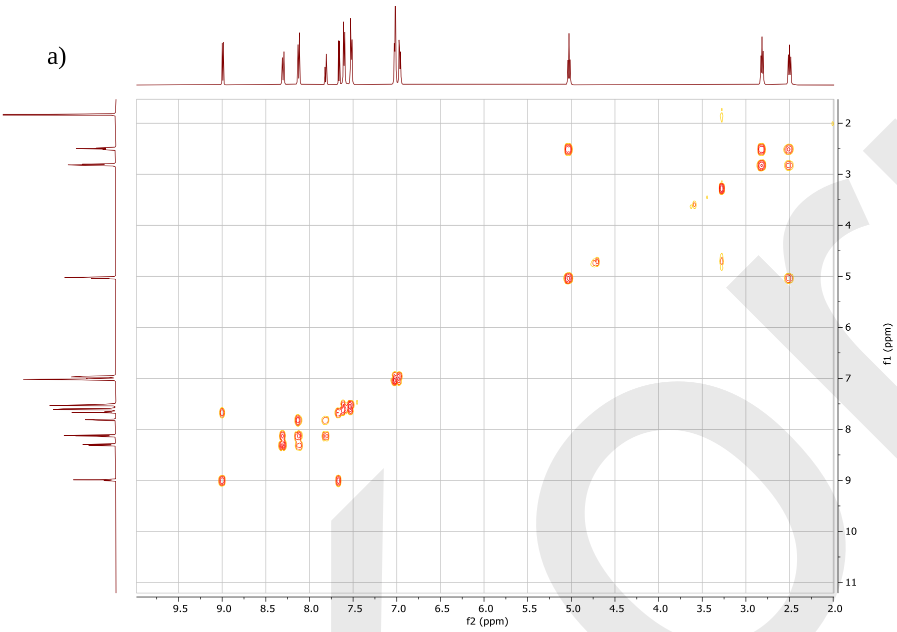

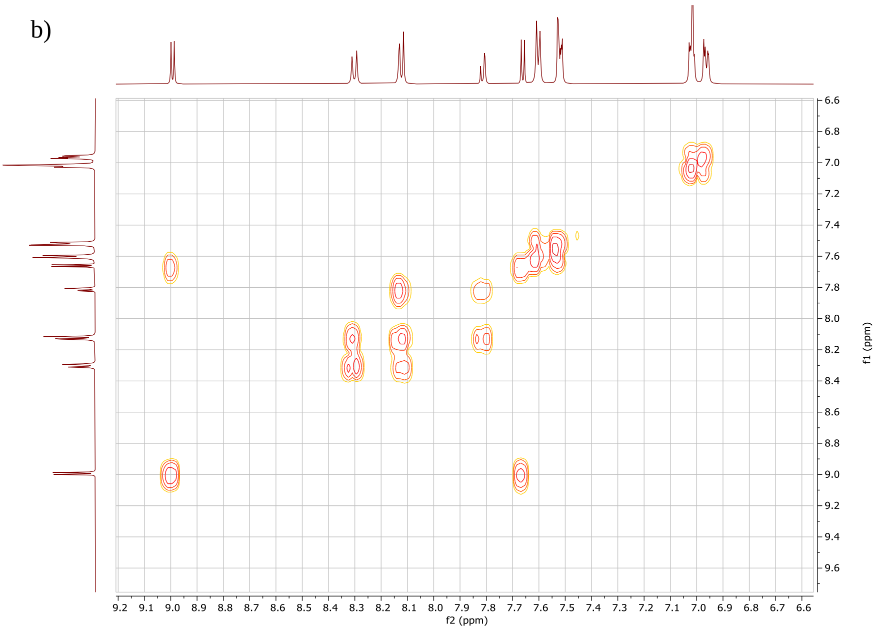

Figure 7. a) COSY ^{1}H NMR in $CDCl_3$ of **3a**, b) Enlargement of the COSY NMR.

When removing the number of carbons and protons, and the unsaturations related to the propyl chain and the two benzene rings from the formula of **3a**, the remainder counts for 9C, 6H, 1N and 7 unsaturations. This is typical of a substituted quinoline scaffold. Thus, it was proposed that the structure of **3a** agrees with that of quaternary quinolinium salt, with a 3-phenylpropyl alkyl chain, and a phenyl substituent on position 4 of the quinoline moiety (Figure 8). A NOE experiment was done on the signal at 5.1 ppm. This demonstrated an expected special proximity with the two other signals at 2.7 and 2.5 ppm, but also with those at 9.0 ppm and 8.4 ppm (Figure 9).

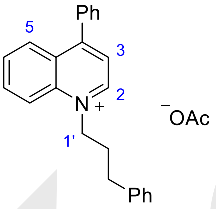

Figure 8. Proposed structure for **3a**.

Kor

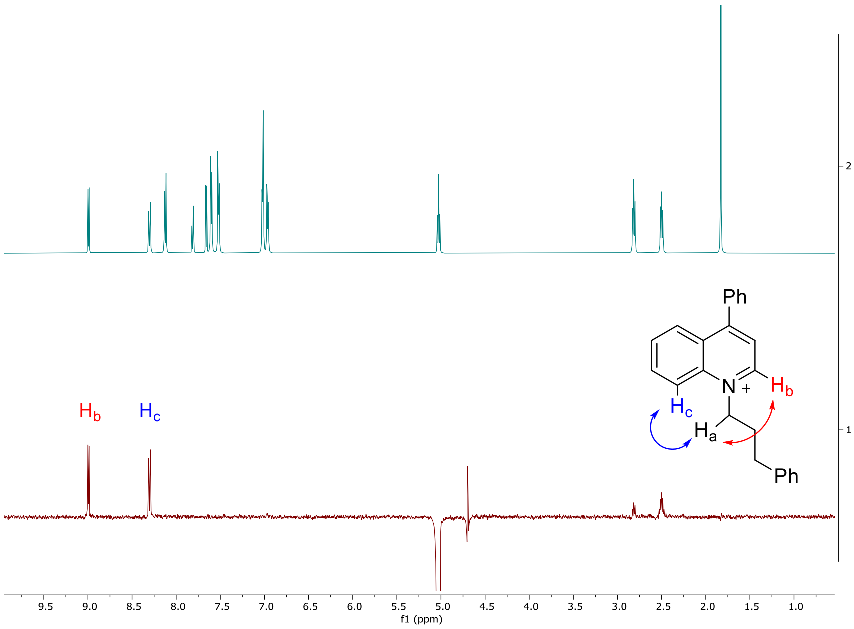

Figure 9. NOE experiment on the signal at 5.1 ppm of compound **3a**.

II.3 Optimization of the reaction conditions

With the structure identified, the optimization of the reaction conditions was carried out. By looking first for other active catalysts, different transition metal salts were tested (Table 1, entry 1). None of them, except palladium acetate (Table 1, entry 3), could afford the product. Other palladium sources like tetrakis(triphenylphosphine)palladium did not yield the product either (Table 1, entry 2). On the side of the oxidant, only silver salts such as silver oxide worked efficiently (Table 1, entries 3-4). Other oxidants[84] commonly used in connection with palladium-mediated transformation did not afford the product, such as nitric acid, oxygenated water or copper acetate (Table 1, entries 5-7). As reported by Bo,[44] silver could play a double role, as oxidant and also to capture the iodine atom during the oxidative addition / reductive elimination steps. Next, the focus was put on the possible solvents for the reaction (Table 1, entries 8-10). It was noticed from the beginning of our study that the presence of acetic acid is essential for the reaction to occur. Therefore, we decided to continue with pure acetic acid (Table 1, entry 4).

Kor

Table 1. Optimization of the reaction conditions.

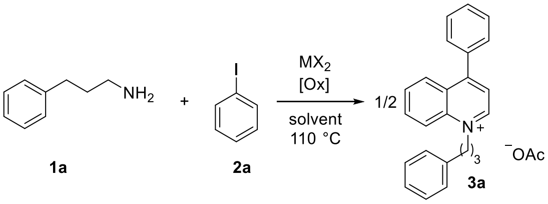

Entry	Catalyst (10 mol%)	oxidant	Solvent	Yield (%)[a]
1[b]	$M(OAc)_2$	CF_3CO_2Ag (1.5 equiv.)	AcOH	0
2	$Pd(PPh_3)_4$	CF_3CO_2Ag (1.5 equiv.)	AcOH	0
3	$Pd(OAc)_2$	CF_3CO_2Ag (1.5 equiv.)	AcOH	16
4	$Pd(OAc)_2$	Ag_2O (2 equiv.)	AcOH	21
5	$Pd(OAc)_2$	HNO_3 (2 equiv.)	AcOH	0
6	$Pd(OAc)_2$	H_2O_2 (2 equiv.)	AcOH	0
7	$Pd(OAc)_2$	$CuOAc_2$ (2 equiv.)	AcOH	0
8	$Pd(OAc)_2$	Ag_2O (2 equiv.)	DMF	0
9	$Pd(OAc)_2$	Ag_2O (2 equiv.)	MeOH	0
10	$Pd(OAc)_2$	Ag_2O (2 equiv.)	Toluene	0

All reactions were performed with 2 equiv. of iodobenzene (**2a**), at 110 °C, overnight. [a]Yields by ^1H NMR spectroscopy with trimethoxybenzene as internal standard. [b]M: Cu, Mn, Co and Zn.

During the reaction, a by-product, acetamide **5**, was detected in the ^1H NMR spectrum of the crude mixtures. The next objective was therefore to reduce the amount of this undesired product. First, larger amounts of silver and iodobenzene (**2a**) substrates were tested in order to increase the rate of formation of the desired product **3a**, however, these changes did not succeed and no significant improvement of yields was observed (Table 2, entries 1-3). Increasing the temperature did not have the expected positive effect (Table 2, entry 4). The solution came with the idea that reducing the amount of acetic acid could decrease the speed of formation of amide **5** by-product. This can be done by using a mixture of acetic acid and water as the solvent mixture, as water was the only other compatible solvent. Different v/v ratios of AcOH and H_2O were investigated, and a 1:1 (v/v) ratio was found to give the best conversion into quinolinium product **3a** with a drastic reduction of amide **5** in the crude mixture. However, the reaction was incomplete at the standard times, so the reaction had to be prolonged for up to 60 h. Those conditions provided the best yields obtained so far (Table 2, entry 7). The number of equivalents of the different starting materials were also optimized, finding that decreasing silver or palladium quantities had a negative impact on the yield (Table 2, entries 8-9), whereas no impact was noted in the case of higher palladium and silver loadings (Table 2, entry 10). Reduction of temperature or time went together with a drop in the yields (Table 2).

Table 2. Optimization of the solvent.

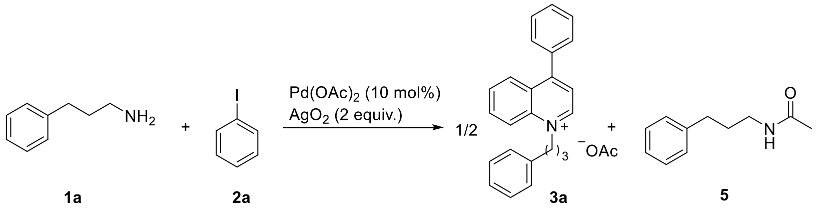

Entry	Ag_2O (equiv.)	PhI (**2a**) (equiv.)	Solvent (*v*/*v*)	Temperature (°C)	Yields (**3a** / **5**, %)[a]
1	2	2	AcOH	110	26 / 47
2	3	2	AcOH	110	31 / 46
3	2	3	AcOH	110	30 / 42
4	2	2	AcOH	130	28 / 49
5	2	2	AcOH/H_2O (1:1)	110	21 / 0
6	2	2	AcOH/H_2O (1:1)	130	35 / 2
7[b]	2	2	AcOH/H_2O (1:1)	130	77 / 4
8[c]	2	2	AcOH/H_2O (1:1)	130	15 / 35
9	1	2	AcOH/H_2O (1:1)	130	22 / 29
10[d]	5	2	AcOH/H_2O (1:1)	130	73 / 3

Reactions were run overnight. [a]Yields by ^{1}H NMR spectroscopy with trimethoxybenzene as internal standard [b]Reaction time was 60 h. [c]Palladium acetate 2 mol%. [d]Palladium acetate 25 mol%.

After optimization, control experiments were done to confirm that in the absence of palladium or iodobenzene (**2a**), the reaction did not occur (Table 3, entries 1 and 3). Meanwhile, it was highlighted that the reaction can proceed in the absence of silver (Table 3, entry 2), although in this case, stoichiometric amounts of palladium are needed (Table 3, entry 4).

Table 3. Control experiments of the reaction.

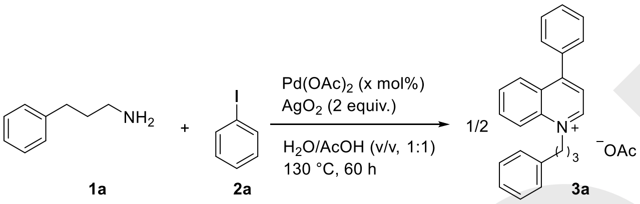

Entry	$Pd(OAc)_2$ (mol%)	Ag_2O (equiv.)	**2a** (equiv.)	Yields (%)[a]
1	0	2	2	0
2	10	0	2	7
3	10	2	0	0
4	100	0	2	42

Conditions: AcOH/H_2O (v/v = 1:1), 130 °C, 60 h. [a]Yields by ^{1}H NMR spectroscopy with trimethoxybenzene as internal standard.

Korr

II.4 Scope

II.4.1 Substrate scope:

For the study of the synthetic scope, 3-aryl propylamines were prepared as follows. Starting from aldehydes **7a-7d**, the corresponding acrylonitriles **9a-9e** were prepared by Horner–Wadsworth–Emmons reactions. For the reduction of the double bond and CN group in **9a-9e** to alkyl amines **10a-10e**, several conditions were proven to be unsuccessful. Only Raney Nickel, utilizing flow reactor at high pressure and temperature was able to provide the product without degradation. However, to avoid formation of secondary or tertiary amines, ammonia was added (Table 4).

Table 4. Synthesis of propyl amines.

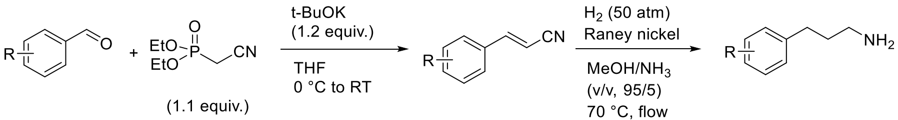

6b-6f **7** **8b-8f** **1b-1f**

Entry	R	**1** (%)[a]
1	4-CH_3 (**1b**)	75
2	4-F (**1c**)	68
3	4-Cl (**1d**)	72
4	4-OMe (**1e**)	65
5	2,6-F (**1f**)	71

[a]Yields of isolated products.

II.4.2 Scope of the reaction

First the reaction between arylated amines **1a-1e** and iodoaryls **2a-2i** was investigated under the optimized conditions (Table 5). When both substrates had the same substitution pattern on the corresponding benzene rings, the products were formed as single isomers (Table 5, entries 1-3) in yields varying from moderate to good, and where fully characterized after isolation. When the substituents on the amine and iodoaryl partners are different, multiple products are obtained in a non-separable mixture. None of the isomers from these mixtures were isolated, and the ratio of the different isomers for each mixture was determined by ^{1}H and ^{19}F NMR, when possible. In the case of *para* substitutions on the iodoaryls, only two isomers are formed (Table 5, entries 5, 7-10), in yields ranging from 31 to 72%. No selectivity was observed, and the method tends to yield equal amounts of both products. With *ortho* substituted iodobenzene derivatives **2e** and **2i**, three isomers were obtained (Table 5, entries 6 and 11). The ratios are, in the case of **3aia-3aic**, not equivalent for all of them (1:6:4).

Table 5. Scope of the reaction.

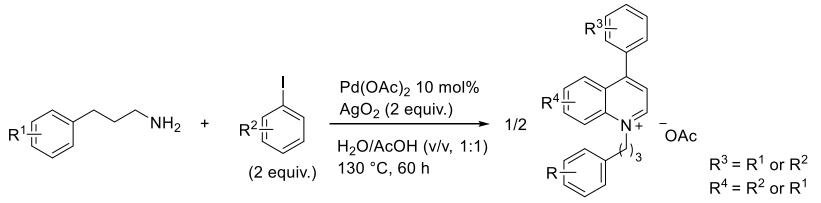
R1
NH2
+
I
R2
(2 equiv.)
Pd(OAc)2 10 mol%
AgO2 (2 equiv.)
H2O/AcOH (v/v, 1:1)
130 °C, 60 h
1/2
R3
R4
N+
−OAc
3
R
R3 = R1 or R2
R4 = R2 or R1

Entry	Amine (**1a**-**1e**)	Iodoaryl (**2**)	Product	Yields (%)^{a}
1	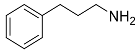 **1a**	**2a**	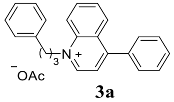 **3a**	55 (77)
2	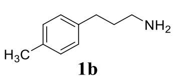 **1b**	4-CH$_3$ (**2b**)	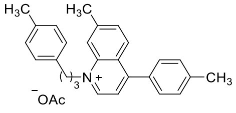 **3bb**	45 (52)
3	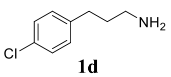 **1d**	4-Cl (**2c**)	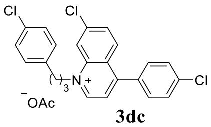 **3dc**	0 (48)
4	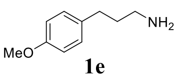 **1e**	4-OMe (**2d**)	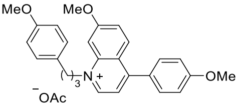 **3ed**	29 (40)
5	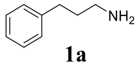 **1a**	4-CH$_3$ (**2b**)	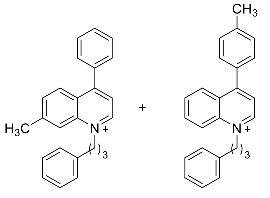 **3ba** 1:4.3 **3bb**	72 (88)
6	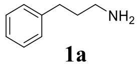 **1a**	3-CH$_3$ (**5e**)	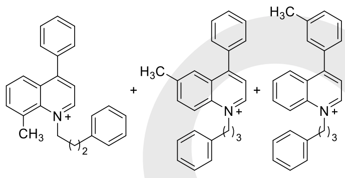 **3aea** **3aeb** **3aec**	47 (65)
7	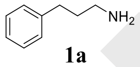 **1a**	4-F (**2f**)	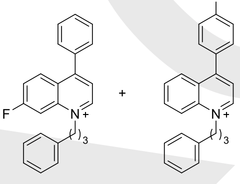 **3afa** 1:1.2 **3afb**	54 (61)

8	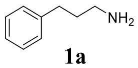 **1a**	4-Cl (**2c**)	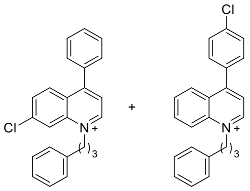 **3aca** **3acb**	43 (54)
9	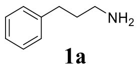 **1a**	4-Br (**2g**)	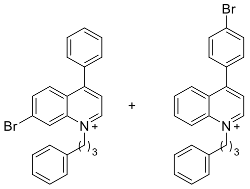 **3aga** **3agb**	39 (48)
10	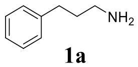 **1a**	4-CF_3 (**2h**)	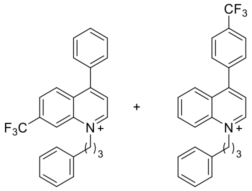 **3aha** 1:1.2 **3ahb**	31 (38)
11	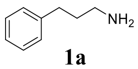 **1a**	3-CF_3 (**2i**)	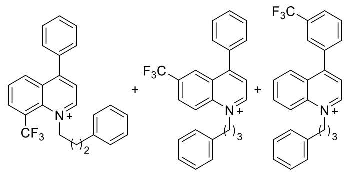 **3aia** **3aib** **3aic** 1:6:4	26 (34)

a) Isolated yields (NMR yields with trimethoxybenzene as internal standard). Ratio was determined by ^{1}H or ^{19}F NMR spectroscopy, if possible.

II.4.3 Propylamine as substrate:

Propylamine (**9**) is a challenging substrate towards C–H activation.[85] However, to our surprise, our conditions can be applied to this simple aliphatic amine to afford the quinolinium adducts by introduction of two equivalents of the aryl iodides (**2a**). As only one single aryl iodide is used in this reaction, the two aryl units introduced in the molecule will be the same on each part of the quinolinium core (Table 6). The yields are significantly lower than previously noted in Tables 4 and 5, ranging now from 16% to 38%. The drawback is counterbalanced by the easiness of using propylamine as substrate, instead of the synthetically more complex phenyl propylamines. Noteworthy, the method allows to functionalize the otherwise very unreactive propylamine (**9**). Also, the increase in complexity from **9** to the final quinolinium product structures in a single reaction is remarkable (Table 6).

Table 6. Synthesis of quinolonium structures from propylamine **9**.

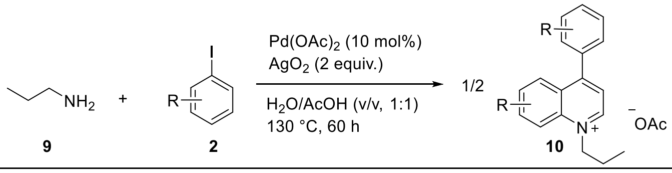
NH$_2$
9
+
R
I
2
Pd(OAc)$_2$ (10 mol%)
AgO$_2$ (2 equiv.)
H$_2$O/AcOH (v/v, 1:1)
130 °C, 60 h
1/2
R
R
N+
⁻OAc
10

Entry	Aryl iodide (R')	Quinolonium	Yields (%)[a]
1	**2a**	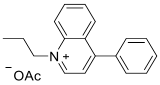 **10a**	32 (38)
2	4-CH$_3$ (**2b**)	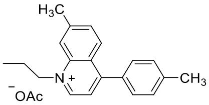 **10b**	38 (43)
3	4-Cl (**2c**)	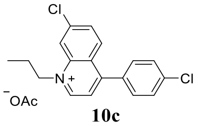 **10c**	16 (23)
4	3-CH$_3$ (**2h**)	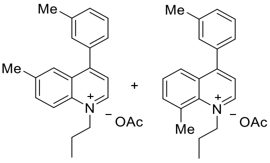	0 (39)

[a] Isolated yields. In parenthesis yields determined by ^{1}H NMR spectroscopy with trimethoxybenzene as internal standard.

Korr

II.5 Mechanistic investigation

For the investigation of the mechanism, the initial literature search suggested a reaction based on multiple Pd-catalyzed activations of C_{sp^3}–H and C_{sp^2}–H bonds. We, thus, hypothesized the participation of a number of singular steps in the mechanism, in an unknown order. These steps were the double arylation of propylamine, C_{sp^2}–H activation and C_{sp^2}–N bond formation on one of the aromatic rings, a cyclization, and a final oxidation of the product to yield the quinolinium form. Based on this assumption, questions remained about the sequence of the different steps. A simple experiment was conducted to know if the amination/cyclization and oxidation can proceed on 3,3-diphenylpropylamine **13**. The product, **14**, was obtained with 43% yield (Scheme 18).

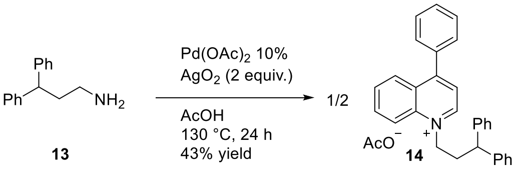

Scheme 18. Reaction from 3,3-diphenylpropylamine **26** as the starting material.

Note that the reaction was conducted in the absence of aryl iodide. Thus, the reaction with iodine containing reagents, like a Hofmann-type elimination was discarded as potential elementary step. In addition, an order for the different steps can be proposed for the case of the propylamine, starting with a double arylation via C_{sp^3}–H activations The reaction needs a directing group, a role that the amine can hardly play, since amines can strongly bind palladium, inhibiting any further reaction.[86] Alternatively, the oxidation of the primary amine to imine by palladium can occur at the outset of the reaction, offering a better directing group for the reaction.

Following our hypothesis, the mechanism in Scheme 19 can be proposed, starting with the oxidation of the amine by the palladium acetate. Then, the first C–H activation occurs, followed by classical oxidative addition/reductive elimination of iodobenzene with Pd^{II}/Pd^{IV} catalytic cycle. The recent literature is in agreement with the possibility of forming Pd^{IV} complex by oxidative addition. Gaunt and co-workers successfully isolated a palladacycle intermediate after oxidative additions.[87,88] Starting from 3-phenylpropylimine, a second identical catalytic cycle could occur. Then, a C_{sp^2}–H activation can follow to complete the first amination of the aromatic ring. When the Aryl-N intermediate is formed, a cyclization to the heterocycle might take place, accompanied by the elimination of ammonia. Finally, the product is obtained after oxidation by palladium of the 3,4-hydroquinolinium to the quaternary quinolinium salt.

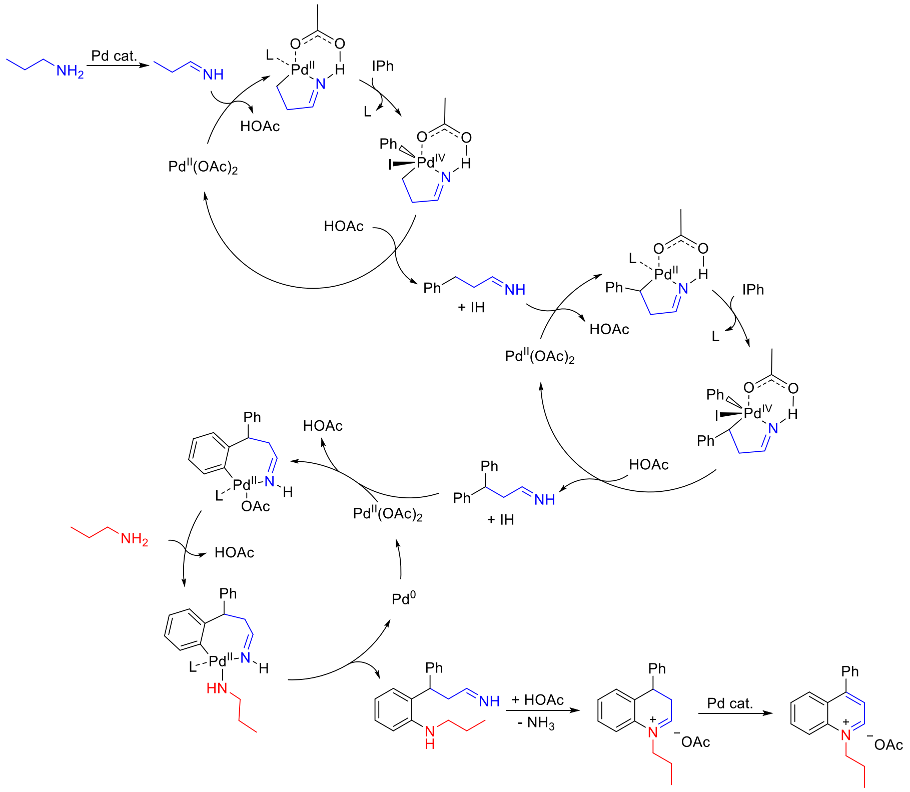

Scheme 19. Proposed mechanism for the reaction.

The different parts of the proposed mechanism were studied by DFT,[89–92] using B97D/6-311g**+SDD (Pd and I) for geometry optimization and M06/DEF2TZVPP for the energy refinements.[93] The final free energies were the result of the thermal correction from B97D/6-311g**/SDD added to the electronic energy from the single point refinement with M06/DEF2TZVPP. As the reaction also works with the palladium complex alone, in dry acetic acid, this solvent has been used for the calculations, and therefore silver was not considered.

The oxidation study starts with the coordination of the palladium to the amine and formation of an N-Pd bond by H transfer to one of the acetates (**I** to **II**), with a downhill energy of -14.4 kcal/mol (Figure 10). Then, the amine / imine transformation occurs through a classical β-hydride elimination reaction, like in **TS1**, with an overall activation energy of 10.2 kcal/mol. If the reference for the energy is the complex **II** (obtained from IRC calculation of the TS), the energy barrier is 24.6 kcal/mol. The energies involved in this transformation, are reasonable and in agreement with the temperature of the experimental conditions. The formation of the imine is uphill from the amide N-Pd complex, but favourable from the separate reactants (amine + Pd(OAc)$_2$), showing an energy of -6.5 kcal/mol for **III**, a complex that evolves by release of the free imine, Pd(0) and two molecules of acetic acid.

The ability of the amine in **I** to function as directing group for the C-H activation was also computed. From **I** to **TS1'**, an activation of 11.0 kcal/mol was found for the C-H cleavage, 1.0 kcal/mol higher than the oxidation step in **TS1**, and therefore, the amine oxidation to imine is slightly favoured. In any case, these data do not allow us to completely discard that the C-H activation occurs first, followed by the amine/imine oxidation. On the other hand, Pd(0) is formed at the end of Figure 1, which has to be re-oxidized to Pd(II) to continue the process.

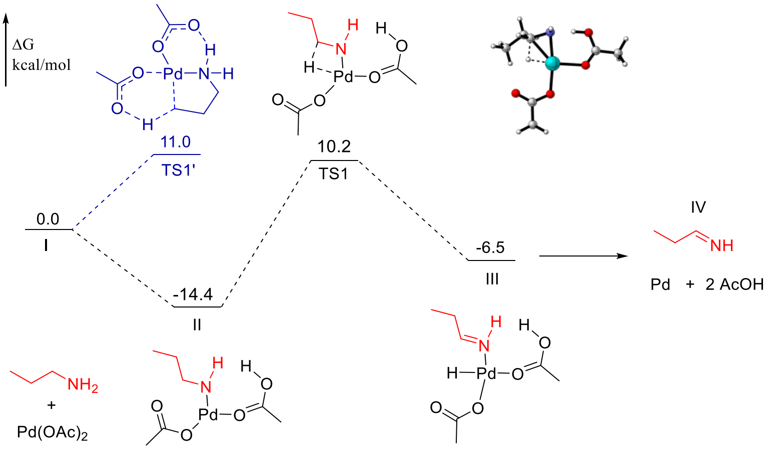

Figure 10. Energetic profile of the oxidation transformation and comparison with amine as directing group of the C-H activation.

Next, the previously formed propylimine coordinates with Pd(OAc)$_2$ in **V**. As this complex is in a different oxidation state from the final adducts in Figure 10, we took **V** as relative G=0 to study the next steps of the reaction. From complex **V**, the following elementary step is the C–H activation in position 3 of the propyl chain, promoted by one of the acetate ligands (Figure 11). The computed energy for **TS2** is 8.7 kcal/mol higher than the palladacycle, while the product **VI** is at –10.0 kcal/mol. After a slight decrease of energy due to the ligand exchange and acetate release from **VI** to **VII**, the oxidative addition to PhI happens with a barrier of 17.4 kcal/mol, affording Pd(IV) complex **VIII**. Then, an easy reductive elimination was computed in **TS4** with only 5.5 kcal/mol over **VIII** kcal/mol activation barrier to provide the formation of the Ph-C bond. Propylimine **IX** is favoured compared to the starting materials, being at an energy of -34.1 kcal/mol.

Kor

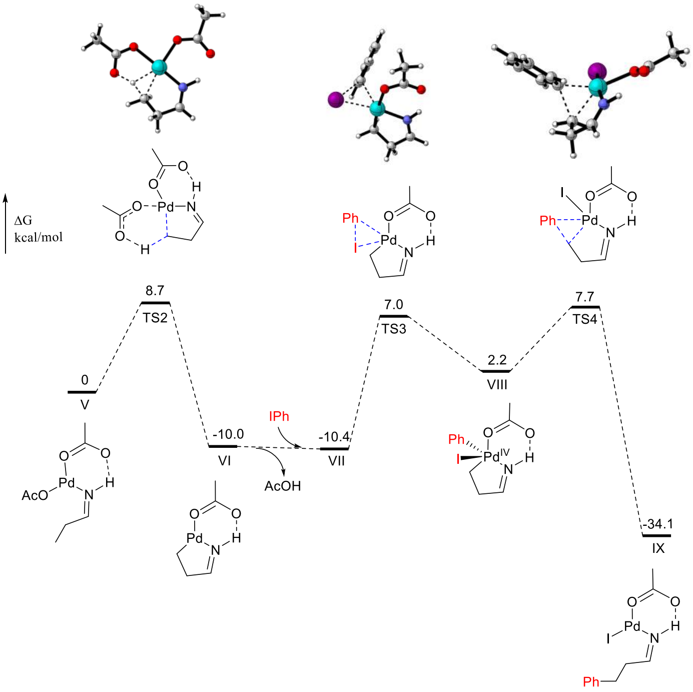
ΔG
kcal/mol
8.7
TS2
0
V
-10.0
VI
IPh
AcOH
-10.4
VII
7.0
TS3
2.2
VIII
7.7
TS4
-34.1
IX
AcO
Pd
Pd^{IV}
Ph
I

Figure 11. DFT computed energy profile of the arylation of propylamine.

Korr

We also studied the feasibility of a second C-H activation and formation of another Ph-C bond in the same position (Figure 12). This step is especially important in the case of substrate **1a**, which already contains a phenyl group, as in **IX**, and must be able to incorporate the second one. Initially, the iodide present in **IX** must be replaced by an acetate ligand. Acetic acid and/or eventually silver salts can participate in this anion exchange, which is difficult to be accurately described. In any case, complex **X** is prone to suffer a similar process as mentioned before for **V**, and in principle Figures 12 and 11 should show similar results. The main difference related to the absence/presence of the phenyl group at C-3 is the general increase of the activation energies due to the larger steric hindrance. For example, the barrier for the C-H activation is quite larger in the presence of the phenyl group (19.3 kcal/mol in **TS5** *vs* 8.7 kcal/mol in **TS2**). A similar trend occurs also during the oxidative addition to PhI (30.0 kcal/mol in **TS6** *vs* 17.4 kcal/mol in **TS3**), and for the final reductive elimination (10.0 kcal/mol in **TS7** *vs* 5.5 kcal/mol in **TS4**). However, the overall pictures stays unaltered, pointing to the oxidative addition to form the Pd(IV) complex as the slowest step.

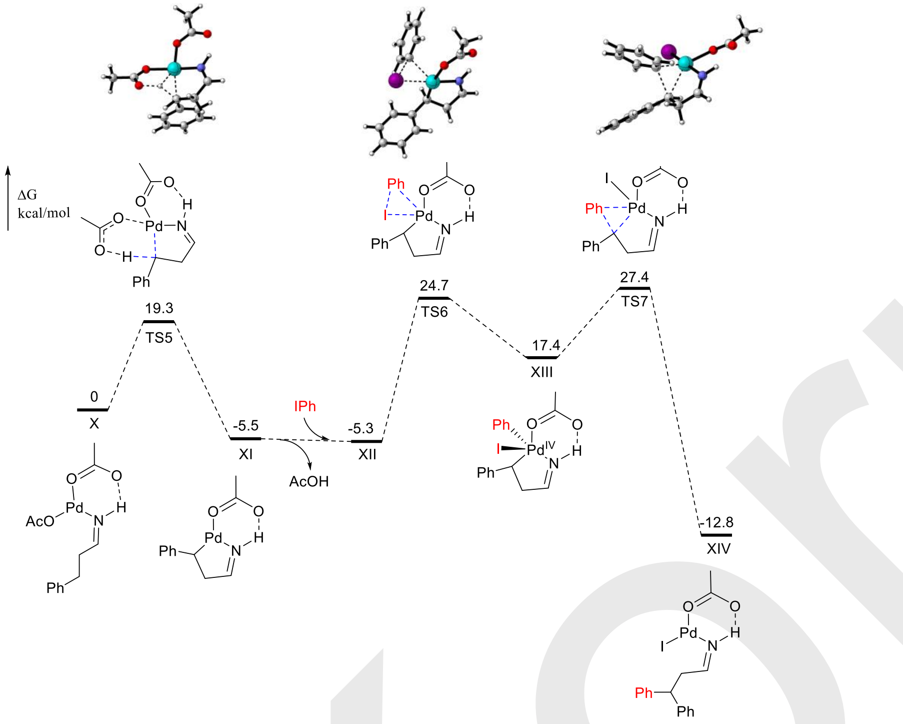

Figure 12. DFT computed energy profile of the arylation of 3-phenyl substituted substrate.

The last steps of the mechanism were also assessed, although we could not locate all structures involved, because of the existing uncertainties about the coordination pattern around palladium in most species. However, we can offer some hints about a few individual steps that might happen to complete the process. For example, after formation of a **XV**-type complex, one of the aromatic rings has to be activated by palladium through a C-H cleavage / Ar-Pd bond formation, like in **TS8** (Figure 13). Our calculation shows that this process is completely feasible, spite the fact that the resulting complex **XVI** is a 7-membered ring palladacycle. Later, the formation of an amide-Pd bond in **XVII** might trigger a Buchwald-Hartwig aryl amination. The computed transition state **TS9** presents a low energy value, leading to an amine-imine adduct **XVIII**, which contains all the atoms and disposition needed for the formation of the final adducts. The hypothetical sequence could probably occur through cyclization to **XIX** and aromatization of **XX**, steps which do not really need the aid of palladium.

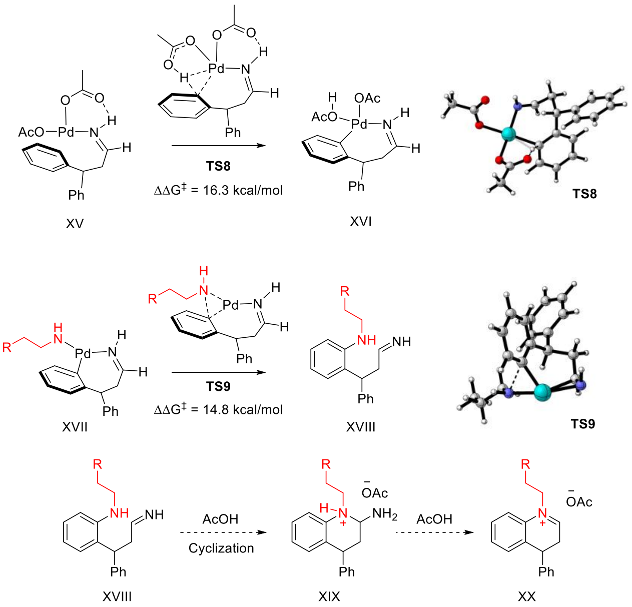

Figure 13. Last steps of the reaction, including calculated aryl CH-activation and aryl amination

Overall, the computed energies for the steps of the process are compatible with the temperature of the reaction, usually at 130 °C. All energies are below 30 kcal/mol, with the maximum at the oxidative addition of **XII** in **TS6**. Noteworthy, we did not locate any intermediate with a significantly lower energy than the rest, and thus, none of them represent a global minimum in the energy surface that could be experimentally isolable.

Those DFT results can explained that the formation of **4** is not observed, as the amine is oxidized to imine quickly. On the other hand, the imine becomes a good directing group for further transformations.

These calculations offer one of the possible pathways that explains some of the experimental observations, and at least shed some light on part of the transition states and intermediates that take place in this intricate transformation. Obviously, more experimental evidence is needed to confirm the different parts of the mechanism. The necessity of the acetic acid as solvent is not fully explained. KIE measurements on deuterated propylamine could confirm that C–H activation is not the rate limiting step. Since two equivalents of amine are needed to complete the reaction, a well designed experiment with ^{15}N labelled amines could be useful to ascertain the amine source of the quinolinium nitrogen. Also, the role of the silver is not taken into account in these mechanistic studies. A recent work[94] shows the important role of the metal for the C–H activation, therefore, investigation of potential ease of the reaction by silver is interesting.[44]

Korr

II.6 Conclusion

In this chapter, a successful and innovative synthesis of quartenary quinolinium salts from propylamines and its derivates is reported, catalyzed by palladium acetate. Aryl-proylamines have been transformed into the desired products, with moderate to good yields. Moreover, the method can be used with propylamine, in a process that involves the activation of two aliphatic C–H bonds.

The mechanism for the reaction has been studied by computational means, and compared with the experimental results and literature precedents. In the case of propylamine, the proposed mechanism starts with the oxidation to imine, then a double C_{sp^3}–H activation/arylation. Then a C_{sp^2}–H bond is activated, followed by a C–N bond formation. The intermediate is cyclized and oxidized to yield the final products.

The interests of the method are, the possibility offered to form quinolines scaffold from simple starting material and to have multiple C–H activations, and creating multiple C–C bonds and a C–N bond, in a single reaction.

Korr

III NHC-catalyzed synthesis of propargylic esters with CO_2 capture (Paper II)

III.1 Introduction

Propargylic esters are present in wide range of compounds. From intermediates for total synthesis of natural products, Diphylin, Justicine B or Tawainin C,[95] to bioactive compounds such as Oxybutynin for the treatment of bladder cancer.[96] Their synthesis can be achieved *via* the esterification of the corresponding carboxylic acid,[97,98] which needs to be prepared before. The group of Prof. Vougioukalakis developed the methodology for the synthesis of the propargylic esters, and the experimental results used for the DFT studies were performed by his group. They reported a method that uses commercially available starting materials and CO_2 for a one-step synthesis of propargylic esters. Because CO_2 is one of the major greenhouse gases and at the same time a cheap and safe reagent, methods using CO_2 as reagent have in general a great interest economically and for the society. A similar reaction to this work has been developed, showing the interest for new routes of synthesis using CO_2.[99]

In the recent literature of CO_2 fixation on terminal alkyls, organocatalyzed by NHC, two methods of synthesis were reported by two different groups.

The first one, by Liu *et al.*,[100] were able to react terminal alkynes with CO2 to form the propargyl carboxylic acid. Then, the treatment with HCl in the presence of alkyl halides led to the corresponding esters.The reaction is carried ut at 60ºC in DMSO, catalyzed by in situ generated NHC (Scheme 20). The mechanism proposed is similar to our proposal[101] and rely on the formation of the NHC-CO_2 adduct.

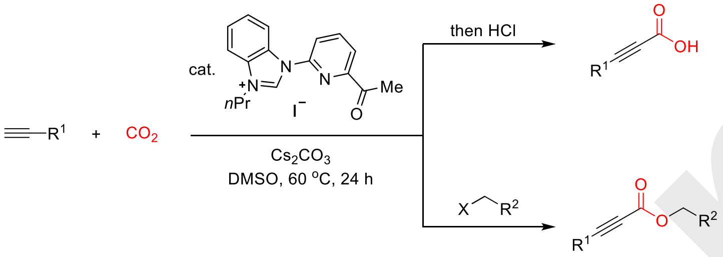

Scheme 20. Synthesis of propargylic acid and esters catalyzed by NHC.

Korr

III.2 Experimental results and scope of the reaction

For the synthesis of propargylic esters, three common reagents are involved: terminal alkynes (**15**), allylic chlorides (**16**) and CO_2. The reaction is catalyzed by NHC **18** (Scheme 21). The experimental results presented in this section (II.2) have been performed by the group of Prof. Vougioukalakis.

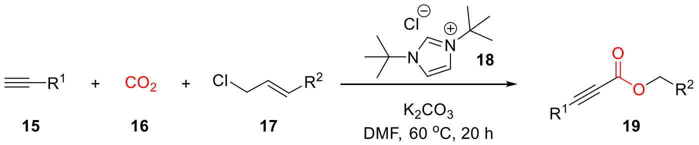

Scheme 21. Three-component reaction for the synthesis of propargylic esters.

After optimization of the reaction conditions, the substrate scope was extended. Aromatic propargylic reagents, with different substituents on the aromatic ring, gave good results (Scheme 22). It was also possible to use different allylic chloride reagents, with various functional groups, such as ester, cinnamyl, benzyl, carbonate or even olefins (Scheme 22). On the other hand, when using 2-picolyl chloride the expected product was not formed (**19m**).

Korr

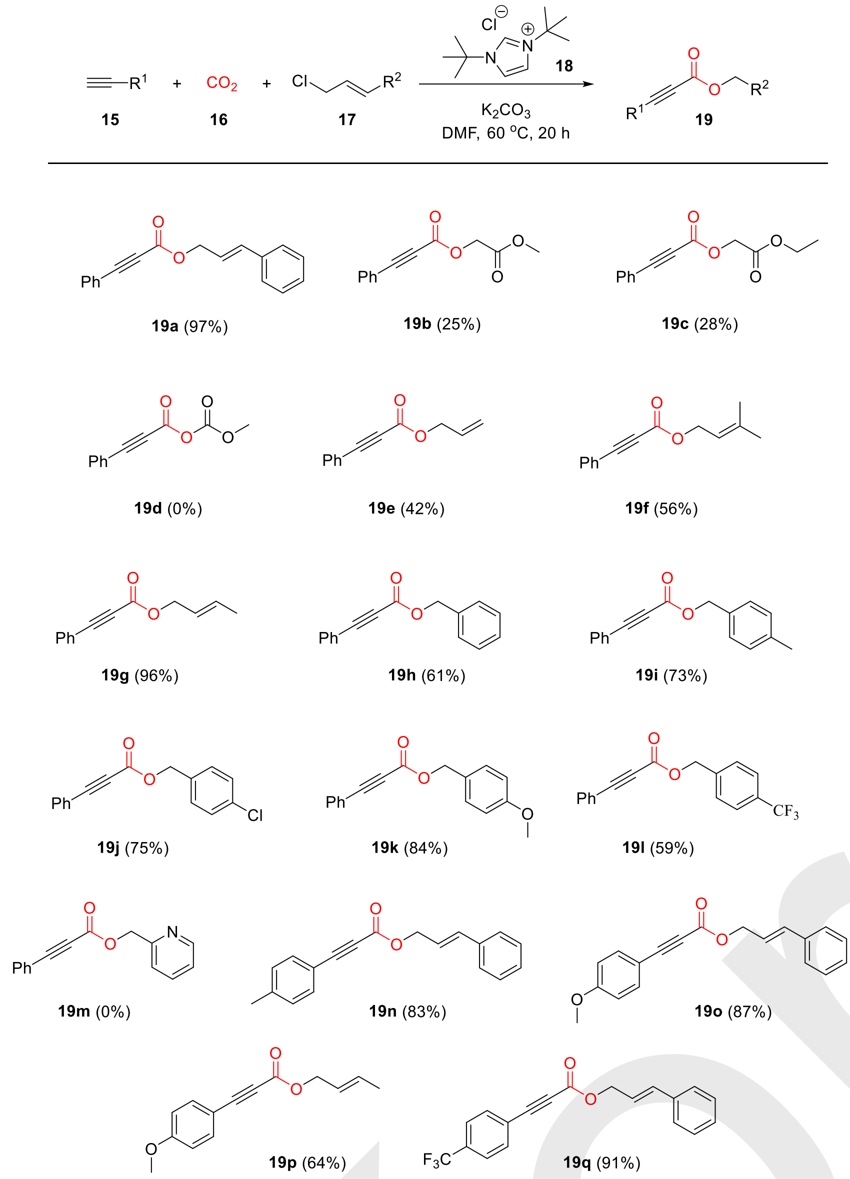
15
16
17
18
19
K2CO3
DMF, 60 °C, 20 h
19a (97%)
19b (25%)
19c (28%)
19d (0%)
19e (42%)
19f (56%)
19g (96%)
19h (61%)
19i (73%)
19j (75%)
19k (84%)
19l (59%)
19m (0%)
19n (83%)
19o (87%)
19p (64%)
19q (91%)

Scheme 22. Scope and limitations of the reaction studied by the group of Prof. Vougioukalakis.

III.3 Mechanistic studies

III.3.1 Proposed mechanism

First, we wanted to identify the rate limiting step of the reaction. Second, we wanted to understand the reactivity trend. In particular, the goal was to understand why aromatic allylic halides (i.e. **17h - 17l**) were active substrates, whilst picolyl chloride **17m** did not react under the reaction conditions (Scheme 22).

Tentatively, a mechanism was proposed, consisting of an initial attack of the NHC catalyst to CO_2. Then, the zwitterionic intermediate formed (**21**) reacts with the allylic chloride (**17a**) through an S_N2 reaction yielding **22**. Next, the deprotonated propargylic moiety (**15a**) reacts with **22** through an addition-elimination mechanism, releasing the NHC catalyst and producing the final ester **19a** (Scheme 23).

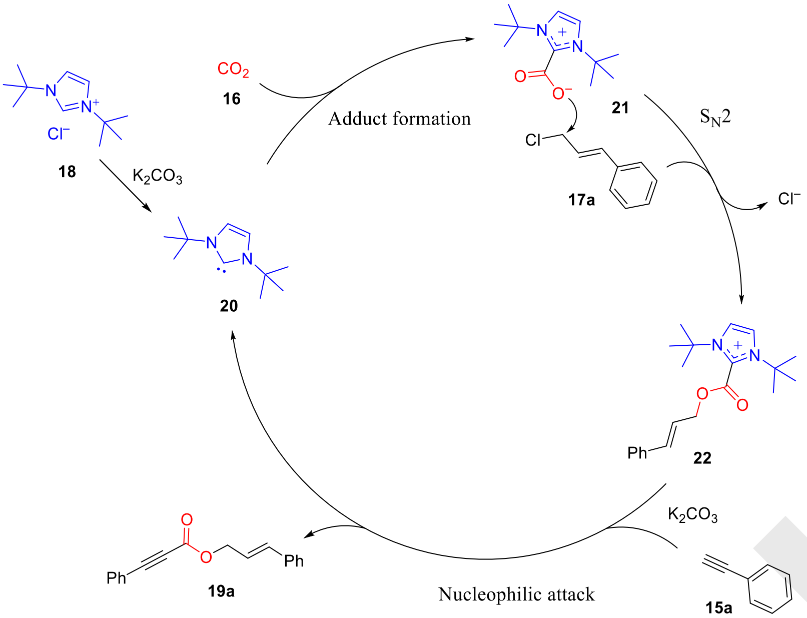

Scheme 23. Proposed mechanism.

III.3.2 Methodology for computational investigations

We used DFT methods to confirm or discard the previously shown mechanism, to identify the possible rate-determining step and to explain the different reactivity of certain chloride substrates. As a model of the reaction, the most reactive substrates, cinnamyl chloride and phenyl acetylene (**17a** and **15a**, respectively), were selected. The calculations were done using Gaussian 16, with M06-2X[102] for the functional and 6-311G(s,p)[103] as the basis sets for the geometry optimization and energies.[104] The solvent model used is IEFPCM with DMF.

III.3.3 Results and discussion

As first step of the proposed mechanism, we investigated the attack of the NHC catalyst to CO_2. An activation energy of 10.9 kcal/mol was found for **TS1** (Figure 14). This low value shows that the first reaction is an easy step and agrees with previous results.[105] The intermediate obtained (**II**) is stable due to its low energy (−2.7 kcal/mol). As the energy of the NHC−CO_2 complex is lower than that of the two reagents (**I** and CO_2), it is possible to isolate it. This is why the intermediate is already reported and is involved in different NHC-catalyzed reactions as a catalyst precursor.[106] The next step is the S_N2 reaction between **II** and allylic chloride **30a**. The computed energy of activation for this step was $\Delta\Delta G^‡ = 22.1$ kcal/mol. Even if this step is more energy demanding, it is affordable at the experimental conditions. The 3D structure of **TS2** shows a typical S_N2 nucleophilic attack (Figure 16). The step yields a more stable intermediate (**III**, −4.2 kcal/mol). Then, the deprotonated alkyne attacks the carbonyl group in **III** (**TS3**, $\Delta\Delta G^‡ =$ 20.9 kcal/mol). A fairly stable tetrahedral intermediate is formed (**IV**), quickly followed by the release of the NHC catalyst, yielding the product **19a** (**TS4**, $\Delta\Delta G^‡ = 5.1$ kcal/mol).

From this point, we have a global view of the energy profile of the reaction. We can highlight that the rate-limiting step is the nucleophilic substitution (**TS2**) of the chloride by the NHC–CO_2 adduct. And, as there are significant differences of reactivity concerning the electrophile, we next focused our attention on this transition state to explain those differences.

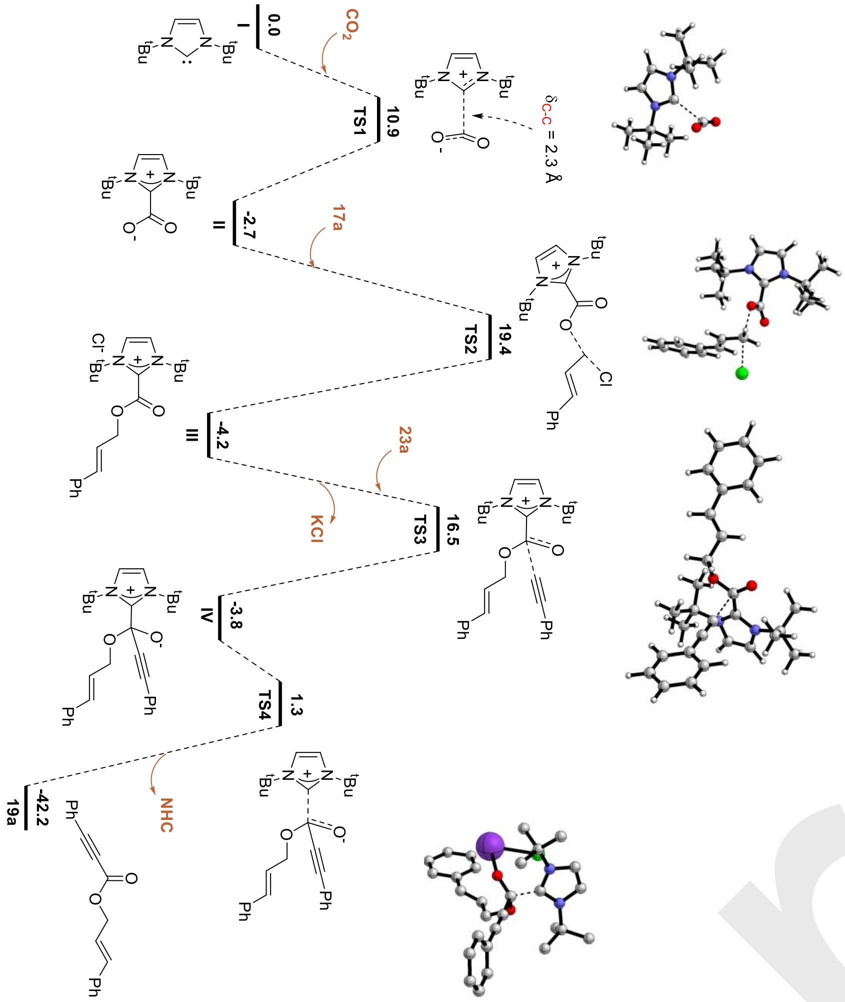

Figure 14. Energy pathway for the reaction.

We were able to locate the transition state for the problematic chlorides, which are benzyl chloride (**17h**) due to its low reactivity, and 2-picolyl chloride (**17m**) for its complete absence of reactivity. The energy of activation of **TS2** in the model reaction (from cinnamyl chloride, **17a**) is $\Delta\Delta G^{\ddagger} = 22.1$ kcal/mol, and was set as the reference for the study. In the case of benzyl chloride (**17h**, 61% yield), we obtained an energy of 23.0 kcal/mol for the corresponding **TS2**. From the Eyring equation, with transmission coefficient set to 1 and a temperature of 333.15 K, we can calculate the half-life times of both intermediates and compare them. For the cinnamyl chloride, we obtained a half-life time of 26.5 s, and for benzyl chloride, of 121.8 s. Those values can give an approximation to the difference of reactivity between the two substrates (97% vs 61%). In the case of the 2-picolyl chloride, **17m**, we obtained an activation energy of 24.7 kcal/mol for the corresponding **TS2-mi**, indicating a half-life time of 25 min. The difference with the previous compounds is significant, but it is not able to explain an absolute absence of reactivity for this substrate. We thought that other factors associated with the pyridine moiety itself could play a crucial inhibiting role in the reaction. To further check this hypothesis experimentally, a control reaction was carried out. Pyridine (1 equiv.) was added to the reaction mixture with cinnamyl chloride (**17h**) and **15a** as substrates, applying the same reaction conditions as before. The expected product was not detected; thus, pyridine inhibits the reaction.

From the three different **TS2** previously found, we can also look at the bond distances. The C−O bonds lengths of the TSs from **17a**, **17h** and **17m** are 2.09 Å, 2.04 Å and 2.00 Å, respectively. And the C−Cl are 2.44 Å, 2.38 Å and 2.34 Å, respectively (Figure 15). Thus, the reactivity increases with increasing bond lengths in the TSs. It seems that the carbon has to be as electropositive as possible, according to the difference between **17k** (84%) and **17i** (59%): The formation of product with pyridine moiety could not be achieved. The calculated energy for the **TS2-m** suggests that the time of reaction should be longer compare to others substrate. But this higher energy level does not correspond with the absence of product, 24.7 kcal/mol of energy of activation is compatible with the experimental conditions.

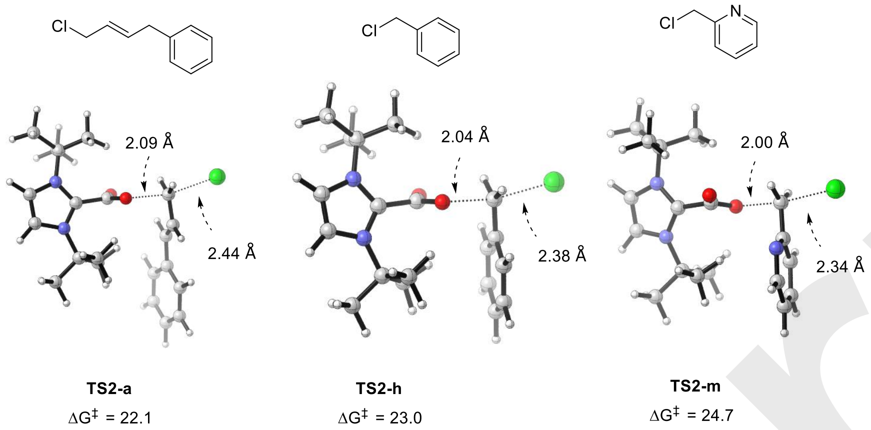

TS2-a $\Delta G^{\ddagger} = 22.1$

TS2-h $\Delta G^{\ddagger} = 23.0$

TS2-m $\Delta G^{\ddagger} = 24.7$

Figure 15. Comparison of energies in kcal/mol with different chains for **TS2**.

III.4 Conclusion

The mechanism of a novel organocatalytic protocol for the multicomponent carboxylative coupling of terminal alkynes with organochlorides and CO_2, catalyzed by an *in situ* generated NHC was studied in collaboration with the group of Prof. Vougioukalakis. The DFT calculations on the mechanism of this transformation indicate that the reaction is initiated with the addition of the carbene to a molecule of CO_2, forming an NHC-carboxylate. This species is nucleophilic enough to react with chlorides, even though the high activation energy of this step suggests that it is the rate-limiting step. This fact explains well the large difference in reactivity of the different allyl and benzyl chlorides and the effect of the substituents. The reaction with substrates with a pyridine moiety could not be formed, which is due to the pyridine acting as inhibitor of the reaction.

Kor

IV Reaction of Catalytic Enols with Nucleophiles (Paper III)

IV.1 Introduction

Functionalization of the Cα of carbonyl moieties using electrophiles is well-known. Ketones can tautomerize to enols or form enolate ions in the presence of base, and then behave as nucleophiles. If the ketone has two enolizable positions that are similar electronically and sterically, both Cα can be functionalized upon reaction with electrophiles (Scheme 24a). To avoid formation of regioisomeric α-functionalized carbonyl compounds, an alternative is to use allylic alcohols as starting materials, and combine a 1,3-hydrogen shift mediated by transition metal catalysts with a functionalization reaction using electrophilic reagents. This approach has been used by us[107–110] and others[111,112] (Scheme 24b). The reaction relies on the formation of enol(ate) intermediates after the isomerization (1,3-hydrogen shift) of the allylic alcohol. This type of reactivity allows the regiospecific formation of α–substituted ketones, and avoids the use of a strong base.

The functionalization of enols or enolates with nucleophiles requires to apply umpolung strategies. Different approaches can be used, employing for example Lewis acid,[113] transition metals[114] or, as in the method developed here, hypervalent iodine reagents.[108,115–118]

In this chapter our work on the use of an umpolung strategy in the stereospecific transformation of allylic alcohols into α-functionalized carbonyl compounds is presented. The electrophilic reagents have been exchanged by nucleophilic ones, (i.e. MeOH). The umpolung is achieved by performing the reaction in the presence of a hypervalent iodine reagent (**24**) (Scheme 24c).[117]

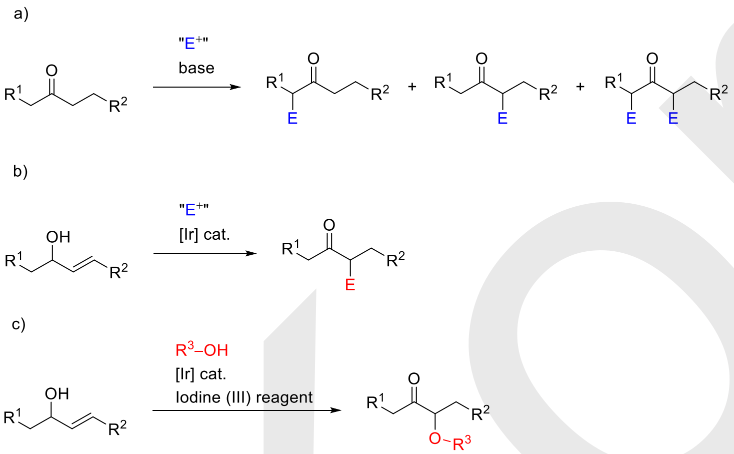

Scheme 24. "E+" = electrophile, a) Classical method for α-functionalization of ketones. b) Regiospecific reaction of allylic alcohols with electrophiles catalyzed by iridium. c) This work: umpolung approach for the synthesis of α-functionalized carbonyls upon reaction of allylic alcohols with nucleophiles.

A recent methodology was developed by Kielf and Gulder,[119] for α-functionalization by nucleophiles of α-pyridyl-ketones with hypervalent reagent. With the same umpolung strategy, they succeeded to form, regioselectively, C–O, C–N and C–S bonds with no enol ether pre-formation needed. The selectivity is driven by the pyridyl group, coordinating weakly but sufficiently with iodine atom. Therefore, the nucleophile reacts only on one side of the ketone (Scheme 25).

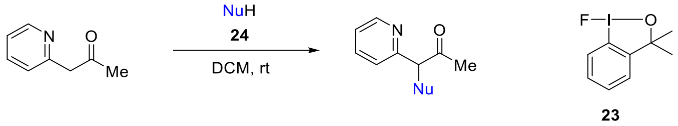

Scheme 25. Functionalization of pyridyl ketone with hypervalent iodine.

IV.2 Experimental results and scope of the reaction

The experimental protocol uses the iridium dimer [Cp*IrCl$_2$]$_2$ as the catalysts for the isomerization of the allylic alcohol. A small excess of the hypervalent iodine reagent **23** is needed (1.2 equiv.), to provide good yields. Importantly, the yields were improved in the presence of 80 mol% of KBF$_4$ as an additive. Methanol is one of the solvents in the mixture used (TFE, 1:3, TFE/MeOH v/v), as well as being the source of the methoxy group (nucleophile). The best yields were obtained at 35 °C.

The method was successfully applied to a wide range of allylic alcohols (Scheme 26). First, allylic alcohols with terminal double bonds gave moderate to quantitative yields of methoxy ketones **25a**-**25h**. The reaction afforded the products without any detectable byproduct when the allylic alcohols contained functional groups such as nitrile, ketone, halogen, or even azide (**25e**-**25h**). It was possible to obtain the ethoxy product using ethanol as the solvent (**25b**), although in lower yields. Allylic alcohols with internal double bonds also afforded the corresponding α-methoxy ketones (**25i**-**25l**) in good yields, ranging from 60 to 79%.

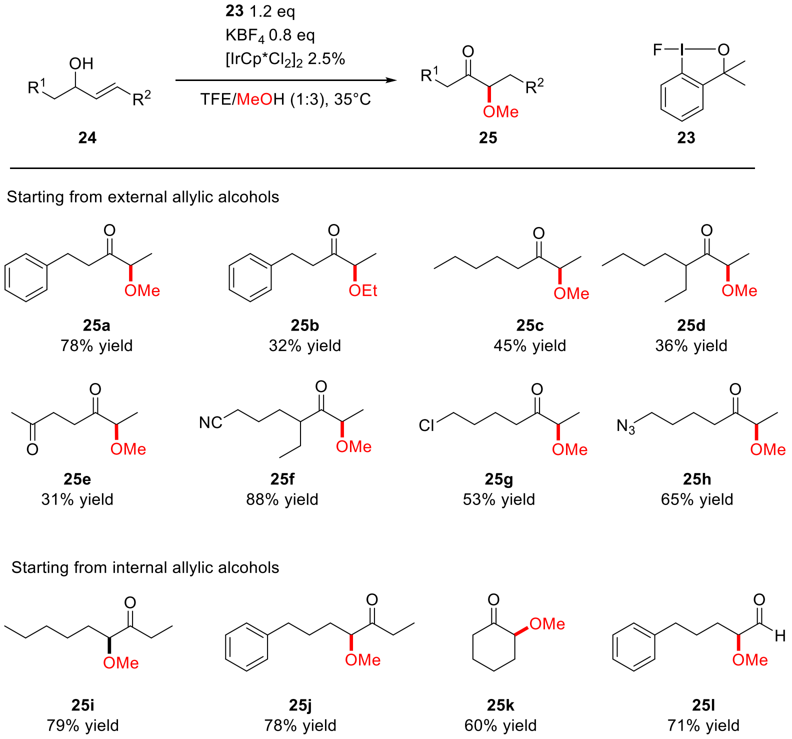
23 1.2 eq
KBF4 0.8 eq
[IrCp*Cl2]2 2.5%
TFE/MeOH (1:3), 35°C
24
25
23
Starting from external allylic alcohols
25a
78% yield
25b
32% yield
25c
45% yield
25d
36% yield
25e
31% yield
25f
88% yield
25g
53% yield
25h
65% yield
Starting from internal allylic alcohols
25i
79% yield
25j
78% yield
25k
60% yield
25l
71% yield

Scheme 26. Scope for the synthesis of α-methoxy ketones from allylic alcohols.Isolated yields*

For the case of allylic alcohol with a ketone in γ position, different products were obtained. The reaction yielded five membered-rings, 3-furanones, **27a-27c** in yields ranging from 46% to 91%. Interestingly, 5-amino-3-furanone **27d** was obtained from the corresponding amide.

---

*Experimental results were obtained by Dr. A. Sanz-Marco and Dr. S. Martinez-Erro.

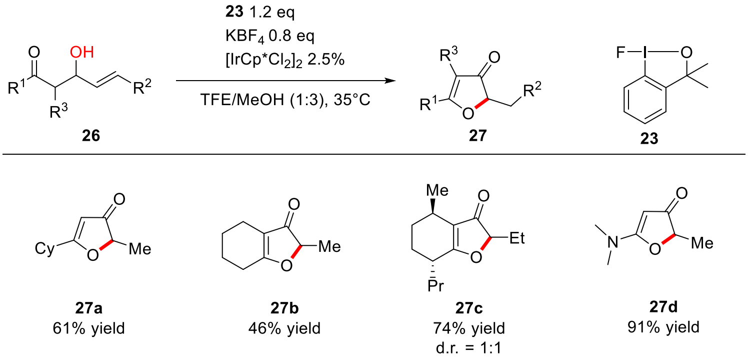

Scheme 27. Scope of the reaction affording 3-furanones.[*]

IV.3 Mechanistic studies

IV.3.1 Method and model selection

To study the mechanism we performed DFT calculations with the help of Gaussian 16 software suit and with M06[102] as functional and 6-31G(d,p)[120] as basis set (SDD for I).[121,122] Different mechanistic pathways were considered. First, we considered a mechanism occurring in two independent stages; first the iridium-mediated isomerization of the allylic alcohol to an enol or enolate, followed by its reaction with the hypervalent iodine reagent **23** and methanol, to yield the product. A more complex mechanism, where all parts (iridium complex, iodine(III) reagent **23** and MeOH) react in a concerted fashion could also be envisioned. The second proposal was evaluated, but the energies obtained were much higher than those expected from the experimental conditions.

An experiment with an isolated silyl enolate reacting under the same conditions of the method yielded the expected product. This result points in the direction of the first mechanism considered. In addition, the possible presence of radical intermediates was tested with radical scavengers such as TEMPO or 2-diphenylethylene and product **27a** was obtained in high yields. Thus, the reaction does not seem to pass through radical intermediates.

From these results, we can hypothesize that the isomerization by iridium and the reaction of the resulting enolate with iodine(III) reagent **23** and methanol are two independent parts of the mechanism. We focused our study here on the second part of the reaction. The mechanism of the isomerization of the allylic alcohol catalyzed by iridium has been in studied in detail by our group recently.[123] The mechanism goes through complex multiple steps, starting with coordination, followed by oxidation of the alcohol, and insertion of an iridium hydride to form an iridium enolate moiety.

---

[*] Experimental results were obtained by Dr. A. Sanz-Marco and Dr. S. Martinez-Erro.

IV.3.2 Intermolecular reactivity mechanism

First, we investigated the mechanism of the reaction using MeOH as the nucleophile (i.e. the intermolecular reaction). The proposed mechanism (Scheme 28) starts with the reaction of enolate **A** and the iodine(III) species **23** to form an enolonium intermediate (**B**). This one reacts with MeOH to render intermediate **C**. A reductive ligand coupling forms the final product **28**. A transition state (**TS1**) was found, showing an activation energy of 16.2 kcal/mol, which is a value that fits well with the experimental conditions.

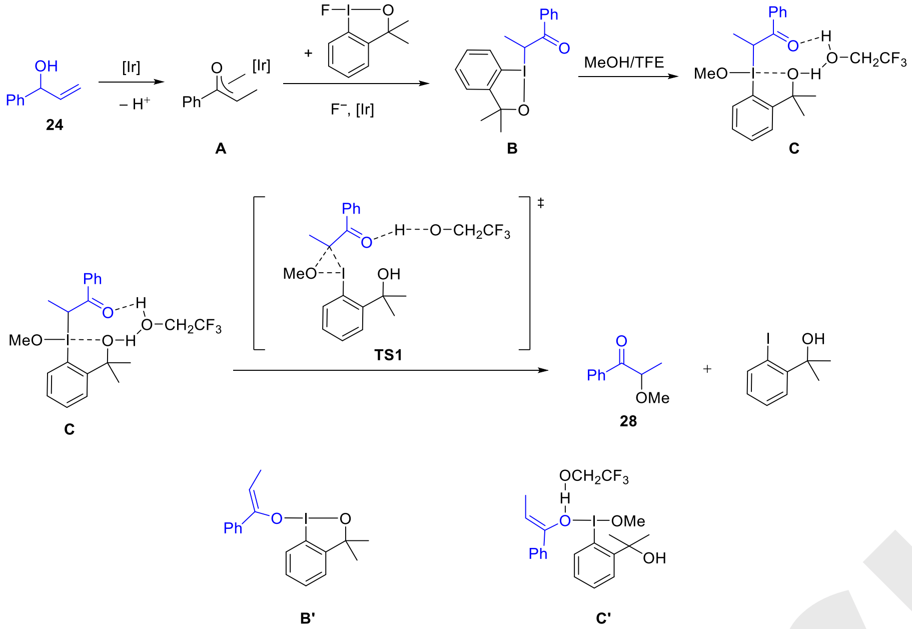

Scheme 28. Proposed mechanism for intermolecular reactivity.

During the calculations, we hypothesized that the addition of a molecule of TFE would activate the carbonyl group of the enolonium through hydrogen bonding. Without this molecule of TFE, the TS1' had an activation energy of 21.8 kcal/mol. These findings illustrate the positive effect of TFE by reducing the electron density of intermediate **C**, what facilitates the ligand coupling. A model with two molecules of TFE was also computed, affording higher activation energy (20 kcal/mol). This effect can be explained by a less significant reduction of the electron density of the complex by the second TFE molecule and an increase of the entropic effect as the structure contains multiple "free" molecules.

Different tautomers have been considered, like the enolonium **B'** and **C'** with I-O bonding. Similar enoloniums have been considered before in the reaction of enolates with non-cyclic iodine(III) reagents.[115] Both structures have significantly higher energies than those of **B** and **C**. Specifically, $\Delta G = 14.1$ kcal/mol higher for **B'** compared to **B**, and $\Delta G = 5.3$ kcal/mol higher for **C'** compared to **C**. A TS starting from **C'** could not be found. For those reasons, **B'** and **C'** have not been considered as possible intermediates of the reaction (Scheme 29).

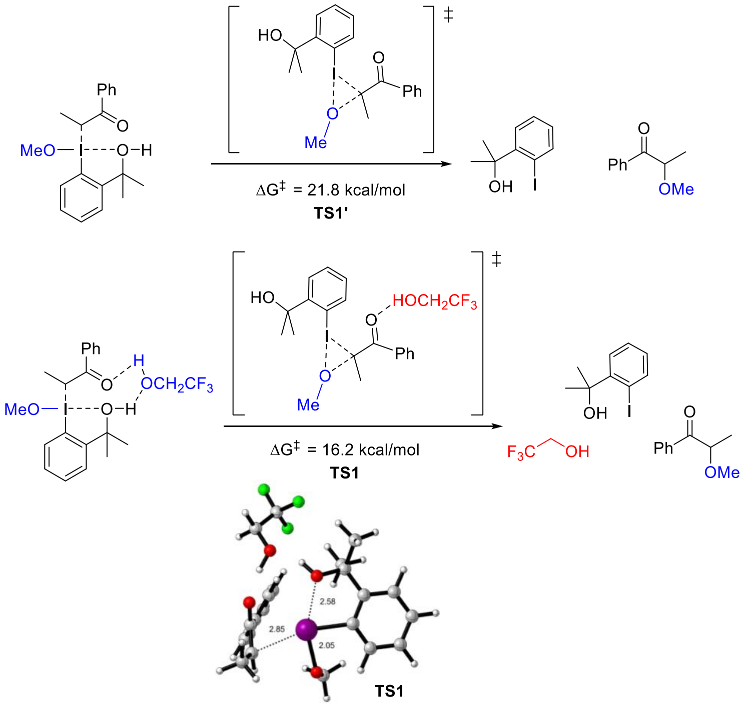
‡
HO
O
Ph
O
Me
Ph
MeO
O–H
OH
I
Ph
O
OMe
ΔG‡ = 21.8 kcal/mol
TS1'
‡
HO
HOCH2CF3
O
Ph
O
Me
Ph
H
O
OCH2CF3
MeO
O–H
OH
I
F3C
OH
Ph
O
OMe
ΔG‡ = 16.2 kcal/mol
TS1
2.58
2.85
2.05
TS1

Scheme 29. Proposed mechanism for intermolecular reactivity

IV.3.3 Intramolecular reactivity mechanism

We then turned our attention to the mechanism of the intramolecular reaction, where the nucleophile is the oxygen of a carbonyl or of a carboxylic acid derivative. Similar to the previous part, enolonium **D** renders the most stable species (**E**, $\Delta G^{\ddagger} = -11.7$ kcal/mol, Scheme 30). This intramolecular rearrangement corresponds to a nucleophilic-addition/tautomerization. As in the intermolecular reaction, the product is obtained *via* a reductive ligand coupling. The energy of activation of **TS2** is 8.0 kcal/mol, resulting in a much faster reaction than the intermolecular reaction.

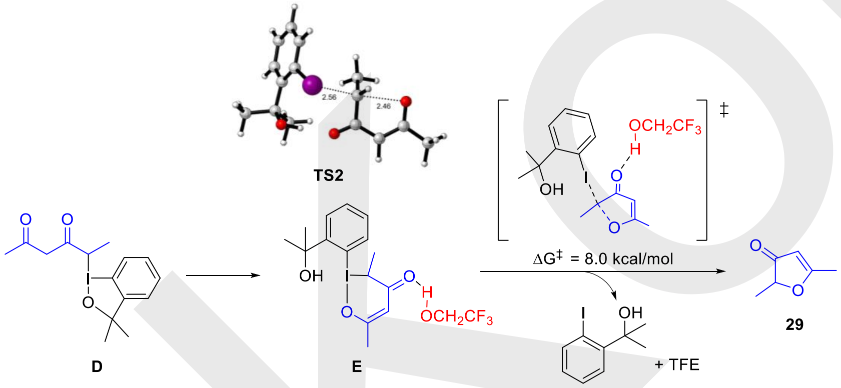
2.56
2.46
TS2
‡
OCH2CF3
H
O
OH
I
O
O
O
O
I
O
D
OH
I
O
O
H
OCH2CF3
E
ΔG‡ = 8.0 kcal/mol
I
OH
+ TFE
O
O
29

Scheme 30. Proposed mechanism for intramolecular reactivity.

IV.3.4 Competitive reactions

In order to explain why only the cyclic product was obtained when both reactions can happen, we computed both TSs for the same substrate. In the case of the first reaction, with the molecule of methanol reacting, the energy of activation is $\Delta G^{‡} = 18.3$ kcal/mol (**TS3**). In addition, for the cyclization, only $\Delta G^{‡} = 8$ kcal/mol were predicted (**TS2**). With a difference of 10 Kcal/mol, we can easily explain the absence of the product derived from the intermolecular reaction with MeOH.

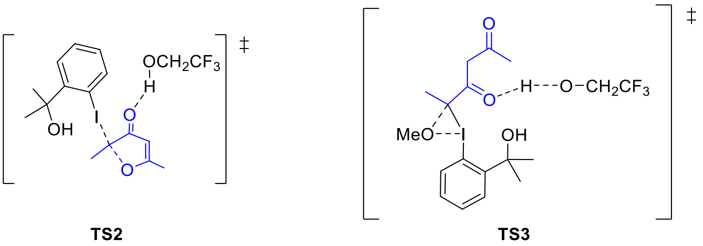

Scheme 31. Key elementary steps for competitive reactions from carbonyl-functionalized allylic alcohols.

IV.4 Conclusion

The mechanism for the synthesis of α-methoxyketones and of 3(2*H*)-furanones from allylic alcohols has been studied by computational means. The iridium catalyst seems to be involved only in the isomerization of the allylic alcohol. The resulting enolate reacts then with the hypervalent iodine reagent. The key step is a ligand coupling, promoted by trifluormethyl ethanol, which allows the formation of a new C–O bond *via* an overall umpolung strategy. Further, we have also concluded that the selectivity of the reaction resulting in formation of 3(2*H*)-furanones as sole products from carbonyl-functionalized allylic alcohols is due to a lower activation energy for the cyclization step than that of the alternative intermolecular reaction with the solvent MeOH.

Kor

V Theoretical study of manganese-catalyzed synthesis of propargylamines (Paper IV)

V.1 Introduction

Propargylamines are common building blocks for the synthesis of N-containing organic molecules.[124] The fact that propargylamines contain multiple functional group allows to use a variety of synthetic tools to transform them. Examples include the synthesis of different heterocycles, such as pyridine,[125] quinoline,[126] hydroquinoline or even oxazolidinones.[127] For example, Yu and coworkers,[126] reported the synthesis of hydroquinolines from *N*-substituted propargyl amines and aldehyde acetals mediated by iron halides salts (Scheme 32a).[126]

The triple bond in propargyl amines can undergo click reactions upon reaction with azides.[128] Cai and coworkers developed a multicomponent one-pot reaction to quickly generate numerous bioactives compounds from a set of azides (Scheme 32b). They used first a metal free triazole synthesis from azide, ketene and the propargylanime, with DBU as base, follow by a classical, copper catalyzed click reaction with a second azide.

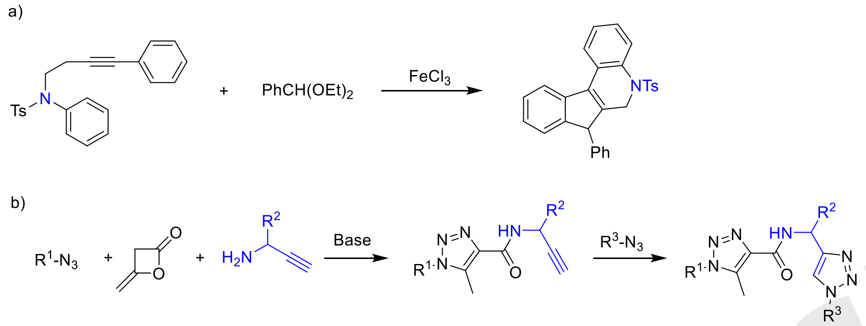

Scheme 32. a) Hydroquinoline synthesis from propargylamine. b) Sequential triazoles formation with propargylamines as intermediate.

Chiral propargylamines can be used for the synthesis of optically active compounds. Innocenti and co-workers used enantioenriched propargylamines to synthetize bicyclic compounds as a single diastereoisomer through a cobalt-mediated Pauson-Khand reaction (Scheme 33).[129]

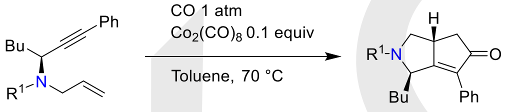

Scheme 33. Pauson-Khand reaction from chiral propargylamines.

In this chapter, the KA^2 reaction has been mediated by manganese catalysts.[130] As an abundant metal, the development of new catalytic methods mediated by manganese are of interest to the industry.[131] Manganese complexes has been used to catalyzed C–H activation reactions with concomitant C–C bond formations,[132] cross-coupling reactions[133] or hydrogenation.[134]

V.2 Scope of reaction

The KA^2 reaction studied in this chapter was experimentally developed by our collaborators, the group of Prof. Vougioukalakis.[101] In this reaction, primary or secondary amines (**30**), terminal alkynes (**31**), and ketones (**29**) are reacted using manganese bromide as catalyst. The reactions are run neat, at 130 °C for 20 h (Scheme 34).

Cyclic amines such as piperidine **30a**, pyrroline **30b**, morpholine **30d** or nornicotine **30i** gave the corresponding propargyl amines (**32a**, **32b**, **32d**, **32i)** in excellent yields. With the latter amine, **32i** was obtained as a single diastereoisomer. In addition, aliphatic, primary or secondary amines afforded their corresponding products, **32g** and **32h**, respectively, in good yields. Regarding the scope of the ketones (**29**), cyclopentanone, cyclohexanone and cycloheptanone could be used successfully, as well as non-cyclic aliphatic ketones. Phenylacetylene derivatives were used in all instances. The reaction was not successful when using 1,2-cyclohexanedione nor with benzophenone.

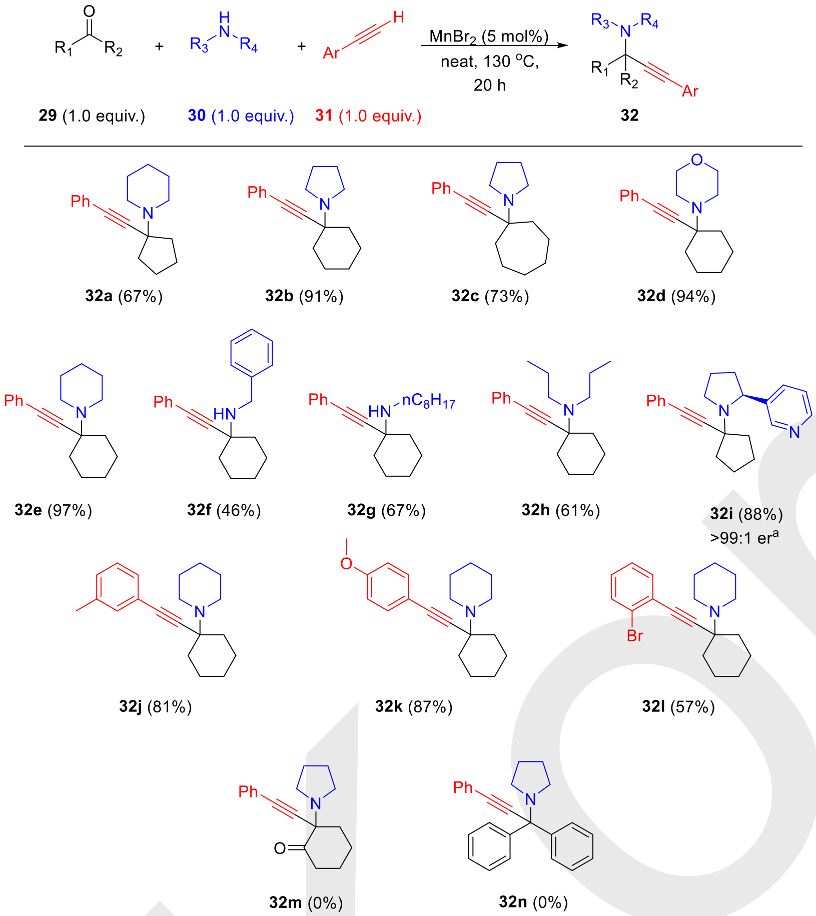

29 (1.0 equiv.)
30 (1.0 equiv.)
31 (1.0 equiv.)
MnBr$_2$ (5 mol%)
neat, 130 °C,
20 h
32
32a (67%)
32b (91%)
32c (73%)
32d (94%)
32e (97%)
32f (46%)
32g (67%)
32h (61%)
32i (88%)
>99:1 er[a]
32j (81%)
32k (87%)
32l (57%)
32m (0%)
32n (0%)

Scheme 34. Scope of the MnBr$_2$-catalyzed KA^2 coupling. [a] enantiomeric ratio determined by ^{1}H NMR spectroscopy.

V.3 Mechanism study

Lee and co-workers proposed a mechanism for the A^3 reaction that we took as the starting point for the mechanistic investigations of the KA^2 coupling.[135] We selected cyclohexyl amine (**30e**), phenyl acetylene (**31e**) and cyclohexanone (**29e**) as the reagents. Condensation of **30e** with **29e** forms iminium **III**. In parallel, acetylene **31e** is deprotonated *in situ by* piperidine **30e**, with the assistance of the manganese salt **I**, forming Mn phenyl acetylide **II**. This intermediate reacts then with iminium **III** affording propargylic amine **32e**, and releasing $MnBr_2$ (Scheme 35).

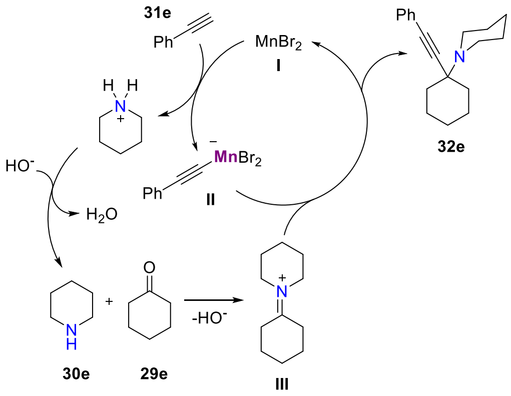

Scheme 35. Proposed mechanism for the KA^2 reaction catalyzed by $MnBr_2$.

There only exist a few computational studies on the mechanism KA^2 reactions.[56] We therefore started the DFT calculations on the model substrates. The experimental reaction is performed in neat conditions, and as solvation is important for accurate calculations, cyclohexanone was used for solvation model for the DFT studies. Since iminium salts can be formed at temperatures lower than 130 °C, their formation was not calculated. We used the B97-D functional for the structure optimizations, together with the 6-31G(d,p) basis sets for all the atoms.

At first, we noticed that the manganese species involved in the catalytic reaction were lower in energy at quartet state instead of doublet state, with an average difference of 10 kcal/mol. This means that the metal complex holds three unpaired electrons during the reaction pathway. As the proposal for the mechanism, phenylacetylene is first deprotonated by a base, being the strongest one in the system piperidine. The triple bond coordinates to $MnBr_2$, leading to an increase acidity of the acetylenic proton. This proton is then removed by piperidine (**30e**), yielding to an ionic pair. The product was found less stable that the starting materials (4.2 kcal/mol higher). This means that the concentration of this species is low in the reaction media (Figure 16a).

The second part of the mechanism is the formation of the imminium salt **III**, by reaction of the ketone and the amine. **III** reacts then with the manganese phenyl acetylide (**II**), generating the product. The energy involved in the transition state, **TS1**, is 23.9 kcal/mol. This energy needs to be added to the energy of the previous complex, leading to a transition state at 28.9 kcal/mol, a reasonable number taking into account the experimental conditions, i.e. a temperature of 130 °C. The product consists then of the expected product (**32e**) coordinated to manganese. The energy of this complex is –1.7

kcal/mol compared to that of the starting materials. Thus, the reaction is driven by the stability of this final compound (**IV**, Figure 16b).

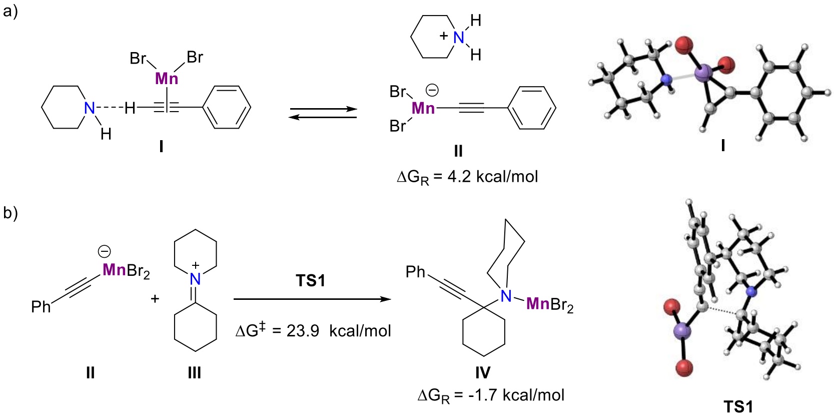

Figure 16. DFT results for: a) the deprotonation of the acetylene, b) Nucleophilic attack of the manganese complex onto the ketamine.

V.4 Conclusion

The mechanism of a manganese-catalyzed KA^2 coupling has been investigated by DFT. It was shown that upon coordination of $MnBr_2$ to the terminal alkyne substrate, a facile deprotonation takes place, forming an anionic manganese phenylacetylide complex. This species reacts with the iminium species. The moderate activation energy of the C–C bond-forming step, together with the low concentration of the manganese phenylacetylide makes this step rate-limiting, and agrees with the need for high temperatures in the experiments. With appropriate ligands on Mn that enables stabilization of the generated anionic Mn acetylide species, its concentration may be increased, which may result in reasonable reaction rates at lower temperatures.

Kor

VI Concluding remarks

The work presently reported in this thesis has the aim of studying new methods of C–C, C–N and C–O bond formations. The experimental and mechanistic aspects of those methods have been investigated with a focus on the utilization of DFT tools.

In the first project, the readily available propylamine and its derivatives demonstrated their capacity to be transformed into quaternary quinolinium salts by a multicomponent process. This reaction, catalyzed by palladium salts, allows to access substituted quinolinium salts in just one step, with a specific substitution pattern. The mechanism proposed for the reaction involves multiple C–H activations, and formation of two new C–C and one C–N bond, in a single transformation.

The second project concerns the study of the mechanism for the NHC-catalyzed formation of propargylic esters from terminal alkynes, allylic chlorides and CO_2. We could propose a mechanism for this new reaction by DFT calculations, consisting on an initial formation of an NHC/CO_2 adduct. Then, this adduct reacts with the allylic chloride reagent, to form an ester as intermediate, before the formation of the product by nucleophilic attack of the alkyne. The experimental limitations found in the scope of the reaction were also investigated.

In the third chapter, the mechanism of an umpolung reaction was studied. The transformation consists on the reaction of catalytic enolates with alcohol nucleophiles. The mechanism through which the final product is formed from the enolate was investigated, which occurs *via* enolonium intermediates. These species render the final products through a reductive elimination. Our studies also explain the selectivity obtained when there exist two competing nucleophiles.

In the last project, the mechanism of a multicomponent reaction for the synthesis of propargylamines was computationally studied by DFT. A mechanism was proposed, which indicates how the reaction may be improved in future experimental investigations.

Korr

Appendix A. Author contribution:

PAPER I:
-Bibliography search of existing reactions, literature of C–H activation of aliphatic amine.
-All experimental results
-Bibliography search of existing mechanisms, optimal basis set and functional.
-All computational results
-Wrote the article
- Wrote the supporting information.

PAPER II:
-Bibliography search of existing mechanisms, optimal basis set and functional.
-Computation of the intermediates and transition states with DFT.
-Wrote the mechanistic part of the paper,
-Wrote of the supporting information for DFT part.

PAPER III:
-Bibliography search of existing mechanisms, optimal basis set and functional.
-Proposition of different models, computation of the intermediates and transition states with DFT.
-Wrote the DFT part of the paper,
- Wrote the supporting information for DFT part.

PAPER IV:
-Bibliography search of existing mechanisms, optimal basis set and functional.
-Proposition of different models, computation of the intermediates and transition states with DFT.
-Wrote the DFT part of the paper,
- Wrote the supporting information for DFT part.

Korr

Acknowledgements

I want to thank here, Professor Enrique Gomez and Professor Belén Martín-Matute, for giving me the opportunity to work on so many interesting projects. Allowing me to discover the world of research with autonomy and support, sharing your knowledge and advices with me in every steps of the PhD program. To make all this project possible even with all the problems faced.

I would like to express my thanks to Professor Kálmán J Szabó and to Víctor García Vázquez for reading this thesis and giving appreciated feedback.

I would like to thanks all my co-workers from the Catmec project, Alba, Giovanna, Victor, Larry and Kenji, for all those great moments. Also the other members of the project, Professor Joseph Harrity and Dr Jennifer Dick.

I want to thank people from Cambrex, Ingrid and Anders for making possible my stay in your team, Lars for being a perfect mentor and all the co-workers who made my stay even better.

Thank you to all people from the UPV, Maite, Lia, Paula, Itziar, Maialen, Arkaitz, Markos and Iñaki for sharing the lab, the nice moments and the good foods from Basque Country. Thank you to all the rest of the people from the 4th floor. I especially thank Nico for all those moments of joy shared inside and outside of the lab. I thank also Marine for we gave to each other during those years.

I thank all the actual and past members of the department of organic chemistry at the University of Stockholm (merci Marie! Notre petit bout de France en Suède). Many thanks to Alba, Amparo, Víctor, Molleti, Sergio, Aitor and Samuel for your help.

Merci papa pour toutes ces années ou tu m’as accompagné et soutenue. De m’avoir poussé et encouragé à aller aussi loin tout en me conseillant de faire ce que j’aime. Tu ne comprendra surement pas la moitier de ce qu’il y dans cette these mais rien n’aurait été possible sans toi et je te dois le plus rand des merci!

Merci Math pour ton soutien durant toutes mes études, d’avoir présent et toujours savoir me faire rire.

Merci Odile et Alix pour votre soutien, tous ces moments tous esembles qui font un bien fou a chacuns de mes passages en France.

Merci Mel, Pilou, Penta, Tofu, Kumquat, Calie, Ben, Boidin, Leny, pour tes ces bons moments ensemble!

Merci a tout le discord du Vortex.

References

1. *IUPAC Compendium of Chemical Terminology*. *IUPAC Compendium of Chemical Terminology* (IUPAC, 2009). doi:10.1351/goldbook.
2. Hagen, J. Homogeneous Catalysis with Transition Metal Catalysts. in *Industrial Catalysis* 17–46 (Wiley-VCH Verlag GmbH & Co. KGaA, 2015).
3. Xu, C., Shen, X. & Hoveyda, A. H. In Situ Methylene Capping: A General Strategy for Efficient Stereoretentive Catalytic Olefin Metathesis. the Concept, Methodological Implications, and Applications to Synthesis of Biologically Active Compounds. *J. Am. Chem. Soc.* **139**, 10919–10928 (2017).
4. List, B. Introduction: Organocatalysis. *Chem. Rev.* **107**, 5413–5415 (2007).
5. Zacuto, M. J. Synthesis of Acrylamides via the Doebner-Knoevenagel Condensation. *J. Org. Chem.* **84**, 6465–6474 (2019).
6. Fioravanti, S., Pellacani, L., Tardella, P. A. & Vergari, M. C. Facile and highly stereoselective one-pot synthesis of either (E)- or (Z)-nitro alkenes. *Org. Lett.* **10**, 1449–1451 (2008).
7. Heck, K. F. & Nolley, J. P. Palladium-Catalyzed Vinylic Hydrogen Substitution Reactions with Aryl, Benzyl, and Styryl Halides. *J. Org. Chem.* **37**, 2320–2322 (1972).
8. Miyaura, N., Yamada, K. & Suzuki, A. A new stereospecific cross-coupling by the palladium-catalyzed reaction of 1-alkenylboranes with 1-alkenyl or 1-alkynyl halides. *Tetrahedron Lett.* **20**, 3437–3440 (1979).
9. Guram, A. S., Rennels, R. A. & Buchwald, S. L. A Simple Catalytic Method for the Conversion of Aryl Bromides to Arylamines. *Angew. Chem. Int. Ed.* **34**, 1348–1350 (1995).
10. Arduengo, A. J., Harlow, R. L. & Kline, M. Additions and Corrections: A Stable Crystalline Carbene. *J. Am. Chem. Soc.* **113**, 2801 (1991).
11. Arduengo, A. J., Dias, H. V. R., Harlow, R. L. & Kline, M. Electronic Stabilization of Nucleophilic Carbenes. *J. Am. Chem. Soc.* **114**, 5530–5534 (1992).
12. Sohn, S. S. & Bode, J. W. Catalytic generation of activated carboxylates from enals: A product-determining role for the base. *Org. Lett.* **7**, 3873–3876 (2005).
13. Breslow, R. On the Mechanism of Thiamine Action. IV. Evidence from Studies on Model Systems. *J. Am. Chem. Soc.* **80**, 3719–3726 (1958).
14. Santra, S., Porey, A., Jana, B. & Guin, J. N-Heterocyclic carbenes as chiral Brønsted base catalysts: a highly diastereo- and enantioselective 1,6-addition reaction. *Chem. Sci.* **9**, 6446–6450 (2018).
15. Benhamou, L., Chardon, E., Lavigne, G., Bellemin-Laponnaz, S. & César, V. Synthetic routes to N-heterocyclic carbene precursors. *Chem. Rev.* **111**, 2705–2733 (2011).
16. Janssen-Müller, D., Schlepphorst, C. & Glorius, F. Privileged chiral N-heterocyclic carbene ligands for asymmetric transition-metal catalysis. *Chem. Soc. Rev.* **46**, 4845–4854 (2017).
17. Menon, R. S., Biju, A. T. & Nair, V. Recent advances in N-heterocyclic carbene (NHC)-catalysed benzoin reactions. *Beilstein J. Org. Chem.* **12**, 444–461 (2016).
18. Agrawal, S., Martínez-Castro, E., Marcos, R. & Martín-Matute, B. Readily available ruthenium complex for efficient dynamic kinetic resolution of aromatic α-hydroxy ketones. *Org. Lett.* **16**, 2256–2259 (2014).
19. Flanigan, D. M., Romanov-Michailidis, F., White, N. A. & Rovis, T. Organocatalytic Reactions Enabled by N-Heterocyclic Carbenes. *Chem. Rev.* **115**, 9307–9387 (2015).
20. Schuster, O., Yang, L., Raubenheimer, H. G. & Albrecht, M. Beyond conventional N-heterocyclic carbenes: Abnormal, remote, and other classes of NHC ligands with reduced heteroatom stabilization. *Chem. Rev.* **109**, 3445–3478 (2009).
21. Alam, K., Kim, S. M., Kim, D. J. & Park, J. K. Development of Structurally Diverse N-Heterocyclic Carbene Ligands *via* Palladium-Copper-Catalyzed Decarboxylative Arylation of Pyrazolo[1,5- *a*]pyridine-3-carboxylic Acid. *Adv. Synth. Catal.* **358**, 2661–2670 (2016).
22. Heckenroth, M., Kluser, E., Neels, A. & Albrecht, M. Neutral ligands with exceptional donor ability for palladium-catalyzed alkene hydrogenation. *Angew. Chem. Int. Ed.* **46**, 6293–6296 (2007).

23. Anderson, D. R., Lavallo, V., O'Leary, D. J., Bertrand, G. & Grubbs, R. H. Synthesis and reactivity of olefin metathesis catalysts bearing cyclic (alkyl)(amino)carbenes. *Angew. Chem. Int. Ed.* **46**, 7262–7265 (2007).

24. Seebach, D. Methods of Reactivity Umpolung. *Angew. Chem. Int. Ed.* **18**, 239–258 (1979).

25. Smith, A. B. & Xian, M. Anion relay chemistry: An effective tactic for diversity oriented synthesis. *J. Am. Chem. Soc.* **128**, 66–67 (2006).

26. Frigerio, M., Santagostino, M. & Sputore, S. A user-friendly entry to 2-iodoxybenzoic acid (IBX). *J. Org. Chem.* **64**, 4537–4538 (1999).

27. Silva, L. F. & Olofsson, B. Hypervalent iodine reagents in the total synthesis of natural products. *Nat. Prod. Rep.* **28**, 1722–1754 (2011).

28. Xing, B., Ni, C. & Hu, J. Hypervalent Iodine(III)-Catalyzed Balz-Schiemann Fluorination under Mild Conditions. *Angew. Chem. Int. Ed.* **57**, 9896–9900 (2018).

29. Jalalian, N., Ishikawa, E. E., Silva, L. F. & Olofsson, B. Room temperature, metal-free synthesis of diaryl ethers with use of diaryliodonium salts. *Org. Lett.* **13**, 1552–1555 (2011).

30. Merritt, E. A. & Olofsson, B. α-Functionalization of carbonyl compounds using hypervalent iodine Reagents. *Synthesis* 517–538 (2011).

31. Chapter 2 The ligand coupling mechanism. *Tetrahedron Org. Chem. Ser.* **18**, 9–46 (1998).

32. Ochiai, M., Takeuchi, Y., Katayama, T., Sueda, T. & Miyamoto, K. Iodobenzene-catalyzed α-acetoxylation of ketones. In situ generation of hypervalent (diacyloxyiodo)benzenes using m-chloroperbenzoic acid. *J. Am. Chem. Soc.* **127**, 12244–12245 (2005).

33. Kuhn, N., Steimann, M. & Weyers, G. Synthesis and Properties of l,3-Diisopropyl-4,5-dimethylimidazolium-2-carboxylate. A Stable Carbene Adduct of Carbon Dioxide. *Z. Naturforsch* **54 b**, 427–433 (1999).

34. Holbrey, J. D., Reichert, W. M., Tkatchenko, I., Bouajila, E., Walter, O., Tommasi, I. & Rogers, R. D. 1,3-Dimethylimidazolium-2-carboxylate: The unexpected synthesis of an ionic liquid precursor and carbene-CO2 adduct. *Chem. Comm.* **9**, 28–29 (2003).

35. Kayaki, Y., Yamamoto, M. & Ikariya, T. N-heterocyclic carbenes as efficient organocatalysts for CO2 fixation reactions. *Angew. Chem. Int. Ed.* **48**, 4194–4197 (2009).

36. Davico, G. E., Bierbaum, V. M., DePuy, C. H., Ellison, G. B. & Squires, R. R. The C—H Bond Energy of Benzene. *J. Am. Chem. Soc.* **117**, 2590–2599 (1995).

37. Shilov, A. E. & Shul'pin, G. B. Activation of C-H bonds by metal complexes. *Chem. Rev.* **97**, 2879–2932 (1997).

38. Crabtree, R. H. & Lei, A. Introduction: CH Activation. *Chem. Rev.* **117**, 8481–8482 (2017).

39. Ackermann, L. Carboxylate-assisted transition-metal-catalyzed C-H bond functionalizations: Mechanism and scope. *Chem. Rev.* **111** 1315–1345 (2011).

40. Xia, G., Zhuang, Z., Liu, L., Schreiber, S. L., Melillo, B. & Yu, J. Ligand-Enabled β-Methylene C(sp^3)−H Arylation of Masked Aliphatic Alcohols. *Angew. Chem. Int. Ed.* **59**, 7783–7787 (2020).

41. Palladacycles - 1st Edition. https://www.elsevier.com/books/palladacycles/kapdi/978-0-12-815505-9.

42. Beccalli, E. M., Broggini, G., Martinelli, M., Masciocchi, N. & Sottocornola, S. New 4-spiroannulated tetrahydroisoquinolines by a one-pot sequential procedure. Isolation and characterization of σ-alkylpalladium Heck intermediates. *Org. Lett.* **8**, 4521–4524 (2006).

43. Ravi Kumar, D. & Satyanarayana, G. Domino Oxidative [Pd]-Catalysis: One-Pot Synthesis of Fluorenones Starting from Simple Benzylamines and Iodo Arenes. *Org. Lett.* **17**, 5894–5897 (2015).

44. Liu, Y. & Ge, H. Site-selective C-H arylation of primary aliphatic amines enabled by a catalytic transient directing group. *Nat. Chem.* **9**, 26–32 (2017).

45. Sambiagio, C., Schönbauer, D., Blieck, R., Dao-Huy, T., Pototschnig, G., Schaaf, P., Wiesinger, T., Zia, M. F., Wencel-Delord, J., Besset, T., Maes, B. U. W. & Schnürch, M. A comprehensive overview of directing groups applied in metal-catalysed C-H functionalisation chemistry. *Chem. Soc. Rev.* vol. 47 6603–6743 (2018).

46. Zhang, M., Zhang, Y., Jie, X., Zhao, H., Li, G. & Su, W. Recent advances in directed C-H

functionalizations using monodentate nitrogen-based directing groups. *Org. Chem. Front.* **1**, 843–895 (2014).

47. Tomberg, A., Muratore, M. É., Johansson, M. J., Terstiege, I., Sköld, C. & Norrby, P. O. Relative Strength of Common Directing Groups in Palladium-Catalyzed Aromatic C−H Activation. *iScience* **20**, 373–391 (2019).
48. Andrade-Sampedro, P., Matxain, J. M. & Correa, A. Pd-Catalyzed C(sp ^{2})−H Alkoxycarbonylation of Phenethyl- and Benzylamines with Chloroformates as CO Surrogates. *Chem Eur. J.* chem.202005338 (2021) doi:10.1002/chem.202005338.
49. Friis, S. D., Johansson, M. J. & Ackermann, L. Cobalt-catalysed C–H methylation for late-stage drug diversification. *Nat. Chem.* **12**, 511–519 (2020).
50. Trowbridge, A., Walton, S. M. & Gaunt, M. J. New Strategies for the Transition-Metal Catalyzed Synthesis of Aliphatic Amines. *Chem. Rev.* **120**, 2613–2692 (2020).
51. Schwarz, M. C., Dastbaravardeh, N., Kirchner, K., Schnürch, M. & Mihovilovic, M. D. First selective direct mono-arylation of piperidines using ruthenium-catalyzed C-H activation. *Monatshefte fur Chemie* **144**, 539–552 (2013).
52. Topczewski, J. J., Cabrera, P. J., Saper, N. I. & Sanford, M. S. Palladium-catalysed transannular C-H functionalization of alicyclic amines. *Nature* **531**, 220–224 (2016).
53. Rodrigalvarez, J., Nappi, M., Azuma, H., Flodén, N. J., Burns, M. E. & Gaunt, M. J. Catalytic C(sp 3)–H bond activation in tertiary alkylamines. *Nat. Chem.* **12**, 76–81 (2020).
54. Wei, C. & Li, C. J. A highly efficient three-component coupling of aldehyde, alkyne, and amines via C-H activation catalyzed by gold in water. *J. Am. Chem. Soc.* **125**, 9584–9585 (2003).
55. McNally, J. J., Youngman, M. A. & Dax, S. L. Mannich reactions of resin-bound substrates: 2. A versatile three- component solid-phase organic synthesis methodology. *Tetrahedron Lett.* **39**, 967–970 (1998).
56. Peshkov, V. A., Pereshivko, O. P. & Van der Eycken, E. V. A walk around the A3-coupling. *Chem. Soc. Rev.* **41**, 3790–3807 (2012).
57. Li, Y., Chen, X., Song, Y., Fang, L. & Zou, G. Well-defined N-heterocyclic carbene silver halides of 1-cyclohexyl-3- arylmethylimidazolylidenes: Synthesis, structure and catalysis in A 3-reaction of aldehydes, amines and alkynes. *Dalt. Trans.* **40**, 2046–2052 (2011).
58. Palchak, Z. L., Lussier, D. J., Pierce, C. J. & Larsen, C. H. Synthesis of tetrasubstituted propargylamines from cyclohexanone by solvent-free copper(ii) catalysis. *Green Chem.* **17**, 1802–1810 (2015).
59. Chen, W. W., Nguyen, R. V. & Li, C. J. Iron-catalyzed three-component coupling of aldehyde, alkyne, and amine under neat conditions in air. *Tetrahedron Lett.* **50**, 2895–2898 (2009).
60. Cao, K., Zhang, F.-M., Tu, Y.-Q., Zhuo, X.-T. & Fan, C.-A. Iron(III)-Catalyzed and Air-Mediated Tandem Reaction of Aldehydes, Alkynes and Amines: An Efficient Approach to Substituted Quinolines. *Chem. Eur. J.* **15**, 6332–6334 (2009).
61. Yoo, W. & Li, C. Copper-Catalyzed Four-Component Coupling between Aldehydes, Amines, Alkynes, and Carbon Dioxide. *Adv. Synth. Catal.* **350**, 1503–1506 (2008).
62. Zorba, L. P. & Vougioukalakis, G. C. The Ketone-Amine-Alkyne (KA2) coupling reaction: Transition metal-catalyzed synthesis of quaternary propargylamines. *Coordination Chemistry Reviews* **429** 213603 (2021).
63. Pierce, C. J., Nguyen, M. & Larsen, C. H. Copper/titanium catalysis forms fully substituted carbon centers from the direct coupling of acyclic ketones, amines, and alkynes. *Angew. Chem. Int. Ed.* **51**, 12289–12292 (2012).
64. Cheng, M., Zhang, Q., Hu, X. Y., Li, B. G., Ji, J. X. & Chan, A. S. C. Gold-catalyzed direct intermolecular coupling of ketones, secondary amines, and alkynes: A facile and versatile access to propargylic amines containing a quaternary carbon center. *Adv. Synth. Catal.* **353**, 1274–1278 (2011).
65. Van Beek, W. E., Van Stappen, J., Franck, P. & Abbaspour Tehrani, K. Copper(I)-Catalyzed Ketone, Amine, and Alkyne Coupling for the Synthesis of 2-Alkynylpyrrolidines and -piperidines. *Org. Lett.* **18**, 4782–4785 (2016).
66. Schrödinger, E. An Undulatory Theory of the Mechanics of Atoms and Molecules. *Phys. Rev.* **28**,

1049 (1926).

67. Cramer, C. J. *Essentials of Computational Chemistry: Theories and Models, 2nd Edition*. (2004).

68. Hohenberg, P. & Kohn, W. Inhomogeneous Electron Gas. *Phys. Rev.* **136**, B864 (1964).

69. Kohn, W. & Sham, L. J. Self-Consistent Equations Including Exchange and Correlation Effects. *Phys. Rev.* **140**, A1133 (1965).

70. Jensen, F. *Introduction to Computational Chemistry*. *Angew. Chem. Int. Ed.* (2007). doi:10.1007/s00214-013-1372-6.

71. Miertuš, S., Scrocco, E. & Tomasi, J. Electrostatic interaction of a solute with a continuum. A direct utilizaion of AB initio molecular potentials for the prevision of solvent effects. *Chem. Phys.* **55**, 117–129 (1981).

72. Hu, L., Cai, A., Wu, Z., Kleij, A. W. & Huang, G. A Mechanistic Analysis of the Palladium-Catalyzed Formation of Branched Allylic Amines Reveals the Origin of the Regio- and Enantioselectivity through a Unique Inner-Sphere Pathway. *Angew. Chem. Int. Ed.* **58**, 14694–14702 (2019).

73. Weigend, F. & Ahlrichs, R. Balanced basis sets of split valence, triple zeta valence and quadruple zeta valence quality for H to Rn: Design and assessment of accuracy. *Phys. Chem. Chem. Phys.* **7**, 3297–3305 (2005).

74. Hamzehloueian, M. A density functional theory study on the reaction mechanism of hydrazones with α-oxo-ketenes: Comparison between stepwise 1,3-dipolar cycloaddition and Diels–Alder pathways. *Comptes Rendus Chim.* **20**, 508–519 (2017).

75. Walker, M., Harvey, A. J. A., Sen, A. & Dessent, C. E. H. Performance of M06, M06-2X, and M06-HF density functionals for conformationally flexible anionic clusters: M06 functionals perform better than B3LYP for a model system with dispersion and ionic hydrogen-bonding interactions. *J. Phys. Chem. A* **117**, 12590–12600 (2013).

76. Yadav, P. & Shah, K. Quinolines, a perpetual, multipurpose scaffold in medicinal chemistry. *Bioorg. Chem.* 104639 (2021) doi:10.1016/j.bioorg.2021.104639.

77. Utreja, D., Sharma, S., Goyal, A., Kaur, K. & Kaushal, S. Synthesis and Biological Activity of Quaternary Quinolinium Salts: A Review. *Curr. Org. Chem.* **23**, 2271–2294 (2019).

78. Wang, Z. Combes Quinoline Synthesis. in *Comprehensive Organic Name Reactions and Reagents* 688–691 (John Wiley & Sons, Inc., 2010). doi:10.1002/9780470638859.conrr151.

79. Xuan, D. D. Recent Progress in the Synthesis of Quinolines. *Curr. Org. Synth.* **16**, 671–708 (2019).

80. Cheng, L.-C., Chen, W.-C., Santhoshkumar, R., Chao, T.-H., Cheng, M.-J. & Cheng, C.-H. Synthesis of Quinolinium Salts from *N* -Substituted Anilines, Aldehydes, Alkynes, and Acids: Theoretical Understanding of the Mechanism and Regioselectivity. *Eur. J. Org. Chem.* **2020**, 2116–2129 (2020).

81. Aksenov, A. V. & Nadein, O. N. Investigation of 2,3′-biquinolyl. 10. The regioselectivity of the reaction of 2,3′-biquinolyl and 1′-alkyl-3-(2-quinolyl)quinolinium halides with halo derivatives in the presence of metallic lithium and magnesium. *Chem. Heterocycl. Compd.* **36**, 1314–1318 (2000).

82. Grozavu, A., Hepburn, H. B., Smith, P. J., Potukuchi, H. K., Lindsay-Scott, P. J. & Donohoe, T. J. The reductive C3 functionalization of pyridinium and quinolinium salts through iridium-catalysed interrupted transfer hydrogenation. *Nat. Chem.* **11**, 242–247 (2019).

83. Dumitraşcu, F., Mitan, C. I., Drăghici, C., Căproiu, M. T. & Răileanu, D. Primary cycloadducts of 1,10-phenanthrolinium and phthalazinium phenacylides with DMAD. *Tetrahedron Lett.* **42**, 8379–8382 (2001).

84. Yun, Y. ling, Yang, J., Miao, Y. hang, Sun, J. & Wang, X. jing. Recent advances in Palladium(II)-catalyzed activation of aromatic ring C–H bonds. *Journal of Saudi Chemical Society* vol. 24 151–185 (2020).

85. Das, J., Guin, S. & Maiti, D. Diverse strategies for transition metal catalyzed distal C(sp3)-H functionalizations. *Chem. Sci.* **11** 10887–10909 (2020).

86. Ryabov, A. D., Sakodinskaya, I. K. & Yatsimirsky, A. K. Kinetics and mechanism of ortho-palladation of ring-substituted NN-dimethylbenzylamines. *J. Chem. Soc. Dalt. Trans.* 2629–2638 (1985) doi:10.1039/DT9850002629.

87. Whitehurst, W. G. & Gaunt, M. J. Synthesis and Reactivity of Stable Alkyl-Pd(IV) Complexes Relevant to Monodentate N-Directed C(sp3)-H Functionalization Processes. *J. Am. Chem. Soc.* **142**, 14169–14177 (2020).

88. McNally, A., Haffemayer, B., Collins, B. S. L. & Gaunt, M. J. Palladium-catalysed C-H activation of aliphatic amines to give strained nitrogen heterocycles. *Nature* **510**, 129–133 (2014).

89. Haines, B. E., Berry, J. F., Yu, J. Q. & Musaev, D. G. Factors Controlling Stability and Reactivity of Dimeric Pd(II) Complexes in C-H Functionalization Catalysis. *ACS Catal.* **6**, 829–839 (2016).

90. Yang, Y. F., Hong, X., Yu, J. Q. & Houk, K. N. Experimental-Computational Synergy for Selective Pd(II)-Catalyzed C-H Activation of Aryl and Alkyl Groups. *Acc. Chem. Res.* **50**, 2853–2860 (2017).

91. Gair, J. J., Haines, B. E., Filatov, A. S., Musaev, D. G. & Lewis, J. C. Mono-: N -protected amino acid ligands stabilize dimeric palladium(II) complexes of importance to C-H functionalization. *Chem. Sci.* **8**, 5746–5756 (2017).

92. Chen, Y. Q., Wang, Z., Wu, Y., Wisniewski, S. R., Qiao, J. X., Ewing, W. R., Eastgate, M. D. & Yu, J. Q. Overcoming the Limitations of γ- And δ-C-H Arylation of Amines through Ligand Development. *J. Am. Chem. Soc.* **140**, 17884–17894 (2018).

93. Davies, D. L., Macgregor, S. A. & McMullin, C. L. Computational Studies of Carboxylate-Assisted C-H Activation and Functionalization at Group 8-10 Transition Metal Centers. *Chem. Rev.* **117**, 8649–8709 (2017).

94. Feng, W., Wang, T., Liu, D., Wang, X. & Dang, Y. Mechanism of the Palladium-Catalyzed C(sp3)-H Arylation of Aliphatic Amines: Unraveling the Crucial Role of Silver(I) Additives. *ACS Catal.* **9**, 6672–6680 (2019).

95. Kocsis, L. S. & Brummond, K. M. Intramolecular dehydro-diels-alder reaction affords selective entry to arylnaphthalene or aryldihydronaphthalene lignans. *Org. Lett.* **16**, 4158–4161 (2014).

96. Kaye, J. A., Margulis, A. V., Fortuny, J., McQuay, L. J., Plana, E., Bartsch, J. L., Bui, C. L., Perez-Gutthann, S. & Arana, A. Cancer Incidence after Initiation of Antimuscarinic Medications for Overactive Bladder in the United Kingdom: Evidence for Protopathic Bias. *Pharmacotherapy* **37**, 673–683 (2017).

97. García, H., Iborra, S., Primo, J. & Miranda, M. A. 6-Endo-Dig vs. 5-Exo-Dig Ring Closure in o-Hydroxyaryl Phenylethynyl Ketones. A New Approach to the Synthesis of Flavones and Aurones. *J. Org. Chem.* **51**, 4432–4436 (1986).

98. Jia, C., Piao, D., Kitamura, T. & Fujiwara, Y. New method for preparation of coumarins and quinolinones via Pd-catalyzed intramolecular hydroarylation of C-C triple bonds. *J. Org. Chem.* **65**, 7516–7522 (2000).

99. Zhang, W. Z., Li, W. J., Zhang, X., Zhou, H. & Lu, X. B. Cu(I)-catalyzed carboxylative coupling of terminal alkynes, allylic chlorides, and CO2. *Org. Lett.* **12**, 4748–4751 (2010).

100. Shi, J. Bin, Bu, Q., Liu, B. Y., Dai, B. & Liu, N. Organocatalytic Strategy for the Fixation of CO2via Carboxylation of Terminal Alkynes. *J. Org. Chem.* **86**, 1850–1860 (2021).

101. Papastavrou, A. T., Pauze, M., Gómez-Bengoa, E. & Vougioukalakis, G. C. Unprecedented multicomponent organocatalytic synthesis of propargylic esters via CO2 activation. *ChemCatChem* **11**, (2019).

102. Zhao, Y. & Truhlar, D. G. The M06 suite of density functionals for main group thermochemistry, thermochemical kinetics, noncovalent interactions, excited states, and transition elements: Two new functionals and systematic testing of four M06-class functionals and 12 other functionals. *Theor. Chem. Acc.* **120**, 215–241 (2008).

103. Krishnan, R., Binkley, J. S., Seeger, R. & Pople, J. A. Self-consistent molecular orbital methods. XX. A basis set for correlated wave functions. *J. Chem. Phys.* **72**, 650–654 (1980).

104. Zhou, Q. & Li, Y. The real role of N-heterocyclic carbene in reductive functionalization of CO2: An alternative understanding from density functional theory study. *J. Am. Chem. Soc.* **137**, 10182–10189 (2015).

105. Zhao, Y. & Truhlar, D. G. A new local density functional for main-group thermochemistry, transition metal bonding, thermochemical kinetics, and noncovalent interactions. *J. Chem. Phys.* **125**, 194101 (2006).

106. Denning, D. M., Thum, M. D. & Falvey, D. E. Photochemical Reduction of CO2 Using 1,3-Dimethylimidazolylidene. *Org. Lett.* **17**, 4152–4155 (2015).

107. Sanz-Marco, A., Martinez-Erro, S. & Martín-Matute, B. Selective Synthesis of Unsymmetrical Aliphatic Acyloins through Oxidation of Iridium Enolates. *Chem. Eur. J.* **24**, 11564–11567 (2018).

108. Sanz-Marco, A., Možina, Š., Martinez-Erro, S., Iskra, J. & Martín-Matute, B. Synthesis of α-Iodoketones from Allylic Alcohols through Aerobic Oxidative Iodination. *Adv. Synth. Catal.* **360**, 3884–3888 (2018).

109. Vázquez-Romero, A., Gómez, A. B. & Martín-Matute, B. Acid- and iridium-catalyzed tandem 1,3-transposition/3,1-hydrogen shift/chlorination of allylic alcohols. *ACS Catal.* **5**, 708–714 (2015).

110. Gómez, A. B., Erbing, E., Batuecas, M., Vázquez-Romero, A. & Martín-Matute, B. Iridium-Catalyzed Isomerization/Bromination of Allylic Alcohols: Synthesis of α-Bromocarbonyl Compounds. *Chem. Eur. J.* **20**, 10703–10709 (2014).

111. Mantilli, L., Gérard, D., Torche, S., Besnard, C. & Mazet, C. Improved Catalysts for the Iridium-Catalyzed Asymmetric Isomerization of Primary Allylic Alcohols Based on Charton Analysis. *Chem. Eur. J.* **16**, 12736–12745 (2010).

112. Akula, R., Doran, R. & Guiry, P. J. Highly Enantioselective Formation of α-Allyl-α-Arylcyclopentanones via Pd-Catalysed Decarboxylative Asymmetric Allylic Alkylation. *Chem. Eur. J.* **22**, 9938–9942 (2016).

113. Lempenauer, L., Duñach, E. & Lemière, G. Tuning the Reactivity of Functionalized Diallylic Alcohols: Brønsted versus Lewis Acid Catalysis. *Chem. Eur. J.* **23**, 10285–10288 (2017).

114. Parchomyk, T. & Koszinowski, K. Electronic and Steric Effects on the Reductive Elimination of Anionic Arylferrate(III) Complexes. *Chem. Eur. J.* **24**, 16342–16347 (2018).

115. Arava, S., Kumar, J. N., Maksymenko, S., Iron, M. A., Parida, K. N., Fristrup, P. & Szpilman, A. M. Enolonium Species-Umpoled Enolates. *Angew. Chem. Int. Ed.* **56**, 2599–2603 (2017).

116. Sanz-Marco, A., Martinez-Erro, S. & Martín-Matute, B. Selective Synthesis of Unsymmetrical Aliphatic Acyloins through Oxidation of Iridium Enolates. *Chem. Eur. J.* **24**, 11564–11567 (2018).

117. Sanz-Marco, A., Martinez-Erro, S., Pauze, M., Gómez-Bengoa, E. & Martín-Matute, B. An umpolung strategy to react catalytic enols with nucleophiles. *Nat. Commun.* **10**, 1–9 (2019).

118. Shneider, O. S., Pisarevsky, E., Fristrup, P. & Szpilman, A. M. Oxidative umpolung α-alkylation of ketones. *Org. Lett.* **17**, 282–285 (2015).

119. Kiefl, G. M. & Gulder, T. α-Functionalization of Ketones via a Nitrogen Directed Oxidative Umpolung. *J. Am. Chem. Soc.* **142**, 20577–20582 (2020).

120. Dong, M., Gao, J., Liu, C. & Zhang, D. DFT Study on the Formation Mechanism of Normal and Abnormal N-Heterocyclic Carbene-Carbon Dioxide Adducts from the Reaction of an Imidazolium-Based Ionic Liquid with CO2. *J. Phys. Chem. B* **121**, 10276–10284 (2017).

121. Zheng, H., Sang, Y., Houk, K. N., Xue, X. S. & Cheng, J. P. Mechanism and Origins of Enantioselectivities in Spirobiindane-Based Hypervalent Iodine(III)-Induced Asymmetric Dearomatizing Spirolactonizations. *J. Am. Chem. Soc.* **141**, 16046–16056 (2019).

122. Koichi, S., Leuthold, B. & Lüthi, H. P. Why do the Togni reagent and some of its derivatives exist in the high-energy hypervalent iodine form? New insight into the origins of their kinetic stability. *Phys. Chem. Chem. Phys.* **19**, 32179–32183 (2017).

123. Li, M., Sanz-Marco, A., Martinez-Erro, S., García-Vázquez, V., Mai, B. K., Fernández-Gallardo, J., Himo, F. & Martín-Matute, B. Unraveling the Mechanism of the IrIII-Catalyzed Regiospecific Synthesis of α-Chlorocarbonyl Compounds from Allylic Alcohols. *Chem. Eur. J.* **26**, 14978–14986 (2020).

124. Lauder, K., Toscani, A., Scalacci, N. & Castagnolo, D. Synthesis and Reactivity of Propargylamines in Organic Chemistry. (2017) doi:10.1021/acs.chemrev.7b00343.

125. Wei, H., Li, Y., Xiao, K., Cheng, B., Wang, H., Hu, L. & Zhai, H. Synthesis of Polysubstituted Pyridines via a One-Pot Metal-Free Strategy. *Org. Lett.* **17**, 5974–5977 (2015).

126. Yang, Q., Xu, T. & Yu, Z. Iron-mediated carboarylation/cyclization of propargylanilines with acetals: A concise route to indeno[2,1- C]quinolines. *Org. Lett.* **16**, 6310–6313 (2014).

127. Yoo, W. J. & Li, C. J. Copper-catalyzed four-component coupling between aldehydes, amines,

alkynes, and carbon dioxide. *Adv. Synth. Catal.* **350**, 1503–1506 (2008).

128. Fantoni, N. Z., El-Sagheer, A. H. & Brown, T. A Hitchhiker's Guide to Click-Chemistry with Nucleic Acids. *Chem. Rev.* **121**, (2021) doi:10.1021/acs.chemrev.0c00928.

129. Innocenti, R., Lenci, E., Menchi, G. & Trabocchi, A. Combination of multicomponent KA2 and Pauson-Khand reactions: Short synthesis of spirocyclic pyrrolocyclopentenones. *Beilstein J. Org. Chem.* **16**, 200–211 (2020).

130. Valyaev, D. A., Lavigne, G. & Lugan, N. Manganese organometallic compounds in homogeneous catalysis: Past, present, and prospects. *Coord. Chem. Rev.* **308**, 191–235 (2016).

131. Carney, J. R., Dillon, B. R. & Thomas, S. P. Recent Advances of Manganese Catalysis for Organic Synthesis. *Eur. J. Org. Chem.* 3912–3929 (2016).

132. Kuninobu, Y., Nishina, Y., Takeuchi, T. & Takai, K. Manganese-catalyzed insertion of aldehydes into a C-H bond. *Angew. Chem. Int. Ed.* **46**, 6518–6520 (2007).

133. Kang, S. K., Kim, J. S. & Choi, S. C. Copper- and Manganese-Catalyzed Cross-Coupling of Organostannanes with Organic Iodides in the Presence of Sodium Chloride. *J. Org. Chem.* **62**, 4208–4209 (1997).

134. Iwasaki, K., Wan, K. K., Oppedisano, A., Crossley, S. W. M. & Shenvi, R. A. Simple, chemoselective hydrogenation with thermodynamic stereocontrol. *J. Am. Chem. Soc.* **136**, 1300–1303 (2014).

135. Afraj, S. N., Chen, C. & Lee, G. H. Manganese(II) chloride catalyzed highly efficient one-pot synthesis of propargylamines and fused triazoles via three-component coupling reaction under solvent-free condition. *RSC Adv.* **4**, 26301–26308 (2014).

Korr

I

Korr

Korr

Synthesis of substituted alkyl quinoliniums from propylamine and its derivatives

Martin Pauze[a] and Enrique Gómez-Bengoa*[a]

[a] Department of Organic Chemistry I, Faculty of Chemistry
University of the Basque Country
UPV/EHU, 20018 Donostia-San Sebastián, Spain

Supporting information for this article containing copies of the ^{1}H and ^{13}C NMR spectra, as well as the Cartesian coordinates to which the present manuscript refers, is given via a link at the end of the document.

Abstract: *The synthesis of a group of quinolinium structures has been achieved starting from aliphatic primary amines, through a palladium catalyzed process. The appropriate combination of the palladium catalyst, silver oxidant and acetic acid / water solvent mixture gives rise to moderate yields of rather complex heterocyclic structures in a single step. Two units of the amine and one or two units of the aryl iodide are incorporated in this multicomponent reaction. In general, unprotected aliphatic primary amines are not suitable substrates for palladium catalyzed processes, due to undesirable side reactions. However, in our case, they can be safely used, giving rise to a remarkable increase in complexity. Some of the elementary steps of the mechanism have also been studied by DFT means.*

Introduction

Azaheterocycles are predominant in the chemical structure of many approved drugs.[1] The subcategory represented by quinoline scaffold (quinolines, quinolones, tetrahydroquinolines), is a significant part of the pharmacophores, offering outstanding bioactivities from antiviral to anticancer and through anti-inflammatory or antibacterial drugs.[2] Furthermore, quaternary quinoliniums are key intermediates of the synthesis of many of those drugs, as their rich reactivity allows to access a wide range of different scaffolds, leading to high structural diversity.[3] In general, quinolinium salts are best prepared by alkylation of quinoline precursors, which is a procedure rather limited by the availability of the corresponding quinolines, depending finally on the methods of their preparation. Thus, a direct access to quinoliniums from simple and inexpensive materials would better fit with the idea of efficient and concise synthesis. However, alkylation remains nowadays the best approach as quinoline synthesis have been intensively studied and, are still the object of new synthetic methodologies.[4] The vast majority of those methods imply starting materials with preformed Aryl–N bond, as aniline or nitrobenzene, and involve the formation of the pyridine ring by reaction with moderate to high complex reactants. Only few examples report the synthesis of quinolines with construction of the critical Aryl–N bond from a C(sp2)–H one.[5]

The C-H activation of sp2 and sp3 carbons is an instrumental new tool for the late stage modification of pre-existing drugs.[6] More specifically, the activation of aliphatic amines has become a valuable tool, due to the inherent difficulty of activating inert C(sp3)-H bonds, and to the preponderant presence of substituted amines in bioactive molecules present in the drug market. Transition metal catalyzed C-H activations allow site selective functionalization of molecules, even if the selectivity is highly dependent on the presence of directing groups. Any kind of amines can act in general as intramolecular directing groups, however, primary amines are the most challenging substrates for different reasons, among them, the irreversible formation of the strong covalent C-N bond, or the easy oxidation of the amine to the imine moiety. In both cases, the further reactivity of the amine is interrupted. Seminal work by Dauglis group used a picolinamide installed in the substrate as directing group (Scheme 1a), yielding γ-arylation of the protected amine.[7] As drawback, the amide had to be prepared initially and cleaved after the functionalization of the substrate. More recently, Ge's group[8] proposed the in situ formation of a carboxy-imine, a transient directing group, formed between the free primary amine and catalytic amounts of glyoxylic acid, which is released after the γ-functionalisation (Scheme 1b). These methods meet some essential criteria in late stage functionalization, like high site selectivity and compatibility with the core structure of the substrates. In parallel, C-H activation processes also offer simple transformation of complex molecules from inexpensive, economically and environmentally friendly starting materials. In our group, by a modification of the existing methods, we have used the γ-functionalization of the aliphatic amines in a different way, developing a different approach, consisting in the polyfunctionalization of aliphatic amines, leading to a remarkable increase of the complexity of the substrates (Scheme 1c). Initially, the method also uses a cascade C-H arylation of the aliphatic amine in the gamma position, and subsequent cyclization, oxidation steps for the formation of quinolinium rings. The substrates are not prefunctionalized, and the method does not require the presence of transient directing groups.

ACCEPTED MANUSCRIPT / AUTHOR VERSION watermark

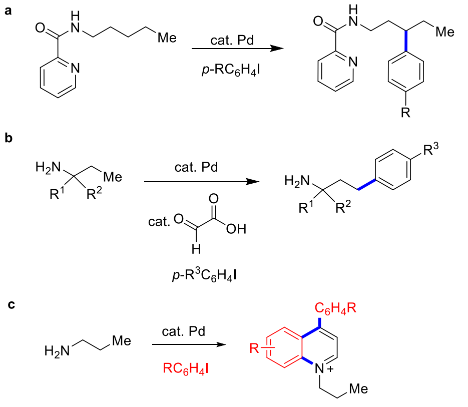

Scheme 1. Palladium catalyzed C-H activation and functionalization of propylamine chains. a) Picolamide directed γ-C–H arylation of protected alkyl amines. b) Site-selective γ-C–H arylation of primary amines with glycoxylic acid as transient directing group. c) In this work, non-directed synthesis of substituted quaternary quinolinium salts from unprotected primary amines.

Results and Discussion

Reaction development and optimization. We began this work by evaluating the suitability of unprotected 3-phenylpropylamine **1a** to the palladium catalysed C-H activation conditions, using iodobenzene **2a** as model arylating agent. We considered that the amine could undergo multiple C-H activation, C-C and C-N bonds formation and oxidation in the presence of palladium acetate catalyst, as this transition metal has demonstrated its ability to participate in such transformations.[9,10] Thus, in the presence of 10 mol% palladium acetate, a stoichiometric amount of silver trifluoroacetate, one equivalent of iodobenzene **2a**, at refluxing conditions in acetic acid, a very polar fluorescent compound was detected. The careful analysis of its NMR and HRMS spectra identified complex the cationic quinolinium structure of **3a**, formed in a 16% yield (entry 2, Table 1). In the structure, two subunits of phenyl-propylamine can be distinguished, one of them forming the pyridine ring of the heterocycle and the other one as the side chain substituent of the N (highlighted in red in **3**). The second aromatic ring comes from the phenyl iodide reagent. Although other metal acetates were initially evaluated, like copper, zinc, manganese and cobalt, we did not observed the formation of any product. Changing the stoichiometric oxidant to a less expensive silver oxide improved the yield to 21%, although the higher reactivity of Ag_2O could arise from its higher solubility or from the use of a higher load (2 equiv.) of the oxidant, which can also be transformed in situ to silver acetate in the reaction medium. The solvent screening showed that only acetic acid, with or without water, can be used for the reaction (entries 7-9, Table 1). The use of the acidic conditions can be explained by the need to destabilize any unreactive amine/palladium complexes. However, the acidity of the medium has to be controlled, as trifluoroacetic acid did not yield the desired compound (entry 10).

Table 1. Investigation of the possible catalyst, oxidants and solvents for the reaction.

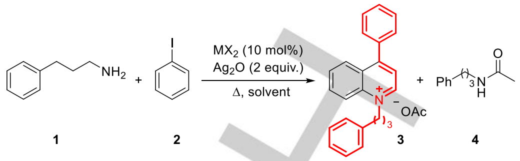

1 2 3 4

Entry	Catalyst 10 mol%	Additives 2 eq.	Solvent	Yield (%)[a]
1[b]	$M(OAc)_2$	CF_3CO_2Ag[c]	AcOH	0
2	$Pd(OAc)_2$	CF_3CO_2Ag[c]	AcOH	16
3	$Pd(OAc)_2$	Ag_2O	AcOH	21
4	$Pd(OAc)_2$	HNO_3	AcOH	0
5	$Pd(OAc)_2$	H_2O_2	AcOH	0
6	$Pd(OAc)_2$	$CuOAc_2$	AcOH	0
7	$Pd(OAc)_2$	Ag_2O	DMF	0
8	$Pd(OAc)_2$	Ag_2O	MeOH	0
9	$Pd(OAc)_2$	Ag_2O	Toluene	0
10	$Pd(OAc)_2$	Ag_2O	TFA	0

All the reaction were done with 2 eq of iodobenzene, at 110°C overnight. [a] Yields by NMR with trimethoxybenzene as internal standard. [b] Metals tried: Cu, Mn, Co and Zn. [c] 1.5 eq of CF_3CO_2Ag used.

An undesired side effect of the use of AcOH is the formation of amide 4a, which appears in the reaction in variable amounts, which were difficult to control initially. The ratio between water and acetic acid (Table 2) was found to have a big impact in the reaction outcome, and a significant reduction of the amount of the amide by-product was accomplished. The optimal ratio was found to be 1:1 (entry 5), at which no more amide formation was noticed. However, the yield remained low (21%), but increasing the temperature to 130°C rendered the product 3a in 35% yield (entry 6). Finally, the yield was improved to 77% after prolonged reaction times (60 h, entry 7).

Table 2. Optimization of the solvent.

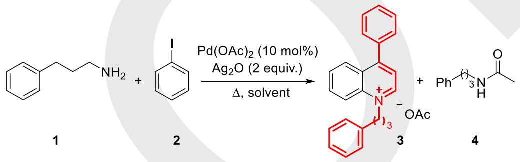

1 2 3 4

Entry	Ag_2O	PhI (eq.)	Solvent	Temp. (°C)	Yield (**3**/**4**,%)[a]
1	2	2	AcOH	110	26/47
2	3	2	AcOH	110	31/46
3	2	3	AcOH	110	30/42

4	2	2	AcOH	130	28/49
5	2	2	AcOH/H_2O[b]	110	21/0
6	2	2	AcOH/H_2O[b]	130	35/2
7[c]	2	2	AcOH/H_2O[b]	130	77/4

[a] Yields by NMR with trimethoxybenzene as internal standard. [b] v/v 1:1. [c] reaction time of 60 h.

To better understand the main features of the process, some control experiments were conducted. For example, in the absence of any palladium catalyst (but in the presence of stoichiometric silver oxide, entry 1, Table 3), the reaction did not proceed. However, in the opposite combination, absence of silver and presence of 10 mol% palladium catalyst (entry 2), a 7% yield of the product was observed, indicating that the palladium is only able to run one turn of the catalytic cycle, the silver oxidant being necessary to re-oxidize the palladium species to its active form. To confirm this idea, a stoichiometric amount of palladium was used in the absence again of silver co-oxidant (entry 3), and in this occasion a 42% yield of the product was obtained. It appears, thus, that the role of the silver is not directly linked to the C-H activation or cyclization steps. Finally, as expected, the aryl iodide is mandatory for the reaction to occur. Phenyl propylamine alone did not cyclize or render any other type of compound, but instead, it decomposed to a complex mixture of materials.

Table 3. Control experiments of the reaction.

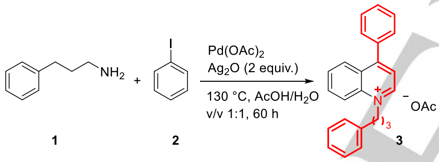

1 2 3

Entry	$Pd(OAc)_2$ (mol%)	Ag_2O (equiv.)	IPh (equiv.)	Yield (%)[a]
1	0	2	2	0
2	10	0	2	7
3	100	0	2	42
4	10	2	0	0

[a] Yields by NMR with trimethoxybenzene as internal standard.

Scope. With the optimal conditions in hands, we next explored the scope of possible aryl iodide reagents, and their regioselectivity in reactions with 3-phenylpropylamine. In principle, if R_1 and R_2 in **1** and **2** are the same substituent, the final rings in **3** are interconvertible ($R_3 = R_4$) and a single isomer is formed. This is the case in compounds of entries 1-4 (Table 4), when applying the reaction to methyl, chloro and methoxy groups in both aromatic substrates. Meanwhile, two possible isomers can arise from mixing differently substituted propylamines and iodides, since the formation of the key C-N bond and cyclization of the initial 3,3-diphenyl propylamine intermediate can happen with either aromatic ring (*vide infra*). For this reason, mixing unsubstituted **1a** (R_1=H) with *p*-iodotoluene (R_2=Me) (**3e**), the two possible isomers arose in 1:4.3 ratio, with the methyl group in the heterocycle or in the peripheral phenyl ring. Seemingly, *o*-iodotoluene also provided the desired products, **3f**, in 40% yield by NMR, (the products could not be isolated in this case). The situation becomes a bit more complex in the case of the *m*-iodotoluene (**3k**), as the cyclization can happen in two regioisomeric aromatic positions (*ortho* and *para* to the methyl group), giving rise to three possible regioisomers in 47% yield. Electron withdrawing groups are also tolerated in the reaction, as *para* fluoro-, chloro- and bromo-toluene derivatives gave the expected mixture of isomers in acceptable yields (54, 43 and 39% respec). In the case of fluorine, **3h**, a ratio of 1:1.2 was determined by ^{19}F NMR. A stronger electron withdrawing group in trifluomethyl iodobenzene was also employed with success. Not surprisingly, two isomers were obtained in a 1:1.2 ratio with the *para* isomer (**3g**), and a mixture of three ismoers for the *meta* analogue (1:6:4, **3l**).

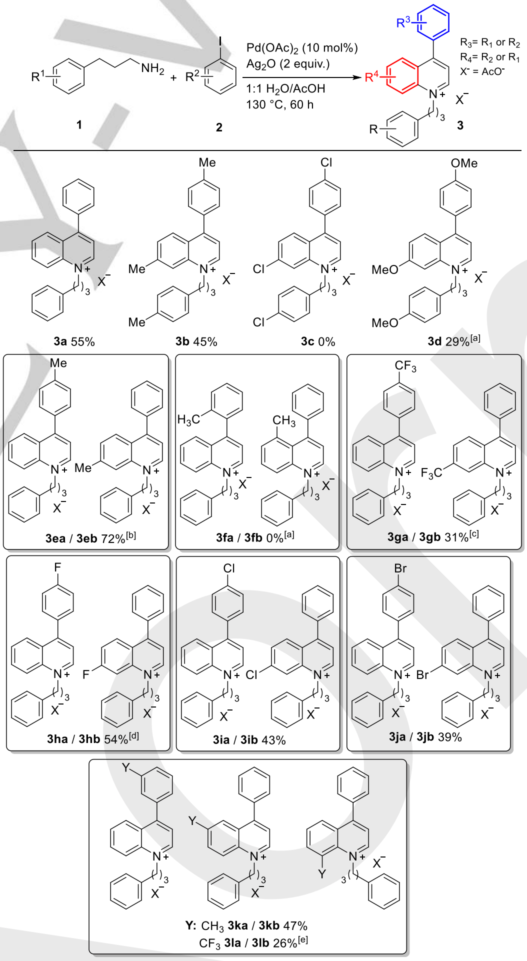

Scheme 2. Scope of the reaction with different 3-arylpropylamine and aryl-iodines. [a] ratio: 1:4.3 by ^{1}H NMR. [b] 40% yields by ^{1}H NMR with trimethoxybenzene as internal standard. [c] ratio: 1:1.2 by ^{19}F NMR. [d] ratio: 1:1.2 by ^{19}F NMR. [e] ratio: 6:4:1 by ^{19}F NMR.

At this point, we wondered about the first elementary steps of this intricate transformation. Indeed, after formation of the amine-Pd complex I, a beta-hydride elimination, followed by oxidation of the Pd(0) species, would lead to imine complex **II** (Scheme 2). This step is lower in energy than the direct C-H activation of the amine at the gamma position (see SI). At this point, the computed activation energy of the C-H activation (**TS1**) is affordable in the reaction conditions ($\Delta\Delta G^{\ddagger}$ = 19.3 kcal/mol) to render **III**, which follows the logical steps of oxidative addition to iodobenzene and reductive elimination to introduce the biaryl system in the gamma position of the imine. We hypothesized that a similar process could also take place in the unsubstituted propyl imine system **IV**, an in fact, the activation energy of **TS2** is much lower (8.7 kcal/mol) than in the previous substituted system **II**. For this reason, it seemed worth to check the suitability of simple, unsubstituted propylamine as a substrate of the reaction, which could suffer a double arylation process en route to the desired quinolinium salts.

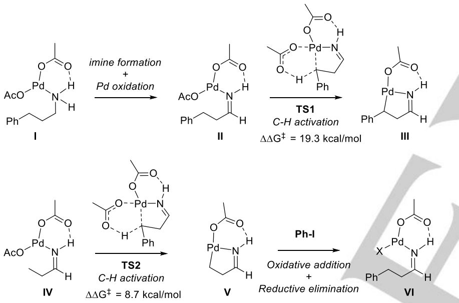

Scheme 3. Mechanism of the formation of the imines as directing group, follow by C-H activation and arylation of the substrate, supported by DFT calculation.

Thus, propylamine was treated with 2 equivalents of iodobenzene in otherwise similar conditions to those described in Table 3, and to our delight, after 60 h at 130 ºC, compound **5a** was obtained as a single product. Although the isolated yield was a low 32%, it can be considered adequate for a process with such a remarkable increase of complexity. As expected, the side alkyl chain at the nitrogen is a propyl group, and since two equal aryl groups are incorporated in the molecule, a single isomer of the final adduct is formed. Similar outcomes were obtained with other aryl iodides, namely *p*-tolyl (**5b**), *p*-chloro (**5c**) and *meta*-methyl (**5d**). In the latter case, the two possible regioisomers is obtained, containing the CH_3 group at the 6 and 8 positions of the heterocyclic with a ration of 3:1. The other position (C8) is probably blocked by steric impediment. The yields of the three compounds range from 32 to 38%, which are values that have to be put again in perspective, taking into account the simplicity of the method and the starting materials and the complexity of the final adducts.

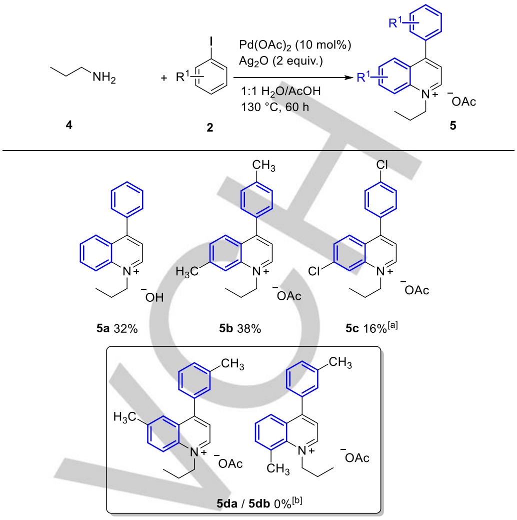

Scheme 4. Scope of the reaction with propylamine and aryl-iodines. [a] Product not isolated. [b] ratio: 3:1

Although the specific nature of all the steps involved in such a complex multicomponent process are impossible to detail at this stage, we have tentatively computed some of the key transition structures that at least are able to explain the key bond formations (Scheme 3). For example, we hypothesize that after the C-H activation previously mentioned, an easy oxidative addition in **TS3** would afford Pd(IV) complex **VII** with an activation barrier of 19.5 kcal/mol. The subsequent reductive elimination presents only 9.9 kcal/mol energy in **TS4** to yield bis-arylated imine **VIII**. After iodide /amine ligand exchange, the C-N bond formation is also energetically accessible (**TS5**¸ 14.8 kcal/mol). The participation of the palladium metal is probably not needed in the final steps, involving cyclization through attach of the amine to the imine functional group, and product yielding oxidative aromatization.

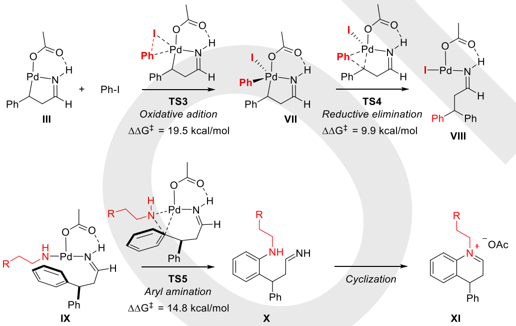

Scheme 5. Mechanism of the C-H activation/arylation of the 3-phenylpropylimine, C-N bond formation and cyclization.

Finally, an interesting result was obtained when *p*-fluorotoluene was used as arylating agent for the reaction with propylamine or

Accepted Manuscript

3-(*p*-fluorophenyl) propyl amine, because instead of the expected single isomer of a quinolinium salt containing two fluorine atoms at C7 position and at the phenyl substituent, the mass spectra showed an adduct containing a single fluorine atom and a new oxygen atom, which had replaced the lacking C-F bond. The transform involved has the characteristics of a aromatic nucleophilic substitution.[11] In addition, the compound was neutral, instead of cationic and much less polar than before. With these data and the NMR traces, the structure of the new adduct was tentatively assigned to compound **8a-8b** or **9a-9b** (Scheme 6). It is worth noting that a single compound, although in different yields, was obtained from the unsubstituted propyl amine or the monosubstituted (4-F-Ph-) derivative.

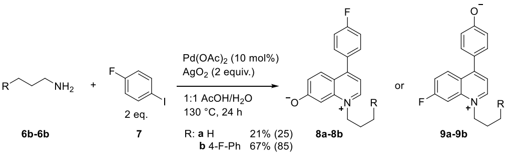

Scheme 6. Reaction with p-f-aryls and by products formation.

Conclusion

In summary, we have developed a simple process for the easy construction of rather complex quinolinium salts, starting from unprotected aliphatic primary amines. The incorporation of two units of the amine and an aryl iodide occurs in a multicomponent process. Even simple propylamine is a suitable substrate, dimerizing and incorporating two units of the aryl iodide reagent. In this case, the increase of complexity is remarkable, but still occurring at acceptable yields for such a complex process. Although the mechanism of this very intricate process contains a large number of individual steps, some tentative computational studies have been carried out, proposing elementary steps such as amine oxidation, C-H activations, oxidative addition, reductive elimination, cyclization and aromatization, all of them occurring at low to moderate activation energies.

Experimental Section

General reagent information

Chemicals were obtained from commercial sources and were used without any further purification, with the exception of substituted 3-aryl-propylamine that was prepare, see SI. All metal sources were anhydrous and at least 98% pure. All reactions were set up under air and carried out screw-cap pressure tubes.

Computational Methods

All reported structures were optimized at Density Functional Theory level by using the unrestricted B97-D functional, which includes Grimme´s dispersion, as implemented in Gaussian 16. Optimizations were carried out with the 6-311G(d,p) basis set taking for all atome except iodine and palladium, where SDD was used.[12–15] The reported energy values correspond to Gibbs Free energies, including a solvent model (IEFPCM, acetic acid), computed with Def2TZVPP. The critical stationary points were characterized by frequency calculations in order to verify that they have the right number of imaginary frequencies, and the intrinsic reaction coordinates (IRC) were followed to verify the energy profiles connecting the key transition structures to the correct associated local minima.

General analytical information

^{1}H, ^{13}C and ^{19}F NMR spectra were measured on a Brucker Avance 400 MHz instrument, using $CDCl_3$ or D_2O as the solvent and its residual solvent peak as a reference. NMR spectroscopic data are given in the order: chemical shift, multiplicity (s, singlet, br. s, broad singlet, d, doublet, t, triplet, q, quartet, m, multiplet), coupling constant in Hertz (Hz), and number of protons. HRMS spectra were recorded by SGIker and were acquired on a time of flight (TOF) mass spectrometer (SYNAPT G2 HDMS from Waters) equipped with an electrospray source in positive mode (ESI+).

General procedure

The following procedure was used for the synthesis of the quinoliniums: in a seal tube, was added, a stirring bar, palladium acetate (6.7 mg, 0.03mmol), silver oxide (140 mg, 0.6 mmol), corresponding iodoaryl (0.6 mmol). Then, 1 ml of water follow by 1 ml of acetic acid was added, and finally the amine (0.3 mmol). The tube was closed with a seal cap, and heat at 130 °C for 60h. The crude mixture was cooled down, 5 ml of methanol was added, and then filtered on cotton to remove salts. To the solution obtained, 5 g of silica was added and the solvent removed under vacuum. The silica was then washed with cyclohexane, then dichloromethane and finally acetone. The product was then remove from the silica by washing with methanol with 1 % (v:v) acetic acid. The solvents was removed under vacuum and the pure product obtained. The products was then characterized by NMR and HRMS.

Characterization data for new compounds

4-phenyl-1-(3-phenylpropyl)quinolin-1-ium acetate (**3a**): Prepared according to the general procedure and obtained as brown oil in 55 % yield (32 mg, 0.82 mmol). ^{1}H NMR (400 MHz, D_2O) δ 8.99 (d, J = 6.1 Hz, 1H), 8.30 (d, J = 8.8 Hz, 1H), 8.17 – 8.05 (m, 2H), 7.81 (dd, J = 8.5, 7.1 Hz, 1H), 7.66 (d, J = 6.1 Hz, 1H), 7.65 – 7.55 (m, 3H), 7.55 – 7.49 (m, 3H), 7.06 – 6.96 (m, 5H), 5.03 (t, J = 6.8 Hz, 2H), 2.82 (t, J = 6.8 Hz, 2H), 2.50 (p, J = 6.8 Hz, 3H), 1.83 (s, 3H). ^{13}C NMR (100 MHz, $CDCl_3$) δ 157.16, 151.36, 139.97, 137.88, 137.68, 134.99, 133.20, 131.50, 131.19, 129.89, 129.77, 129.67, 129.05, 128.99, 128.85, 128.64, 128.56, 128.07, 128.01, 126.71, 123.24, 118.43, 57.08, 32.55, 31.12. HRMS m/z $[M\text{-}OAc^-]^+$ calcd for $C_{24}H_{22}N^+$ 324.1700; Found 324.1745.

7-methyl-4-(p-tolyl)-1-(3-(p-tolyl)propyl)quinolin-1-ium acetate (**3b**): Prepared according to the general procedure and obtained as brown oil in 45 % yield (28.7 mg, 6.75 mmol). ^{1}H NMR (400 MHz, $CDCl_3$) δ 9.32 (s, 1H), 8.01 (d, J = 8.7 Hz, 1H), 7.59 (d, J = 5.9 Hz, 1H), 7.51 (d, J = 8.8 Hz, 1H), 7.43 (s, 1H), 7.05 – 6.85 (m, 8H), 4.85 – 4.78 (m, 2H), 3.31 (d, J = 35.5 Hz, 3H), 2.68 (t, J = 6.9 Hz, 2H), 2.41 (d, J = 38.7 Hz, 3H), 2.30 – 2.06 (m, 5H), 1.12 (s, 3H). ^{13}C NMR (100 MHz, $CDCl_3$) δ 13C NMR (101 MHz, CDCl3) δ 177.89, 158.85, 148.33, 147.25, 141.48, 138.14, 136.49, 136.10, 135.45, 133.59, 131.77, 131.55, 129.89, 129.55, 129.29, 128.97, 128.85, 128.71, 128.24, 126.74, 126.30, 121.42, 117.08, 56.33, 49.84, 49.62, 49.40, 49.19, 48.98, 48.76, 48.55, 48.34, 43.39, 31.66, 30.84, 29.52, 28.88, 22.52, 22.34, 21.24, 20.75. HRMS m/z $[M\text{-}OAc^-]^+$ calcd for $C_{27}H_{28}N^+$ 366,2222; Found 366.2231.

7-chloro-4-(4-chlorophenyl)-1-(3-(4-chlorophenyl)propyl)quinolin-1-ium acetate (**3c**): Prepared according to the general procedure, product not isolated. HRMS m/z [M-OAc-]+ calcd for C24H19Cl3N+ 426.0583 Found 426.0588.

7-methoxy-4-(4-methoxyphenyl)-1-(3-(4-methoxyphenyl)propyl)quinolin-1-ium acetate (**3d**): Prepared

WILEY-VCH

according to the general procedure and obtained as brown oil in 29 % yield (19.1 mg, 0.044 mmol). 1H NMR (400 MHz,) δ 10.13 (d, J = 6.2 Hz, 1H), 8.14 (d, J = 9.4 Hz, 1H), 7.72 (d, J = 6.1 Hz, 1H), 7.49 (d, J = 8.5 Hz, 2H), 7.37 (d, J = 9.5 Hz, 2H), 7.29 (s, 1H), 7.21 – 7.16 (m, 3H), 7.12 (dd, J = 14.5, 8.5 Hz, 1H), 7.04 (s, 2H), 6.83 (t, J = 7.5 Hz, 6H), 5.30 – 5.07 (m, 2H), 4.15 – 3.64 (m, 3H), 2.80 – 2.50 (m, 3H), 2.00 (s, 3H), 1.90 – 1.77 (m, 2H). 13C NMR (126 MHz, CD3CN) δ 159.1, 151.6, 147.2, 132.5, 131.9, 122.6, 120.2, 116.5, 115.5, 115.5, 99.2, 57.5, 56.2, 56.0, 22.9. HRMS m/z [M-OH$^-$]$^+$ calcd for C27H28NO3+ 414.2069; Found 414.2048.

7-methyl-4-phenyl-1-(3-phenylpropyl)quinolin-1-ium acetate and 1-(3-phenylpropyl)-4-(p-tolyl)quinolin-1-ium acetate (**3e**): Prepared according to the general procedure and obtained as brown oil in 72 % yield (47.5 mg, 0.108 mmol). Mixture of the two compounds: ^{1}H NMR (400 MHz, CDCl$_3$) δ 10.32 (d, J = 5.4 Hz, 1H), 8.29 (d, J = 8.5 Hz, 1H), 7.98 – 7.91 (m, 2H), 7.91 – 7.79 (m, 1H), 7.46 (s, 3H), 7.30 (d, J = 4.9 Hz, 5H), 7.27 – 7.04 (m, 6H), 5.35 – 5.26 (m, 2H), 2.95 (t, J = 7.2 Hz, 2H), 2.51 (d, J = 19.1 Hz, 5H), 2.30 (s, 1H), 2.09 (s, 3H). ^{13}C 13C NMR (126 MHz, CDCl3) δ 161.77, 158.76, 151.15, 150.97, 141.47, 141.17, 139.88, 139.35, 138.58, 137.86, 134.83, 134.57, 134.21, 131.87, 131.45, 130.69, 130.46, 130.01, 129.70, 129.56, 129.37, 129.33, 129.22, 129.19, 128.82, 128.72, 128.63, 128.59, 128.48, 128.44, 128.41, 128.12, 128.08, 127.94, 126.55, 126.44, 126.09, 122.89, 121.61, 121.08, 120.83, 118.05, 117.12, 114.29, 56.62, 41.74, 33.20, 32.41, 31.19, 29.68, 28.78, 21.45, 21.28, 20.93. HRMS m/z [M-OAc$^-$]$^+$ calcd for C$_{25}$H$_{24}$N$^+$ 338.1909; Found 338.1924.

1-(3-phenylpropyl)-4-(4-(trifluoromethyl)phenyl)quinolin-1-ium acetate and 4-phenyl-1-(3-phenylpropyl)-7-(trifluoromethyl)quinolin-1-ium acetate (**3g**): Prepared according to the general procedure and obtained as brown oil in 31 % yield (21.0 mg, 0.047 mmol). Mixture of the two compounds: ^{1}H NMR (400 MHz, CDCl$_3$) δ 10.38 (d, J = 5.1 Hz, 1H), 8.10 (d, J = 8.5 Hz, 1H), 8.07 – 8.02 (m, 1H), 7.98 (d, J = 5.1 Hz, 1H), 7.90 (td, J = 13.4, 8.4 Hz, 4H), 7.67 (d, J = 8.0 Hz, 2H), 7.42 (q, J = 8.3 Hz, 4H), 7.34 – 7.17 (m, 8H), 5.29 – 5.21 (m, 2H), 2.90 (t, J = 7.1 Hz, 2H), 2.50 – 2.38 (m, 2H), 2.03 (s, 3H). ^{19}F NMR (376 MHz, CDCl$_3$) -62.29, -62.94. ^{13}C NMR (100 MHz, CDCl$_3$) δ 156.67, 151.29, 141.86, 139.56, 138.02, 137.65, 134.97, 132.86, 132.52, 130.90, 130.64, 129.95, 129.81, 129.76, 129.30, 128.77, 128.61, 128.54, 128.47, 128.35, 127.83, 127.45, 126.53, 126.18, 125.62, 124.72, 123.24, 122.92, 122.14, 121.95, 121.54, 118.26, 114.51, 57.14, 41.86, 33.16, 32.33, 30.98, 29.67. HRMS m/z [M-OAc$^-$]$^+$ calcd for C$_{25}$H$_{21}$F$_3$N$^+$ 392.1626; Found 392.1638.

4-(4-fluorophenyl)-1-(3-phenylpropyl)quinolin-1-ium acetate and 7-fluoro-4-phenyl-1-(3-phenylpropyl)quinolin-1-ium acetate (**3h**): Prepared according to the general procedure and obtained as brown oil in 54 % yield (32.5 mg, 0.081 mmol). ^{1}H NMR (400 MHz, CDCl$_3$) δ 9.95 (d, J = 5.8 Hz, 1H), 8.19 (d, J = 8.5 Hz, 1H), 8.09 – 7.90 (m, 4H), 7.89 – 7.81 (m, 1H), 7.58 (dd, J = 8.7, 5.1 Hz, 2H), 7.40 – 7.12 (m, 19H), 6.91 (t, J = 8.7 Hz, 2H), 5.27 – 5.02 (m, 2H), 2.89 (t, J = 7.2 Hz, 2H), 2.49 – 2.37 (m, 2H), 2.03 (s, 3H). ^{19}F NMR (376 MHz, CDCl$_3$) -108.47, -116.60. ^{13}C NMR (100 MHz, CDCl$_3$) δ 176.75, 165.48, 162.97, 162.83, 160.40, 157.62, 150.39, 139.68, 137.89, 134.82, 131.91, 131.83, 131.27, 130.90, 130.82, 129.55, 129.23, 128.98, 128.89, 128.64, 128.38, 128.11, 126.51, 123.06, 118.38, 116.74, 116.52, 115.10, 114.89, 57.24, 32.40, 31.00, 29.66, 21.67.HRMS m/z [M-OAc$^-$]$^+$ calcd for C$_{24}$H$_{21}$FN$^+$ 342.1658; Found 342.1668.

4-(4-chlorophenyl)-1-(3-phenylpropyl)quinolin-1-ium acetate and 7-chloro-4-phenyl-1-(3-phenylpropyl)quinolin-1-ium acetate (**3i**): Prepared according to the general procedure and obtained as brown oil in 43 % yield (26.9 mg, 0.065 mmol). ^{1}H NMR (400 MHz, CDCl$_3$) δ 10.04 (s, 1H), 8.16 (d, J = 8.5 Hz, 1H), 8.02 (d, J = 7.3 Hz, 1H), 7.87 (m, 4H), 7.62 (d, J = 8.4 Hz, 2H), 7.49 (d, J = 8.4 Hz, 2H), 7.33 – 6.86 (m, 8H), 5.17 – 5.08 (m, 2H), 2.85 (t, J = 7.1 Hz, 2H), 2.45 – 2.35 (m, 2H), 2.03 (s, 3H). ^{13}C NMR (100 MHz, CDCl$_3$) δ 157.32, 150.77, 139.67, 137.82, 137.46, 134.82, 133.02, 132.13, 131.01, 130.85, 129.64, 128.80, 128.65, 128.40, 128.22, 127.97, 126.53, 123.08, 118.32, 57.21, 32.40, 31.00, 29.67.HRMS m/z [M-OAc$^-$]$^+$ calcd for C$_{24}$H$_{21}$ClN$^+$ 358.1363; Found 358.1371.

4-(4-bromophenyl)-1-(3-phenylpropyl)quinolin-1-ium acetate and 7-bromo-4-phenyl-1-(3-phenylpropyl)quinolin-1-ium acetate (**3j**): Prepared according to the general procedure and obtained as brown oil in 39 % yield (23.5 mg, 0.059 mmol). ^{1}H NMR (400 MHz, CDCl$_3$) δ 10.06 – 10.00 (m, 1H), 8.17 (d, J = 8.5 Hz, 1H), 8.03 (d, J = 7.3 Hz, 1H), 7.98 – 7.57 (m, 3H), 7.43 (d, J = 8.4 Hz, 1H), 7.38 – 7.17 (m, 3H), 7.13 (d, J = 8.2 Hz, 2H), 5.18 – 5.10 (m, 2H), 2.87 (t, J = 7.1 Hz, 2H), 2.46 – 2.34 (m, 2H), 2.02 (s, 3H). ^{13}C NMR (101 MHz, CDCl3) δ 207.14, 176.15, 157.34, 150.74, 139.66, 137.81, 135.39, 134.86, 133.48, 132.60, 131.19, 131.13, 129.61, 129.41, 128.81, 128.66, 128.40, 127.90, 126.54, 125.76, 122.99, 120.12, 118.31, 57.16, 32.39, 31.00, 30.93. HRMS m/z [M-OAc$^-$]$^+$ calcd for C$_{24}$H$_{21}$BrN$^+$ 402.0857; Found 402.0873.

1-(3-phenylpropyl)-4-(p-tolyl)quinolin-1-ium acetate, 6-methyl-4-phenyl-1-(3-phenylpropyl)quinolin-1-ium acetate and 8-methyl-4-phenyl-1-(3-phenylpropyl)quinolin-1-ium acetate (**3k**): Prepared according to the general procedure and obtained as brown oil in 47 % yield (28.0 mg, 0.071 mmol). ^{1}H NMR (400 MHz, CDCl$_3$) δ 1H NMR (400 MHz, CDCl3) δ 10.34 (s, 1H), 8.24 (d, J = 8.5 Hz, 1H), 8.06 – 7.95 (m, 1H), 7.92 (dd, J = 9.4, 6.0 Hz, 3H), 7.82 (t, J = 7.6 Hz, 1H), 7.67 – 7.60 (m, 1H), 7.56 – 7.40 (m, 3H), 7.40 – 6.98 (m, 6H), 6.91 (d, J = 7.3 Hz, 1H), 5.30 – 5.21 (m, 2H), 3.80 (s), 3.59 (s), 2.91 (t, J = 7.1 Hz, 2H), 2.44 (s), 2.03 (s, 3H). ^{13}C NMR (101 MHz, CDCl3) δ 175.91, 158.94, 150.93, 139.85, 139.28, 137.81, 137.49, 137.04, 134.72, 134.63, 131.54, 130.61, 130.26, 130.16, 129.53, 129.33, 129.28, 129.06, 128.61, 128.46, 128.17, 127.91, 126.82, 126.67, 126.46, 122.96, 118.10, 92.85, 56.84, 55.31, 32.40, 31.15, 29.67, 22.66, 21.44, 21.29. HRMS m/z [M-OAc$^-$]$^+$ calcd for C$_{25}$H$_{24}$N$^+$ 338.1909; Found 338.1918.

1-(3-phenylpropyl)-4-(3-(trifluoromethyl)phenyl)quinolin-1-ium acetate, 4-phenyl-1-(3-phenylpropyl)-6-(trifluoromethyl)quinolin-1-ium acetate and 4-phenyl-1-(3-phenylpropyl)-8-(trifluoromethyl)quinolin-1-ium acetate (**3l**): Prepared according to the general procedure and obtained as brown oil in 26 % yield (15.3 mg, 0.039 mmol). ^{1}H NMR (400 MHz, CDCl$_3$) δ 10.24 – 10.18 (m, 1H), 8.04 (m, 2H), 7.95 – 7.68 (m, 4H), 7.64 – 6.98 (m, 5H), 5.23 – 5.14 (m, 2H), 2.84 (t, J = 6.9 Hz, 2H), 2.46 – 2.34 (m, 2H), 1.99 (s, 3H). ^{19}F NMR (376 MHz, CDCl$_3$) -62.43, -62.48, -62.70. ^{13}C NMR (101 MHz, CDCl3) δ 156.59, 151.17, 139.52, 137.85, 137.68, 135.33, 134.91, 133.01, 132.84, 131.83, 130.09, 129.85, 128.60, 128.41, 128.34, 127.86, 127.38, 126.50, 126.12, 123.24, 122.81, 118.26, 57.16, 43.28, 32.27, 30.82, 29.68. HRMS m/z [M-OAc$^-$]$^+$ calcd for C$_{25}$H$_{21}$F$_3$N$^+$ 392.1626; Found 392.1635.

4-phenyl-1-propylquinolin-1-ium acetate (**5a**): Prepared according to the general procedure and obtained as brown oil in 32 % yield (14.7 mg, 0.048 mmol). ^{1}H NMR (400 MHz, CDCl$_3$) δ 10.28 (s, 1H), 8.28 – 8.18 (m, 2H), 8.15 – 8.07 (m, 1H), 7.91 – 7.80 (m, 1H), 7.53 (d, J = 6.3 Hz, 2H), 7.28 (d, J = 7.9 Hz, 2H), 7.15 (t, J = 7.3 Hz, 1H), 5.14 (s, 2H), 3.57 (s, 2H), 2.07 (s, 3H), 1.05 (t, J = 6.8 Hz, 3H). ^{13}C NMR (101 MHz, CDCl3) δ 158.55, 150.84, 137.89, 137.74, 134.71, 130.76, 129.67, 129.47, 129.41, 129.24, 128.56, 128.15, 127.93, 125.68, 122.99, 118.35, 58.94, 29.66, 23.34, 10.85. HRMS m/z [M-OAc$^-$]$^+$ calcd for C$_{18}$H$_{18}$N$^+$ 248.1439; Found 248.1450.

7-methyl-1-propyl-4-(p-tolyl)quinolin-1-ium acetate (**5b**): Prepared according to the general procedure and obtained as brown oil in 38 % yield (19.1 mg, 0.057 mmol). ^{1}H NMR (400 MHz, CDCl$_3$) δ 10.45 (s, 1H), 8.19 (d, J = 8.7 Hz, 1H), 7.98 (s, 1H), 7.87 (s, 1H), 7.67 (d, J = 8.7 Hz, 1H), 7.22 (d, J = 7.7 Hz, 1H), 6.97 (d, J = 7.7 Hz, 1H), 5.21 (s, 2H), 2.76 (s, 3H), 2.52 (s, 2H), 2.17 – 2.08 (m, 3H), 1.12 (t, J = 7.3 Hz, 3H). ^{13}C NMR (101 MHz, CDCl3) δ 158.42, 150.24, 146.83, 141.35, 138.33, 132.02, 131.43, 129.98, 129.66, 129.32, 129.01, 128.60, 126.41, 121.91, 117.25, 58.53, 29.66, 23.29, 22.79, 21.44, 10.90. HRMS m/z [M-OAc$^-$]$^+$ calcd for C$_{20}$H$_{22}$N$^+$ 276.1752; Found 276.1768.

7-chloro-4-(4-chlorophenyl)-1-propylquinolin-1-ium acetate (**5c**): Prepared according to the general procedure, not isolated. HRMS m/z [M-OAc$^-$]$^+$ calcd for C$_{18}$H$_{16}$Cl$_2$N$^+$ 316.0660; Found 316.0679.

6-methyl-1-propyl-4-(m-tolyl)quinolin-1-ium acetate and 8-methyl-1-propyl-4-(m-tolyl)quinolin-1-ium acetate (**5d**): Prepared according to the general procedure and obtained as brown oil in 32 % yield (23.5 mg, 0.048 mmol). Major product: ^{1}H NMR (400 MHz, $CDCl_3$) δ 10.32 (s, 1H), 8.19 (d, J = 9.0 Hz, 1H), 8.02 (s, 1H), 7.97 (d, J = 8.9 Hz, 1H), 7.58 – 7.49 (m, 1H), 7.47 (d, J = 7.7 Hz, 2H), 7.45 – 7.31 (m, 3H), 5.25 (s, 2H), 2.57 (s, 3H), 2.18 (m, 2H), 2.07 (s, 3H), 1.15 (t, J = 7.1 Hz, 3H).^{13}C NMR (101 MHz, CDCl3) δ HRMS m/z $[M\text{-}OAc^-]^+$ calcd for $C_{20}H_{22}N^+$ 276.1752; Found 276.1768.

4-(4-fluorophenyl)-1-propylquinolin-1-ium-7-olate (**8a**): Prepared according to the general procedure and obtained as brown oil in 21 % yield (8.9 mg, 0.032 mmol). ^{1}H NMR (500 MHz, CDCl3) δ 7.80 (d, J = 6.6 Hz, 1H), 7.58 (d, J = 9.6 Hz, 1H), 7.49 – 7.41 (m, 2H), 7.27 (d, J = 12.9 Hz, 4H), 6.73 (s, 1H), 6.67 (d, J = 6.5 Hz, 1H), 4.32 – 4.18 (m, 2H), 2.11 – 2.00 (m, 7H). ^{19}F NMR (376 MHz, $CDCl_3$) -110.98. ^{13}C NMR (126 MHz, CDCl3) δ 139.46, 131.36, 131.06, 130.99, 129.03, 116.12, 115.95, 111.23, 100.70, 57.54, 29.68, 21.17, 11.09.. HRMS m/z $[M+H]^+$ calcd for $C_{18}H_{17}FON^+$ 282.1294; Found 282.1308.

4-(4-fluorophenyl)-1-(3-(4-fluorophenyl)propyl)quinolin-1-ium-7-olate (**8b**): Prepared according to the general procedure and obtained as brown oil in 67 % yield (37.7 mg, 0.101 mmol). ^{1}H NMR (400 MHz, CDCl3) δ 7.72 (d, J = 6.5 Hz, 1H), 7.58 (d, J = 9.6 Hz, 1H), 7.48 – 7.40 (m, 2H), 7.30 – 7.22 (m, 3H), 7.18 (dd, J = 8.4, 5.4 Hz, 2H), 7.08 (dd, J = 9.6, 1.8 Hz, 1H), 7.01 (t, J = 8.6 Hz, 2H), 6.78 (s, 1H), 6.65 (d, J = 6.4 Hz, 1H), 4.31 (t, J = 7.4 Hz, 2H), 2.79 (t, J = 7.5 Hz, 2H), 2.35 (p, J = 7.6 Hz, 2H). ^{13}C NMR (101 MHz, CDCl3) δ 164.37, 162.44, 151.62, 142.94, 139.39, 134.85, 132.31, 130.76, 130.68, 129.36, 128.83, 120.39, 115.86, 115.65, 115.30, 115.10, 111.40, 100.33, 55.09, 31.53, 29.36, 28.70. HRMS m/z $[M+H]^+$ calcd for $C_{25}H_{19}F_2ON^+$ 376.1512; Found 376.1527.

Acknowledgements

This work was supported by European Funding: Horizon 2020-MSCA (ITN-EJD CATMEC 14/06-721223). The contribution of COST Action CA15106 (C-H Activation in Organic Synthesis - CHAOS) is also gratefully acknowledged. Moreover, we are thankful to the human and technical support provided by the IZO-SGI SGIker of UPV/EHU.

Keywords: C-H activation • Quinolinium • C-C bond formation • C-N bond formation • multicomponent reactions • DFT calculations

[1] P. Kittakoop, C. Mahidol, S. Ruchirawat, *Curr. Top. Med. Chem.* **2013**, *14*, 239–252.

[2] P. Yadav, K. Shah, *Bioorg. Chem.* **2021**, 104639.

[3] D. Utreja, S. Sharma, A. Goyal, K. Kaur, S. Kaushal, *Curr. Org. Chem.* **2019**, *23*, 2271–2294.

[4] D. D. Xuan, *Curr. Org. Synth.* **2019**, *16*, 671–708.

[5] M. Austin, O. J. Egan, R. Tully, A. C. Pratt, *Org. Biomol. Chem.* **2007**, *5*, 3778–3786.

[6] S. D. Friis, M. J. Johansson, L. Ackermann, *Nat. Chem.* **2020**, *12*, 511–519.

[7] V. G. Zaitsev, D. Shabashov, O. Daugulis, *J. Am. Chem. Soc.* **2005**, *127*, 13154–13155.

[8] Y. Liu, H. Ge, *Nat. Chem.* **2017**, *9*, 26–32.

[9] T. Tanaka, K. I. Okunaga, M. Hayashi, *Tetrahedron Lett.* **2010**, *51*, 4633–4635.

[10] P. Ruiz-Castillo, S. L. Buchwald, *Chem. Rev.* **2016**, *116*, 12564–12649.

[11] O. Van Den Berg, W. F. Jager, S. J. Picken, *J. Org. Chem.* **2006**, *71*, 2666–2676.

[12] R. W. Counts, *J. Comput. Aided. Mol. Des.* **1987**, *1*, 177–178.

[13] Y. F. Yang, X. Hong, J. Q. Yu, K. N. Houk, *Acc. Chem. Res.* **2017**, *50*, 2853–2860.

[14] J. J. Gair, B. E. Haines, A. S. Filatov, D. G. Musaev, J. C. Lewis, *Chem. Sci.* **2017**, *8*, 5746–5756.

[15] Y. Q. Chen, Z. Wang, Y. Wu, S. R. Wisniewski, J. X. Qiao, W. R. Ewing, M. D. Eastgate, J. Q. Yu, *J. Am. Chem. Soc.* **2018**, *140*, 17884–17894.

WILEY-VCH

WILEY-VCH
Korr

Supporting Information for

Synthesis of substituted alkyl quinoliniums from propylamine and its derivatives

by

Martin Pauze, Enrique Gómez-Bengoa*

M. Pauze, E. Gómez-Bengoa, Department of Organic Chemistry I, Faculty of Chemistry, University of the Basque Country, UPV-EHU, 20018 Donostia - San Sebastian, Spain

Korr

Synthesis of 3-aryl-propylamine:

t-BuOK (5.66 g, 50.0 mmol) was added to a stirred solution of anhydrous THF containing the substituted benzaldehyde (42.0 mmol) and 2-diethoxyphosphorylacetonitrile (8.10 g, 6.0 mmol) at 0 °C for 30 min. Then, the reaction was maintained at 25 °C for a further 30 min. The mixture was extracted with ethyl acetate and the combined organics were washed with brine, dried over magnesium sulfate, and concentrated, flash column chromatography was done to recover the pure corresponding acrylonitrile (90:10, hexane/ethyl acetate). Then, the acrylonitrile was dissolve in 100 ml of a solution of 5 % ammonia in methanol (v:v), and hydrogenated with 50 bars, 70 °C, 1 ml/min with Raney nickel as catalyst on a flow hydrogenation reactor. The solvent was remove under vacuum, and product obtained without any further purification.

Synthesis of the quinoliniums:

In a sealed tube, was added, a stirring bar, palladium acetate (6.7 mg, 0.03mmol), silver oxide (140 mg, 0.6 mmol) and the corresponding iodoaryl (0.6 mmol). Then, 1 ml of water followed by 1 ml of acetic acid was added, and finally the amine (0.3 mmol). The tube was closed with a seal cap, and heated at 130 °C for 60h. The crude mixture was cooled down to room temperature, 5 ml of methanol was added, and then filtered on cotton to remove salts. To the solution obtained, 5 g of silica were added and the solvent removed under vacuum. The silica was then washed with cyclohexane, then dichloromethane and finally acetone. The product was then remove from the silica by washing with methanol with 1 % (v:v) acetic acid. The solvents were removed under vacuum and the pure product obtained.

3-(p-tolyl)propan-1-amine (1b):

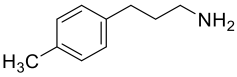

Prepared from 4-methylbenzaldehyde with the described method, isolated as a white solid, 75% yield after both steps. ^{1}H NMR (400 MHz, CDCl$_3$) δ 7.12 (s, 3H), 2.76 (t, *J* = 7.0 Hz, 2H), 2.69 – 2.57 (m, 2H), 2.35 (s, 3H), 1.79 (p, *J* = 7.5 Hz, 2H). ^{13}C NMR (101 MHz, CDCl$_3$) δ 138.9, 135.12, 129.0, 128.2, 41.7, 35.4, 32.7, 20.9. HRMS m/z [M+H]$^+$ calcd for $C_{10}H_{16}N+$ 150.1283; Found 150.1291.

3-(4-chlorophenyl)propan-1-amine (1c):

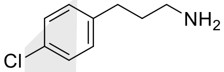

Prepared from 4-chlorobenzaldehyde with the described method, isolated as an white solid, 72% yield after both steps. ^{1}H NMR (400 MHz, CDCl$_3$) δ 7.35 – 7.19 (m, 2H), 7.14 (d, *J* = 8.5 Hz, 2H), 2.76 (t, *J* = 7.0 Hz, 2H), 2.69 – 2.60 (m, 2H), 1.89 – 1.68 (m, 2H). ^{13}C NMR (101 MHz, CDCl$_3$) δ 140.5, 131.5, 129.7, 128.4, 41.6, 35.2, 32.6. HRMS m/z [M+H]$^+$ calcd for $C_9H_{12}ClN+$ 169.0669; Found 169.0669.

3-(4-methoxyphenyl)propan-1-amine (1d):

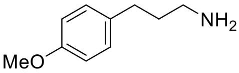

Prepared from 4-methoxybenzaldehyde with the described method, isolated as an off-white solid, 65% yield after both steps. ^{1}H NMR (400 MHz, CDCl$_3$) δ 7.13 (d, *J* = 8.5 Hz, 2H), 6.86 (d, *J* = 8.5 Hz, 2H), 3.82 (s, 3H), 2.75 (t, *J* = 7.0 Hz, 2H), 2.63 (t, *J* = 7.0 Hz, 2H), 1.77 (p, *J* = 7.5 Hz, 2H). Result in agreement with the literature.[1]

3-(4-fluorophenyl)propan-1-amine (6b):

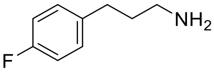

Prepared from 4-flurorobenzaldehyde with the described method, isolated as an off-white solid, 68% yield after both steps. ^{1}H NMR (400 MHz, CDCl3) δ 7.16 (dd, J = 8.5, 5.5 Hz, 2H), 7.07 – 6.89 (m, 2H), 2.75 (t, *J* = 7.0 Hz, 2H), 2.72 – 2.58 (m, 2H), 1.89 – 1.66 (m, 2H). ^{19}F NMR (376 MHz, CDCl$_3$) δ -117.91. ^{13}C NMR (101 MHz, CDCl$_3$) δ 161.2 (d, *J* = 243Hz), 129.6 13 (d, *J* = 7.5 Hz), 115.0 13 (d, *J* = 21.0 Hz), 41.66, 35.49, 32.42. HRMS m/z [M+H]$^+$ calcd for $C_9H_{12}FN^+$ 153.0954; Found 153.0950.

3-(2,6-difluorophenyl)propan-1-amine:

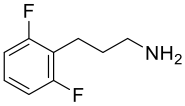

Prepared from 4-methoxybenzaldehyde with the described method, isolated as an oil, 71% yield after both steps. ^{1}H NMR (400 MHz, CDCl$_3$) δ 7.25 – 7.06 (m, 1H), 6.87 (t, *J* = 8.0 Hz, 2H), 2.77 (dt, *J* = 12.0, 7.5 Hz, 4H), 1.81 (p, *J* = 7.5 Hz, 2H). ^{19}F NMR (376 MHz, CDCl3) δ -116.1. ^{13}C NMR (101 MHz, CDCl3) δ 127.4 (t, *J* = 8.5 Hz), 111.0 (d, *J* = 8.0 Hz), 41.2, 32.5, 19.5. HRMS m/z [M+H]$^+$ calcd for $C_9H_{11}F_2N^+$ 171.0860; Found 171.0853.

---

[1] William F. McCalmont, Jaclyn R. Patterson, Michael A. Lindenmuth, Tiffany N. Heady, Doris M. Haverstick, Lloyd S. Gray, Timothy L. Macdonald. Bioorganic & Medicinal Chemistry, 13, 11, 2005, 3821-3839,

4-phenyl-1-(3-phenylpropyl)quinolin-1-ium acetate (3a):

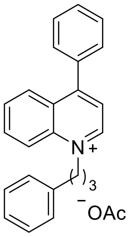

Prepared according to the general procedure and obtained as brown oil in 55 % yield (32 mg, 0.82 mmol). ^{1}H NMR (500 MHz, CD_3CN) δ 9.09 (d, 4.4 Hz, 1H), 8.39 (d, J = 8.9 Hz, 1H), 8.27 (d, J = 8.5 Hz, 1H), 8.23 (t, J = 8.0 Hz, 1H), 8.00 – 7.93 (t, J = 7.5 Hz, 1H), 7.89 (d, J = 4.5 Hz, 1H), 7.74 – 7.68 (m, 3H), 7.64 (m, 2H), 7.24 (d, J = 7.5 Hz, 5H), 5.03 (t, J = 7.0 Hz, 2H), 2.87 (t, J = 8.0 Hz, 2H), 2.47 – 2.43 (m, 2H), 1.97 (s, 3H). ^{13}C NMR (126 MHz, CD_3CN) δ 180.0, 160.3, 148.6, 140.9, 136.2, 136.1, 131.5, 130.9, 130.6, 130.2, 130.0, 130.0, 129.3, 129.0, 129.0, 127.1, 122.9, 119.6, 58.5, 32.8, 31.3. HRMS m/z $[M\text{-}OAc^-]^+$ calcd for $C_{24}H_{22}N^+$ 324.1700; Found 324.1745.

7-methyl-4-(p-tolyl)-1-(3-(p-tolyl)propyl)quinolin-1-ium acetate (3b):

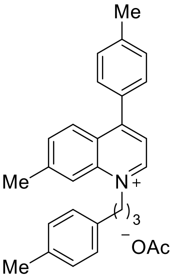

Prepared according to the general procedure and obtained as brown oil in 45 % yield (28.7 mg, 6.75 mmol). ^{1}H NMR (400 MHz, CD_3CN) δ 9.10 (d, J = 6.0 Hz, 1H), 8.16 (d, J = 9.0 Hz, 1H), 8.01 (s, 1H), 7.80 – 7.71 (m, 2H), 7.51 (s, 4H), 7.12 (d, J = 5.0 Hz, 2H), 7.03 (d, J = 8.0 Hz, 2H), 4.93 (t, J = 7.5 Hz, 2H), 2.80 (t, J = 7.5 Hz, 2H), 2.69 (s, 3H), 2.51 (s, 3H), 2.44 – 2.31 (m, 2H), 2.28 (s, 3H). ^{13}C NMR (126 MHz, CD_3CN) δ 175.4, 159.5, 148.4, 148.0, 142.0, 139.3, 137.8, 136.4, 135.4, 132.9, 132.5, 130.5, 130.4, 129.9, 129.7, 129.6, 129.3, 129.1, 128.8, 121.7, 57.7, 32.1, 31.1, 22.2, 21.0, 20.6, 20.60. HRMS m/z $[M\text{-}OAc^-]^+$ calcd for $C_{27}H_{28}N^+$ 366,2222; Found 366.2231.

7-chloro-4-(4-chlorophenyl)-1-(3-(4-chlorophenyl)propyl)quinolin-1-ium acetate (3c):

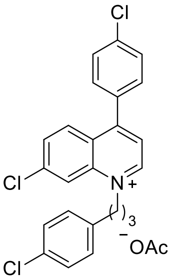

Prepared according to the general procedure, product not isolated. HRMS m/z [M-OAc$^-$]$^+$ calcd for $C_{24}H_{19}Cl_3N^+$ 426.0583 Found 426.0588.

7-methoxy-4-(4-methoxyphenyl)-1-(3-(4-methoxyphenyl)propyl)quinolin-1-ium hydroxyde (3d):

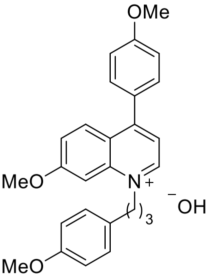

Prepared according to the general procedure and obtained as brown oil in 29 % yield (19.1 mg, 0.044 mmol). ^{1}H NMR (400 MHz,) δ 10.13 (d, *J* = 6.2 Hz, 1H), 8.14 (d, *J* = 9.4 Hz, 1H), 7.72 (d, *J* = 6.1 Hz, 1H), 7.49 (d, *J* = 8.5 Hz, 2H), 7.37 (d, *J* = 9.5 Hz, 2H), 7.29 (s, 1H), 7.21 – 7.16 (m, 3H), 7.12 (dd, *J* = 14.5, 8.5 Hz, 1H), 7.04 (s, 2H), 6.83 (t, *J* = 7.5 Hz, 6H), 5.30 – 5.07 (m, 2H), 4.15 – 3.64 (m, 3H), 2.80 – 2.50 (m, 3H), 2.00 (s, 3H), 1.90 – 1.77 (m, 2H). ^{13}C NMR (126 MHz, CD_3CN) δ 159.1, 151.6, 147.2, 132.5, 131.9, 122.6, 120.2, 116.5, 115.5, 115.5, 99.2, 57.5, 56.2, 56.0, 22.9. HRMS m/z [M-OH$^-$]$^+$ calcd for $C_{27}H_{28}NO_3^+$ 414.2069; Found 414.2048.

7-methyl-4-phenyl-1-(3-phenylpropyl)quinolin-1-ium acetate (3e):

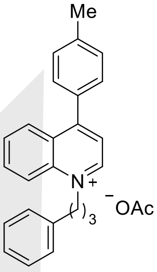

Prepared according to the general procedure and obtained as brown oil in 72 % yield (47.5 mg, 0.108 mmol). ^{1}H NMR (400 MHz, $CDCl_3$) δ 10.32 (d, *J* = 5.5 Hz, 1H), 8.29 (d, *J* = 8.5 Hz, 1H), 7.98 – 7.91 (m, 2H), 7.91 – 7.79 (m, 1H), 7.46 (s, 3H), 7.30 (d, *J* = 4.9 Hz, 5H), 7.27 – 7.04 (m, 6H), 5.35 – 5.26 (m, 2H), 2.95 (t, J = 7.0 Hz, 2H), 2.51 (d, J = 19.0 Hz, 5H), 2.30 (s, 1H), 2.09 (s, 3H). ^{13}C NMR (126 MHz, CDCl3) δ 161.8, 158.7, 151.2, 151.0, 141.5, 141.2, 139.9, 139.4, 138.6, 137.9, 134.8, 134.6, 134.2, 131.9, 131.5, 130.7, 130.5, 130.0, 129.7, 129.6, 129.4, 129.3, 129.2, 129.2, 128.8, 128.7, 128.6, 128.6, 128.8, 128.4, 128.4, 128.1, 128.1, 127.9, 126.6, 126.4, 126.09, 122.9, 121.6, 121.1, 120.8, 118.1, 117.1, 114.3, 56.6, 41.7, 33.2, 32.41 31.2, 29.7, 28.8, 21.5, 21.3, 20.9. HRMS m/z [M-OAc$^-$]$^+$ calcd for $C_{25}H_{24}N^+$ 338.1909; Found 338.1924.

1-(3-phenylpropyl)-4-(4-(trifluoromethyl)phenyl)quinolin-1-ium acetate and 4-phenyl-1-(3-phenylpropyl)-7-(trifluoromethyl)quinolin-1-ium acetate (3g):

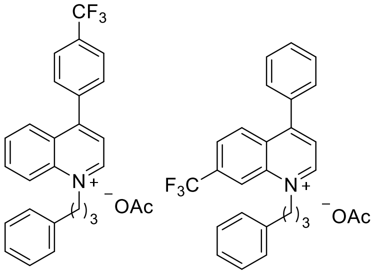

Prepared according to the general procedure and obtained as brown oil in 31 % yield (21.0 mg, 0.047 mmol). Mixture of 1:0.8. ^{1}H NMR (400 MHz, CDCl$_3$) δ 10.38 (d, J = 5.0 Hz, 1H), 8.10 (d, J = 8.5 Hz, 1H), 8.07 – 8.02 (m, 1H), 7.98 (d, J = 5.0 Hz, 1H), 7.90 (td, J = 13.4, 8.5 Hz, 4H), 7.67 (d, J = 8.0 Hz, 2H), 7.42 (q, J = 8.5 Hz, 4H), 7.34 – 7.17 (m, 8H), 5.29 – 5.21 (m, 2H), 2.90 (t, J = 7.0 Hz, 2H), 2.50 – 2.38 (m, 2H), 2.03 (s, 3H). ^{19}F NMR (376 MHz, CDCl$_3$) -62.29, -62.94. ^{13}C NMR (100 MHz, CDCl$_3$) δ 156.7, 151.3, 141.9, 139.6, 138.0, 137.7, 135.0, 132.9, 132.5, 130.9, 130.6, 130.0, 129.8, 129.8, 129.3, 128.8, 128.6, 128.5, 128.5, 128.4, 127.8, 127.5, 126.5, 126.2, 125.6, 124.7, 123.2, 122.9, 122.1, 122.0, 121.5, 118.3, 114.5, 57.1, 41.9, 33.2, 32.3, 31.0, 29.8. HRMS m/z [M-OAc$^-$]$^+$ calcd for $C_{25}H_{21}F_3N^+$ 392.1626; Found 392.1638.

4-(4-fluorophenyl)-1-(3-phenylpropyl)quinolin-1-ium acetate and 7-fluoro-4-phenyl-1-(3-phenylpropyl)quinolin-1-ium acetate (3h):

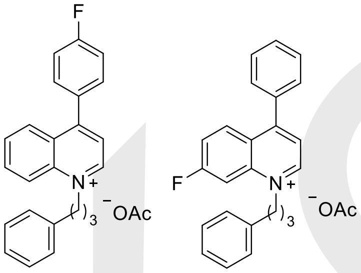

Prepared according to the general procedure and obtained as brown oil in 54 % yield (32.5 mg, 0.081 mmol). Mixture of 1:1. ^{1}H NMR (400 MHz, CDCl$_3$) δ 9.95 (d, J = 6.0 Hz, 1H), 8.19 (d, J = 8.5 Hz, 1H), 8.09 – 7.90 (m, 4H), 7.89 – 7.81 (m, 1H), 7.58 (dd, J = 8.5, 5.0

Hz, 2H), 7.40 – 7.12 (m, 2H), 6.91 (t, *J* = 8.7 Hz, 2H), 5.27 – 5.02 (m, 2H), 2.89 (t, *J* = 7.2 Hz, 2H), 2.49 – 2.37 (m, 2H), 2.03 (s, 3H). ^{19}F NMR (376 MHz, $CDCl_3$) -108.47, -116.60. ^{13}C NMR (100 MHz, $CDCl_3$) δ 176.8, 165.5, 163.0, 162.8, 160.4, 157.6, 1504., 139.7, 137.9, 134.8, 131.9, 131.8, 131.3, 130.9, 130.8, 129.6, 129.2, 129.0, 128.9, 128.6, 128.4, 128.1, 126.51, 123.1, 118.4, 116.7, 116.5, 115.1, 114.9, 57.2, 32.4, 31.0, 29.7, 21.7. HRMS m/z $[M\text{-}OAc^-]^+$ calcd for $C_{24}H_{21}FN^+$ 342.1658; Found 342.1668.

4-(4-chlorophenyl)-1-(3-phenylpropyl)quinolin-1-ium acetate and 7-chloro-4-phenyl-1-(3-phenylpropyl)quinolin-1-ium acetate (3i):

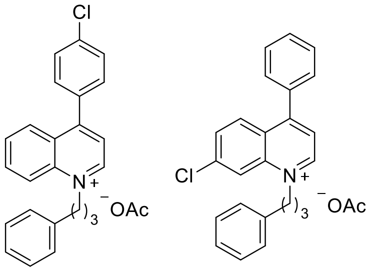

Prepared according to the general procedure and obtained as brown oil in 43 % yield (26.9 mg, 0.065 mmol). ^{1}H NMR (400 MHz, $CDCl_3$) δ 10.04 (s, 1H), 8.16 (d, *J* = 8.5 Hz, 1H), 8.02 (d, *J* = 7.5 Hz, 1H), 7.87 (m, 4H), 7.62 (d, *J* = 8.5 Hz, 2H), 7.49 (d, *J* = 8.5 Hz, 2H), 7.33 – 6.86 (m, 8H), 5.17 – 5.08 (m, 2H), 2.85 (t, *J* = 7.0 Hz, 2H), 2.45 – 2.35 (m, 2H), 2.03 (s, 3H). ^{13}C NMR (100 MHz, $CDCl_3$) δ 157.3, 150.8, 139.7, 137.8, 137.5, 134.8, 133.0, 132.1, 131.0, 130.9, 129.6, 128.8, 128.7, 128.4, 128.2, 128.0, 126.5, 123.1, 118.3, 57.2, 32.4, 31.0, 29.7. HRMS m/z $[M\text{-}OAc^-]^+$ calcd for $C_{24}H_{21}ClN^+$ 358.1363; Found 358.1371.

4-(4-bromophenyl)-1-(3-phenylpropyl)quinolin-1-ium acetate and 7-bromo-4-phenyl-1-(3-phenylpropyl)quinolin-1-ium acetate (3j):

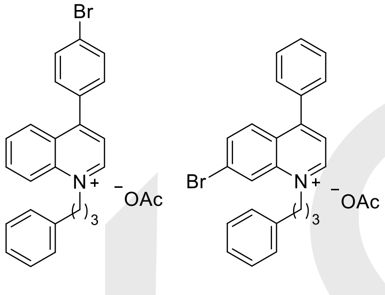

Prepared according to the general procedure and obtained as brown oil in 39 % yield (23.5 mg, 0.059 mmol). ^{1}H NMR (400 MHz, $CDCl_3$) δ 10.06 – 10.00 (m, 1H), 8.17 (d, *J* = 8.5 Hz, 1H), 8.03 (d, *J* = 7.5 Hz, 1H), 7.98 – 7.57 (m, 3H), 7.43 (d, *J* = 8.5 Hz, 1H), 7.38 – 7.17 (m, 3H), 7.13 (d, *J* = 8.0 Hz, 2H), 5.18 – 5.10 (m, 2H), 2.87 (t, *J* = 7.0 Hz, 2H), 2.46 – 2.34 (m, 2H), 2.02 (s, 3H). ^{13}C NMR (101 MHz, $CDCl_3$) δ 207.1, 176.2, 157.3, 150.7, 139.7, 137.8, 135.4, 134.9, 133.5, 132.6, 131.2, 131.1, 129.6, 129.4, 128.8, 128.7, 128.4, 127.9, 126.5, 125.8, 123.0, 120.1, 118.3, 57.2, 32.4, 31.0, 30.9. HRMS m/z [M-OAc$^-$]$^+$ calcd for $C_{24}H_{21}BrN^+$ 402.0857; Found 402.0873.

1-(3-phenylpropyl)-4-(p-tolyl)quinolin-1-ium acetate, 6-methyl-4-phenyl-1-(3-phenylpropyl)quinolin-1-ium acetate and 8-methyl-4-phenyl-1-(3-phenylpropyl)quinolin-1-ium acetate (3k):

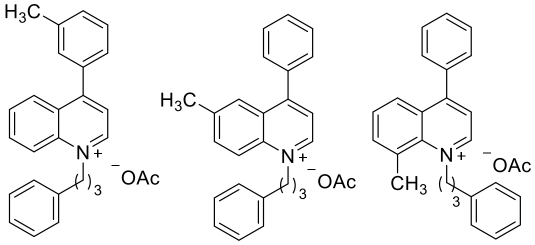

Prepared according to the general procedure and obtained as brown oil in 47 % yield (28.0 mg, 0.071 mmol). ^{1}H NMR (400 MHz, $CDCl_3$) δ 10.34 (s, 1H), 8.24 (d, *J* = 8.5 Hz, 1H), 8.06 – 7.95 (m, 1H), 7.92 (dd, *J* = 9.5, 6.0 Hz, 3H), 7.82 (t, *J* = 7.5 Hz, 1H), 7.67 – 7.60 (m, 1H), 7.56 – 7.40 (m, 3H), 7.40 – 6.98 (m, 6H), 6.91 (d, *J* = 7.0 Hz, 1H), 5.30 – 5.21 (m, 2H), 3.80 (s, 0.6H), 3.59 (s, 1.1H), 2.91 (t, *J* = 7.0 Hz, 2H), 2.51 (s, 2.3H), 2.44 (m, 2H), 2.03 (s, 3H). ^{13}C NMR (101 MHz, $CDCl_3$) δ 175.9, 158.9, 150.9, 139.9, 139.3, 137.8, 137.5, 137.0, 134.7, 134.6, 131.5, 130.6, 130.3, 130.2, 129.5, 129.3, 129.3, 129.1, 128.6, 128.5, 128.2, 127.9, 126.8, 126.7, 126.5, 123.0, 118.1, 92.9, 56.8, 55.3, 32.4, 31.2, 29.7, 22.7, 21.4, 21.3. HRMS m/z [M-OAc$^-$]$^+$ calcd for C25H24N+ 338.1909; Found 338.1918.

1-(3-phenylpropyl)-4-(3-(trifluoromethyl)phenyl)quinolin-1-ium acetate, 4-phenyl-1-(3-phenylpropyl)-6-(trifluoromethyl)quinolin-1-ium acetate and 4-phenyl-1-(3-phenylpropyl)-8-(trifluoromethyl)quinolin-1-ium acetate (3l):

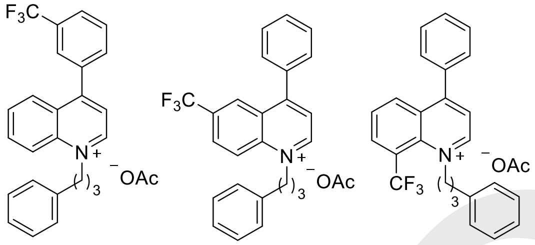

Prepared according to the general procedure and obtained as brown oil in 26 % yield (15.3 mg, 0.039 mmol). ^{1}H NMR (400 MHz, $CDCl_3$) δ 10.24 – 10.18 (m, 1H), 8.04 (m, 2H), 7.95 – 7.68 (m, 4H), 7.64 – 6.98 (m, 5H), 5.23 – 5.14 (m, 2H), 2.84 (t, *J* = 6.9 Hz, 2H), 2.46 – 2.34 (m, 2H), 1.99 (s, 3H). ^{19}F NMR (376 MHz, $CDCl_3$) -62.43, -62.48, -62.70. ^{13}C NMR (101 MHz, $CDCl_3$) δ 156.59, 151.17, 139.52, 137.85, 137.68, 135.33, 134.91, 133.01, 132.84, 131.83, 130.09, 129.85, 128.60, 128.41, 128.34, 127.86, 127.38, 126.50, 126.12, 123.24, 122.81, 118.26, 57.16, 43.28, 32.27, 30.82, 29.68. HRMS m/z [M-OAc$^-$]$^+$ calcd for $C_{25}H_{21}F_3N^+$ 392.1626; Found 392.1635.

4-phenyl-1-propylquinolin-1-ium hydroxyde (5a):

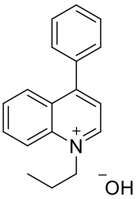

Prepared according to the general procedure and obtained as brown oil in 32 % yield (14.7 mg, 0.048 mmol). ^{1}H NMR (500 MHz, CD_3CN) δ 9.15 (d, *J* = 6.0 Hz, 1H), 8.49 (d, *J* = 9.0 Hz, 1H), 8.31 (dd, *J* = 8.6, 1.0 Hz, 1H), 8.26 (ddd, *J* = 8.8, 7.0, 1.4 Hz, 1H), 8.03 – 7.93 (m, 2H), 7.75 – 7.63 (m, 5H), 5.03 – 4.90 (t, *J* = 7.7 Hz, 2H), 2.15 (sex, *J* = 7.4 Hz, 2H), 1.10 (t, *J* = 7.4 Hz, 3H). ^{13}C NMR (126 MHz, CD_3CN) δ 160.16, 148.30, 136.06, 135.96, 131.34, 130.72, 130.40, 129.80, 129.73, 122.77, 119.52, 59.97, 23.52, 10.60. HRMS m/z $[M\text{-}OH^-]^+$ calcd for $C_{18}H_{18}N^+$ 248.1439; Found 248.1450.

7-methyl-1-propyl-4-(p-tolyl)quinolin-1-ium acetate (5b):

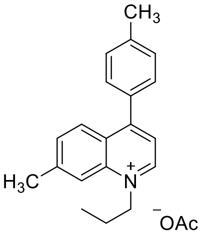

Prepared according to the general procedure and obtained as brown oil in 38 % yield (19.1 mg, 0.057 mmol). ^{1}H NMR (500 MHz, CD_3CN) δ 8.99 (d, *J* = 6.0 Hz, 1H), 8.25 (s, 1H), 8.23 (d, *J* = 9.0 Hz, 1H), 7.85 (d, *J* = 6.0 Hz, 1H), 7.82 (d, *J* = 8.0 Hz, 1H), 7.60 – 7.49 (m, 3H), 4.93 – 4.85 (t, 7.5 Hz, 2H), 2.76 (s, 3H), 2.52 (s, 3H), 2.13 (m, 2H), 1.09 (t, J = 7.5 Hz, 3H). ^{13}C NMR (101 MHz, $CDCl_3$) δ 158.4, 150.2, 146.8, 141.5, 138.3, 132.0, 131.4, 130.0, 129.7, 129.3, 129.0, 128.6, 126.4, 121.9, 117.3, 58.5, 29.7, 23.3, 22.8, 21.4, 10.9. HRMS m/z $[M\text{-}OAc^-]^+$ calcd for $C_{20}H_{22}N^+$ 276.1752; Found 276.1768.

7-chloro-4-(4-chlorophenyl)-1-propylquinolin-1-ium acetate (5c):

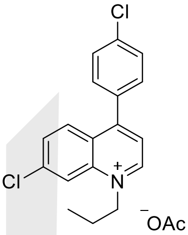

Prepared according to the general procedure and obtained as brown oil in 16% (9.0 mg, 0.024 mmol). ^{1}H NMR (500 MHz, CD_3CN) δ 9.21 (s, 1H), 8.56 (s, 1H), 8.24 (d, *J* = 9.0 Hz, 1H), 7.95 (d, *J* = 8.0 Hz, 2H), 7.73 (d, *J* = 8.0 Hz, 2H), 7.63 (d, *J* = 8.5 Hz, 2H), 4.93 (t, *J* = 7.5 Hz, 2H), 2.16 – 2.09 (m, 2H), 1.09 (t, *J* = 7.5 Hz, 3H). ^{13}C NMR (126 MHz, CD_3CN) δ 158.8, 138.3, 137.7, 133.9, 132.1, 131.7, 131.3, 131.2, 130.0, 128.5, 128.0, 123.1, 60.1, 23.5, 10.5. HRMS m/z [M-OAc$^-$]$^+$ calcd for $C_{18}H_{16}Cl_2N^+$ 316.0660; Found 316.0679.

6-methyl-1-propyl-4-(m-tolyl)quinolin-1-ium acetate and 8-methyl-1-propyl-4-(m-tolyl)quinolin-1-ium acetate (5d):

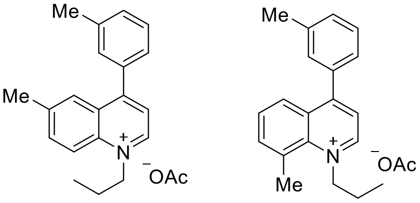

Prepared according to the general procedure not isolated. HRMS m/z [M-OAc$^-$]$^+$ calcd for $C_{20}H_{22}N^+$ 276.1752; Found 276.1768.

4-(4-fluorophenyl)-1-propylquinolin-1-ium-7-olate (8a):

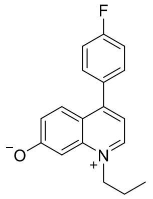

Prepared according to the general procedure and obtained as brown oil in 21 % yield (8.9 mg, 0.032 mmol). ^{1}H NMR (500 MHz, $CDCl_3$) δ 8.68 (s, 1H), 7.82 (d, *J* = 9.5 Hz, 1H), 7.63 (s, 1H), 7.51 (dd, *J* = 8.5, 5.2 Hz, 2H), 7.36 (d, *J* = 9.5 Hz, 1H), 7.33 – 7.26 (m, 2H), 7.23 (s, 1H), 4.66 (s, 2H), 2.11 (d, *J* = 6.0 Hz, 2H), 1.08 (t, *J* = 7.0 Hz, 3H). ^{19}F NMR (471 MHz, $CDCl_3$) δ -109.49. ^{13}C NMR (126 MHz, $CDCl_3$) δ 163.9 (d, J = 250 Hz), 155.2, 143.4, 142.1, 131.8, 131.5 (d, *J* = 9 Hz), 129.8, 126.7, 121.8, 116.4 (d, *J* = 22 Hz), 115.6, 101.1, 58.7, 29.7, 22.1, 11.0. HRMS m/z [M+H]$^+$ calcd for $C_{18}H_{17}FON^+$ 282.1294; Found 282.1308.

4-(4-fluorophenyl)-1-(3-(4-fluorophenyl)propyl)quinolin-1-ium-7-olate (8b):

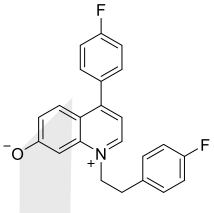

Prepared according to the general procedure and obtained as brown oil in 67 % yield (37.7 mg, 0.101 mmol). ^{1}H NMR (500 MHz, $CDCl_3$) δ 8.45 (s, 1H), 7.72 (d, J = 10.0 Hz, 1H), 7.49 – 7.41 (m, 2H), 7.31 – 7.23 (m, 5H), 7.15 (dd, *J* = 8.5, 5.5 Hz, 2H), 7.00 (d, *J* = 6.0 Hz, 1H), 6.92 (t, *J* = 8.5 Hz, 2H), 4.60 (t, *J* = 7.0 Hz, 3H), 2.80 (t, *J* = 7.5 Hz, 2H), 2.35 (p, *J* = 8.0 Hz, 3H). ^{19}F NMR (471 MHz, CDCl3) δ -109.95, -116.40. ^{13}C NMR (126 MHz, $CDCl_3$) δ 174.8, 163.8 (d, *J* = 250Hz), 161.7 (d, *J* = 242Hz), 154.3, 142.8, 142.6, 135.5, 135.5, 132.3, 131.5 (d, *J* = 8 Hz), 130.0 (d, *J* = 8 Hz), 128.5, 121.4, 116.5 (d, *J* = 21 Hz), 115.7 (d, J = 21 Hz), 114.5, 101.0, 77.5, 77.3, 77.0, 56.3, 32.0, 29.8. HRMS m/z $[M+H]^+$ calcd for $C_{25}H_{19}F_2ON^+$ 376.1512; Found 376.1527.

3-(p-tolyl)propan-1-amine (1b):

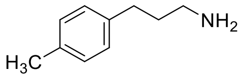

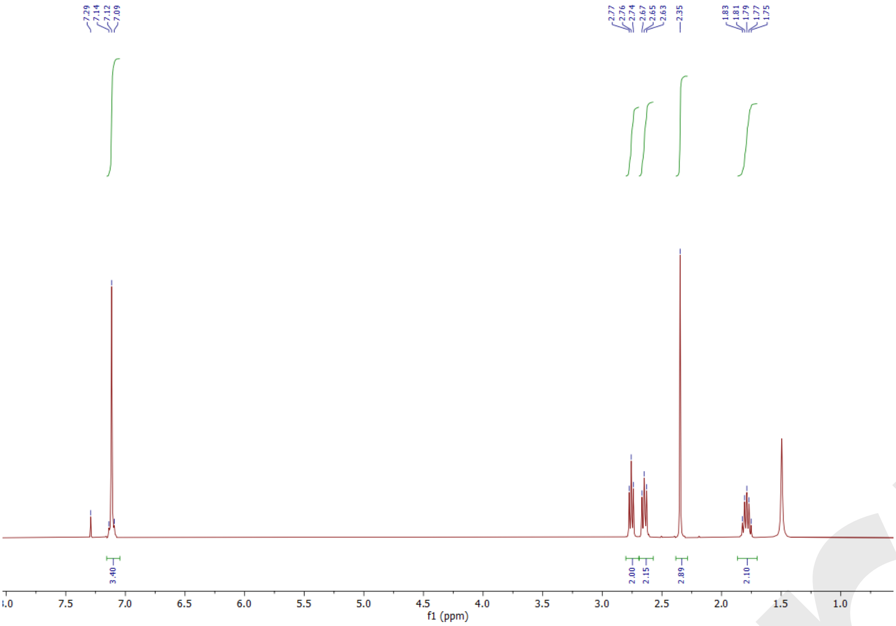

Kor

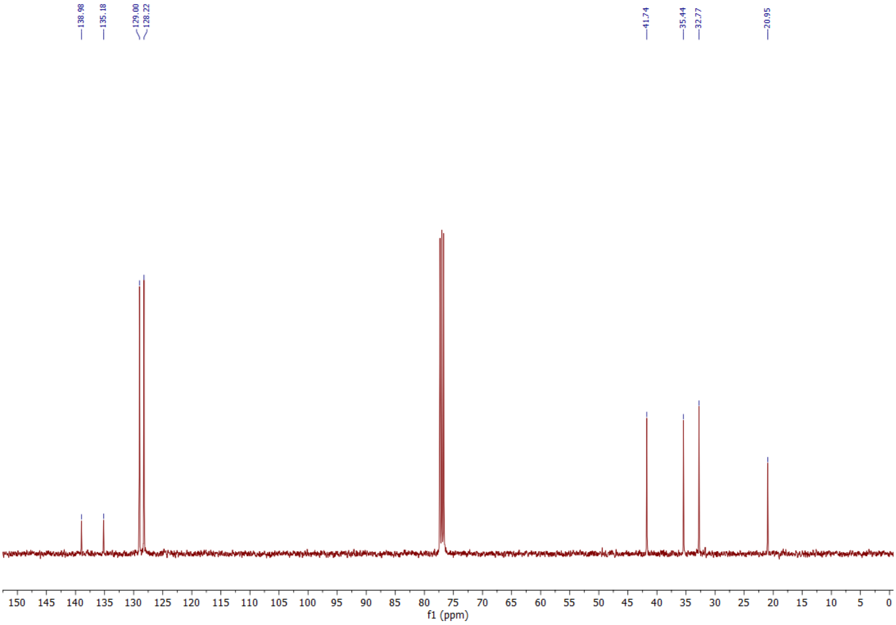

3-(4-chlorophenyl)propan-1-amine (1c):

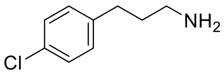

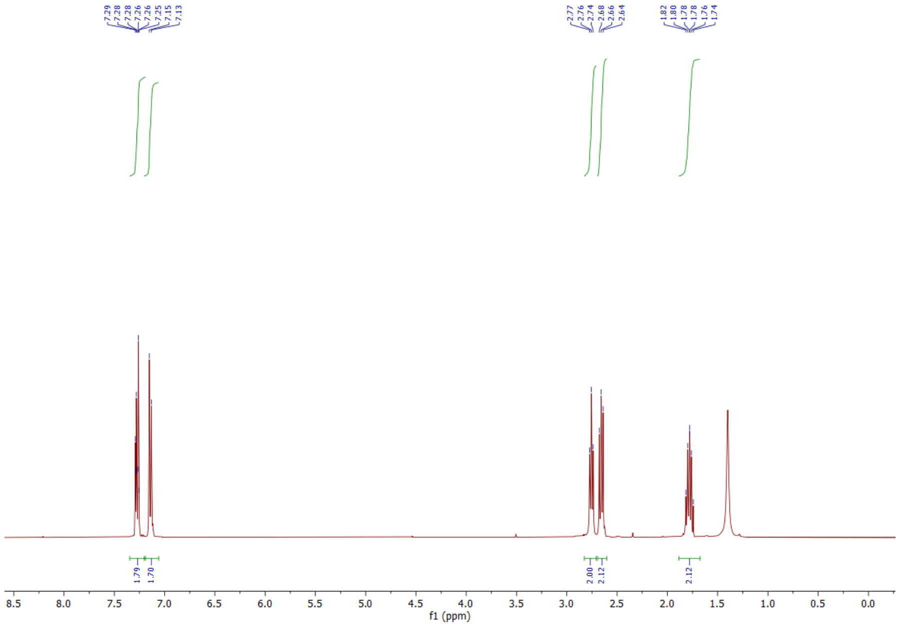

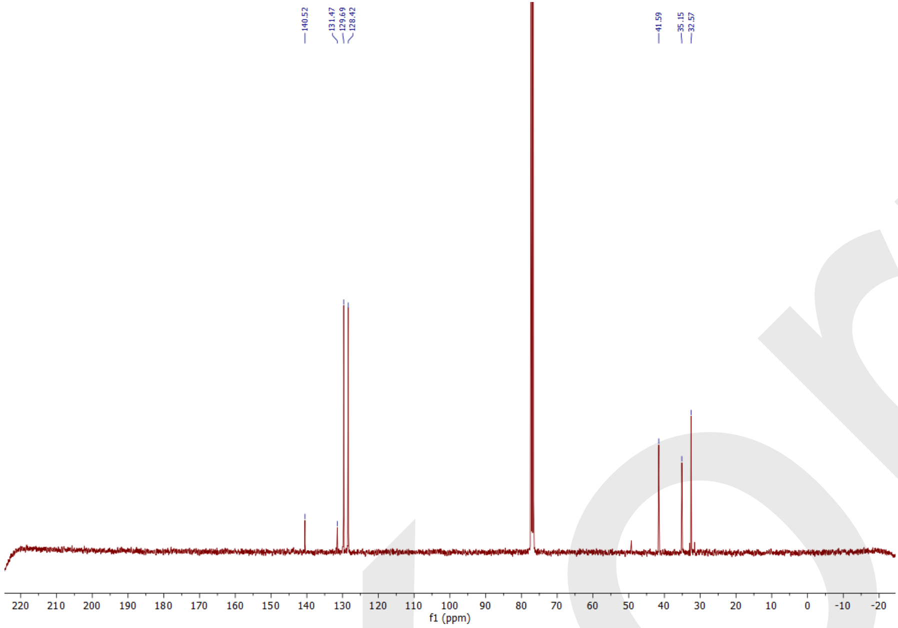

3-(4-methoxyphenyl)propan-1-amine (1d):

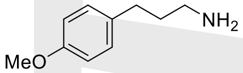

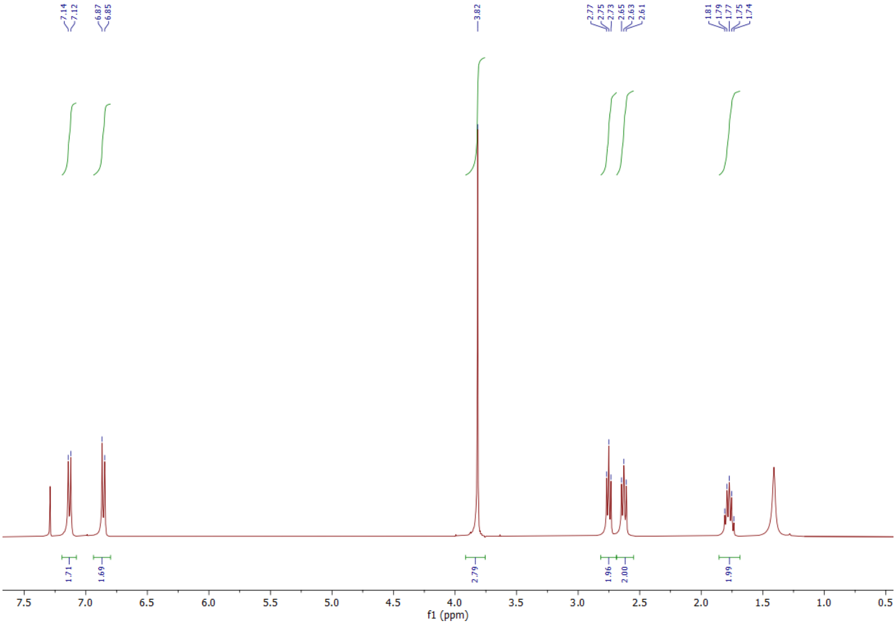

3-(4-fluorophenyl)propan-1-amine (6b):

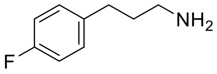

Korr

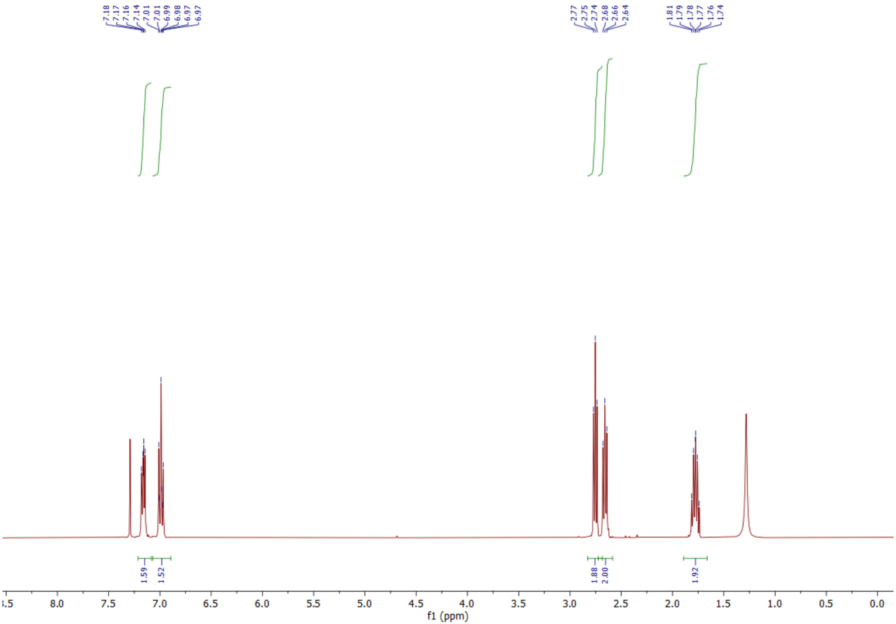
7.18
7.17
7.16
7.14
7.01
7.01
6.99
6.98
6.97
6.97
2.77
2.75
2.74
2.68
2.66
2.64
1.81
1.79
1.78
1.77
1.76
1.74
1.59
1.52
1.88
2.00
1.92
8.0
7.5
7.0
6.5
6.0
5.5
5.0
4.5
4.0
3.5
3.0
2.5
2.0
1.5
1.0
0.5
0.0
f1 (ppm)

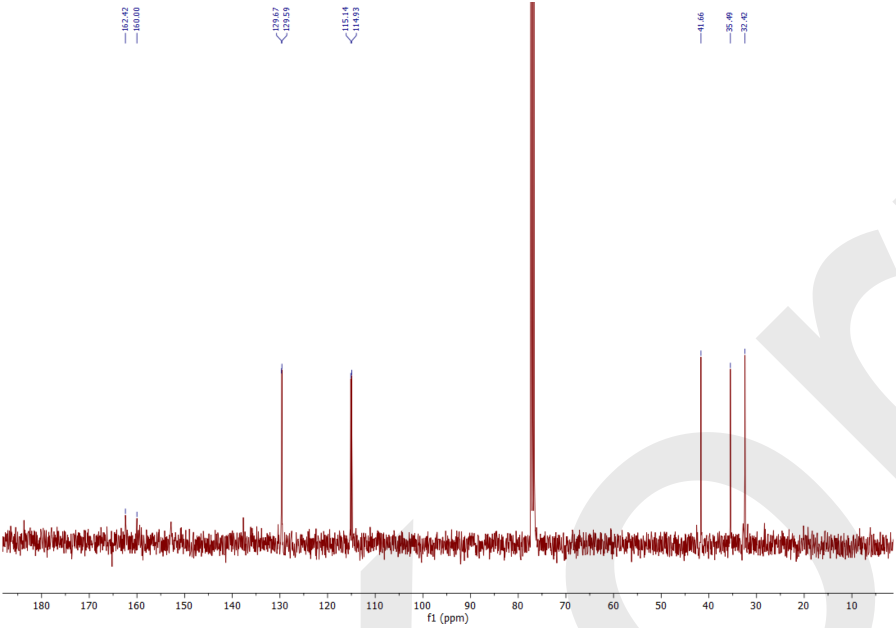
162.42
160.00
129.67
129.59
115.14
114.93
41.66
35.49
32.42
180
170
160
150
140
130
120
110
100
90
80
70
60
50
40
30
20
10
f1 (ppm)

kor

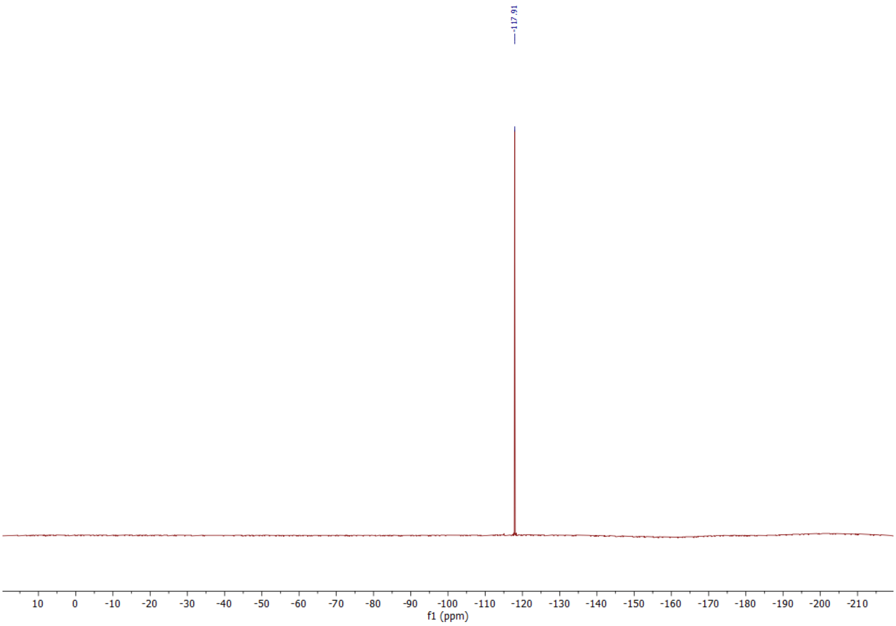

3-(2,6-difluorophenyl)propan-1-amine:

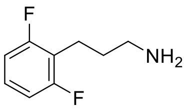

Korr

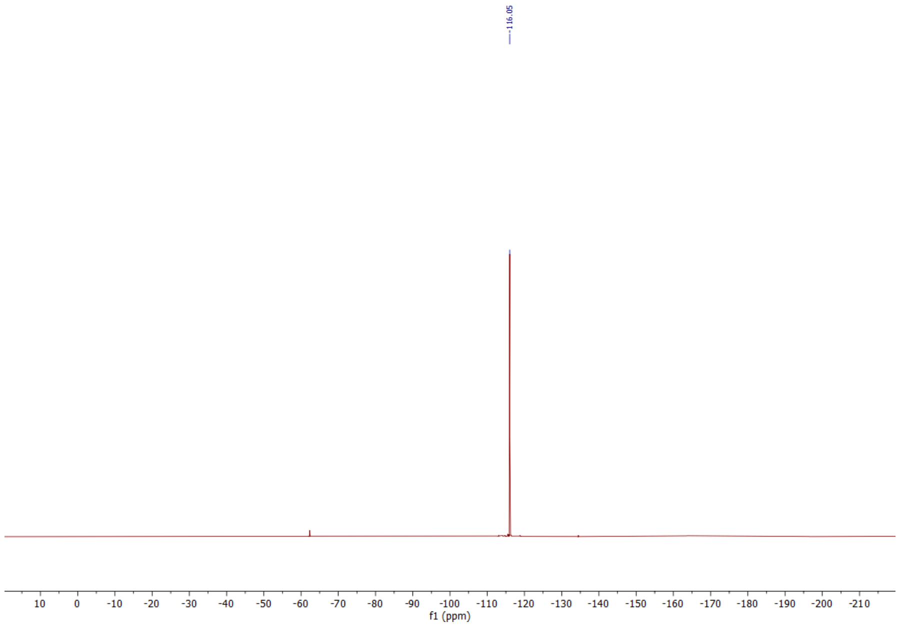
-116.05
10
0
-10
-20
-30
-40
-50
-60
-70
-80
-90
-100
-110
-120
-130
-140
-150
-160
-170
-180
-190
-200
-210
f1 (ppm)

Korr

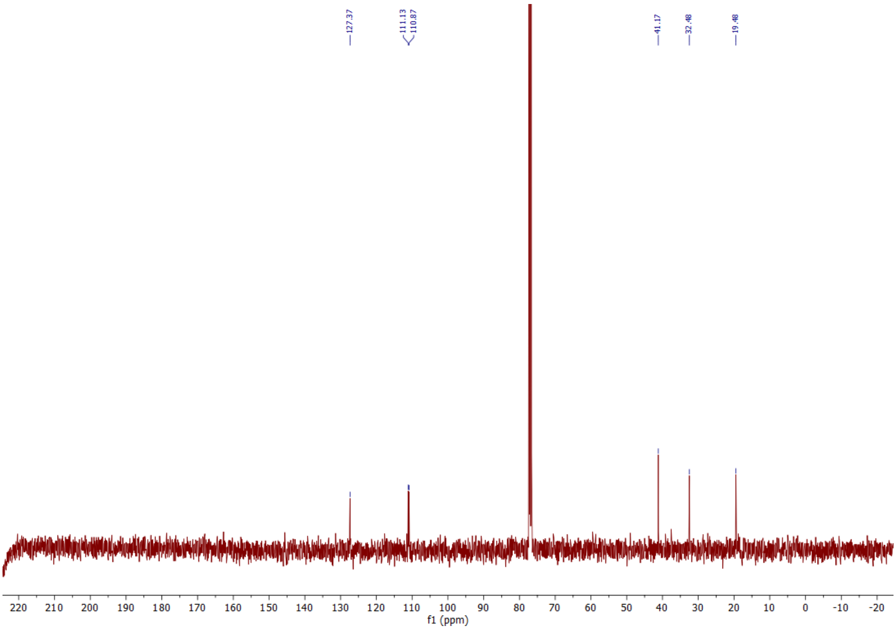

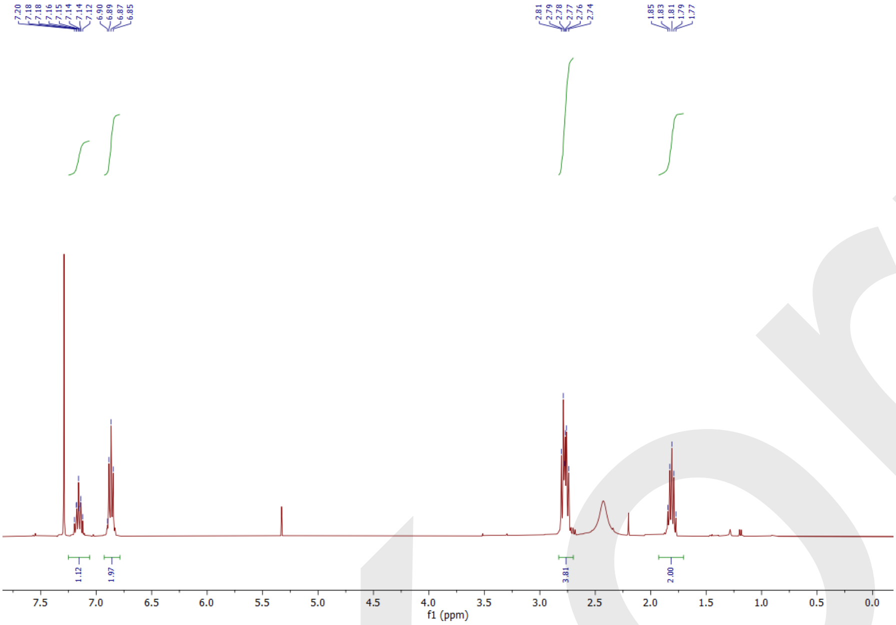

4-phenyl-1-(3-phenylpropyl)quinolin-1-ium acetate (3a):

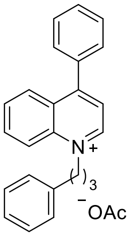

Korr

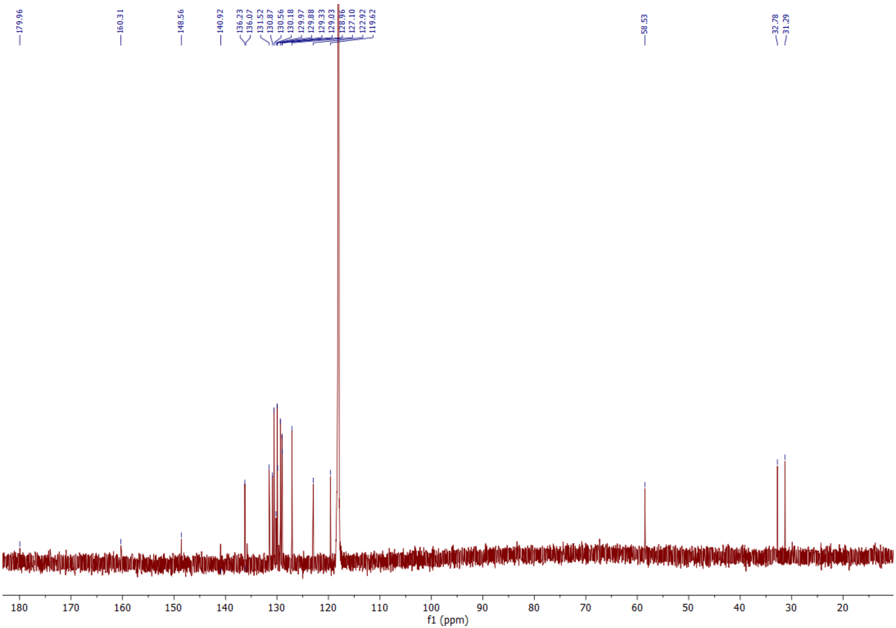

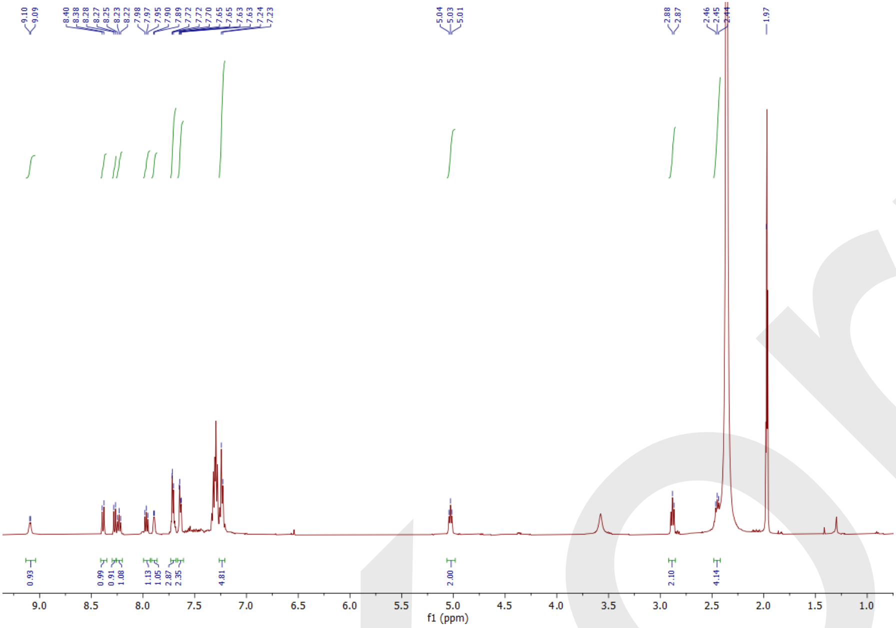

7-methyl-4-(p-tolyl)-1-(3-(p-tolyl)propyl)quinolin-1-ium acetate (3b):

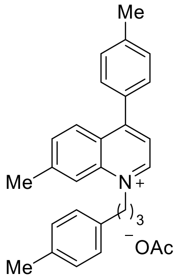
Me
Me
N+
( )3
−OAc
Me

Korr

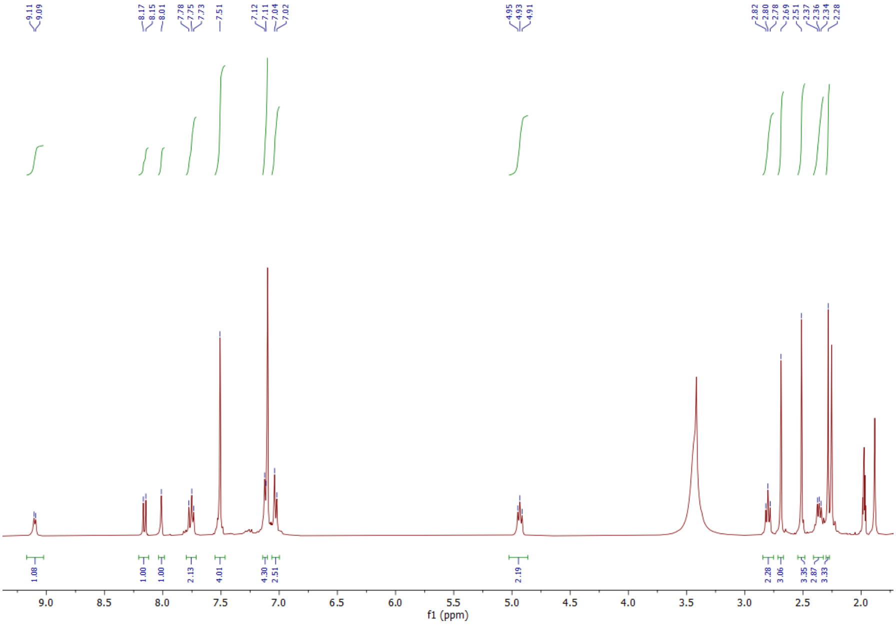
9.11
9.09
8.17
8.15
8.01
7.78
7.75
7.73
7.51
7.12
7.11
7.04
7.02
4.95
4.93
4.91
2.82
2.80
2.78
2.69
2.51
2.37
2.36
2.34
2.28
1.08
1.00
1.00
2.13
4.01
4.30
2.51
2.19
2.28
3.06
3.35
2.87
3.33
9.0
8.5
8.0
7.5
7.0
6.5
6.0
5.5
5.0
4.5
4.0
3.5
3.0
2.5
2.0
f1 (ppm)

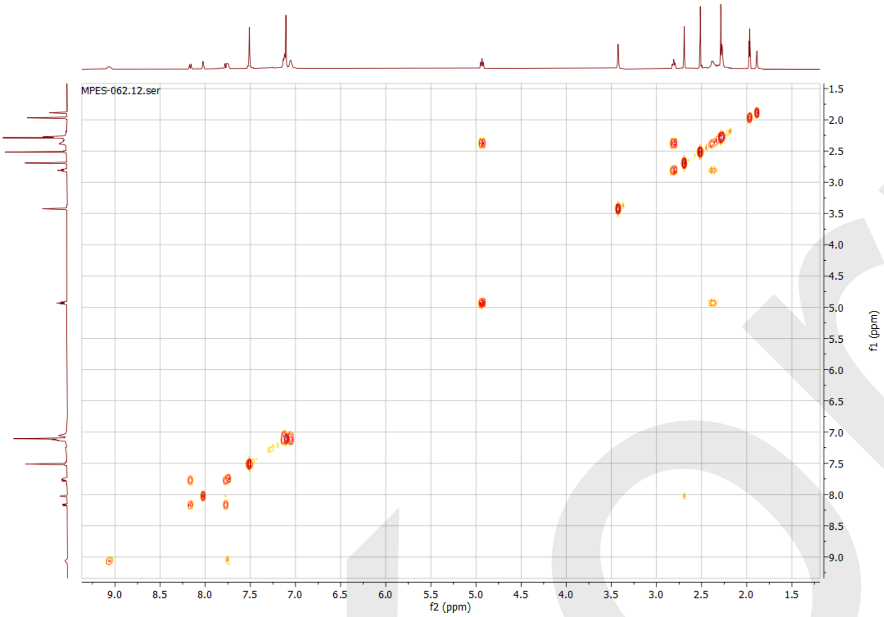
MPES-062.12.ser
1.5
2.0
2.5
3.0
3.5
4.0
4.5
5.0
5.5
6.0
6.5
7.0
7.5
8.0
8.5
9.0
f1 (ppm)
9.0
8.5
8.0
7.5
7.0
6.5
6.0
5.5
5.0
4.5
4.0
3.5
3.0
2.5
2.0
1.5
f2 (ppm)

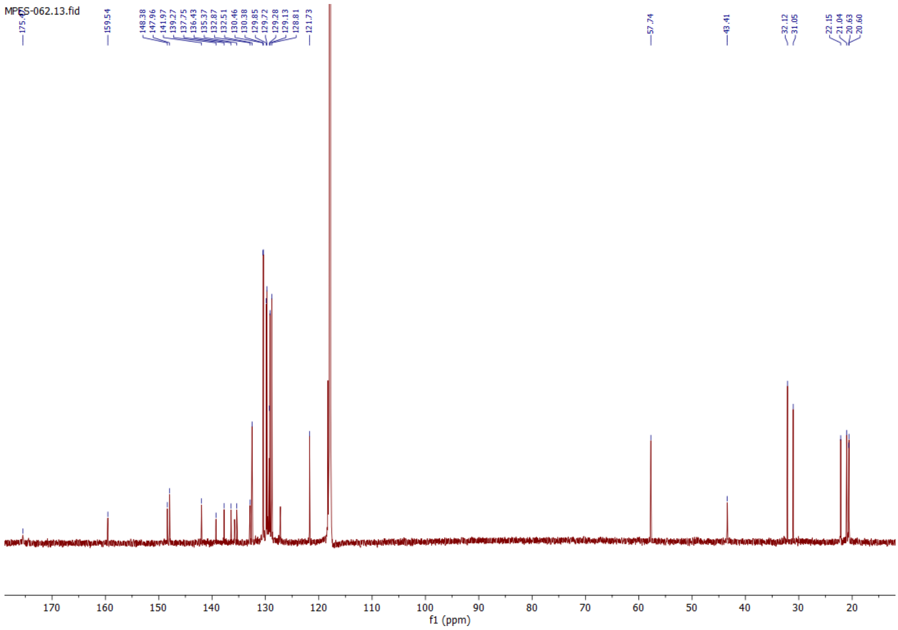

7-methoxy-4-(4-methoxyphenyl)-1-(3-(4-methoxyphenyl)propyl)quinolin-1-ium hydroxyde (3d):

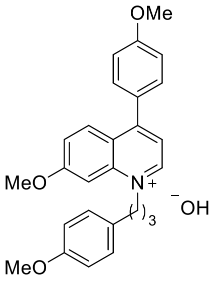
OMe
MeO
N+
3
−OH
MeO

Korr

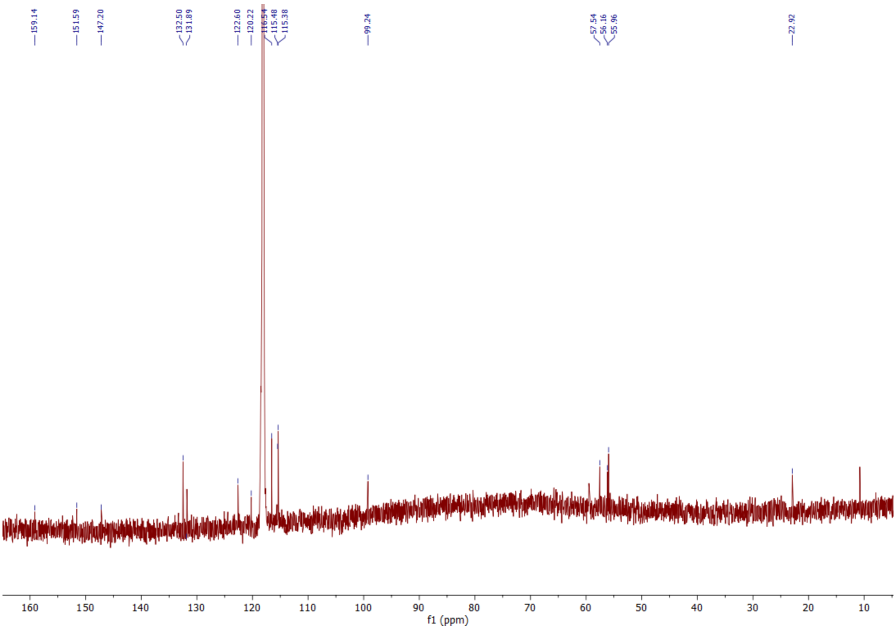

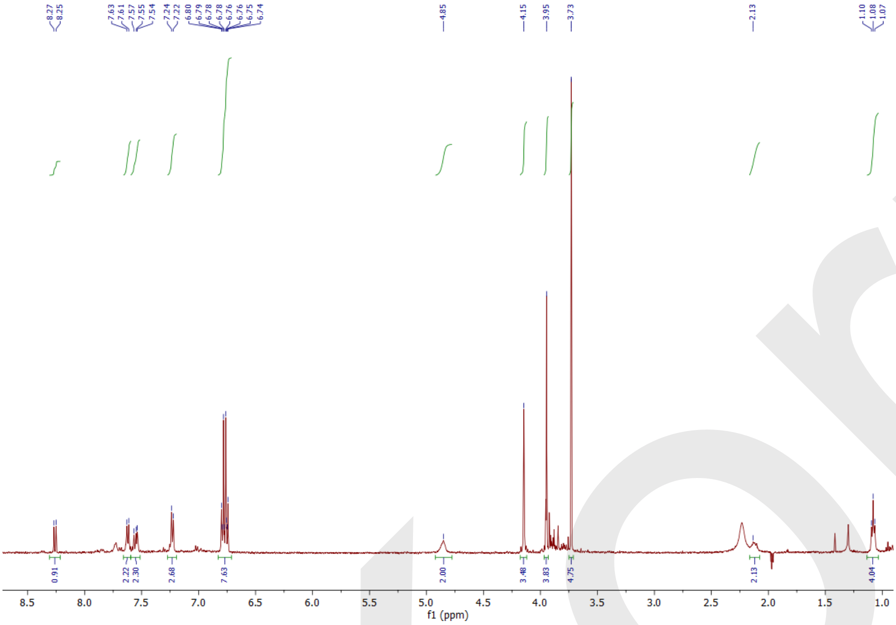

7-methyl-4-phenyl-1-(3-phenylpropyl)quinolin-1-ium acetate and 1-(3-phenylpropyl)-4-(p-tolyl)quinolin-1-ium acetate (3e):

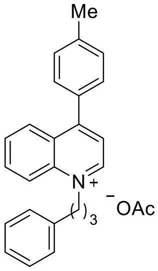

Kor

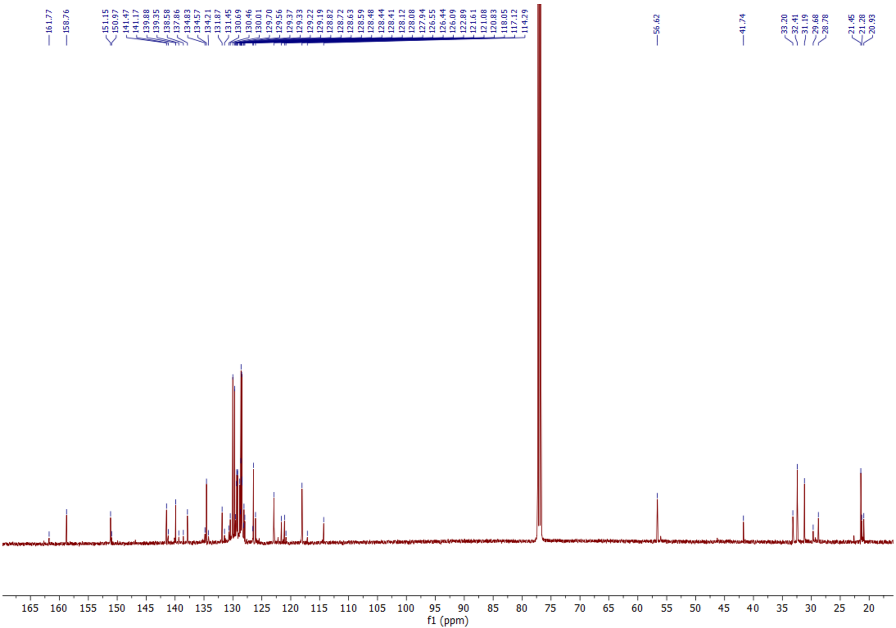

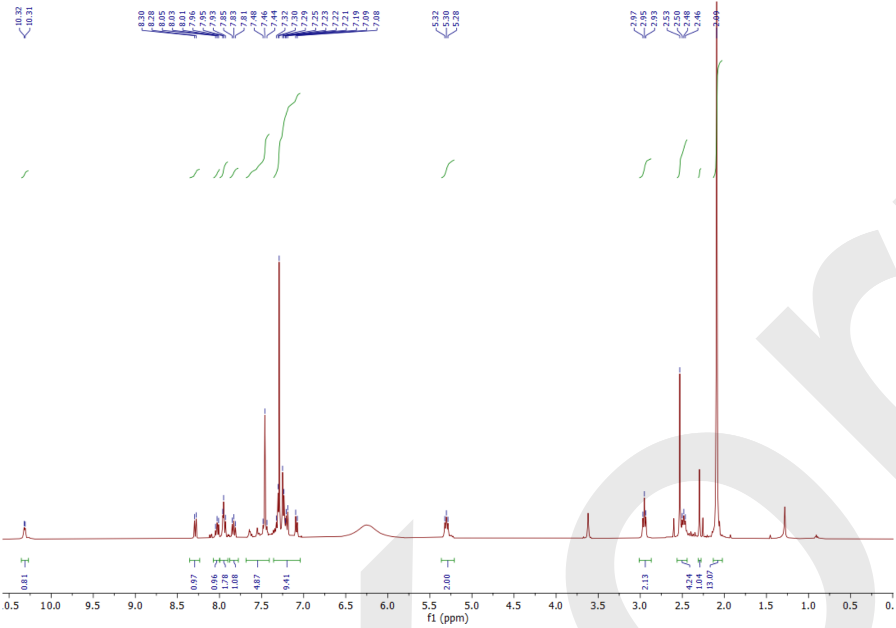

1-(3-phenylpropyl)-4-(4-(trifluoromethyl)phenyl)quinolin-1-ium acetate and 4-phenyl-1-(3-phenylpropyl)-7-(trifluoromethyl)quinolin-1-ium acetate (3g):

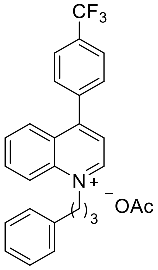

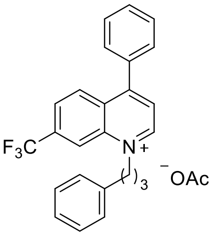

Korr

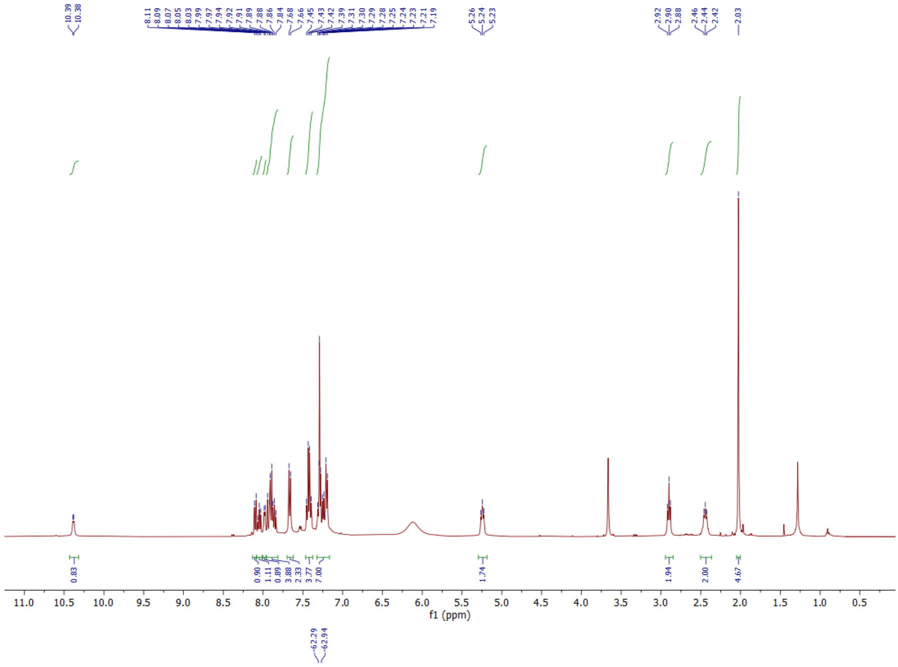
10.39
10.38
8.11
8.09
8.07
8.05
8.03
7.99
7.97
7.94
7.92
7.91
7.89
7.88
7.86
7.84
7.68
7.66
7.45
7.43
7.42
7.39
7.31
7.30
7.29
7.28
7.25
7.24
7.23
7.21
7.19
5.26
5.24
5.23
2.92
2.90
2.88
2.46
2.44
2.42
2.03
0.83
0.90
1.11
0.89
3.88
2.33
3.77
7.00
1.74
1.94
2.00
4.67
11.0
10.5
10.0
9.5
9.0
8.5
8.0
7.5
7.0
6.5
6.0
5.5
5.0
4.5
4.0
3.5
3.0
2.5
2.0
1.5
1.0
0.5
f1 (ppm)
-62.29
-62.94

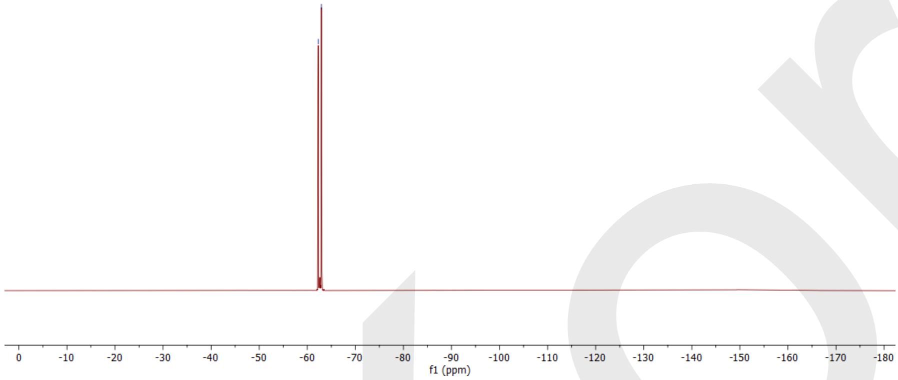
0
-10
-20
-30
-40
-50
-60
-70
-80
-90
-100
-110
-120
-130
-140
-150
-160
-170
-180
f1 (ppm)

Korr

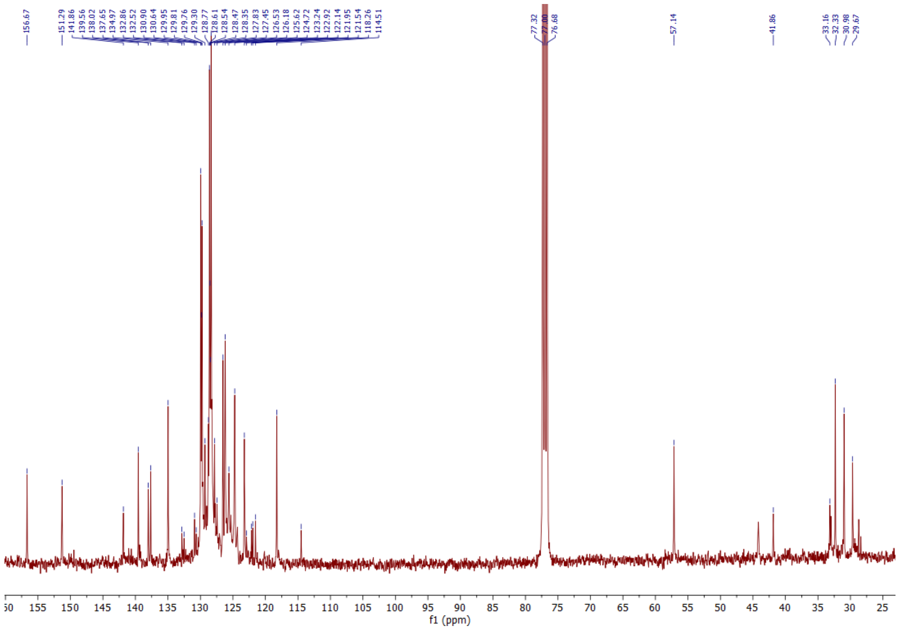

4-(4-fluorophenyl)-1-(3-phenylpropyl)quinolin-1-ium acetate and 7-fluoro-4-phenyl-1-(3-phenylpropyl)quinolin-1-ium acetate (3h):

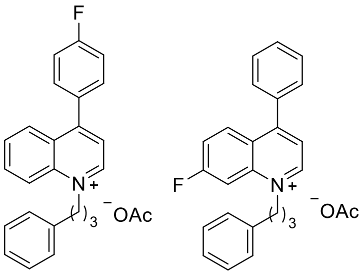
F
N+
3
‾OAc
F
N+
3
‾OAc

Kor

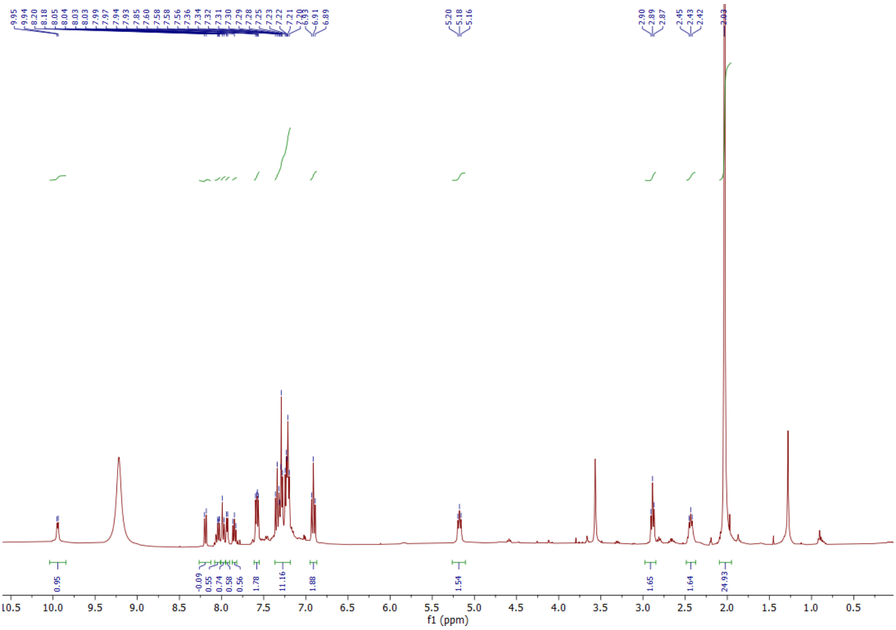
9.95
9.94
8.20
8.18
8.05
8.04
8.03
8.03
7.99
7.97
7.94
7.93
7.85
7.60
7.58
7.58
7.56
7.36
7.34
7.32
7.31
7.30
7.29
7.28
7.25
7.23
7.22
7.21
7.20
6.93
6.91
6.89
5.20
5.18
5.16
2.90
2.89
2.87
2.45
2.43
2.42
2.03
0.95
-0.09
0.55
0.74
0.58
0.56
1.78
11.16
1.88
1.54
1.65
1.64
24.93
10.5
10.0
9.5
9.0
8.5
8.0
7.5
7.0
6.5
6.0
5.5
5.0
4.5
4.0
3.5
3.0
2.5
2.0
1.5
1.0
0.5
f1 (ppm)

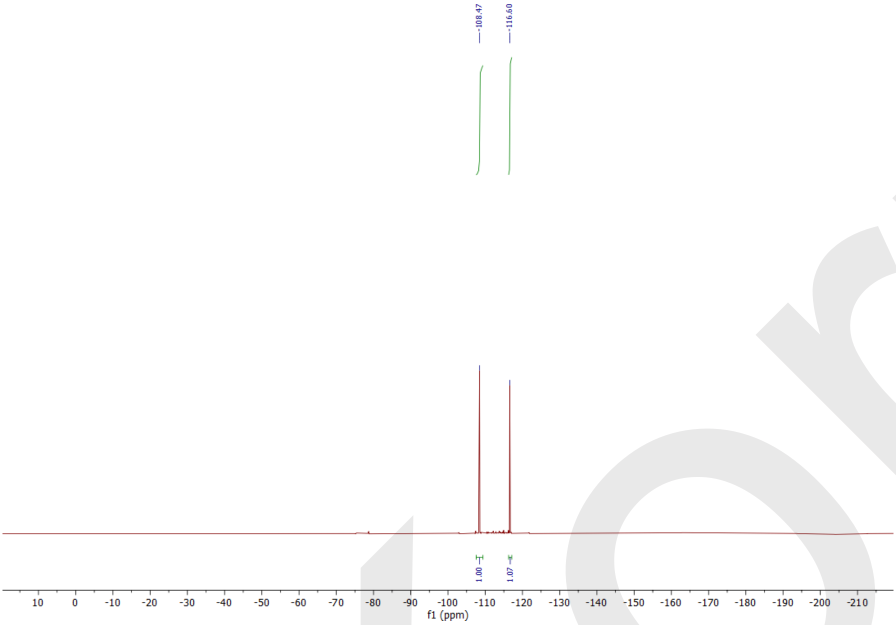
-108.47
-116.60
1.00
1.07
10
0
-10
-20
-30
-40
-50
-60
-70
-80
-90
-100
-110
-120
-130
-140
-150
-160
-170
-180
-190
-200
-210
f1 (ppm)

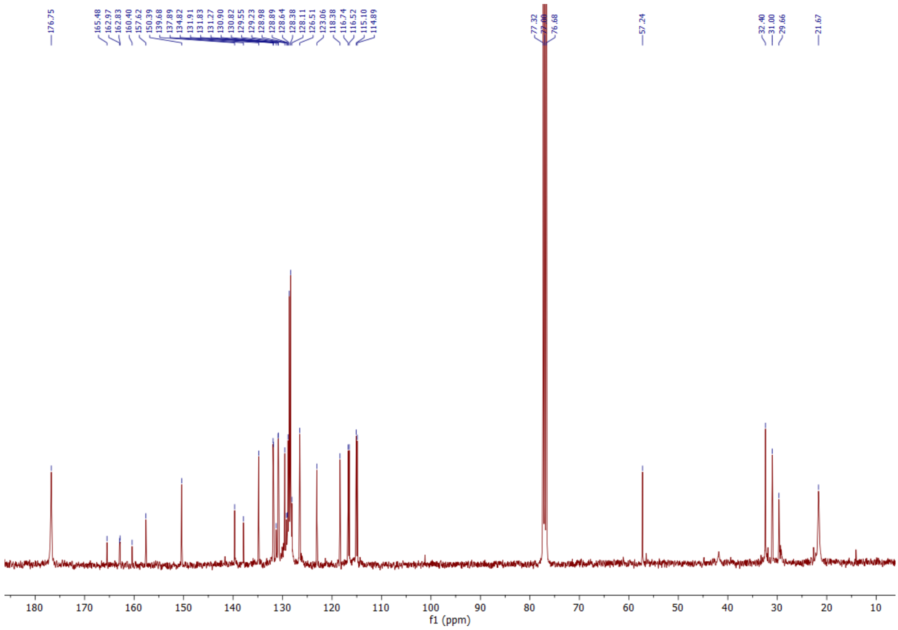

4-(4-chlorophenyl)-1-(3-phenylpropyl)quinolin-1-ium acetate and 7-chloro-4-phenyl-1-(3-phenylpropyl)quinolin-1-ium acetate (3i):

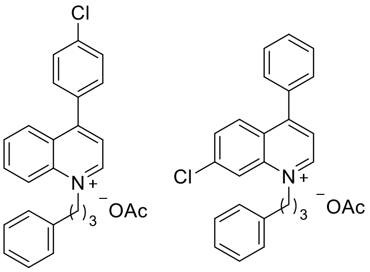
Cl
N+
( )3
−OAc
Cl
N+
( )3
−OAc

Kor

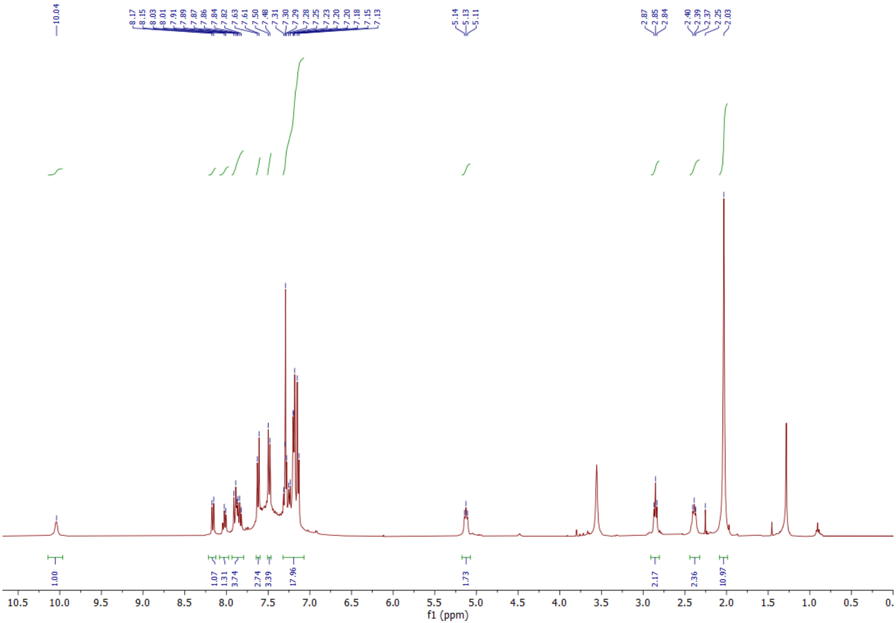

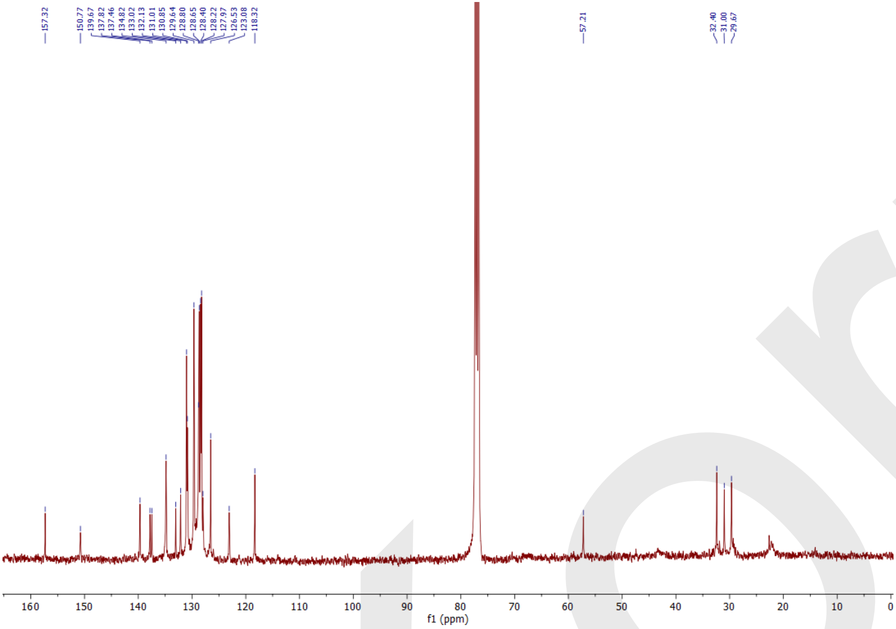

4-(4-bromophenyl)-1-(3-phenylpropyl)quinolin-1-ium acetate and 7-bromo-4-phenyl-1-(3-phenylpropyl)quinolin-1-ium acetate (3j):

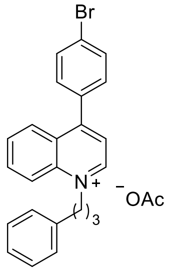

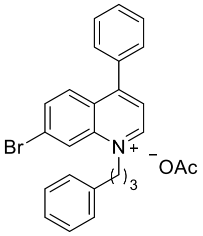

Korr

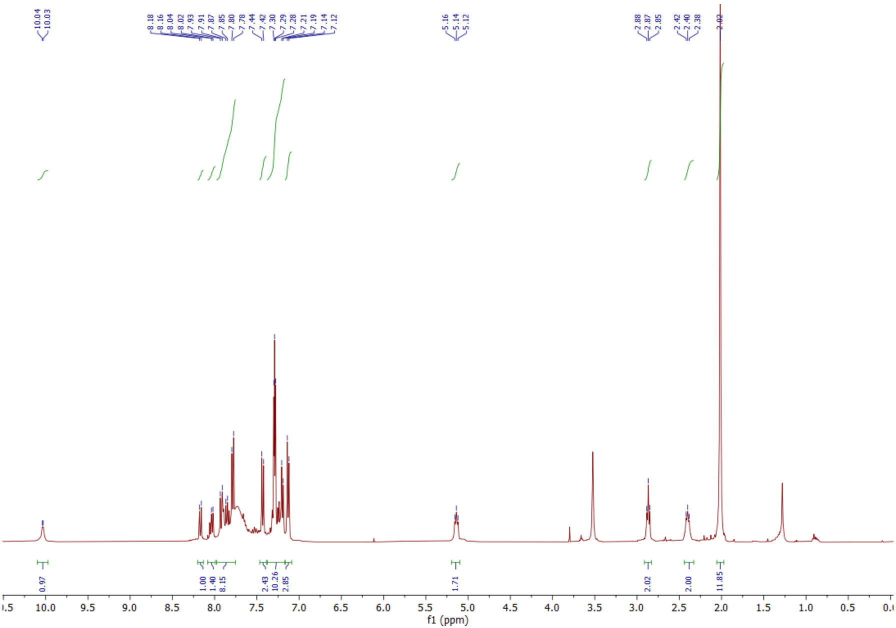

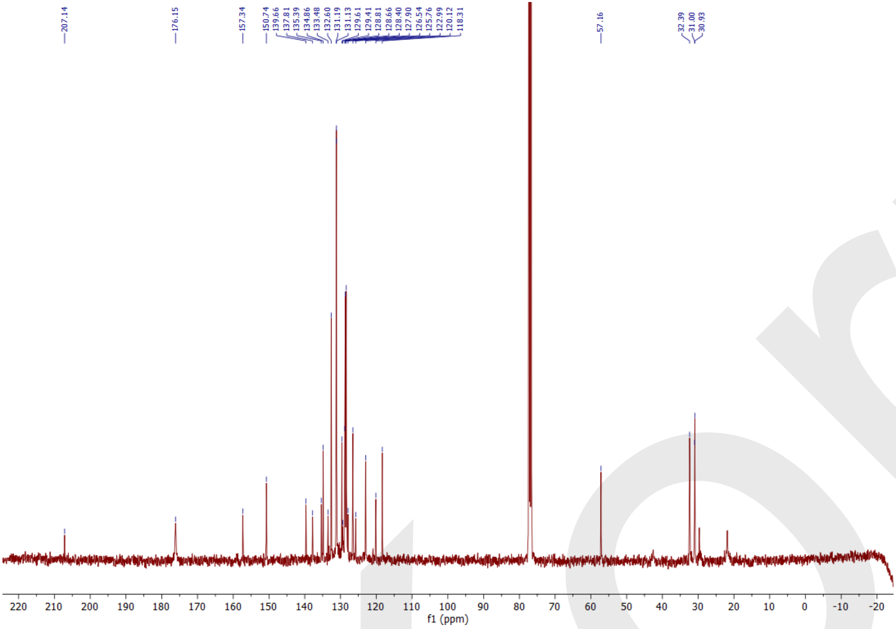

1-(3-phenylpropyl)-4-(p-tolyl)quinolin-1-ium acetate, 6-methyl-4-phenyl-1-(3-phenylpropyl)quinolin-1-ium acetate and 8-methyl-4-phenyl-1-(3-phenylpropyl)quinolin-1-ium acetate (3k):

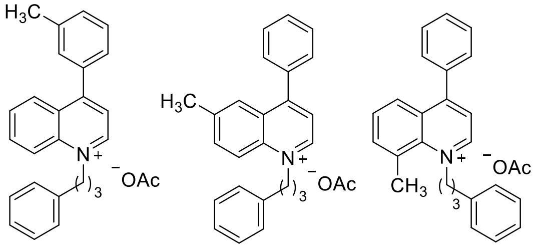
H3C
N+
−OAc
( )3
H3C
N+
−
( )3
OAc
N+
−OAc
CH3
( )3

Korr

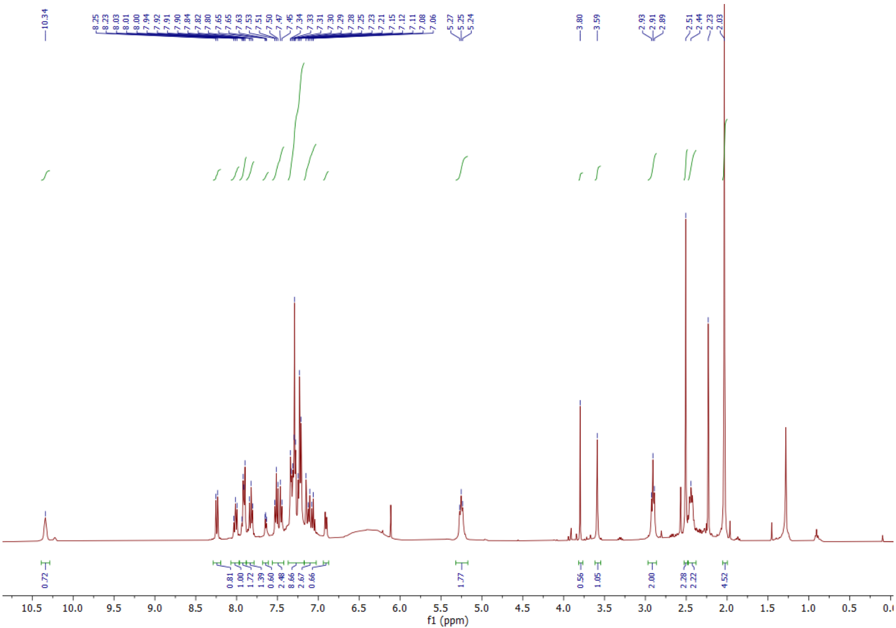

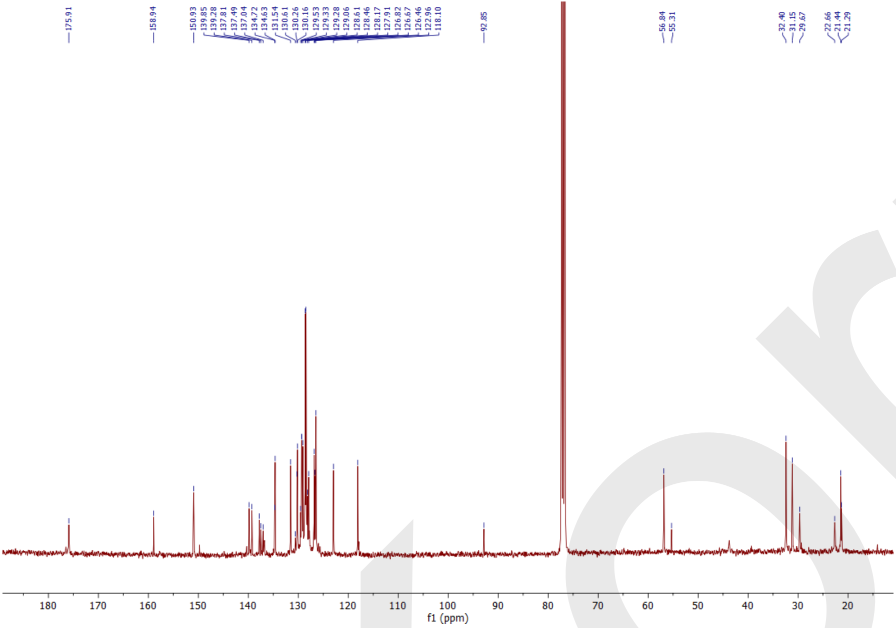

1-(3-phenylpropyl)-4-(3-(trifluoromethyl)phenyl)quinolin-1-ium acetate, 4-phenyl-1-(3-phenylpropyl)-6-(trifluoromethyl)quinolin-1-ium acetate and 4-phenyl-1-(3-phenylpropyl)-8-(trifluoromethyl)quinolin-1-ium acetate (3l):

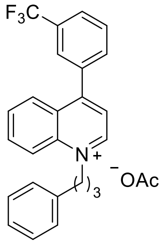

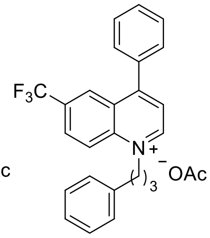

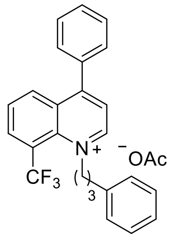

Korr

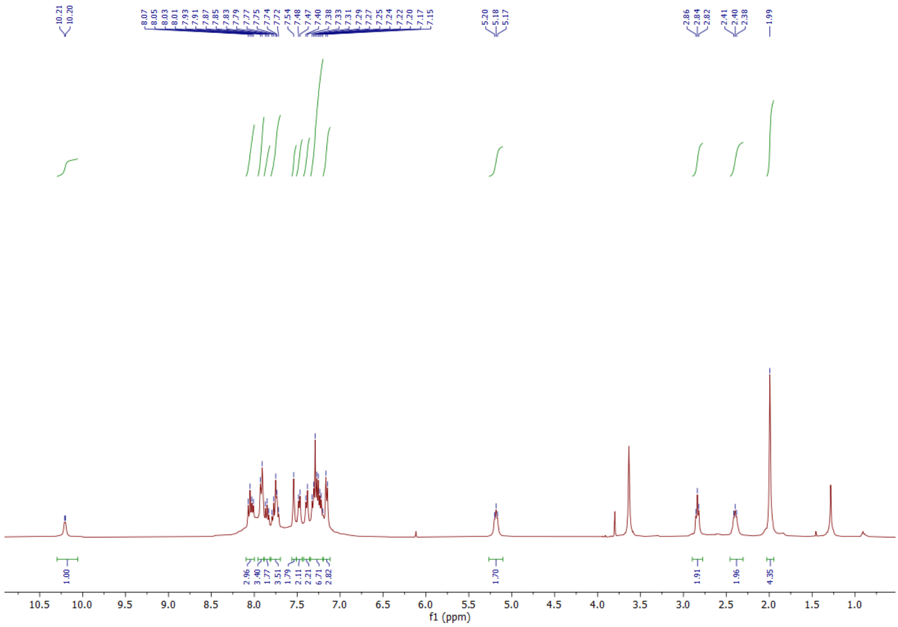
10.21
10.20
8.07
8.05
8.03
8.01
7.93
7.91
7.87
7.85
7.83
7.79
7.77
7.75
7.74
7.72
7.54
7.48
7.47
7.40
7.38
7.33
7.31
7.29
7.27
7.25
7.24
7.22
7.20
7.17
7.15
5.20
5.18
5.17
2.86
2.84
2.82
2.41
2.40
2.38
1.99
1.00
2.96
3.40
1.77
3.51
1.79
2.11
2.21
6.71
2.82
1.70
1.91
1.96
4.35
10.5
10.0
9.5
9.0
8.5
8.0
7.5
7.0
6.5
6.0
5.5
5.0
4.5
4.0
3.5
3.0
2.5
2.0
1.5
1.0
f1 (ppm)

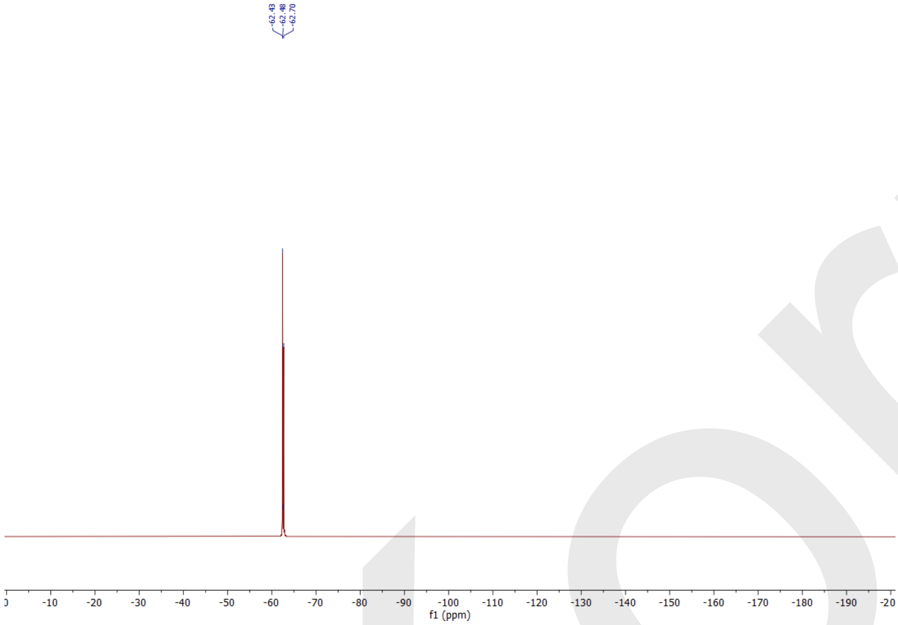
-62.43
-62.48
-62.70
0
-10
-20
-30
-40
-50
-60
-70
-80
-90
-100
-110
-120
-130
-140
-150
-160
-170
-180
-190
-20
f1 (ppm)

korr

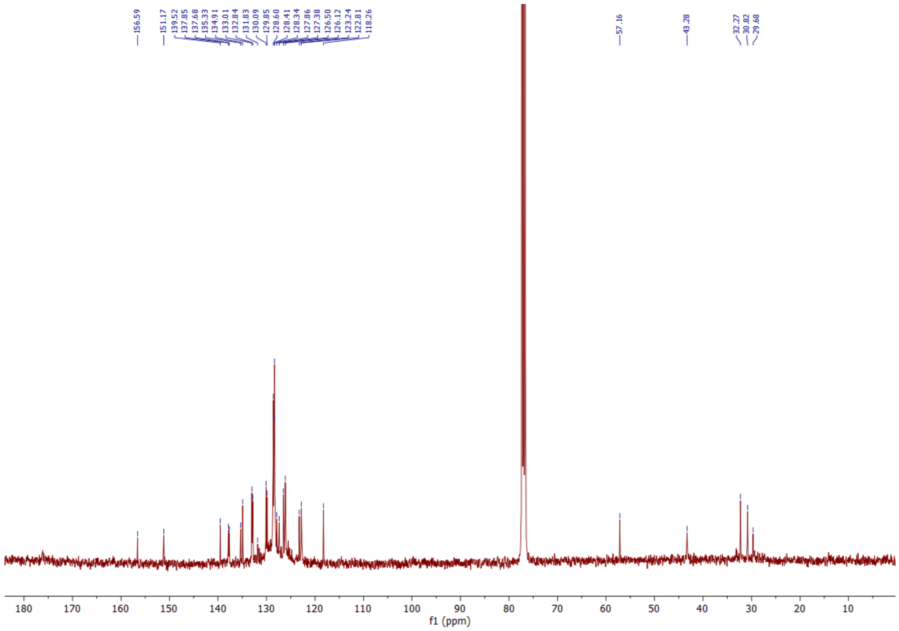

4-phenyl-1-propylquinolin-1-ium acetate (5a):

Kor

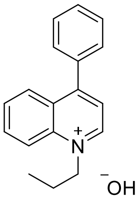

+
N
–OH

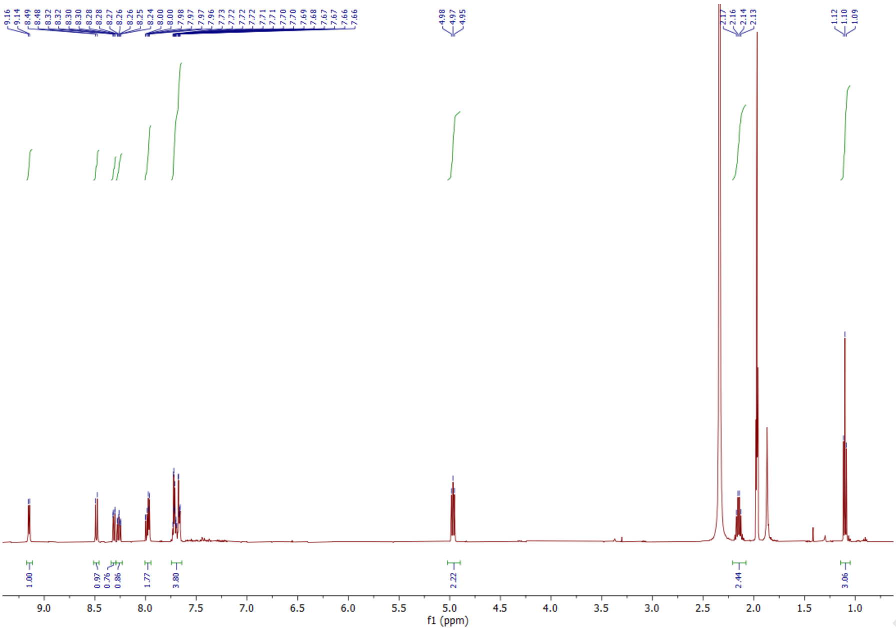

9.16
9.14
8.49
8.48
8.32
8.32
8.30
8.30
8.28
8.28
8.27
8.26
8.26
8.25
8.24
8.00
8.00
7.98
7.97
7.97
7.96
7.73
7.72
7.72
7.72
7.71
7.71
7.70
7.70
7.69
7.68
7.67
7.67
7.66
7.66
4.98
4.97
4.95
2.17
2.16
2.14
2.13
1.12
1.10
1.09
1.00
0.97
0.76
0.86
1.77
3.80
2.22
2.44
3.06
9.0
8.5
8.0
7.5
7.0
6.5
6.0
5.5
5.0
4.5
4.0
3.5
3.0
2.5
2.0
1.5
1.0
f1 (ppm)

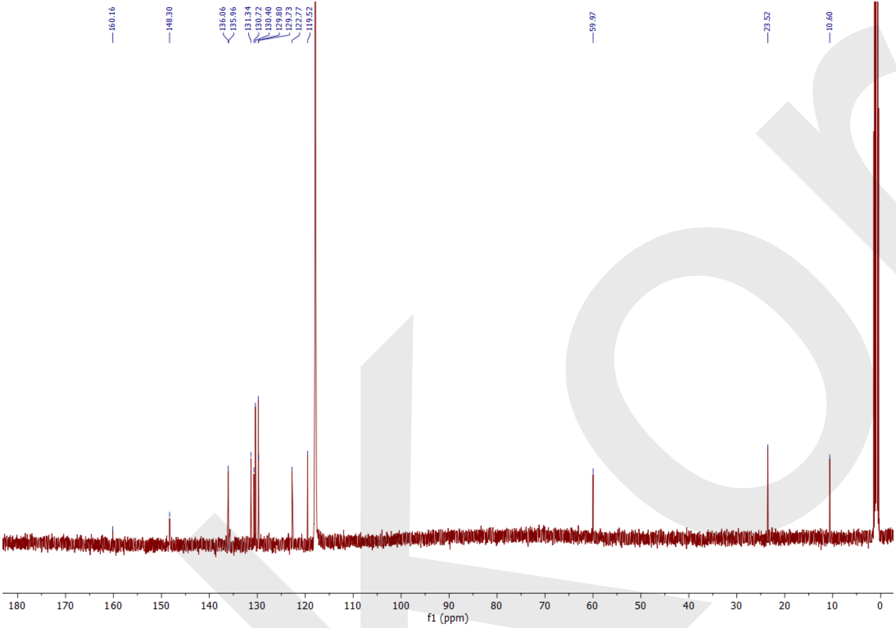

160.16
148.30
136.06
135.96
131.34
130.72
130.40
129.80
129.73
122.77
119.52
59.97
23.52
10.60
180
170
160
150
140
130
120
110
100
90
80
70
60
50
40
30
20
10
0
f1 (ppm)

7-methyl-1-propyl-4-(p-tolyl)quinolin-1-ium acetate (5b):

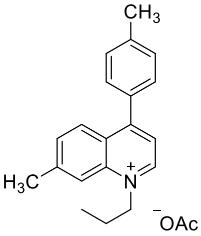
CH3
H3C
N
+
−OAc

Korr

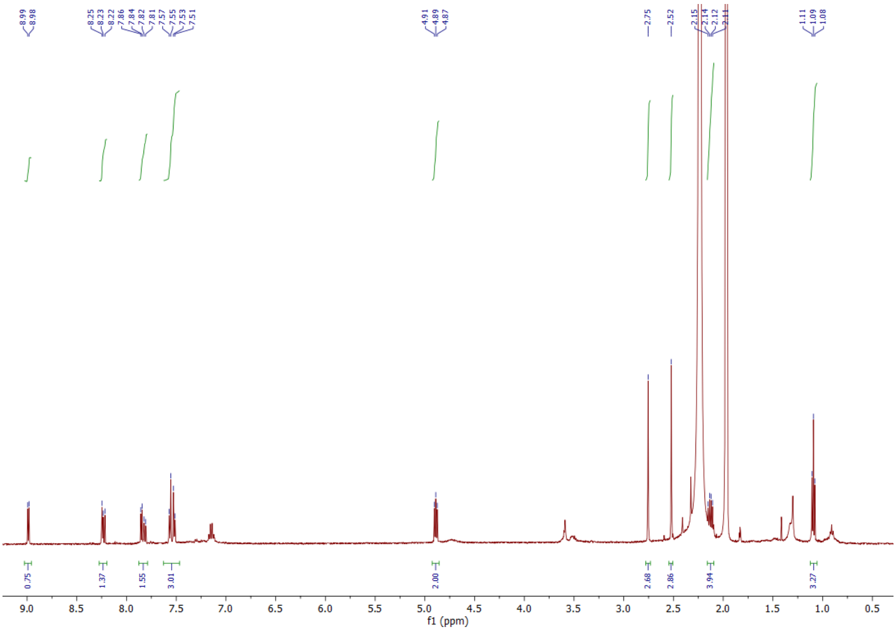

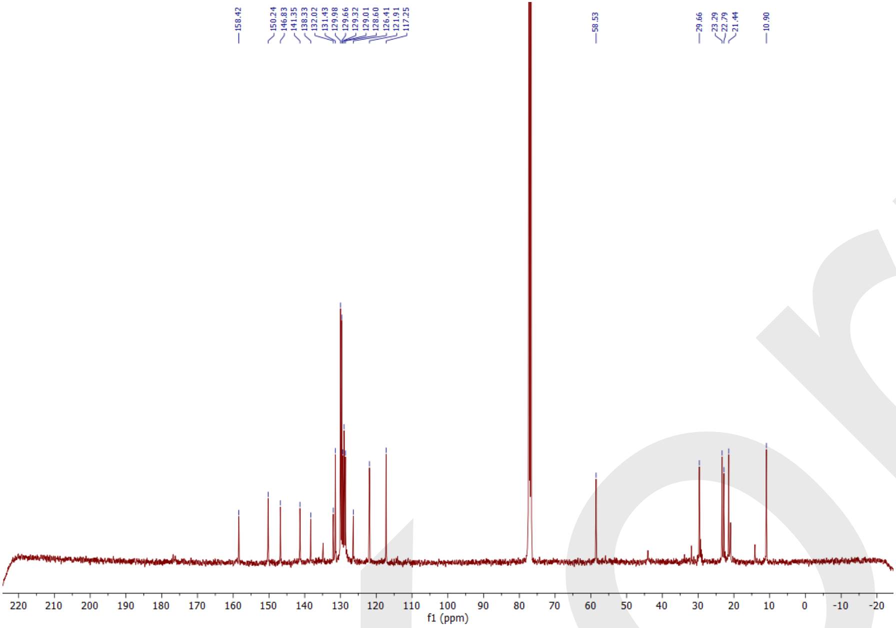

7-chloro-4-(4-chlorophenyl)-1-propylquinolin-1-ium acetate (5c):

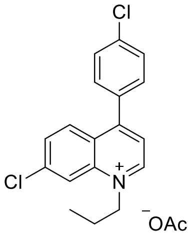

Korr

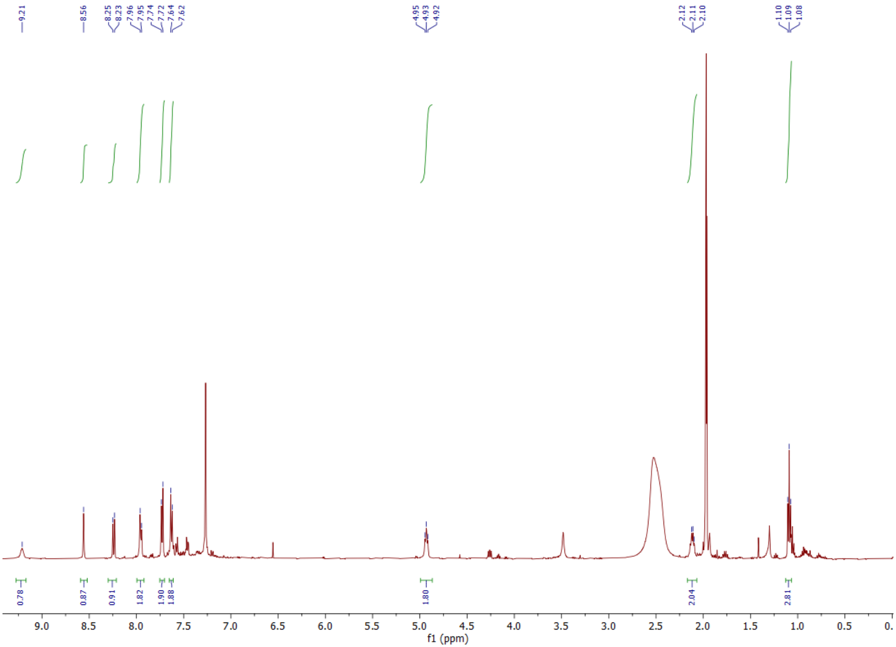

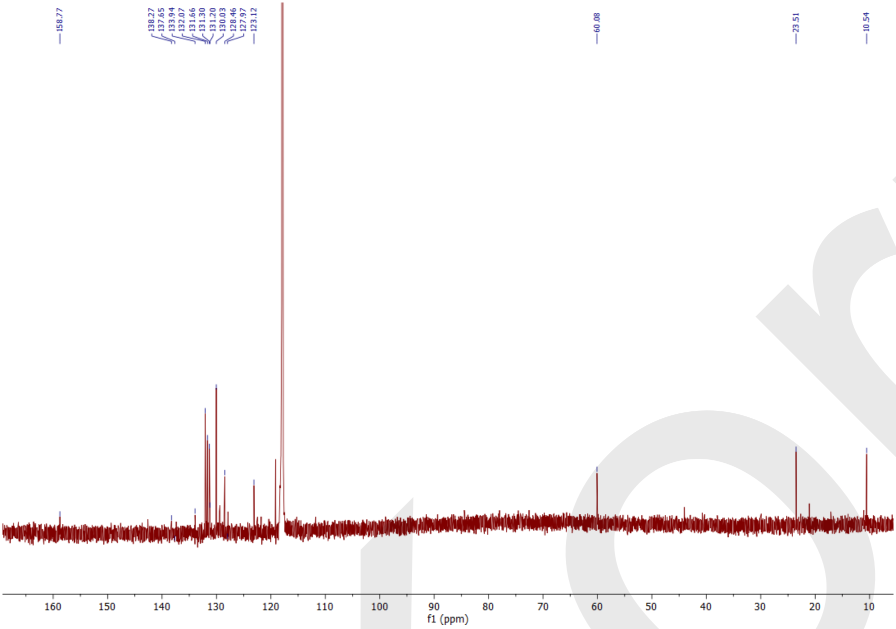

4-(4-fluorophenyl)-1-propylquinolin-1-ium-7-olate (8a):

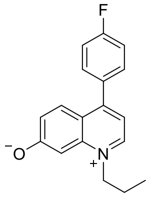
F
O
−
N
+

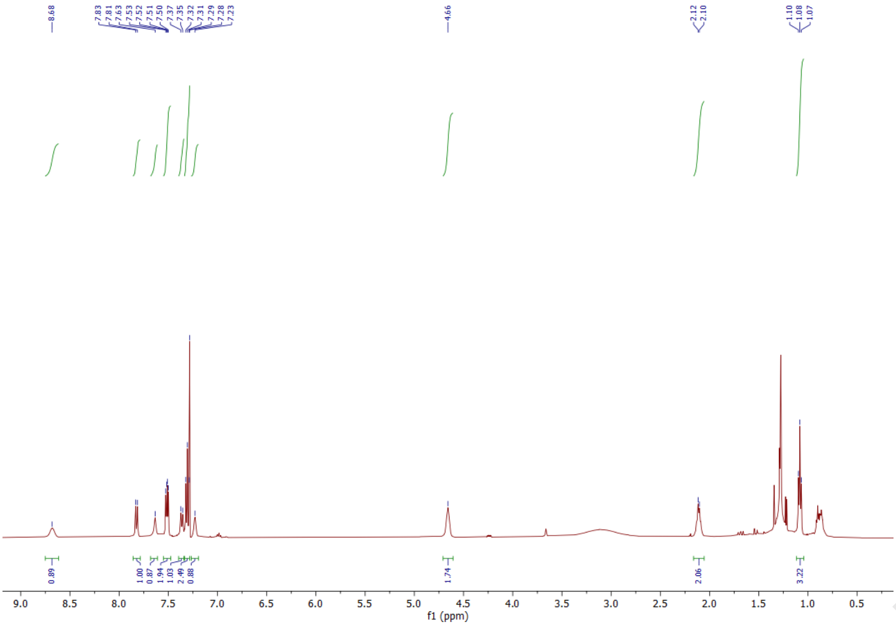
8.68
7.83
7.81
7.63
7.53
7.52
7.51
7.50
7.37
7.35
7.32
7.31
7.29
7.28
7.23
4.66
2.12
2.10
1.10
1.08
1.07
0.89
1.00
0.87
1.94
1.03
2.49
0.88
1.74
2.06
3.22
9.0
8.5
8.0
7.5
7.0
6.5
6.0
5.5
5.0
4.5
4.0
3.5
3.0
2.5
2.0
1.5
1.0
0.5
f1 (ppm)

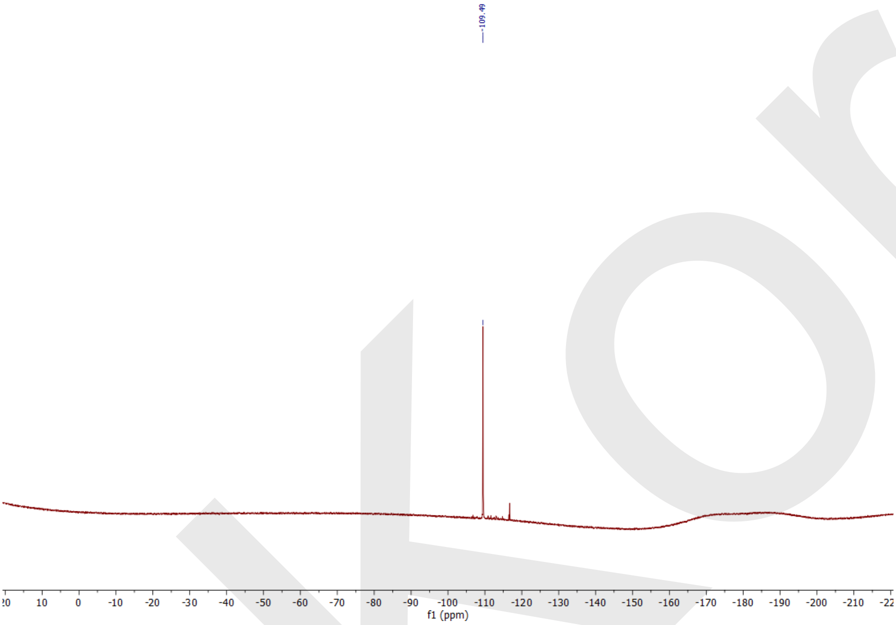
-109.49
20
10
0
-10
-20
-30
-40
-50
-60
-70
-80
-90
-100
-110
-120
-130
-140
-150
-160
-170
-180
-190
-200
-210
-22
f1 (ppm)

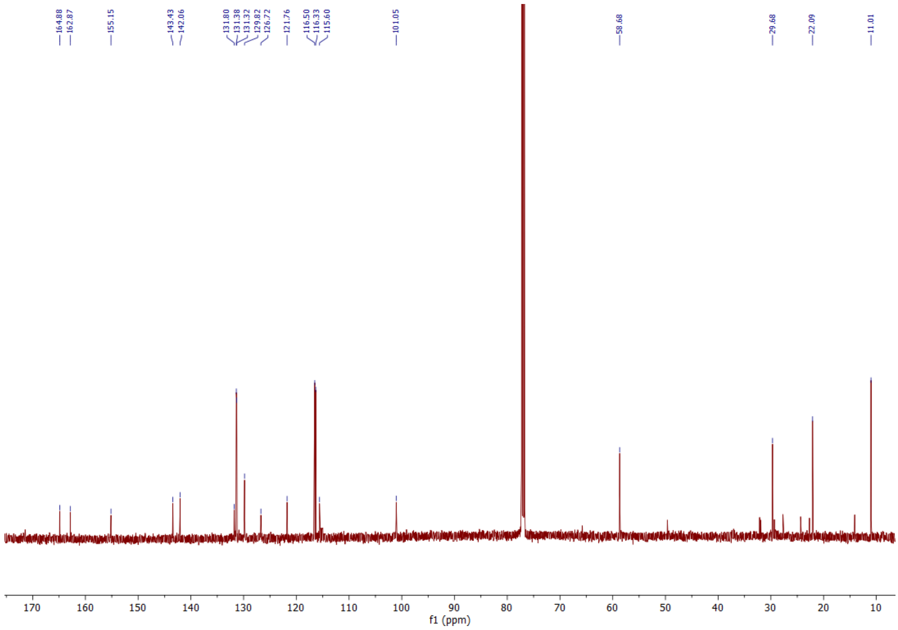

4-(4-fluorophenyl)-1-(3-(4-fluorophenyl)propyl)quinolin-1-ium-7-olate (8b):

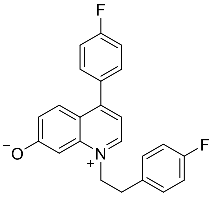

Korr

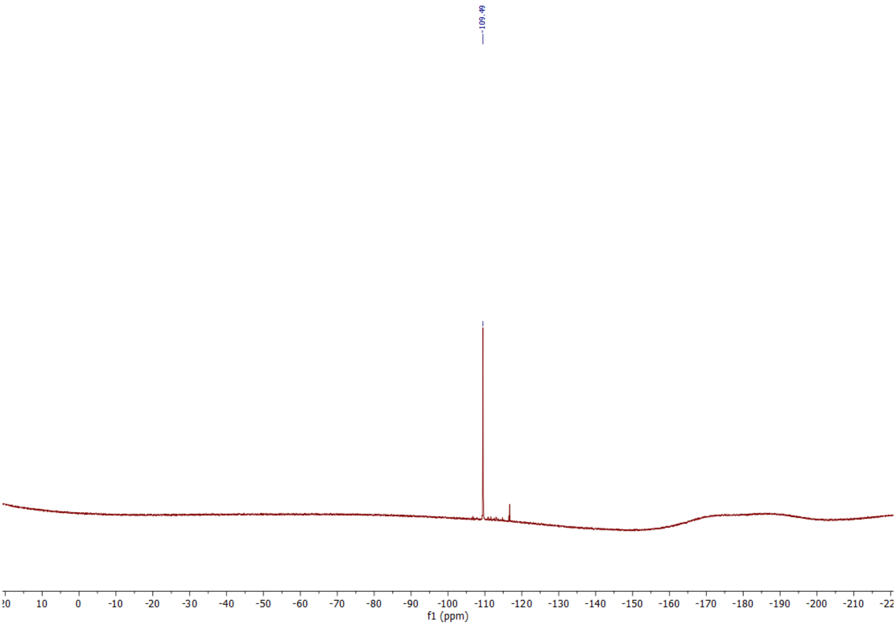
-109.49
20
10
0
-10
-20
-30
-40
-50
-60
-70
-80
-90
-100
-110
-120
-130
-140
-150
-160
-170
-180
-190
-200
-210
-22
f1 (ppm)

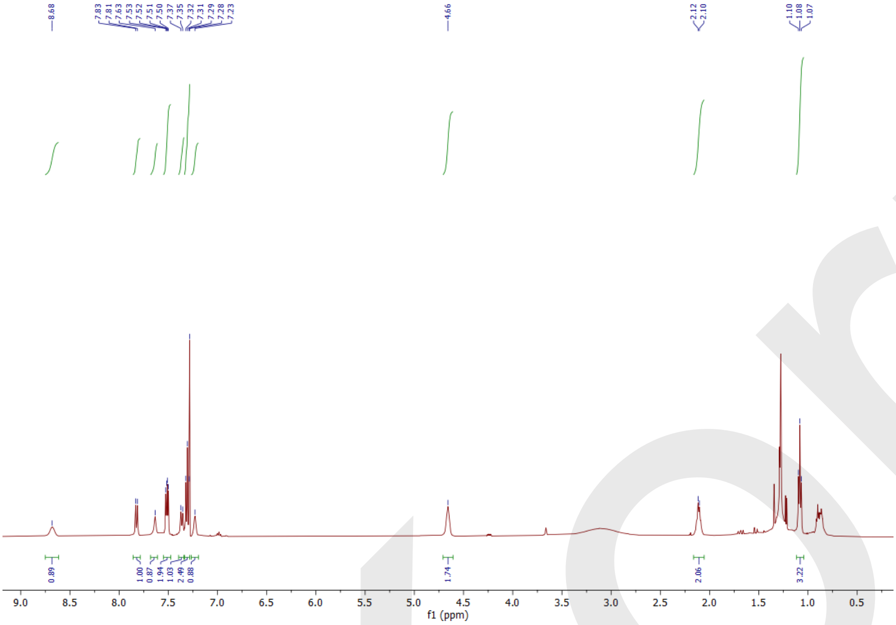
8.68
7.83
7.81
7.63
7.53
7.52
7.51
7.50
7.37
7.35
7.32
7.31
7.29
7.28
7.23
4.66
2.12
2.10
1.10
1.08
1.07
0.89
1.00
0.87
1.94
1.03
2.49
0.88
1.74
2.06
3.22
9.0
8.5
8.0
7.5
7.0
6.5
6.0
5.5
5.0
4.5
4.0
3.5
3.0
2.5
2.0
1.5
1.0
0.5
f1 (ppm)

korr

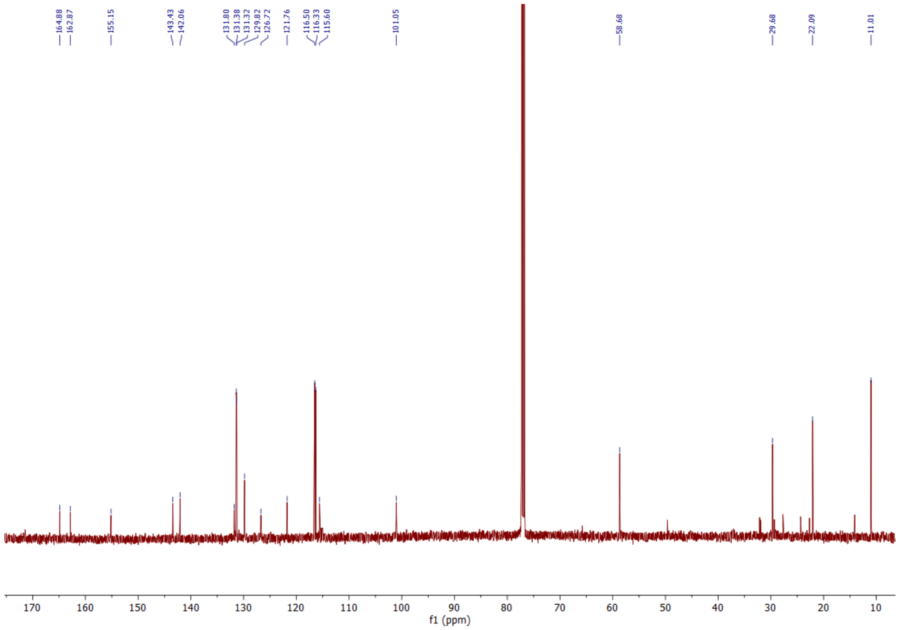

Computational Methods:

All reported structures were optimized at Density Functional Theory level by using the B97D functional as implemented in Gaussian 09. Optimizations were carried out with the 6-311G(d,p) basis set for all atoms except iodine and palladium with SDD. The reported energy values correspond to Gibbs Free energies, including single point refinements at M06/def2tzvpp level of theory in a solvent model (IEFPCM, acetic acid) on the previously optimized structures. The critical stationary points were characterized by frequency calculations in order to verify that they have the right number of imaginary frequencies, and the intrinsic reaction coordinates (IRC) were followed to verify the energy profiles connecting the key transition structures to the correct associated local minima.

Cartesian Coordinates of the computed structures:

I

SCF = -759.3378114

Thermal correction to Gibbs Free Energy = 0.171592

C	1.349912	3.347791	0.159645
C	0.173724	2.833264	1.005005
H	-0.158753	3.611387	1.707232
H	0.492896	1.965649	1.601939
C	-1.037130	2.424459	0.162458
H	-1.443427	3.295710	-0.375432
N	-0.698691	1.380372	-0.850917
H	-0.103977	1.775281	-1.580898
Pd	0.190553	-0.336366	-0.108045

H	2.164478	3.704276	0.803726
O	1.543511	-1.909744	0.469578
C	2.513173	-1.226445	-0.008915
C	3.932027	-1.708335	0.075542
H	4.366177	-1.361517	1.024467
H	3.958801	-2.803628	0.061573
H	4.522991	-1.295022	-0.749409
O	2.236948	-0.088314	-0.545802
H	1.756404	2.547586	-0.473193
O	-1.607549	-1.025168	0.572346
C	-2.758221	-0.879861	-0.034709
C	-3.875509	-1.682956	0.632755
H	-3.761990	-1.685876	1.723002
H	-4.848476	-1.268903	0.346786
H	-3.814054	-2.723561	0.283317
O	-2.976374	-0.201588	-1.050589
H	1.034829	4.182104	-0.485333
H	-1.572574	1.014536	-1.268111
H	-1.828069	2.003216	0.791865

II

SCF = 0.223377

Thermal correction to Gibbs Free Energy = -989.0637912

C	1.264997	-2.276843	-1.348930
C	0.363251	-3.413325	-0.846150
H	0.855612	-3.966020	-0.027200
H	0.233881	-4.150505	-1.650712
C	-1.002884	-3.028634	-0.363834
H	-1.755276	-3.824501	-0.316263
N	-1.343345	-1.852953	0.005940
H	-2.323325	-1.696454	0.312902
Pd	-0.342692	-0.097771	0.138541
H	2.185137	-2.739190	-1.734393
O	0.542193	1.729505	0.398113
C	0.828691	2.413999	-0.683172
C	1.485702	3.759090	-0.361105
H	1.064410	4.204729	0.547890
H	2.558204	3.585452	-0.189075
H	1.369965	4.440746	-1.211322
O	0.652450	2.040077	-1.846371
H	0.787224	-1.776777	-2.202814
O	-2.124697	0.987707	-0.097452
C	-3.317911	0.592996	0.247643
C	-4.373320	1.683764	0.042148
H	-4.255362	2.147972	-0.944806
H	-5.376599	1.257014	0.147454
H	-4.227878	2.467787	0.798408
O	-3.634143	-0.516500	0.713574
C	1.683620	-1.217697	-0.336167
C	2.650283	-0.255800	-0.767172
C	1.422981	-1.316084	1.068986
C	3.325502	0.530149	0.147620

H	2.859330	-0.169748	-1.831036
C	2.137729	-0.504845	1.994374
H	0.848259	-2.153276	1.457677
C	3.070531	0.408533	1.537078
H	4.065197	1.248381	-0.201486
H	1.940194	-0.618358	3.057935
H	3.616802	1.032746	2.241540

TS1

SCF = -989.0265426

Thermal correction to Gibbs Free Energy = 0.216946

C	-1.306702	-0.265929	1.401824
C	-0.877210	-1.309168	2.463922
H	-1.684271	-2.040038	2.626568
H	-0.727331	-0.801110	3.430518
C	0.401927	-1.999523	2.129350
H	0.701177	-2.922949	2.635462
N	1.162078	-1.460390	1.250160
H	2.073483	-1.860214	0.964799
Pd	0.626629	0.219196	0.310868
H	-2.004615	0.415249	1.905673
O	0.113630	2.058760	-0.600016
C	-0.544070	2.825156	0.183773
C	-0.917989	4.201346	-0.327189
H	-1.939602	4.149923	-0.730599
H	-0.911908	4.922244	0.497412
H	-0.239657	4.517137	-1.125737
O	-0.922630	2.472325	1.344582
H	-0.664457	1.045549	1.346130
O	2.325109	0.296810	-0.888402
C	3.319143	-0.549187	-0.916896
C	4.372406	-0.165021	-1.961636
H	5.211498	-0.867846	-1.923782
H	3.918380	-0.179989	-2.961705
H	4.727158	0.857152	-1.775337
O	3.462150	-1.566379	-0.217971
C	-2.016405	-0.771089	0.172697
C	-2.887789	0.103569	-0.509662
C	-1.844330	-2.075732	-0.329932
C	-3.556676	-0.307638	-1.666113
H	-3.031371	1.112016	-0.123098
C	-2.522618	-2.491060	-1.481773
H	-1.172369	-2.768271	0.171702
C	-3.376595	-1.608803	-2.158897
H	-4.223078	0.384239	-2.179510
H	-2.378975	-3.504656	-1.853643
H	-3.898192	-1.932368	-3.058217

III

SCF = -989.0659778

Thermal correction to Gibbs Free Energy = 0.220032

C	-1.228497	-0.162970	1.289458

Korr

C	-1.078803	-1.304121	2.343882
H	-2.020386	-1.855711	2.496527
H	-0.817066	-0.870262	3.323497
C	0.027145	-2.233543	1.965723
H	0.164284	-3.209105	2.445001
N	0.845025	-1.818468	1.064855
H	1.670561	-2.353154	0.745584
Pd	0.563006	-0.044832	0.216194
H	-1.410263	0.800022	1.783052
O	0.160937	1.965372	-0.498955
C	0.362743	2.944926	0.231833
C	0.080591	4.354104	-0.196743
H	1.004239	4.943762	-0.134075
H	-0.307294	4.361575	-1.217833
H	-0.647096	4.802586	0.492325
O	0.842794	2.839097	1.471830
H	0.995792	1.879222	1.653272
O	2.399233	-0.026065	-0.938158
C	3.242615	-1.006800	-1.005895
C	4.450563	-0.714011	-1.910230
H	4.975013	0.181495	-1.548781
H	5.139068	-1.566449	-1.925032
H	4.104061	-0.499855	-2.930884
O	3.159125	-2.111832	-0.428408
C	-2.242551	-0.395820	0.223000
C	-2.959137	0.693725	-0.320818
C	-2.492919	-1.683029	-0.305588
C	-3.884001	0.507972	-1.353120
H	-2.778327	1.692125	0.076140
C	-3.420433	-1.870543	-1.334794
H	-1.945425	-2.538849	0.085797
C	-4.119906	-0.776122	-1.867076
H	-4.425652	1.363955	-1.754635
H	-3.595782	-2.871929	-1.726754
H	-4.840350	-0.923090	-2.670380

IV

SCF = -758.0970982

Thermal correction to Gibbs Free Energy = 0.147708

C	1.458007	2.292404	-0.481816
C	0.522978	3.354844	0.118384
H	0.564146	4.279875	-0.475258
H	0.855106	3.636283	1.131560
C	-0.901523	2.908315	0.227269
H	-1.679056	3.655381	0.418105
N	-1.233798	1.672647	0.130050
H	-2.220552	1.383112	0.226556
Pd	0.055366	0.156874	-0.145974
H	2.510384	2.598075	-0.439327
O	1.389096	-1.367638	-0.468706
C	2.511230	-1.324514	0.212650
C	3.410548	-2.530168	-0.061622

H	2.952774	-3.427154	0.378317
H	3.506079	-2.701869	-1.141254
H	4.396502	-2.366597	0.386436
O	2.828954	-0.431985	1.008028
H	1.506732	1.358956	0.173675
O	-1.342846	-1.339225	-0.087991
C	-2.637754	-1.201512	0.076646
C	-3.336432	-2.566041	0.077301
H	-3.022426	-3.132876	0.963889
H	-4.421341	-2.418906	0.095778
H	-3.043747	-3.142469	-0.808890
O	-3.274168	-0.152245	0.225219
H	1.214559	2.082227	-1.530403

TS2

SCF = -758.0794011

Thermal correction to Gibbs Free Energy = 0.143856

C	1.500726	1.809621	-0.541215
C	0.905356	3.026760	0.200104
H	1.181696	3.972447	-0.292336
H	1.305634	3.090952	1.225945
C	-0.579495	2.906785	0.307022
H	-1.213384	3.773235	0.519954
N	-1.099837	1.743154	0.161425
H	-2.115317	1.560259	0.238701
Pd	0.040137	0.142419	-0.175084
H	2.596226	1.892442	-0.560800
O	1.300687	-1.540301	-0.393507
C	2.447811	-1.367026	0.139238
C	3.385286	-2.553078	0.220148
H	3.464219	-2.861460	1.271714
H	3.011706	-3.389527	-0.377233
H	4.384773	-2.252587	-0.116243
O	2.835449	-0.250634	0.616926
H	1.895972	0.645338	0.190260
O	-1.522035	-1.227717	-0.057981
C	-2.793088	-0.968844	0.088041
C	-3.642721	-2.244178	0.111842
H	-3.319645	-2.888144	0.940700
H	-4.701063	-1.988078	0.228623
H	-3.493253	-2.806080	-0.819771
O	-3.325304	0.148382	0.199703
H	1.201368	1.799786	-1.597839

V

SCF = -758.1092181

Thermal correction to Gibbs Free Energy = 0.148277

C	1.158581	2.005780	-0.450460
C	0.401265	3.200154	0.203417
H	0.551304	4.150727	-0.334929
H	0.765260	3.376884	1.230420
C	-1.050800	2.872854	0.309720

H	-1.816408	3.627048	0.521577
N	-1.370947	1.633586	0.173005
H	-2.337598	1.272618	0.256339
Pd	0.020921	0.291550	-0.243303
H	2.172983	1.899648	-0.042438
O	1.667609	-1.029730	-0.674416
C	2.574354	-1.218772	0.149950
C	3.728313	-2.141185	-0.106905
H	3.715865	-2.946364	0.639489
H	3.655245	-2.558672	-1.113625
H	4.669679	-1.590108	0.014694
O	2.608293	-0.623640	1.341722
H	1.812985	-0.042342	1.409824
O	-1.269404	-1.444158	-0.083203
C	-2.550913	-1.406113	0.096658
C	-3.207889	-2.794994	0.137550
H	-2.719067	-3.417406	0.899670
H	-4.278920	-2.711687	0.354372
H	-3.066409	-3.294384	-0.831479
O	-3.261893	-0.385805	0.225591
H	1.235059	2.147951	-1.540137

VI

SCF = -989.063791

Thermal correction to Gibbs Free Energy = 0.223427

C	1.158581	2.005780	-0.450460
C	0.401265	3.200154	0.203417
H	0.551304	4.150727	-0.334929
H	0.765260	3.376884	1.230420
C	-1.050800	2.872854	0.309720
H	-1.816408	3.627048	0.521577
N	-1.370947	1.633586	0.173005
H	-2.337598	1.272618	0.256339
Pd	0.020921	0.291550	-0.243303
H	2.172983	1.899648	-0.042438
O	1.667609	-1.029730	-0.674416
C	2.574354	-1.218772	0.149950
C	3.728313	-2.141185	-0.106905
H	3.715865	-2.946364	0.639489
H	3.655245	-2.558672	-1.113625
H	4.669679	-1.590108	0.014694
O	2.608293	-0.623640	1.341722
H	1.812985	-0.042342	1.409824
O	-1.269404	-1.444158	-0.083203
C	-2.550913	-1.406113	0.096658
C	-3.207889	-2.794994	0.137550
H	-2.719067	-3.417406	0.899670
H	-4.278920	-2.711687	0.354372
H	-3.066409	-3.294384	-0.831479
O	-3.261893	-0.385805	0.225591
H	1.235059	2.147951	-1.540137

TS3

SCF = 0.245198

Thermal correction to Gibbs Free Energy = -1289.283792

C	1.226123	-0.995649	1.391125
C	1.087530	-2.427837	1.990489
H	1.589442	-2.492494	2.969378
H	1.583979	-3.169945	1.344114
C	-0.352301	-2.811573	2.070596
H	-0.717459	-3.596163	2.742388
N	-1.143279	-2.194244	1.273953
H	-2.154837	-2.392220	1.174514
Pd	-0.404399	-0.766037	0.033888
O	-2.136865	-0.902919	-1.336412
C	-3.280810	-1.423928	-1.031978
C	-4.348390	-1.249988	-2.123316
H	-3.913027	-1.385772	-3.121223
H	-5.176126	-1.951668	-1.967904
H	-4.740736	-0.223191	-2.068733
O	-3.588277	-1.998950	0.035130
H	1.012683	-0.260312	2.173899
C	-2.217783	2.869734	2.489690
C	-0.829565	2.704394	2.596868
C	-0.111383	2.042256	1.591180
C	-0.819058	1.515996	0.506270
C	-2.195130	1.713514	0.343049
C	-2.891830	2.378959	1.362705
H	-2.767536	3.390516	3.271422
H	-0.290132	3.097666	3.457654
H	0.965300	1.929794	1.659679
H	-2.704355	1.322037	-0.530390
H	-3.968389	2.510442	1.262328
I	0.503153	1.288970	-1.520195
C	2.526369	-0.724668	0.731773
C	3.292679	0.407398	1.078171
C	3.002151	-1.566033	-0.298558
C	4.486108	0.700853	0.408641
H	2.950025	1.053703	1.885440
C	4.189569	-1.273792	-0.971215
H	2.409240	-2.431486	-0.592613
C	4.935988	-0.134891	-0.623019
H	5.064347	1.579592	0.691114
H	4.534202	-1.926517	-1.772193
H	5.861123	0.094526	-1.149617

VII

SCF = 0.246677

Thermal correction to Gibbs Free Energy = -1289.29682

C	1.076221	-0.255836	-1.631177
C	0.532306	0.532789	-2.850242

Korr

H	-0.249216	-0.063559	-3.348572
H	1.320610	0.710448	-3.597078
C	-0.117574	1.813108	-2.435591
H	-0.323808	2.614135	-3.153112
N	-0.462833	1.920918	-1.209459
H	-1.007050	2.699775	-0.788795
Pd	-0.127229	0.328088	0.029863
O	-1.019968	1.332400	1.780707
C	-1.670792	2.449077	1.750960
C	-2.188692	2.898485	3.121359
H	-2.568989	3.924896	3.073454
H	-3.000508	2.224206	3.429799
H	-1.392847	2.819995	3.872842
O	-1.924114	3.141185	0.736702
H	0.974220	-1.333349	-1.768815
C	-4.122695	-1.575922	-1.890790
C	-2.933355	-2.311821	-1.956555
C	-1.744744	-1.802303	-1.404303
C	-1.780951	-0.547507	-0.793560
C	-2.951766	0.208693	-0.714194
C	-4.130037	-0.321019	-1.269360
H	-5.038778	-1.979144	-2.319223
H	-2.915770	-3.294272	-2.426905
H	-0.835713	-2.393244	-1.437415
H	-2.954439	1.191663	-0.250555
H	-5.047446	0.263683	-1.212654
I	0.391833	-1.809095	1.573595
C	2.431439	0.106493	-1.147168
C	3.284906	-0.909823	-0.658526
C	2.899213	1.441172	-1.131897
C	4.561569	-0.606687	-0.185003
H	2.927465	-1.937279	-0.652750
C	4.176300	1.744770	-0.649275
H	2.263701	2.245816	-1.492719
C	5.011255	0.723920	-0.173610
H	5.207113	-1.404215	0.179165
H	4.519133	2.778096	-0.643767
H	6.004618	0.961672	0.203386

TS4

SCF = 0.247048

Thermal correction to Gibbs Free Energy = -1289.281401

C	-1.103945	-0.874337	-1.241416
C	-0.989200	-2.360035	-1.559801
H	-1.356761	-2.517007	-2.588004
H	-1.628748	-2.977900	-0.913118
C	0.413884	-2.866522	-1.451633
H	0.668846	-3.838442	-1.886657
N	1.299814	-2.181072	-0.837997
H	2.284506	-2.495294	-0.752381

Pd	1.003104	-0.287432	-0.113137
O	3.049700	0.153107	-0.462938
C	4.033812	-0.702153	-0.437702
C	5.399055	-0.019953	-0.572495
H	5.626743	0.501899	0.367586
H	6.173691	-0.768793	-0.770227
H	5.377040	0.730923	-1.371748
O	3.955783	-1.936562	-0.303723
C	-2.197841	-1.439476	3.282548
C	-2.329548	-0.185588	2.666727
C	-1.647608	0.094105	1.481519
C	-0.782883	-0.860034	0.903714
C	-0.671040	-2.127023	1.519391
C	-1.370349	-2.407692	2.701213
H	-2.744583	-1.662497	4.197354
H	-2.981435	0.573478	3.096549
H	-1.811810	1.045482	0.988275
H	-0.024916	-2.894299	1.108130
H	-1.257911	-3.387344	3.163676
I	0.789404	2.375162	0.445172
H	-0.421965	-0.298041	-1.875022
C	-2.434418	-0.245779	-1.258853
C	-3.603589	-0.947745	-0.895216
C	-2.538800	1.106440	-1.646899
C	-4.846348	-0.315279	-0.938478
H	-3.536027	-1.981591	-0.563684
C	-3.783319	1.742051	-1.678666
H	-1.632365	1.654881	-1.898437
C	-4.940066	1.032429	-1.325634
H	-5.743716	-0.865710	-0.661322
H	-3.850794	2.787345	-1.974614
H	-5.910356	1.525859	-1.346834

VIII

SCF = 0.249876

Thermal correction to Gibbs Free Energy = -1289.348197

C	-2.039162	-0.967353	-0.177005
C	-1.996950	-2.227489	0.716572
H	-2.655581	-2.989054	0.275259
H	-2.442272	-2.006810	1.701495
C	-0.669889	-2.871038	0.955040
H	-0.681270	-3.895223	1.346170
N	0.458241	-2.307751	0.749347
H	1.305617	-2.845123	0.976744
Pd	1.018272	-0.424025	0.155052
O	2.638544	-1.307377	-0.826220
C	3.415365	-2.173986	-0.229700
C	4.607624	-2.577823	-1.101844
H	5.413186	-1.847956	-0.937143

H	4.962175	-3.569917	-0.800756
H	4.348858	-2.564367	-2.166533
O	3.268774	-2.634230	0.912063
C	-0.662579	2.750197	1.587674
C	-1.224665	2.707200	0.288870
C	-1.515038	1.497879	-0.315599
C	-1.290725	0.262599	0.363792
C	-0.673783	0.318078	1.652149
C	-0.372862	1.572829	2.253372
H	-0.447697	3.710181	2.052367
H	-1.431792	3.635997	-0.238900
H	-1.979119	1.473142	-1.298980
H	-0.652888	-0.563374	2.287342
H	0.067721	1.586420	3.247647
I	2.174364	1.918854	-0.534224
H	-1.594138	-1.226281	-1.147925
C	-3.509902	-0.622624	-0.415747
C	-4.286949	-0.066995	0.615977
C	-4.107584	-0.885563	-1.656797
C	-5.640754	0.218646	0.408818
H	-3.824700	0.154563	1.577749
C	-5.464443	-0.599617	-1.867653
H	-3.506028	-1.310892	-2.459916
C	-6.233599	-0.047438	-0.835232
H	-6.232134	0.652533	1.213872
H	-5.916312	-0.804229	-2.837210
H	-7.286329	0.178359	-0.998092

IX
SCF = 0.298171
Thermal correction to Gibbs Free Energy = -936.2500241

C	-0.958551	-1.330962	2.151059
C	-0.456930	-0.866211	0.922782
C	0.892070	-0.463534	0.809298
C	1.713551	-0.559449	1.949699
C	1.217989	-1.034967	3.170379
C	-0.121352	-1.425844	3.273505
H	-2.004201	-1.626319	2.232403
H	2.754594	-0.249912	1.878779
H	1.877411	-1.092835	4.035382
H	-0.521881	-1.795844	4.217087
C	2.824854	0.627165	-0.463926
C	3.997983	-0.143705	-0.539393
C	5.258433	0.457331	-0.419710
C	5.362788	1.840688	-0.218625
C	4.198620	2.618398	-0.138678
C	2.941590	2.012649	-0.259515
H	3.927260	-1.219946	-0.688589
H	6.157418	-0.154684	-0.482535
H	6.341955	2.308693	-0.127092
H	4.269697	3.694544	0.014746
H	2.036011	2.616251	-0.193797

C	1.443352	0.000283	-0.543706
H	0.753230	0.771690	-0.918067
C	1.372054	-1.195823	-1.550676
H	1.720009	-2.118657	-1.067700
H	2.032156	-0.979506	-2.403639
C	-0.026466	-1.381877	-2.085207
H	-0.315592	-0.659461	-2.861522
N	-0.798193	-2.459602	-1.962027
H	-0.341610	-3.139245	-1.341020
N	-2.982217	0.239428	0.329994
H	-2.787197	0.294416	1.333564
C	-3.085059	1.626004	-0.154437
H	-2.189564	2.228447	0.094418
H	-3.175802	1.613964	-1.251736
C	-4.323135	2.329021	0.439455
H	-4.242032	2.313382	1.538175
H	-5.220472	1.750601	0.174309
C	-4.452601	3.778513	-0.056971
H	-3.564866	4.367035	0.218492
H	-4.549952	3.807604	-1.152513
H	-5.335112	4.269733	0.376122
Pd	-1.694646	-0.930105	-0.650284

TS5

SCF = -936.2287843

Thermal correction to Gibbs Free Energy = 0.300464

C	-1.700761	-0.434812	2.273402
C	-1.073697	-0.255403	1.019793
C	0.316110	-0.496373	0.876844
C	1.033309	-0.913351	2.015670
C	0.414679	-1.089613	3.257907
C	-0.964831	-0.860994	3.381998
H	-2.766977	-0.228832	2.370034
H	2.099358	-1.112416	1.915071
H	1.002648	-1.401640	4.119620
H	-1.466006	-0.996678	4.340243
C	2.470079	-0.260699	-0.463876
C	3.400979	-1.312210	-0.418666
C	4.776132	-1.048864	-0.335677
C	5.239090	0.272868	-0.295728
C	4.317953	1.330266	-0.339663
C	2.946595	1.061922	-0.420950
H	3.052449	-2.343296	-0.446731
H	5.483619	-1.876613	-0.302341
H	6.306916	0.478122	-0.233575
H	4.668249	2.361534	-0.313262
H	2.230207	1.882848	-0.450362
C	0.968621	-0.498121	-0.510217
H	0.532178	0.328505	-1.083295
C	0.564677	-1.817757	-1.262444
H	0.613732	-2.672861	-0.574410
H	1.282811	-1.988156	-2.078491

C	-0.820207	-1.718703	-1.870100
H	-0.865863	-1.145267	-2.806965
N	-1.872552	-2.502348	-1.601430
H	-1.631510	-3.136746	-0.830182
N	-1.961050	1.340328	0.137478
H	-2.428280	1.609023	0.999889
C	-0.907055	2.300519	-0.185387
H	-0.016646	2.166421	0.461650
H	-0.580346	2.133764	-1.221748
C	-1.405920	3.747509	-0.041734
H	-1.761292	3.897351	0.990515
H	-2.268808	3.899847	-0.706608
C	-0.294581	4.760261	-0.364545
H	0.565584	4.622231	0.306945
H	0.059404	4.632722	-1.398240
H	-0.653687	5.792408	-0.252446
Pd	-2.224121	-0.551452	-0.662118

X

SCF = -936.2857884

Thermal correction to Gibbs Free Energy = 0.301818

C	-1.465800	-1.018233	1.642226
C	-0.748290	0.003068	0.907623
C	0.651054	-0.233478	0.591691
C	1.283575	-1.352451	1.134964
C	0.601413	-2.296651	1.932184
C	-0.763661	-2.146030	2.161510
H	-2.454748	-0.794303	2.037002
H	2.336236	-1.513760	0.911636
H	1.140460	-3.148059	2.344509
H	-1.313061	-2.872934	2.758498
C	2.859431	0.710566	-0.221595
C	3.762932	-0.157709	-0.857122
C	5.137906	-0.082124	-0.589144
C	5.628526	0.864017	0.319514
C	4.734339	1.735417	0.959963
C	3.363440	1.655020	0.690649
H	3.395318	-0.900182	-1.562627
H	5.823092	-0.764353	-1.091041
H	6.696166	0.924230	0.526279
H	5.105227	2.477009	1.666581
H	2.668035	2.327622	1.193406
C	1.352375	0.638569	-0.442903
H	1.000869	1.675844	-0.360992
C	0.997218	0.129286	-1.911920
H	1.090306	-0.964399	-1.916750
H	1.747742	0.560649	-2.589415
C	-0.357264	0.509705	-2.409853
H	-0.470551	1.511399	-2.845988
N	-1.388042	-0.283492	-2.308787
H	-2.220187	0.156952	-2.708352
N	-1.275327	1.306142	0.779073

H	-0.899477	1.778404	-0.036332
C	-2.730314	1.492052	0.823240
H	-3.231346	0.761086	0.155023
H	-3.085368	1.293354	1.844536
C	-3.103613	2.919579	0.415426
H	-2.733309	3.104182	-0.606708
H	-2.587009	3.629986	1.077861
C	-4.621697	3.148268	0.467838
H	-5.145169	2.453009	-0.204578
H	-5.003938	2.985629	1.486102
H	-4.878010	4.173025	0.167101
Pd	-1.691894	-1.415786	-0.548337

XI

SCF = -980.8603258

Thermal correction to Gibbs Free Energy = 0.326588

C	-1.511212	2.266862	0.408815
C	-0.812214	1.189890	-0.219201
C	0.621376	1.107323	-0.093320
C	1.305241	2.067774	0.684083
C	0.604479	3.123296	1.323989
C	-0.799189	3.222134	1.171273
H	-2.603786	2.352302	0.302934
H	2.403616	1.998189	0.773542
H	1.154864	3.868191	1.924454
H	-1.352722	4.046892	1.655664
C	2.815354	-0.230056	-0.525875
C	3.174991	-0.605034	0.800046
C	4.530766	-0.818819	1.144826
C	5.546684	-0.661912	0.166503
C	5.198503	-0.289082	-1.155564
C	3.839580	-0.074160	-1.498354
H	2.382993	-0.719745	1.561623
H	4.797539	-1.107081	2.177887
H	6.605415	-0.828682	0.435323
H	5.985618	-0.164419	-1.921351
H	3.566702	0.217997	-2.528731
C	1.329137	-0.011680	-0.905869
H	1.279474	0.266624	-1.985489
C	0.528970	-1.356007	-0.726970
H	0.618074	-1.682484	0.328256
H	0.961089	-2.145153	-1.376114
C	-1.005217	-1.193140	-1.090430
H	-1.207468	-1.588604	-2.121158
N	-1.462933	0.231618	-1.081772
C	-2.888858	0.457872	-1.509602
H	-2.987319	1.539430	-1.754327
H	-3.042289	-0.128959	-2.444965
C	-3.999787	0.055904	-0.465087
H	-3.737038	0.469502	0.530461
H	-4.027298	-1.049256	-0.377480
C	-5.393481	0.592730	-0.917582

H	-5.376632	1.699013	-0.985824
H	-5.660145	0.184584	-1.913085
H	-6.177104	0.294925	-0.192624
O	-1.204262	-0.927479	1.733316
C	-1.855192	-1.842928	1.163744
C	-2.824684	-2.879154	1.847345
H	-3.875101	-2.655589	1.566062
H	-2.584430	-3.910464	1.517487
H	-2.721136	-2.807881	2.947978
O	-1.869971	-2.135212	-0.253908

Pd

SCF = -127.9039946

Thermal correction to Gibbs Free Energy = -0.016592

Pd	0.000000	0.000000	0.000000

Pd(OAc)$_2$

SCF = -584.8746247

Thermal correction to Gibbs Free Energy = 0.060018

Pd	0.000006	-0.011553	0.000811
O	1.555603	-1.072723	0.201690
C	2.345800	0.016622	-0.009851
C	3.885453	0.039374	0.013671
H	4.223069	1.002874	0.333955
H	4.242876	-0.707318	0.691609
H	4.260171	-0.161627	-0.968207
O	1.554900	1.049951	-0.241742
O	-1.541419	0.207319	1.078968
C	-2.345923	0.004906	-0.001604
C	-3.885358	0.046228	-0.007453
H	-4.214614	1.042844	-0.215409
H	-4.257087	-0.616671	-0.760634
H	-4.253978	-0.258779	0.949621
O	-1.569151	-0.236133	-1.043521

AcOH

SCF = 0.084651

Thermal correction to Gibbs Free Energy = -458.1481866

C	3.436011	0.056536	0.000792
C	1.926093	0.061312	-0.000232
H	3.800275	-0.485572	-0.881794
H	3.814004	1.082191	-0.002592
H	3.798569	-0.478748	0.888289
O	1.401067	-1.158512	-0.000033
O	1.258886	1.100248	-0.000885
H	-0.393273	1.103216	-0.000539
C	-3.435989	-0.056572	0.000738
H	-3.800166	0.484463	-0.882555
H	-3.798805	0.479680	0.887531
H	-3.813827	-1.082291	-0.001590

Korr

C	-1.926065	-0.061264	-0.000148
O	-1.401047	1.158560	0.000064
O	-1.258948	-1.100267	-0.000808
H	0.393266	-1.103245	-0.000361

IPh

SCF = -529.3104838

Thermal correction to Gibbs Free Energy = 0.05543

C	3.381071	0.000006	-0.000002
C	2.678475	1.212176	-0.000003
C	1.275218	1.223341	0.000005
C	0.597518	-0.000018	0.000002
C	1.275227	-1.223349	-0.000003
C	2.678509	-1.212157	0.000002
H	4.469400	0.000039	0.000005
H	3.214932	2.159722	-0.000012
H	0.732192	2.164623	0.000009
H	0.732252	-2.164660	0.000008
H	3.214945	-2.159715	0.000002
I	-1.578865	0.000000	0.000000

HI

SCF = -298.3676773

Thermal correction to Gibbs Free Energy = -0.024998

I	0.000000	0.000000	0.030078
H	0.000000	0.000000	-1.594154

NH_4OAc

SCF = -285.5988315

Thermal correction to Gibbs Free Energy = 0.07218

N	-2.388400	0.085263	0.000676
H	-3.144836	0.827158	-0.039487
H	-2.632349	-0.488757	0.857834
H	-2.609883	-0.556771	-0.813200
H	-1.000475	0.643921	-0.001290
O	-0.016333	1.122655	-0.001581
C	0.945235	0.108868	-0.000019
C	0.384092	-1.393950	-0.000665
H	-0.233967	-1.585191	-0.902102
H	1.235202	-2.103299	0.003722
H	-0.242030	-1.583468	0.895520
O	2.187730	0.372353	0.001378

Korr

II

Korr

Korr

ChemPubSoc Europe
DOI: 10.1002/cctc.201900207
CHEMCATCHEM Full Papers

Unprecedented Multicomponent Organocatalytic Synthesis of Propargylic Esters via CO_2 Activation

Argyro T. Papastavrou,[a] Martin Pauze,[b] Enrique Gómez-Bengoa,[b] and Georgios C. Vougioukalakis*[a]

An efficient and straightforward organocatalytic method for the direct, multicomponent carboxylation of terminal alkynes with CO_2 and organochlorides, towards propargylic esters, is reported for the first time. 1,3-Di-tert-butyl-1H-imidazol-3-ium chloride, a simple, widely-available, stable, and cost-efficient *N*-heterocyclic carbene (NHC) precursor salt was used as the (pre) catalyst. A wide range of phenylacetylenes, bearing electron-withdrawing or electron-donating substituents, react with allyl-chlorides, benzyl chlorides, or 2-chloroacetates, providing the corresponding propargylic esters in low to excellent yields. DFT calculations on the mechanism of this transformation indicate that the reaction is initiated with the formation of an NHC-carboxylate, by addition of the carbene to a molecule of CO_2. Then, the nucleophilic addition of this species to the corresponding chlorides has been computed to be the rate limiting step of the process.

Introduction

Carbenes are neutral compounds bearing a divalent carbon atom having six valence electrons. Due to the fact that the number of carbene electrons deviates from the ''octet rule'', carbenes were initially considered to be non-isolable. The distribution of the carbenes' electrons in their orbitals is the factor that defines their ground state, characteristics, and reactivity. More specifically, carbenes are of singlet or triplet ground state. In singlet carbenes, the two electrons that do not participate in σ-bonds occupy the highest occupied molecular orbital (HOMO) of the carbon atom. Therefore, the carbenic carbon's p_π orbital is empty. This distribution of valence electrons makes singlet carbenes both nucleophilic and electrophilic at the same time. In contrast, triplet carbenes carry a single electron in each p_χ and p_ψ orbital and behave as biradicaloid species.[1] *N*-heterocyclic carbenes (NHCs) were successfully isolated and characterized for the first time by Arduengo in 1991.[2] The term NHC is used to describe molecules bearing the carbenic carbon in a ring containing at least one α-amino substituent.[3] The nitrogen atom at this position thermodynamically stabilizes the carbenic center of a singlet carbene, both due to its π-electron donating and σ-electron withdrawing character (Figure 1).[4]

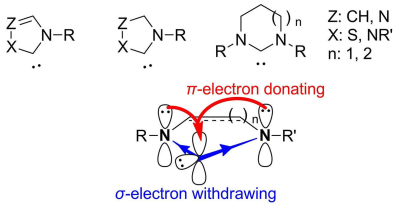

Figure 1. Some frequently encountered types of NHCs and the visualization of the stabilization of singlet carbenes originating from the α-amino substituent(s).

Among others, NHCs have been studied as ligands that can substitute phosphines in metal complexes. Indeed, many metal complexes of NHCs efficiently catalyze a plethora of reactions, including olefin metathesis and cross-couplings.[5] Moreover, catalytic systems of "green" metals, such as copper and iron, with NHCs as ligands find numerous applications in sustainable catalytic systems.[6] Equally important, NHCs serve as excellent organocatalysts in many organic transformations. The benzoin reaction is one of the earliest known carbon-carbon bond-forming reactions catalyzed by *N*-heterocyclic carbenes.[7] Ever since, NHCs organocatalysis has been employed in many different transformations. In addition to the benzoin reaction,[8] these include the Stetter reaction,[9] Heck-type reactions,[10] NHC-catalyzed umpolung of imines for intramolecular reactions, as well as many other valuable transformations employing NHCs' peculiar behavior and balance between nucleophilicity and electrophilicity (Scheme 1).[11]

Recently-reported transformations, catalyzed by NHCs, deal with the utilization of nitroalkenes to prepare three- to five-carbon-atom building blocks,[12] the synthesis of 4-difluoromethylquinolines,[13] polymerization reactions,[14] 1,6-conjugate addition reactions,[15] Michael additions,[16] and various enantioselective functionalizations.[17]

---

[a] A. T. Papastavrou, Prof. Dr. G. C. Vougioukalakis
Laboratory of Organic Chemistry, Department of Chemistry
National and Kapodistrian University of Athens
Athens GR-15771 (Greece)
E-mail: vougiouk@chem.uoa.gr
[b] M. Pauze, Prof. Dr. E. Gómez-Bengoa
Department of Organic Chemistry I, Faculty of Chemistry
University of the Basque Country
UPV-EHU, 20018 Donostia-San Sebastian (Spain)

Supporting information for this article is available on the WWW under https://doi.org/10.1002/cctc.201900207

This manuscript is part of the Special Issue on New Concepts in Homogeneous Catalysis.

© 2019 Wiley-VCH Verlag GmbH & Co. KGaA, Weinheim

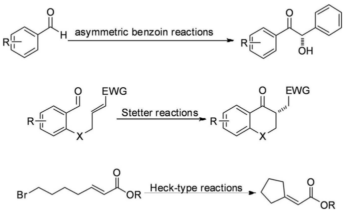

Scheme 1. Examples of useful organic transformations catalyzed by NHCs.

On a different note, propargylic esters can be prepared via several synthetic pathways. One of the simplest methods involves the esterification of the corresponding propiolic acid. The desired propiolic acid has to be synthesized first, which is then coupled with the corresponding alcohol.[18] Propargylic esters can be also obtained from the transformation of lithium phenylacetylide, as demonstrated in the synthesis of Taxoids.[19] Other propargylic esters synthetic methods utilize carbon monoxide as the carbonyl source of the final molecule.[20] However, carbon monoxide is highly toxic and dangerous. Alternatively, carbon dioxide can be used as the source of the carbonyl group of the desired compounds. Besides leading to a highly useful family of organic synthons, these CO_2 monetization methodologies utilize one of the most harmful pollutants, the main "greenhouse effect" gas, transforming it into useful organic compounds.[21] Catalytic systems that are known to achieve the direct preparation of propargylic esters via CO_2 activation are currently based on rather complicated copper complexes or silver salts.[22,23] Note that propargylic esters are invaluable organic synthons, among others utilized in the preparation of arylnaphthalenes, via intramolecular dehydro-Diels-Alder reactions (Scheme 2). Arylnaphthalenes and their dihydro- and tetrahydronaphthalene derivatives are compounds of medicinal interest, with a wide range of pharmacological activity. For example, diphyllin and justicidin B are both cytotoxic compounds and demonstrate anticancer, antiparasitic, and antiviral activities.[18d]

Herein, we report a novel, straightforward organocatalytic approach for the multicomponent conjugation of terminal alkynes, carbon dioxide and organochlorides, affording propargylic esters with variable structural characteristics in a single step. 1,3-Di-tert-butyl-1H-imidazol-3-ium chloride, a simple, widely-available, stable, and cost-efficient NHC precursor salt was used as the (pre)catalyst. The reaction between phenylacetylene, cinnamyl chloride and CO_2 was the model reaction employed to probe the activity of a series of NHC salts as (pre) catalysts, as well as in order to determine the optimum reaction conditions. Then, a series of phenyl acetylene derivatives and organohalides were utilized to investigate the scope of the reaction. 18 different propargylic esters were synthesized and isolated, with isolated yields ranging from 25 to 97 %. Finally, DFT studies were carried out to clarify the mechanism of the transformation. These studies suggest that the NHC moiety is crucial for the activation of CO_2 at the outset of the reaction, forming an NHC-carboxylate, which is then esterified with the allyl halide. In the last step, the NHC acts as an efficient leaving group, leading to the final adducts upon attack of the potassium acetylide. Thus, NHC is acting as a catalytic activator of CO_2, enhancing its nucleophilicity in the first step and its electrophilicity during the final alkyne attack.

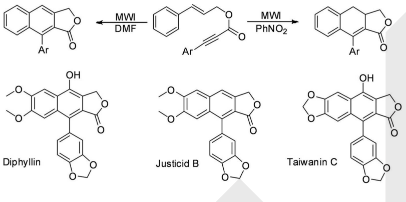

Scheme 2. Propargylic esters as valuable intermediates in organic synthesis.[18d]

Results and Discussion

To determine which NHC catalyzes the reaction most efficiently, a number of NHC salts precursors with variable structural characteristics were screened in the reaction between phenylacetylene (**1a**), CO_2 (**2**), and cinnamyl chloride (**3a**) towards propargylic ester **4a** (Scheme 3). K_2CO_3 was used as the base and DMF as the solvent, at 60 °C and under 14.8 Atm of CO_2 pressure. NHC precursors utilized bear saturated (**8**–**12**) or unsaturated (**5**–**7**) NHC backbones, are of symmetrical (**5**–**7** and **11**, **12**) or unsymmetrical (**8**–**10**) nature with regards to their exocyclic substituents, have aliphatic (**5**, **6**), aromatic (**7** and **9**–**12**) or both aliphatic and aromatic exocyclic substituents (**8**), or even exocyclic substituents bearing heteroatoms able to act as base and/or nucleophile when appropriately rotated close to the carbenic center (**9**, **10**). NHC precursors bearing the aliphatic, bulky, electron-donating exocyclic substituents tert-butyl (**5**) and cyclohexyl (**6**) groups afforded the desired product

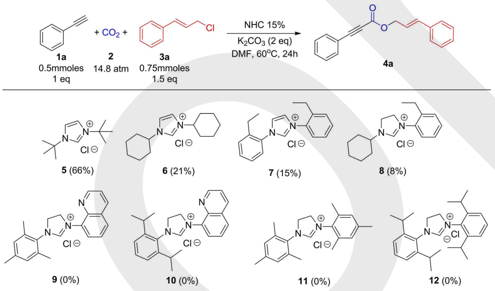

Scheme 3. Investigation of the catalytic activity of *N*-heterocyclic carbene salt precursors. (Experimental conditions: NHC precursor 15 mol %, phenylacetylene 0.5 mmol, cinnamyl chloride 0.75 mmol, carbon dioxide 14.8 Atm, K_2CO_3 1 mmol, DMF 4 mL, temperature 60 °C, reaction time 24 h.Yields were measured by GC/MS.)

© 2019 Wiley-VCH Verlag GmbH & Co. KGaA, Weinheim

in **66** and **21%** yields, respectively. The rest of the NHC precursors utilized, afforded very low yields of the targeted propargylic ester (**7**–**8**), or no product at all (**9**–**12**). Therefore, among the NHC salts tested in the model reaction, 1,3-di-tert-butyl-1H-imidazol-3-ium chloride (**5**) exhibits the optimum catalytic behavior. This was the NHC precursor we utilized in the rest of our studies.

With the most efficient NHC salt (pre)catalyst in hand, we investigated the influence of the other reaction parameters. More specifically, we investigated the influence of the base used, the solvent of the reaction, the catalytic amount of the NHC precursor, and the reaction temperature (Table 1). Among the bases used, in DMF, potassium carbonate provided the best results (Entry 3). Sodium carbonate provided the desired product, albeit with significantly lower yields (Entries 4 and 9). This result is attributed to the size and the nature of the counterion of carbonate. Sodium bicarbonate was found to be an inappropriate base for the reaction (Entry 1), as also did sodium hydroxide (Entry 5). Besides DMF, four other solvents were used to carry out the reaction. Those were toluene, acetonitrile, dichloromethane and tetrahydrofuran (Entries 6 to 11). When acetonitrile was used as the solvent (Entries 7 to 9) the targeted propargylic ester was formed efficiently, but in slightly lower yields than those observed in the case of DMF. All other solvents either did not yield the product at all, or the product was formed in traces. By increasing the NHC (pre) catalyst loading from 15 to 20% (Entry 12), phenylacetylene is quantitatively converted to the desired product, as was also observed under 25% catalyst loading (Entry 13). The reaction also takes place at room temperature (Entry 14) affording a 55% yield of the propargylic ester, which is, however, lower than the 99% GC/MS yield obtained at 60 °C. In a series of blank tests, it was found that the presence of base (Entry 17), NHC precursor (Entry 18) and a high pressure of carbon dioxide (Entry 16) were all necessary for the three-component reaction to occur.

Table 1. Investigation of the conditions of the three-component coupling of phenylacetylene, cinnamyl chloride and carbon dioxide towards the corresponding propargylic ester.

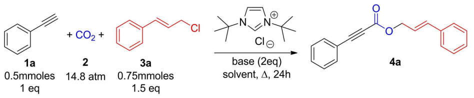

Entry	Base	Solvent	Catalyst loading [%]	T	Yield [a]
1	$NaHCO_3$	DMF	15	60 °C	–
2	CsF	DMF	15	60 °C	9%
3	K_2CO_3	DMF	15	60 °C	66%
4	Na_2CO_3	DMF	15	60 °C	11%
5	NaOH	DMF	15	60 °C	–
6	K_2CO_3	Toluene	15	60 °C	–
7	K_2CO_3	CH_3CN	15	60 °C	53%
8	K_2CO_3	CH_3CN	20	60°C	78%
9	Na_2CO_3	CH_3CN	15	60°C	Traces
10	K_2CO_3	CH_2Cl_2	15	60 °C	Traces
11	K_2CO_3	THF	15	60 °C	–
12	K_2CO_3	DMF	20	60 °C	>99%
13	K_2CO_3	DMF	25	60 °C	>99%
14	K_2CO_3	DMF	20	r.t.	55%
15[b]	K_2CO_3	DMF	20	60 °C	–
16[c]	K_2CO_3	DMF	20	60 °C	17%
17	–	DMF	20	60 °C	–
18	K_2CO_3	DMF	–	60 °C	–

[a] Experimental conditions:1,3-di-tert-butyl-1H-imidazol-3-ium chloride (NHC precursor salt), phenylacetylene 0.5 mmol, cinnamyl chloride 0.75 mmol, carbon dioxide 14.8 Atm, base 1 mmol, solvent 4 mL, reaction time 24 h. Yields were measured by GC/MS. [b] In the absence of CO_2. [c] CO_2 pressure of 4.9 Atm.

We then carried out a kinetic study, in order to find the optimum reaction time. More specifically, we studied the catalytic activity of our optimized organocatalytic system in the reaction of phenylacetylene (**1a**), CO_2, and cinnamyl chloride (**3a**) towards propargylic ester **4a** via GC/MS. The conversion to the product **4a** over time is represented in Figure 2. Interestingly, the reaction has a relatively long induction period of about 10 hours (about 20% conversion in the first 10 hours). This long induction period could be rationalized by the necessity for the formation of an important intermediate in the catalytic cycle, or by some kind of an off-cycle process (also see the discussion with regards to the theoretical calculations below). After the necessary induction period, the reaction speeds up, reaching completion in about 10 additional hours, that is, in 20 hours total reaction time.

Prior to investigating the reaction scope, we also carried out a series of control experiments towards shedding some light on the possible role of the NHC in the generation of the acetylide. It is known that the deprotonation of phenylacetylene readily occurs in the presence of carbonates to provide the corresponding acetylide.[24] Nevertheless, carbenes have been also shown to be able to insert into C–H bonds.[25] Therefore, we were intrigued to study whether the in situ generated NHC could somehow increase the rate of the acetylide formation. Unfortunately, though, despite our efforts to trap the generated acetylide under conditions analogous to our reaction conditions, our experiments were inconclusive in this regard.

With the optimum reaction conditions in hand, we investigated the scope of the organohalides (Scheme 4). The two 2-chloroacetate esters probed yield the corresponding coupling products **4b** and **4c**, albeit at relatively low yields. Moreover, organochlorides bearing the chlorine atom on the carbonyl carbon do not provide the desired propargyl ester, as found in the case of **4d**. On the contrary, allylic chlorides are very good

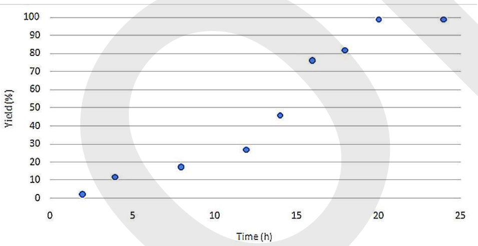

Figure 2. Reaction profile of the organocatalytic multicomponent coupling of phenylacetylene (**1a**), cinnamyl chloride (**3a**) and carbon dioxide towards propargylic ester **4a**.

© 2019 Wiley-VCH Verlag GmbH & Co. KGaA, Weinheim

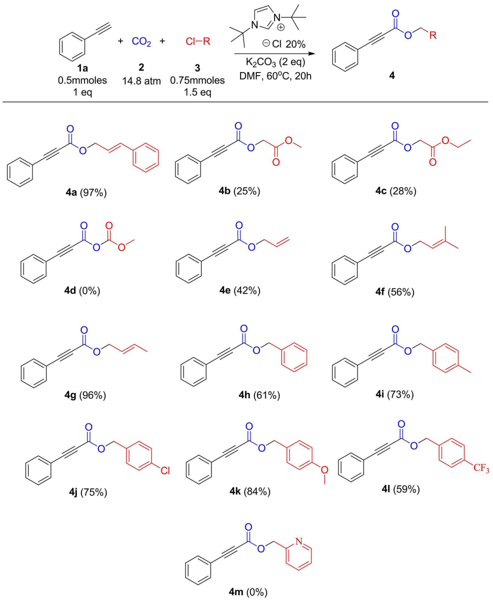

Scheme 4. Investigation of the scope of the reaction with regards to the organochloride. (Experimental conditions: 1,3-di-tert-butyl-1H-imidazol-3-ium chloride (NHC precursor salt) 20 %, phenylacetylene 0.5 mmol, organochloride 0.75 mmol, carbon dioxide 14.8 Atm, K_2CO_3 1 mmol, DMF 4 mL, reaction time 20 h, reaction temperature 60 °C. All yields provided are isolated.)

substrates for this reaction, leading to propargylic esters **4a**, **4e**, **4f** and **4g** in good to excellent yields. The relatively low yield in the reaction of chloropropene (leading to propargylic ester **4e**) can be attributed to the fact that this substrate has a relatively low boiling point (46 °C, while the reaction temperature is 60 °C). The same rationale can be also true in the case of propargylic ester **4f** (56 % yield), given that chlorobutene has a boiling point of 59 °C, also lower that the reaction temperature. Along these lines, crotyl chloride, with a boiling point of 85 °C, yields the corresponding propargylic ester **4g** in an excellent, 96 % yield. Benzyl chlorides are also very good substrates under these conditions, leading to propargylic esters **4h** to **4l**, in isolated yields ranging from 59 to 84 %. Picolyl chloride does not provide the targeted ester **4m**, most probably due to the existence of the pyridine moiety in its structure. This was shown during control experiments, in which the reaction of phenylacetylene with benzylchloride was completely quenched in the presence of one equivalent (in relation to benzylchloride) of pyridine- in the absence of pyridine this reaction provides propargylic ester **4h** in 61 % isolated yield. Interestingly, in addition to the parent benzyl chloride (**4h**), both electron-poor (**4j** and **4l**) and electron-rich (**4i** and **4k**) benzyl chlorides afford very good yields, while the co-existence of a second chlorine atom on the aromatic ring (**4j**) does not impose any problem to the reaction. Note, finally, that all organobromides probed

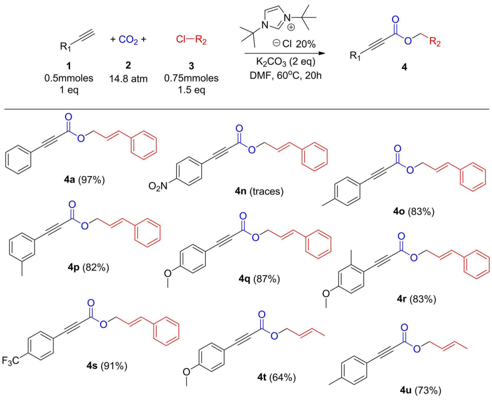

Scheme 5. Investigation of the scope of the multicomponent organocatalytic carboxylative coupling of terminal alkynes and organohalides with CO_2. (Experimental conditions: 1,3-di-tert-butyl-1H-imidazol-3-ium chloride (NHC precursor salt) 20 %, terminal alkyne 0.5 mmol, organochloride 0.75 mmol, carbon dioxide 14.8 Atm, K_2CO_3 1 mmol, DMF 4 mL, reaction time 20 h, reaction temperature 60 °C. All yields provided are isolated.)

(results not shown: 1-bromobutane, bromoethene, 1-bromododecane, 3-bromopropanenitrile, 2-bromo-1-phenylethanone) were found to be unsuitable substrates for the reaction.

Subsequently, the scope of the multicomponent organocatalytic coupling towards propargylic esters was investigated with regards to the terminal alkyne utilized. The results of this study are shown in Scheme 5. Alkyl-substituted terminal alkynes (results not shown: 1-pentyne and 3,3-dimethylbut-1-yne) do not afford the targeted propargylic esters under our protocol's conditions. The same is true for a hydroxyl-bearing alkyne we tested (results not shown: 2-methylbut-3-yn-2-ol), as well as a phenyl acetylene bearing a bromide (results not shown: 1-bromo-2-ethynylbenzene). Moreover, the electron poor, p-NO_2-substituted phenyl acetylene affords the targeted propargylic ester **4n**, albeit in traces. On the other hand, the p-CF_3-substituted phenyl acetylene, which is also electron-poor, gives an excellent isolated yield of 91 % of propargylic ester **4s**. This finding suggests the reaction is not problematic with electron-poor terminal alkynes in general, but, most probably, it is not compatible with the -NO_2 moiety (also see the discussion that follows). Phenylacetylenes bearing no aromatic substituents or methyl and/or methoxy moieties on the aromatic ring are excellent substrates under our protocol, affording the corresponding propargylic esters in very good to excellent yields (**4a**, **4o**–**4r**, and **4t**–**4u**).

Theoretical Calculations

We next turned our attention to the study of the mechanism of the reaction, by means of DFT methods. The calculations were carried out with the Gaussian 16 set of programs, using the M06-2X functional together with the 6-311G(d,p) basis sets for full structure optimization. An implicit solvent model (IEFPCM, solvent = dimethyl formamide) was also incorporated to all calculations.[26]

We wanted to get information about the energy profile of the reaction, which is crucial to clarify some important issues about the mechanism, like: a) the identification of the rate limiting step of the process, b) the understanding of the origin of the induction period observed at the outset of the reaction, and c) the determination of the underlying reasons for the large difference of reactivity between the different electrophiles, like, for example, cinnamyl chloride **3 a** *vs* picolyl chloride **3 m** (Scheme 4). We assumed that the fundamental steps of the reaction would be the attack of the NHC catalyst to CO_2 (**TS1**, Figure 3), the S_N2-type nucleophilic substitution of the chloride by the carboxylate (**TS2**) and the final introduction of the propargylic system with concomitant recovery of the catalytic NHC carbene (**TS3** and **TS4**). For the initial calculations, those substrates affording the best results were selected, including the di-tertbutylcarbene catalyst derived from **5**, cinnamyl chloride **3 a**, and phenylacetylene **1 a**.

As previously mentioned, we envisioned that the first step of the reaction was the attack of NHC carbene to a molecule of CO_2 (Figure 3). As described by others,[27] this step was computed to be easy and low in energy (**TS1**, $\Delta G^{\neq} = 10.9$ kcal/mol), with a very early transition state that bears a long carbon-carbon bond distance (2.3 Å). The intermediate formed in this step (**II**) is fairly stable and low in energy (−2.7 kcal/mol). These carbene-CO_2 adducts are known and extensively studied. Amongst others, they are used as non-ionic NHC precursors, delivering the free carbene in the reaction mixture upon thermal decomposition, circumventing the need for the use of a base.[28] The intermediate formed in step (**II**) shows kinetic resistance to react with cinnamyl chloride **3 a**, as can be inferred from its moderate activation energy ($\Delta\Delta G^{\neq} = 22.1$ kcal/mol). This value is perfectly affordable at the experimental reaction temperature. The structure of the transition state follows a standard S_N2-type nucleophilic displacement of the chloride anion (see 3D structure in Figure 4), leading to the second intermediate of the reaction (**III**), which is rather stable ($\Delta G = -4.2$ kcal/mol). The process continues with the nucleophilic attack of the propargylic unit (**1 a**) to intermediate **III** through a classical two-step addition to the carbonyl group (transition states **TS3** and **TS4**) with formation of the tetrahedral intermediate **IV**. The addition of the acetylide in **TS3** is higher in energy ($\Delta\Delta G^{\neq} = 20.7$ kcal/mol) than the detachment of the carbene leaving group in **TS4**, which is very fast ($\Delta\Delta G^{\neq} = 5.1$ kcal/mol), but both steps are lower in energy than **TS2**.

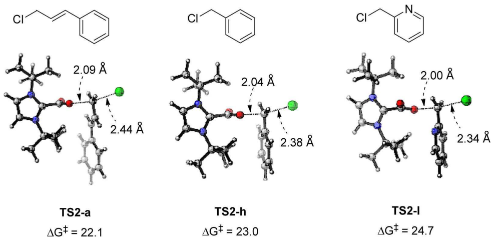

Figure 4. Activation free energies for the substitution step of chloride (**TS2**) in the cinnamyl (**3 a**), benzyl (**3 h**) and picolyl substrates (**3 m**).

Thus, the energy profile points to the nucleophilic displacement of the chloride by NHC-carboxylate (**TS2**) as the rate limiting step of the process, as it shows the highest energy of the catalytic cycle. Thus, the comparison of the reactivity of the different substrates should be done at this point. In fact, we were able to locate the transition states for the substitution of intermediate II to benzyl chloride (**3 h**) and picolyl chloride (**3 m**). The computed structures of **TS2h**, and **TS2m** were structurally very similar to that of cinnamyl chloride **TS2a** (Figure 4).[29] The computed activation energies show the lowest

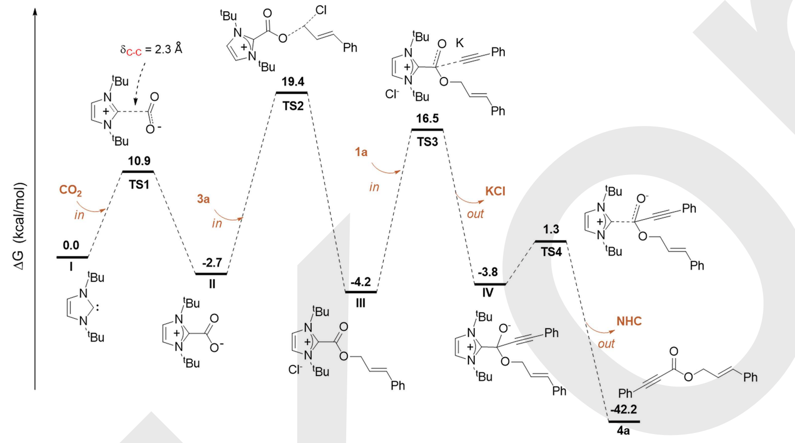

Figure 3. Energy profile for the catalytic cycle of the reaction between **1 a**, **3 a**, and CO_2.

© 2019 Wiley-VCH Verlag GmbH & Co. KGaA, Weinheim

value ($\Delta G^{\neq}=22.1$ kcal/mol) for the most reactive substrate of the three (**3a**), in agreement with the experimental results shown in Scheme 4. The activation energy for the benzyl derivative **3h** lies 0.9 kcal/mol higher, which is not a very significant difference, but enough to explain the decrease in yield noted experimentally (97% vs 61%, Scheme 4). Interestingly, the unreactive picolyl derivative **3m** shows an activation energy of $\Delta G^{\neq}=24.7$ kcal/mol). While this value is 2.6 kcal/mol higher than for **3a**, allowing us to explain a significant decrease in yield for substrate **3m**, it does not seem enough to account for its complete lack of reactivity. Therefore, the presence of a pyridine moiety has a deleterious effect on the reactivity by some other undisclosed mechanism. As previously discussed, the addition of 1 eq of pyridine to the reaction medium quenches the reaction completely. Finally, the structures of the three transition states in Figure 4 present forming O–C bond distances between 2.00 Å and 2.09 Å, and breaking C–Cl bond distances between 2.34 Å and 2.44 Å. Interestingly, the distances slightly increase with the increasing reactivity of the substrates (Figure 4). These data suggest that the reacting sp3 carbon develops a relative positive charge during **TS2**, explaining why electron donating substituents, like **3k**, show higher reactivity than electron withdrawing groups, like **3l** (Scheme 4).

Finally, we were intrigued by the long induction period that we observed in our reactions (Figure 2). In fact, nothing, in the computed cycle shown in Figure 3, points to the existence of such an initial delay, which has to be related to some off-cycle process. One hypothesis is that the initial formation of the active NHC carbene from the imidazolium precursor in the presence of a base could be slow in the reaction scale, and, therefore, the necessary concentration of NHC carbene (I) would need some time to evolve.

Conclusions

A novel organocatalytic protocol for the multicomponent carboxylative coupling of terminal alkynes with organochlorides and CO_2, catalyzed by an in situ generated NHC derived from the widely-available, cost-efficient and stable 1,3-di-tert-butyl-1H-imidazol-3-ium chloride was developed. The protocol is user-friendly, straightforward and highly efficient against a number of substrates and functionalities. In addition to the parent phenylacetylene, a wide range of substituted phenylacetylenes, bearing electron-withdrawing or electron-donating aromatic substituents, react with allyl-chlorides, benzyl chlorides, or 2-chloroacetates, providing the corresponding propargylic esters in low to excellent yields. DFT calculations on the mechanism of this transformation indicate that the reaction is initiated with the addition of the carbene to a molecule of CO_2, forming an NHC-carboxylate. This species is nucleophilic enough to react with chlorides, although the high activation energy of this process suggests that it is the rate limiting step. This fact would explain the large difference in reactivity of the different allyl and benzyl chlorides and the effect of the substituents.

Experimental Section

General Reagent Information. Unless otherwise noted, chemicals were obtained from commercial sources and were purified according to literature procedures. Solvents were purified according to published procedures, distilled and stored under argon over 3 Å molecular sieves. All reactions were set up under argon and carried out under carbon dioxide in sealed, high pressure reactor. The course of the reactions was followed with GC/MS. The purification of the products was carried out by flash column chromatography, using silica gel 60 (230–400 mesh).

General Analytical Information. ^{1}H, ^{13}C NMR spectra were measured on a Varian Mercury 200 MHz spectrometer using $CDCl_3$ as the solvent and its residual solvent peak as a reference. NMR spectroscopic data are given in the order: chemical shift, multiplicity (s, singlet, br. s, broad singlet, d, doublet, t, triplet, q, quartet, m, multiplet), coupling constant in Hertz (Hz), and number of protons. Peaks at 0 and 1.5 ppm of spectra are attributed to impurities of laboratory solvents, organics, and gases in deuterated solvents.[30] HRMS spectra were recorded in a QTOF maxis Impact (Bruker) spectrometer with Electron Spray Ionization (ESI). The GC/MS spectra were recorded with a Shimadzu R GCMS-QP2010 Plus Chromatograph Mass Spectrometer using a MEGAR (MEGA-5, F.T: 0.25 μm, I.D.: 0.25 mm, L: 30 m, Tmax: 350 °C, Column ID# 11475) column, using *n*-octane as the internal standard.

Synthetic Protocols. The synthetic protocols for NHC ligand precursors **5** to **10** are reported in the literature.[6b,31] NHC ligand precursors **11** and **12** were purchased and used without any further purification.

Unless otherwise mentioned, the following procedure was used for the synthesis of all products: A flame-dried vial with a stirring bar and a rubber septum was charged with 20 mol% of 1,3-di-tert-butyl-1H-imidazol-3-ium chloride (0.1 mmol), K_2CO_3 (1 mmol) and DMF (4 mL). Under a flow of argon, the terminal alkyne (0.5 mmol) and organohalide (0.75 mmol) were added and the mixture was placed in the pressure reactor. The reactor was purged three times with carbon dioxide, the pressure was finally fixed to 14.8 Atm and the reaction was allowed to stir in an oil bath, preheated at 60 °C, for 20 hours. After this time, the pressure reactor was cooled to room temperature and ventilated carefully. Water was added to the reaction mixture and was extracted with ethyl acetate (3×5 ml). The organic phase was dried with $MgSO_4$ and the solvent was removed under reduced pressure to afford the crude mixture of the reaction. Gradient column chromatography with ethyl acetate/petroleum ether furnished the desired product. Products prepared for the first time were characterized by ^{1}H NMR, ^{13}C NMR, and HRMS, which are all in agreement with the assigned structures. Known compounds were characterized by ^{1}H NMR and ^{13}C NMR with all their spectroscopic characteristics in agreement with those reported in the literature.

1-(2,6-Diisopropylphenyl)-3-(quinolin-8-yl)-4,5-dihydro-1H-imidazol-3-ium chloride (**10**): ^{1}H NMR (200 MHz, $CDCl_3$) δ 9.62 (s, 1H), 8.74 (s, 1H), 8.28 (d, J=7.9 Hz, 1H), 7.99 (d, J=7.4 Hz, 1H), 7.79 (d, J=8.1 Hz, 1H), 7.66–7.36 (m, 3H), 7.24 (d, J=7.6 Hz, 2H), 5.24 (t, J=10.5 Hz, 2H), 4.57 (t, J=10.5 Hz, 2H), 3.17 (hept, J=13.2, 6.9 Hz, 2H), 1.26 (t, J=6.9 Hz, 12H). ^{13}C NMR (50 MHz, $CDCl_3$) δ 158.36, 150.58, 146.73, 140.17, 137.79, 131.80, 131.72, 130.20, 129.42, 128.06, 127.01, 125.34, 122.84, 122.27, 53.35, 29.07, 25.48, 24.44. HRMS (ESI) m/z calculated for $C_{12}H_{10}O_4Na$ $[M]^+$ requires m/z 358.5085. Found m/z: 358.2321.

Cinnamyl 3-phenylpropiolate (**4a**):[22c] Prepared according to the general procedure and obtained in 97% yield (127 mg, 0.485 mmol). ^{1}H NMR (200 MHz, $CDCl_3$) δ 7.70–7.52 (m, 2H), 7.51–7.16 (m, 8H), 6.74 (d, J=15.8 Hz, 1H), 6.34 (dt, J=15.9, 6.5 Hz, 1H),

© 2019 Wiley-VCH Verlag GmbH & Co. KGaA, Weinheim

4.90 (d, J = 6.5 Hz, 2H).^{13}C NMR (50 MHz, $CDCl_3$) δ 154.0, 136.2, 135.5, 133.2, 130.9, 128.8, 128.8, 128.5, 126.9, 122.3, 119.7, 86.8, 80.7, 66.7.

2-Methoxy-2-oxoethyl 3-phenylpropiolate (**4b**): Prepared according to the general procedure and obtained in 25% yield (27 mg, 0.125 mmol).^{1}H NMR (200 MHz, $CDCl_3$) δ 7.65–7.56 (m, 2H), 7.48–7.32 (m, 3H), 4.76 (s, 2H), 3.80 (s, 3H).^{13}C NMR (50 MHz, $CDCl_3$) δ 167.7, 153.4, 133.4, 131.2, 128.8, 119.3, 88.4, 79.9, 61.7, 52.8. HRMS (ESI) m/z calculated for $C_{12}H_{10}O_4Na$ $[M+Na]^+$ requires m/z 241.0579. Found m/z: 241.0472.

2-Ethoxy-2-oxoethyl 3-phenylpropiolate (**4c**):[22c] Prepared according to the general procedure and obtained in 28% yield (32 mg, 0.14 mmol).^{1}H NMR ($CDCl_3$) δ 7.68–7.55 (m, 2H), 7.51–7.31 (m, 3H), 4.74 (s, 2H), 4.27 (q, J = 7.1 Hz, 2H), 1.31 (t, J = 7.1 Hz, 3H).^{13}C NMR ($CDCl_3$) δ 167.1, 153.4, 133.3, 131.1, 128.8, 119.4, 88.3, 79.9, 61.9, 61.8.

Allyl 3-phenylpropiolate (**4e**):[22c] Prepared according to the general procedure and obtained in 42% yield (39 mg, 0.21 mmol). ^{1}H NMR ($CDCl_3$) δ 7.65–7.52 (m, 2H), 7.50–7.30 (m, 3H), 5.97 (m, 1H), 5.41 (dd, J = 17.2, 1.4 Hz, 1H), 5.32 (dd, J = 10.3, 1.2 Hz, 1H), 4.73 (d, J = 5.9 Hz, 2H). ^{13}C NMR ($CDCl_3$) δ 153.9, 133.2, 131.3, 130.9, 128.8, 119.7, 119.6, 86.7, 80.6, 66.8.

3-Methylbut-2-en-1-yl 3-phenylpropiolate (**4f**):[22c] Prepared according to the general procedure and obtained in 56% yield (60 mg, 0.28 mmol).^{1}H NMR ($CDCl_3$) δ 7.58–7.30 (m, 5H), 5.44–5.40 (m, 1H), 4.73 (d, J = 7.4 Hz, 2H), 1.79 (s, 3H), 1.75 (s, 3H). ^{13}C NMR ($CDCl_3$) δ 154.3, 140.8, 133.2, 130.8, 128.7, 119.8, 117.8, 86.3, 80.8, 63.1, 26.0, 18.3.

(E)-But-2-en-1-yl 3-phenylpropiolate (**4g**):[32] Prepared according to the general procedure and obtained in 94% yield (94 mg, 0.47 mmol).^{1}H NMR ($CDCl_3$) δ 7.65–7.50 (m, 2H), 7.48–7.27 (m, 3H), 6.01–5.72 (m, 1H), 5.71–5.51 (m, 1H), 4.63 (d, 2H), 1.72 (d, J = 6.3 Hz, 3H).^{13}C NMR ($CDCl_3$) δ 154.0, 133.1, 133.0, 130.8, 128.7, 124.4, 119.8, 86.4, 80.8, 66.9, 18.0.

Benzyl 3-phenylpropiolate (**4h**):[22i] Prepared according to the general procedure and obtained in 61% yield (72 mg, 0.30 mmol).^{1}H NMR (200 MHz, $CDCl_3$) δ 7.66–7.55 (m, 2H), 7.50–7.31 (m, 8H), 5.29 (s, 2H).^{13}C NMR (50 MHz, $CDCl_3$) δ 154.1, 135.1, 133.2, 130.9, 128.9, 128.9, 128.8, 128.8, 119.7, 86.9, 80.8, 67.9.

4-Methylbenzyl 3-phenylpropiolate (**4i**):[22i] Prepared according to the general procedure and obtained in 73% yield (91 mg,0.365 mmol).^{1}H NMR ($CDCl_3$) δ 7.63–7.55 (m, 2H), 7.46–7.32 (m, 4H), 7.22 (d, J = 7.9 Hz, 2H), 5.25 (s, 2H), 2.38 (s, 3H).^{13}C NMR ($CDCl_3$) δ 154.20, 138.80, 133.25, 132.18, 130.93, 129.61, 129.08, 128.83, 119.81, 86.82, 80.86, 67.96, 21.52.

4-Chlorobenzyl 3-phenylpropiolate (**4j**):[22i] Prepared according to the general procedure and obtained in 75% yield (101 mg, 0.375 mmol).^{1}H NMR ($CDCl_3$) δ 7.61–7.51 (m, 2H), 7.50–7.31 (m, 7H), 5.22 (s, 2H).^{13}C NMR ($CDCl_3$) δ 153.5, 134.4, 133.3, 132.8, 130.6, 129.8, 128.7, 128.4, 119.2, 86.8, 80.2, 66.6.

4-Methoxybenzyl 3-phenylpropiolate (**4k**):[22i] Prepared according to the general procedure and obtained in 84% yield (112 mg, 0.42 mmol).^{1}H NMR (200 MHz, $CDCl_3$) δ 7.77–7.45 (m, 2H), 7.46–7.28 (m, 5H), 6.98–6.86 (m, 2H), 5.21 (s, 2H), 3.81 (s, 3H).^{13}C NMR (50 MHz, $CDCl_3$) δ 160.16, 154.22, 133.23, 130.92, 130.84, 128.81, 127.23, 119.77, 114.26, 86.75, 80.84, 67.86, 55.54.

4-(Trifluoromethyl)benzyl 3-phenylpropiolate (**4l**):[20] Prepared according to the general procedure and obtained in 59% yield (89 mg, 0.29 mmol). ^{1}H NMR ($CDCl_3$) δ 7.68–7.62 (d, J = 8.1 Hz, 2H), 7.62–7.57 (m, 2H), 7.56–7.52 (d, J = 8.1 Hz, 2H), 7.49–7.43 (m, 1H), 7.41–7.35 (m, 2H), 5.31 (s, 2H). ^{13}C NMR ($CDCl_3$) δ 153.8, 139.1, 133.3, 131.1, 128.7, 125.8, 119.5, 87.5, 80.4, 66.8.

Cinnamyl 3-(p-tolyl)propiolate (**4o**):[22c] Prepared according to the general procedure and obtained in 83% yield (115 mg, 0.41 mmol). ^{1}H NMR ($CDCl_3$) δ 7.48 (d, J = 7.9 Hz, 2H), 7.41–7.24 (m, 5H), 7.16 (d, J = 7.9 Hz, 2H), 6.71 (d, J = 15.9 Hz, 1H), 6.32 (dt, J = 15.9, 6.6 Hz, 1H), 4.87 (d, J = 6.6 Hz, 2H), 2.36 (s, 3H). ^{13}C NMR ($CDCl_3$) δ 153.9, 141.3, 136.0, 135.2, 133.0, 129.4, 128.6, 128.2, 126.7, 122.1, 116.4, 87.2, 80.2, 66.4, 21.7.

Cinnamyl 3-(m-tolyl)propiolate (**4p**): Prepared according to the general procedure and obtained in 82% yield (113 mg, 0.41 mmol). ^{1}H NMR (200 MHz, $CDCl_3$) δ 7.73–7.08 (m, 9H), 6.74 (d, J = 15.9 Hz, 1H), 6.34 (dt, J = 15.9, 6.5 Hz, 1H), 4.90 (d, J = 6.5 Hz, 2H), 2.35 (s, 3H). ^{13}C NMR (50 MHz, $CDCl_3$) δ 154.1, 138.6, 136.2, 135.5, 133.7, 131.9, 130.4, 128.9, 128.7, 128.5, 126.9, 122.3, 119.5, 87.2, 80.4, 66.7, 21.4. HRMS (ESI) m/z calculated for $C_{19}H_{16}O_2Na^+$ $[M+Na]^+$ requires 299.1150. Found m/z: 299.1047.

Cinnamyl 3-(4-methoxyphenyl)propiolate (**4q**):[22c] Prepared according to the general procedure and obtained in 87% yield (123 mg, 0.43 mmol). ^{1}H NMR (200 MHz, $CDCl_3$) δ 7.54 (d, J = 8.9 Hz, 2H), 7.47–7.23 (m, 5H), 7.01–6.81 (m, 2H), 6.79–6.66 (m, 1H), 6.33 (dt, 1H), 4.88 (d, J = 6.5 Hz, 2H), 3.80 (s, 3H). ^{13}C NMR (50 MHz, $CDCl_3$) δ 161.8, 154.3, 136.2, 135.4, 135.2, 128.9, 128.5, 126.9, 122.4, 114.5, 111.4, 87.7, 80.2, 66.6, 55.6.

Cinnamyl 3-(4-methoxy-2-methylphenyl)propiolate (**4r**): Prepared according to the general procedure and in 91% yield (136 mg, 0.45 mmol). ^{1}H NMR (200 MHz, $CDCl_3$) δ 7.50 (d, J = 8.4 Hz, 1H), 7.46–7.21 (m, 5H), 6.82–6.63 (m, 3H), 6.34 (dt, J = 15.9, 6.5 Hz, 1H), 4.89 (dd, J = 6.5, 1.1 Hz, 2H), 3.80 (s, 3H), 2.48 (s, 3H). ^{13}C NMR (50 MHz, $CDCl_3$) δ 161.6, 154.4, 144.8, 136.2, 135.5, 135.3, 128.8, 128.4, 126.9, 122.5, 115.6, 111.9, 111.5, 86.8, 83.8, 66.6, 55.5, 21.1. HRMS (ESI) m/z calculated for $C_{20}H_{18}O_3Na^+$ $[M+Na]^+$ requires 329.1256. Found m/z: 329.1158.

Cinnamyl 3-(4-(trifluoromethyl)phenyl)propiolate (**4s**):[22c] Prepared according to the general procedure and obtained in 91% yield (150 mg, 0.45 mmol). ^{1}H NMR ($CDCl_3$) δ 7.67 (d, J = 8.2 Hz, 2H), 7.61 (d, J = 8.2 Hz, 2H), 7.41–7.23 (m, 5H), 6.72 (d, J = 15.9 Hz, 1H), 6.32 (dt, J = 15.9, 6.6 Hz, 1H), 4.90 (d, J = 6.6 Hz, 2H). ^{13}C NMR ($CDCl_3$) δ 153.4, 135.9, 135.7, 133.2, 132.2, 128.7, 128.4, 126.8, 125.6, 123.4, 121.9, 121.8, 84.3, 82.1, 66.9.

(E)-But-2-en-1-yl 3-(4-methoxyphenyl)propiolate (**4t**):[33] Prepared according to the general procedure and obtained in 64% yield (74 mg, 0.32 mmol). ^{1}H NMR ($CDCl_3$) δ 7.51 (d, J = 9.0 Hz, 2H), 6.86 (d, J = 9.0 Hz, 2H), 5.85 (dq, J = 15.0, 6.5 Hz, 1H), 5.64 (dt, J = 15.0, 6.5 Hz, 1H), 4.63 (d, J = 6.5 Hz, 2H), 3.81 (s, 3H), 1.73 (d, J = 2.0 Hz, 3H). ^{13}C NMR ($CDCl_3$) δ 161.4, 154.1, 134.9, 132.6, 124.2, 114.2, 111.3, 87.1, 80.0, 66.5, 55.3, 17.7.

(E)-But-2-en-1-yl 3-(p-tolyl)propiolate (**4u**):[33] Prepared according to the general procedure and obtained in 73% yield (78 mg, 0.36 mmol). ^{1}H NMR ($CDCl_3$) δ 7.46 (d, J = 8.5 Hz, 2H), 7.15 (d, J = 8.5 Hz, 2H), 5.85 (dq, J = 15.0, 7.0 Hz, 1H), 5.64 (tq, J = 15.0, 7.0 Hz, 1H), 4.63 (d, J = 7.0 Hz, 2H), 2.36 (s, 3H), 1.73(d, J = 7.0 Hz, 3H). ^{13}C NMR ($CDCl_3$) δ 154.0, 141.2, 132.9, 132.7, 129.3, 124.2, 116.5, 86.8, 80.2, 66.6, 21.7, 17.6.

Computational Details. The computational details of the calculations carried out are provided at the supporting information of this article.

© 2019 Wiley-VCH Verlag GmbH & Co. KGaA, Weinheim

Acknowledgements

We acknowledge the contribution of COST Action CA15106 (C–H Activation in Organic Synthesis-CHAOS). The Special Account for Research Grants of the National and Kapodistrian University of Athens is also gratefully acknowledged for funding (Research Program 70/3/14872). Moreover, we are thankful for the technical and human support provided by IZO-SGI SGIker of UPV/EHU, and the European Funding Horizon 2020-MSCA (ITN-EJD CATMEC 14/06-721223).

Conflict of Interest

The authors declare no conflict of interest.

Keywords: NHCs · organocatalysis · propargylic esters · CO$_2$ · multicomponent

[1] a) D. Bourissou, O. Guerret, F. P. Gabbai, G. Bertrand, *G. Chem. Rev.* **2000**, *100*, 39–92; b) K. Hirai, T. Itoh, H. Tomioka, *Chem. Rev.* **2009**, *109*, 3275–3332; c) M. Fèvre, J. Pinaud, Y. Gnanou, J. Vignolle, D. Taton, *Chem. Soc. Rev.* **2013**, *42*, 2142–2173.

[2] A. J. Arduengo, R. L. Harlow, M. Kline, *J. Am. Chem. Soc.* **1991**, *113*, 361–363.

[3] a) M. Feroci, I. Chiarotto, F. D'Anna, F. Gala, R. Noto, L. Ornano, G. Zollo, A. Inesi, *ChemElectroChem* **2016**, *3*, 1133–1141; b) D. M. Flanigan, F. Romanov-Michailidis, N. A. White, T. Rovis, *Chem. Rev.* **2015**, *115*, 9307–9387; c) R. S. Menon, A. T. Biju, V. Nair, *Chem. Soc. Rev.* **2015**, *44*, 5040–5052.

[4] a) Y. Canac, M. Soleilhavoup, S. Conejero, G. Bertrand, *J. Organomet. Chem.* **2004**, *689*, 3857–3865; b) J. Vignolle, X. Cattoen, D. Bourissou, *Chem. Rev.* **2009**, *109*, 3333–3384.

[5] a) G. C. Vougioukalakis, R. H. Grubbs, *Chem. Rev.* **2010**, *110*, 1746–1787; b) E. Kantchev, C. O'Brien, M. Organ, *Angew. Chem.* **2007**, *46*, 2768–2813; c) J. Farmer, M. Pompeo, M. Organ, in Ligand Design in Metal Chemistry: Reactivity and Catalysis, chap. 6 (Eds.: M. Stradiotto, R. J. Lundgren), John Wiley & Sons, Ltd, **2016**, pp. 134–175.

[6] a) N. V. Tzouras, I. K. Stamatopoulos, A. T. Papastavrou, A. Liori, G. C. Vougioukalakis, *Coord. Chem. Rev.* **2017**, *343*, 25–138; b) A. A. Liori, I. K. Stamatopoulos, A. T. Papastavrou, A. Pinaka, G. C. Vougioukalakis, *Eur. J. Org. Chem.* **2018**, *2018*, 6134–6139; c) S. Nolan, *Acc. Chem. Res.* **2010**, *44*, 91–100; d) K. Riener, S. Haslinger, A. Raba, M. Högerl, M. Cokoja, W. Herrmann, F. Kühn, *Chem. Rev.* **2014**, *114*, 5215–5272; e) Y. Zhang, J. Chan, *Energy Environ. Sci.* **2010**, *3*, 408–417.

[7] R. Menon, A. Biju, V. Nair, *Beilstein J. Org. Chem.* **2016**, *12*, 444–461.

[8] D. Enders, T. Balensiefer, *Acc. Chem. Res.* **2004**, *37*, 534–541.

[9] a) R. Breslow, *J. Am. Chem. Soc.* **1958**, *80*, 3719–3726; b) H. Stetter, *Angew. Chem. Int. Ed.* **1976**, *15*, 639–647; *Angew. Chem.* **1976**, *88*, 695–704; c) M. Christmann, *Angew. Chem. Int. Ed.* **2005**, *44*, 2632–2634; *Angew. Chem.* **2005**, *117*, 2688–2690; d) J. De Alaniz, M. Kerr, J. Moore, T. Rovis, *J. Org. Chem.* **2008**, *73*, 2033–2040.

[10] C. Fischer, S. Smith, D. Powell, G. Fu, *J. Am. Chem. Soc.* **2006**, *128*, 1472–1473.

[11] a) A. Patra, S. Mukherjee, T. Das, S. Jain, R. Gonnade, A. Biju, *Angew. Chem. Int. Ed.* **2017**, *56*, 2730–2734; *Angew. Chem.* **2017**, *129*, 2774–2778; b) M. Schumacher, B. Goldfuss, *New J. Chem.* **2015**, *39*, 4508–4518; c) C. Mayor, C. Wentrup, *J. Am. Chem. Soc.* **1975**, *97*, 7467–7480; d) N. Lán, C. Wentrup, *Helv. Chim. Acta* **1976**, *59*, 2068–2073; e) N. Marion, S. Díez-González, S. Nolan, *Angew. Chem. Int. Ed.* **2007**, *46*, 2988–3000; *Angew. Chem.* **2007**, *119*, 3046–3058.

[12] B. Maji, *Asian J. Org. Chem.* **2017**, *7*, 70–84.

[13] A. Patra, F. Gelat, X. Pannecoucke, T. Poisson, T. Besset, A. Biju, *Org. Lett.* **2018**, *20*, 1086–1089.

[14] H. Li, B. Ai, M. Hong, *Chin. J. Polym. Sci.* **2017**, *36*, 231–236.

[15] S. Santra, A. Porey, J. Guin, *Asian J. Org. Chem.* **2018**, *7*, 477–486.

[16] F. Xing, Z. Feng, Y. Wang, G. Du, C. Gu, B. Dai, L. He, *Adv. Synth. Catal.* **2018**, *360*, 1704–1710.

[17] a) X. Chen, Q. Liu, P. Chauhan, D. Enders, *Angew. Chem. Int. Ed.* **2018**, *57*, 3862–3873; *Angew. Chem.* **2018**, *130*, 3924–3935; b) M. Zhao, Y. Zhang, J. Chen, L. Zhou, *Asian J. Org. Chem.* **2017**, *7*, 54–69.

[18] a) H. Garcia, S. Iborra, J. Primo, M. A. Miranda, *J. Org. Chem.* **1986**, *51*, 4432–4436; b) C. Jia, D. Piao, T. Kitamura, Y. Fujiwara, *J. Org. Chem.* **2000**, *65*, 7516–7522; c) K. Ishihara, S. Nakagawa, A. Sakakura, *J. Am. Chem. Soc.* **2005**, *127*, 4168–4169 d) L. S. Kocsis, K. M. Brummond, *Org. Lett.* **2014**, *16*, 4158–4161.

[19] a) K. C. Nicolaou, E. A. Couladouros, P. G. Nantermet, J. Renaud, R. K. Guy, W. Wrasidlo, *Angew. Chem.* **1994**, *33*, 15–44; b) K. C. Nicolaou, J. Renaud, P. G. Nantermet, E. A. Couladouros, R. K. Guy, W. Wrasidlo, *J. Am. Chem. Soc.* **1995**, *117*, 2409–2420.

[20] a) K. Ohe, H. Takahashi, S. Uemura, N. Sugita, *J. Org. Chem.* **1987**, *52*, 4859–4863; b) R. Takeuchi, Y. Tsuji, M. Fujita, T. Kondo, Y. Watanabe, *J. Org. Chem.* **1989**, *54*, 1831–1836; c) T. Kitamura, I. Mihara, H. Taniguchi, P. J. Stang, *J. Chem. Soc. Chem. Commun.* **1990**, *8*, 614–615; d) Q. Cao, N. L. Hughes, M. J. Muldoon, *Chem. Eur. J.* **2016**, *22*, 11982–11985.

[21] A. Pinaka, G. C. Vougioukalakis, *Coord. Chem. Rev.* **2015**, *288*, 69–97.

[22] a) Y. Fukue, S. Oi, Y. Inoue, *J. Chem. Soc. Chem. Commun.* **1994**, *18*, 2091–2092; b) N. Eghbali, J. Eddy, P. T. Anastas, *J. Org. Chem.* **2008**, *73*, 6932–6935; c) W. Z. Zhang, W. J. Li, X. Zhang, H. Zhou, X. B. Lu, *Org. Lett.* **2010**, *12*, 4748–4751; d) K. Inamoto, N. Asano, K. Kobayashi, M. Yonemoto, Y. Kondo, *Org. Biomol. Chem.* **2012**, *10*, 1514–1516; e) X. Zhang, W. Z. Zhang, L. L. Shi, C. Zhu, J. L. Jiang, X. B. Lu, *Tetrahedron* **2012**, *68*, 9085–9089; f) B. Yu, Z. F. Diao, C. X. Guo, C. L. Zhong, L. N. He, Y. N. Zhao, Q. W. Song, A. H. Liu, J. Q. Wang, *Green Chem.* **2013**, *15*, 2401–2407; g) J. N. Xie, B. Yu, C. X. Guo, L. N. He, *Green Chem.* **2015**, *17*, 4061–4067; h) J. N. Xie, B. Yu, Z. H. Zhou, H. C. Fu, N. Wang, L. N. He, *Tetrahedron Lett.* **2015**, *56*, 7059–7062; i) F. J. Guo, Z. Z. Zhang, J. Y. Wang, J. Sun, X. C. Fang, M. D. Zhou, *Tetrahedron* **2017**, *73*, 900–906; j) G. Xiong, B. Yu, J. Dong, Y. Shi, B. Zhao, L. N. He, *Chem. Commun.* **2017**, *53*, 6013–6016; k) G. N. Bondarenko, E. G. Dvurechenskaya, E. S. Magommedov, I. P. Beletskaya, *Catal. Lett.* **2017**, *147*, 2570–2580.

[23] For a pioneering work on the stoichiometric carbon dioxide insertion into organocopper and organosilver compounds see: T. Tsuda, K. Ueda, T. Saegusa, *Chem. Commun.* **1974**, 380–381.

[24] Y. Dingyi, Z. Yugen, *Green Chem.* **2011**, *13*, 1275–1279.

[25] A. Arduengo III, J. Calabrese, F. Davidson, H. Rasika Dias, J. Goerlich, R. Krafczyk, W. Marshall, M. Tamm, R. Schmutzler, *Helv. Chim. Acta* **1999**, *82*, 2348–2364.

[26] For full Computational Details, see Supporting Information.

[27] a) D. M. Denning, D. E. Faley, *J. Org. Chem.* **2017**, *82*, 1552–1557; b) M. J. Ajitha, C. H. Suresh, *J. Org. Chem.* **2012**, *77*, 1087–1094.

[28] a) A. Voutchkova, M. Feliz, E. Clot, O. Eisenstein, R. Crabtree, *J. Am. Chem. Soc.* **2007**, *129*, 12834-12846. b) H. Zhou, W. Zhang, C. Liu, J. Qu, X. Lu, *J. Org. Chem.* **2008**, *73*, 8039–8044. c) M. Fèvre, P. Coupillaud, K. Miqueu, J. Sotiropoulos, J. Vignolle, D. Taton, *J. Org. Chem.* **2012**, *77*, 10135–10144.

[29] 3D structures are represented with CYL*view*, Legault, C. Y. CYLview 1.0b; University of Sherbrooke, Canada, **2009** (http://www.cylview.org).

[30] a) G. Fulmer, A. Miller, N. Sherden, H. Gottlieb, A. Nudelman, B. Stoltz, J. Bercaw, K. Goldberg, *Organometallics* **2010**, *29*, 2176–2179; b) H. Gottlieb, V. Kotlyar, A. Nudelman, *J. Org. Chem.* **1997**, *62*, 7512–7515.

[31] B. Prasad, S. Gilbertson, *Org. Lett.* **2009**, *11*, 3710–3713.

[32] Y. Lee, Y. Kang, Y. Chung, *J. Org. Chem.* **2009**, *74*, 7922–7934.

[33] T. Lyons, M. Sanford, *Tetrahedron* **2009**, *65*, 3211–3221.

Manuscript received: February 1, 2019
Accepted manuscript online: February 19, 2019
Version of record online: March 12, 2019

© 2019 Wiley-VCH Verlag GmbH & Co. KGaA, Weinheim

III

Korr

Korr

nature
COMMUNICATIONS

ARTICLE

https://doi.org/10.1038/s41467-019-13175-5

OPEN

An umpolung strategy to react catalytic enols with nucleophiles

Amparo Sanz-Marco[1], Samuel Martinez-Erro[1], Martin Pauze[1,2], Enrique Gómez-Bengoa[2] & Belén Martín-Matute[1*]

The selective synthesis of α-functionalized ketones with two similar enolizable positions can be accomplished using allylic alcohols and iridium(III) catalysts. A formal 1,3-hydrogen shift on allylic alcohols generates catalytic iridium-enolates in a stereospecific manner, which are able to react with electrophiles to yield α-functionalized ketones as single constitutional isomers. However, the employment of nucleophiles to react with the nucleophilic catalytic enolates in this chemistry is still unknown. Herein, we report an umpolung strategy for the selective synthesis of α-alkoxy carbonyl compounds by the reaction of iridium enolates and alcohols promoted by an iodine(III) reagent. Moreover, the protocol also works in an intramolecular fashion to synthesize 3(2*H*)-furanones from γ-keto allylic alcohols. Experimental and computational investigations have been carried out, and mechanisms are proposed for both the inter- and intramolecular reactions, explaining the key role of the iodine(III) reagent in this umpolung approach.

Kor

---

[1] Department of Organic Chemistry, Stockholm University, Stockholm SE-10691, Sweden. [2] Departamento de Química Orgánica I, Universidad del País Vasco/UPV-EHU, Manuel de Lardizabal 3, Donostia – San Sebastián 20018, Spain. *email: belen.martin.matute@su.se

Umpolung reactions represent a powerful approach for the introduction of functional groups into organic molecules where this would not otherwise be possible due to electronic mismatch[1]. This term was introduced by D. Seebach and E. J. Corey to refer the inversion of reactivity of acyl carbon atoms in their reactions with electrophiles[2]. Analogous methods based on switching the reactivity of amines[3], imines[4–6], or carbonyl groups[7–13] have been developed in recent decades. This approach has played a pivotal role in the design of synthetic procedures, allowing access to target molecules that would be difficult to obtain by classical processes.

One example of a reaction where it is necessary to use an umpolung approach is the functionalization of ketones in the α position using nucleophiles[14]. To achieve this goal, iodine(III) compounds[15–18], transition metals[19], Lewis acids[20,21], and other reagents[22] have been used. For the synthesis of α-functionalized ketones with iodine(III) compounds, several reagents have been successfully used. These include Koser's reagent[23], (diacetoxyiodo)benzene (PIDA)[24], *p*-iodotoluene difluoride[25], and benzioxol(on)es (BX)[26]. When acyclic I(III) reagents are used, the nucleophile can be either an external nucleophile or a ligand of the I(III) center. However, for cyclic hypervalent iodine reagents, only examples where the nucleophile is part of the reagent have been reported, what requires an enormous synthetic effort as every reaction requires the synthesis of a new I(III) reagent[27–30]. In terms of the reaction substrates, dicarbonyl compounds, aromatic and cyclic ketones, and silyl enol ethers have all been used. However, no regiocontrol was achieved for ketones containing two enolizable α carbons with similar electronic/steric properties (Fig. 1a)[31].

Allylic alcohols have been proven to be a very useful class of compounds as ketone synthons during the last decades[32,33]. Our group has reported the use of allylic alcohols as enolate equivalents for the preparation of α-functionalized carbonyl compounds as single constitutional isomers[34–41]. This approach relies on the generation of iridium enolates as catalytic intermediates through 1,3-hydrogen transfer, and the in situ reaction of these intermediates with a variety of heteroatomic electrophiles, including halogen and oxygen-based electrophilic species. The stoichiometric synthesis of enolates is avoided, and the reaction takes place under base-free conditions; as a result, a single substituent may be introduced at the desired α carbon. This is difficult to achieve starting from ketones with no clear electronic or steric bias (Fig. 1b). This approach has been successful, but it relies on the use of heteroatomic electrophiles. These are highly reactive species, and are less readily available than their nucleophilic counterparts. In this paper, we report an approach that inverts the polarity of the iridium enolate intermediate, allowing it to react with O-nucleophiles (Fig. 1c). In a reaction mediated by an iridium(III) complex, allylic alcohols react with nucleophiles to yield α-alkoxy ketones as single constitutional isomers. The reaction is mediated by 1-fluoro-3,3-dimethyl-1,3-dihydro-$1\lambda^3$-benzo[*d*][1,2]iodaoxole. Furthermore, under the same conditions β-keto allylic alcohols cyclize yielding 3(2*H*)-furanones.

Results

Reaction development and optimization. We focused on the use of alcohols as nucleophiles; this would lead to the formation of α-alkoxy ketones. α-Alkoxy ketones are important building blocks for synthesis, and they are also present in many natural products[42,43]. We selected allylic alcohol **1a** as a model substrate and methanol as a nucleophile. A preliminary screening of iodine (III) reagents (Fig. 2) revealed that 1-fluoro-3,3-dimethyl-1,3-dihydro-$1\lambda^3$-benzo[*d*][1,2]iodaoxole (**I**) gave α-methoxy ketone **2a** in a promising 43% yield as a single constitutional isomer (see Supplementary Table 1). In contrast, **II**–**IX** resulted in lower yields, ranging from 0 to 15%. **I** is a stable compound, and it is commercially available and easy to handle. Taking all this into account, **I** was chosen for further optimization studies in combination with the commercially available $[Cp^*IrCl_2]_2$[44,45].

It should be noted that the selective formation of the desired product **2** in this reaction represents an enormous challenge (Table 1). Several by-products may be formed from the allylic alcohol substrates **1**, including unsubstituted ketone **3**, and also enone **4**. Furthermore, other nucleophiles such as water could

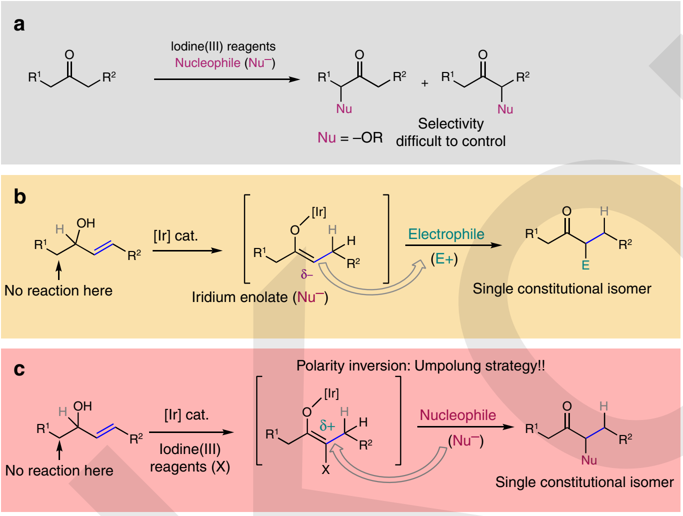

Fig. 1 Synthesis of α-substituted carbonyl compounds. **a** α-Functionalization of ketones through umpolung reactions. **b** Isomerization/functionalization of allylic alcohols with electrophiles. **c** Our approach: Isomerization/umpolung functionalization of allylic alcohols

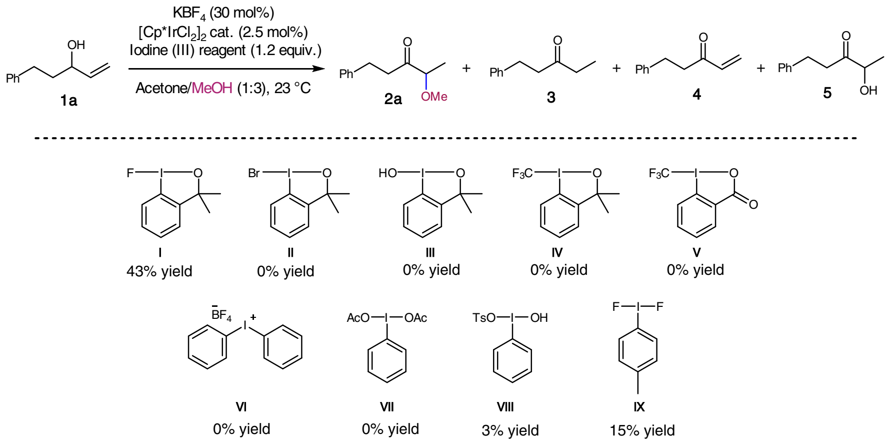

Fig. 2 Iodine(III) reagents screened. Yields of **2a** determined by ^{1}H NMR spectroscopy using an internal standard (1,2,4,5-tetrachloro-3-nitrobenzene) (Supplementary Table 1)

also react, leading to the formation of α-hydroxy ketone **5**. All these by-products were observed in our initial test reactions (Table 1, entry 1 and Supplementary Table 1), where common solvents previously used in related reactions were tested[35–41]. When either acetone or THF was used (Table 1, entries 1 and 2), **2a** was formed in moderate yield (up to 43%) together with by-products **3**–**6** in yields ranging from 6 to 12%. Further testing led us to the use of 2,2,2-trifluoroethanol (TFE) (entries 3–5), which gave α-methoxy ketone **2a** in 54% yield along with the same by-products in a similar ratio (Table 1, entry 4). A slightly better yield of **2a** was obtained when the temperature was raised to 35 ° C (57%; Table 1, entry 6). Increasing the temperature further did not prove beneficial (Table 1, entry 7). Remarkably, **2a** was formed in 75% yield when the reaction mixture was diluted (from 0.2 to 0.02 M). The amounts of by-products **3** and **4** decreased, and the formation of **5** was suppressed (Table 1, entry 8). When the amount of KBF_4 was increased (from 0.3 to 0.8 equiv.), **2a** was formed in an excellent yield of 89% (Table 1, entry 9). The use of other additives failed to give higher yields of **2a** (Table 1, entries 10 and 11). No conversion was observed when the chloride-free $[Cp^*Ir(H_2O)_3]SO_4$ complex was used as the catalyst. It has previously been shown that a halide ligand is essential in the isomerization of allylic alcohols[45]. In fact, when a chlorinated agent such as *N*-chlorosuccinimide is added in combination with $[Cp^*Ir(H_2O)_3]SO_4$, the desired product is observed (Supplementary Fig. 4). Control experiments were also carried out (Table 1, entries 13–15). In the absence of the iridium catalyst, allylic alcohol **1a** was recovered in 86% yield (Table 1, entry 13), and **2a** was not detected. The presence of the additive as well as TFE as cosolvent was necessary for the desired product **2a** to be formed in high yield (Table 1, entry 9 vs entries 14 and 15). Saturated ketone **3** was obtained in quantitative yield when the reaction was carried out in the absence of **I** (Table 1, entry 16). Thus, we found that the umpolung reaction of **1a** was best carried out using **I** in a TFE/MeOH mixture with KBF_4 as additive at 35 °C catalyzed by $[Cp^*IrCl_2]_2$ at a 0.02 M concentration of the allylic alcohol (Table 1, entry 9). We went on to study the substrate scope of the reaction under these optimal reaction conditions.

Reaction scope. For our studies of the substrate scope of the reaction (Fig. 3), we focused on allylic alcohols that would lead to α-methoxy ketones that are not accessible by the alternative direct α-functionalization of ketones, due to poor regioselectively. Allylic alcohols bearing terminal double bonds generally gave the corresponding α-methoxy ketones **2a**–**2n** in moderate to good yields. Steric effects play an important role, and a more hindered allylic alcohol **1d** gave **2d** in only 45% yield. Aromatic allylic alcohols were found to be well tolerated, and **1e** gave a 64% yield of **2e**. Substrates bearing other functional groups such as an alkene, an ether, or a silyl ether (**1f**–**1h**) gave the corresponding products in excellent yields (84%, 99%, and 80%, respectively). This highlights the functional-group compatibility of the method. Remarkably, the reaction is chemoselective for the allylic alcohol functionality. Other functional groups with acidic α-methylene groups remain untouched. Allylic alcohol substrates bearing additional ketone (**2i**, 42% yield), nitrile (**2j**, 91% yield), or sulfone groups (**2k**, 74% yield) all gave the desired products with the reaction only taking place at the allylic alcohol. Furthermore, the reaction of chloride-containing allylic alcohol **1l** proceeded in high yield (89%), and also diverse functionalized α-methoxy ketones, such as azide **2m** (69%) and morpholine **2n** (77%), were prepared in good yields from **1l** in a one-pot two-step procedure. By simply selecting the starting allylic alcohol, constitutional isomers were prepared selectively. For instance, α-methoxy ketones **2b** and **2q** were selectively synthesized from allylic alcohols **1b** (external double bond) and **1q** (internal double bond), respectively. Allylic alcohols with internal 1,2-disubstituted double bonds (**1o**–**1u**) also reacted smoothly to give generally good yields of the corresponding products. Other alcohols such as ethanol and propanol afforded also the corresponding products, α-ethoxy ketone **6a** in 40% and α-propoxy ketone **7a** in 20% yield, respectively. In all examples shown in Fig. 3, the products were obtained as single constitutional isomers. Remarkably, this efficient umpolung protocol was extended to primary allylic alcohols (**1v**–**1w**) to give α-methoxy aldehydes in high yields. The method was also extended to more complex molecules derived from *trans*-androsterone (**1x**) and lythocolic acid (**1y**), which bear multiple functional groups such as esters and ketones, in addition to several stereocenters, and the desired products were obtained in high yields.

We also found that the reaction could be carried out in an intramolecular manner, with the oxygen of a carbonyl group acting as the nucleophile (Fig. 4). Thus, allylic alcohols **8a**–**8h**,

Table 1 Optimization studies[a]

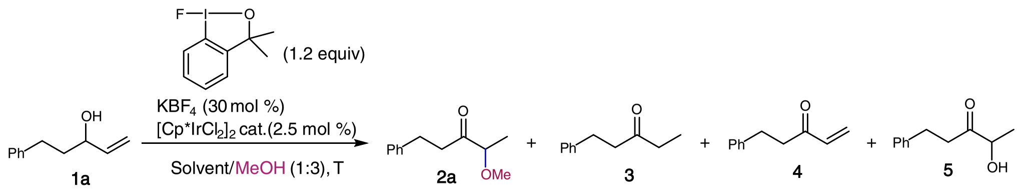

Entry	Solvent	*T* [°C]	Additive	Yield [%][b] 2a/3/4/5
1	Acetone	23	KBF$_4$	43/12/12/10
2	THF	23	KBF$_4$	27/11/6/12
3	HFIP[c]	23	KBF$_4$	45/-/29/-
4	TFE	23	KBF$_4$	54/9/10/10
5	PhCF$_3$	23	KBF$_4$	52/6/7/9
6	TFE	35	KBF$_4$	57/10/10
7	TFE	45	KBF$_4$	48/7/2/-
8[d]	TFE	35	KBF$_4$	75/8/2/-
9[d,e]	TFE	35	KBF$_4$	89/4/6/-
10[d,e]	TFE	35	NaBF$_4$	85/7/5/-
11[d,e]	TFE	35	TBAF	65/20/-/10
12[d,e,f]	TFE	35	KBF$_4$	-
13[d,e,g]	TFE	35	KBF$_4$	-
14[d]	TFE	35	-	67/5/3/10
15[d,e]	-	35	KBF$_4$	68/5/2/11
16[d,e,h]	TFE	35	KBF$_4$	-/99/-/-

[a] Unless otherwise noted, all experiments were carried out under an atmosphere of air on a scale of 0.15 mmol of **1a** (0.2 M), with KBF$_4$ (0.3 equiv.) for 2 h

[b] Determined by ^{1}H NMR spectroscopy using an internal standard (1,2,4,5-tetrachloro-3-nitrobenzene)

[c] HFIP = 1,1,1,3,3,3-hexafluoroisopropanol

[d] 0.02 M instead of 0.2 M

[e] 0.8 equiv. of additive instead of 0.3 equiv

[f] [Cp*Ir(H$_2$O)$_3$]SO$_4$ instead of [Cp*IrCl$_2$]$_2$

[g] In the absence of catalyst, 86% of **1a** was recovered

[h] In the absence of **I**

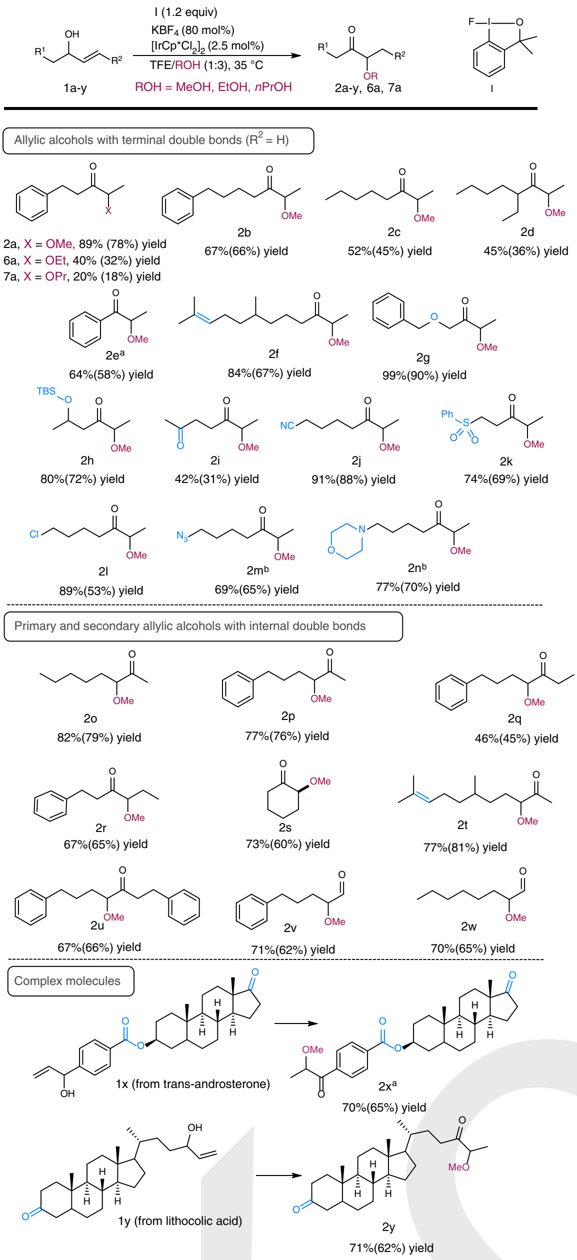
I (1.2 equiv)
KBF4 (80 mol%)
[IrCp*Cl2]2 (2.5 mol%)
TFE/ROH (1:3), 35 °C
ROH = MeOH, EtOH, nPrOH
1a-y
2a-y, 6a, 7a
I
Allylic alcohols with terminal double bonds (R2 = H)
2a, X = OMe, 89% (78%) yield
6a, X = OEt, 40% (32%) yield
7a, X = OPr, 20% (18%) yield
2b 67%(66%) yield
2c 52%(45%) yield
2d 45%(36%) yield
2ea 64%(58%) yield
2f 84%(67%) yield
2g 99%(90%) yield
2h 80%(72%) yield
2i 42%(31%) yield
2j 91%(88%) yield
2k 74%(69%) yield
2l 89%(53%) yield
2mb 69%(65%) yield
2nb 77%(70%) yield
Primary and secondary allylic alcohols with internal double bonds
2o 82%(79%) yield
2p 77%(76%) yield
2q 46%(45%) yield
2r 67%(65%) yield
2s 73%(60%) yield
2t 77%(81%) yield
2u 67%(66%) yield
2v 71%(62%) yield
2w 70%(65%) yield
Complex molecules
1x (from trans-androsterone)
2xa 70%(65%) yield
1y (from lithocolic acid)
2y 71%(62%) yield

Fig. 3 Scope of allylic alcohols **1**. Yields by ^{1}H NMR spectroscopy (isolated yields in parentheses). **a** By slow addition of the reactants. **b** From **2l** in a one-pot two-step procedure

which have a ketone group in a 1,3-relationship with the alcohol functionality, were efficiently transformed into 3(2*H*)-furanones **9**. This five-membered ring system is an important structural unit, and it can be found in a large number of natural products and other compounds with applications in medicine and biology[46–49].

Allylic alcohol **8a**, with $R^3 = H$, gave 3(2*H*)-furanone **9a** in 65% yield. The introduction of a substituent at R^3 had a

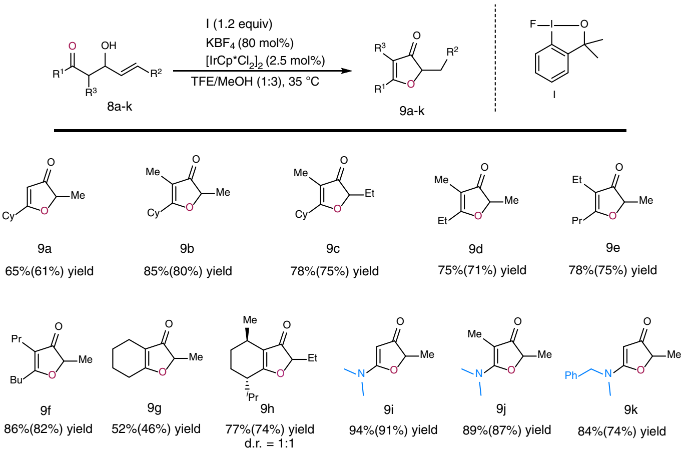

Fig. 4 Scope of allylic alcohols **8**. Yields by ^{1}H NMR spectroscopy (isolated yields in parentheses)

significant positive effect on the yield of the tandem reaction. Thus, alcohols **8b**–**8f** gave the corresponding 3(2*H*)-furanones in excellent yields. Furthermore, allylic alcohols containing a cyclic ketone moiety **8g** and **8h** reacted well to give bicyclic products **9g** and **9h** (as a mixture of two diastereomers). The intramolecular umpolung reaction was extended to allylic alcohols **8i**–**8k**, which contain an amide group that can act as an internal nucleophile. These substrates gave highly functionalized aminofuranones in excellent yields. Our umpolung strategy allows the construction of these highly important heterocycles from easily accessible starting materials.

Mechanism. To gain some insight into the reaction mechanism, and in particular into the role of the iodine(III) reagent **I**, we carried out DFT calculations at the M06/6-31G(d,p) level using the Gaussian 16 suit of programs (see the Supplementary Figs. 7 and 8, and Supplementary Data 1). In analogy with our previous work on the [Cp*Ir(III)]-catalyzed isomerization of allylic alcohols[34,37,45,50] we propose that the reaction starts with the allylic alcohol undergoing a hydrogen-transfer step (1,3-hydride shift) mediated by the metal catalyst. This leads to iridium enolate species **A** (represented as an η^3-enolate in Fig. 5)[51]. Our hypothesis is that the role of the additive (KBF_4) is to increase the rate of the formation of iridium enolate species **A**. We carried out kinetic studies on the isomerisation of allylic alcohols, and found that the reaction is faster in the presence of KBF_4 than in its absence (Supplementary Fig. 1). The initial reaction rate of **1a**-*d* was found to be comparable to that of **1a**, indicating that the 1,3-H shift is not rate determing (Supplementary Fig. 5).

The reaction of enolate **A** with **I** forms an enolonium intermediate **B**, which then reacts further with MeOH to form enolonium **C**[52,53]. From **C**, the final product **2** is obtained by reductive ligand coupling via **TS1**[28,54]. This step has an activation energy of 16.2 kcal mol^{-1}, which is perfectly attainable under the experimental reaction conditions. In the computational model of **TS1**, a molecule of TFE was introduced to activate the carbonyl group of the substrate by hydrogen bonding, and thus lower the activation barrier. When this step was modeled in the absence of TFE, the activation energy increased to 21.8 kcal mol^{-1} (Supplementary Fig. 8). Enolonium intermediates **B**′ and **C**′, tautomers containing an I–O bond instead of an I–C bond were also considered, but these species were excluded as they have higher energies than **B** and **C** ($\Delta G = 14.1$ and 5.3 kcal mol^{-1}, respectively). The energies of other isomeric forms of the enolonium intermediate (with a different arrangement of the substituents around the I(III) center) were also calculated, and these were all found to be much higher in energy (Supplementary Fig. 7). Besides, we could not locate any transition structure to form **2** starting from tautomer **C**′. Thus, **C** was the most plausible intermediate for this mechanism.

To investigate whether the iridium complex or KBF_4 are involved in the reaction mechanism after enolonium **B** is formed, we performed control experiments in the laboratory where a preformed silyl enol ether was used as the starting material instead of the allylic alcohol. Neither the presence of KBF_4 nor that of the iridium catalyst in the reactions from the silyl enol ether had any effect on the yield of the product (Supplementary Figs. 2 and 3). This suggests that none of them participates in the mechanism after enolonium **B** has been formed.

Further, reactions tested in the presence of radical scavengers, such as 2,2,6,6-tetramethylpiperidin-1-yl)oxidanyl (TEMPO) or 2-diphenylethylene, afforded the product (**2a**) in high yields (Supplementary Fig. 6). This suggests that a single-electron transfer mechanism is not operating.

We also investigated the mechanism of the cyclization reaction of type-**8** allylic alcohols. An analogous enolonium species **D** is transformed into enolonium **E** by a downhill nucleophilic-addition/proton-transfer process ($\Delta G = -11.7$ kcal mol^{-1}, Fig. 6). The intramolecular displacement of the aryliodonium group via **TS2** leads to the final (2*H*)-furan-3-one **9** in a very fast step, with a calculated activation energy of 8.0 kcal mol^{-1}. Such intramolecular nucleophilic displacement reactions of aryliodonium groups have previously been suggested by Jacobsen and coworkers among others[55,56].

We also investigated why we never observed α-methoxylated products when we used **8**-type substrates in our experimental work, and found out that starting from **D**, the competing transition state leading to the α-methoxy carbonyl compound (**TS3**) is higher in energy than **TS2** by ca. 10 kcal mol^{-1} (18.2 kcal mol^{-1}, Fig. 6).

Discussion

We have described a selective umpolung strategy which involves the reaction of an enolate species, formed from an allylic alcohol

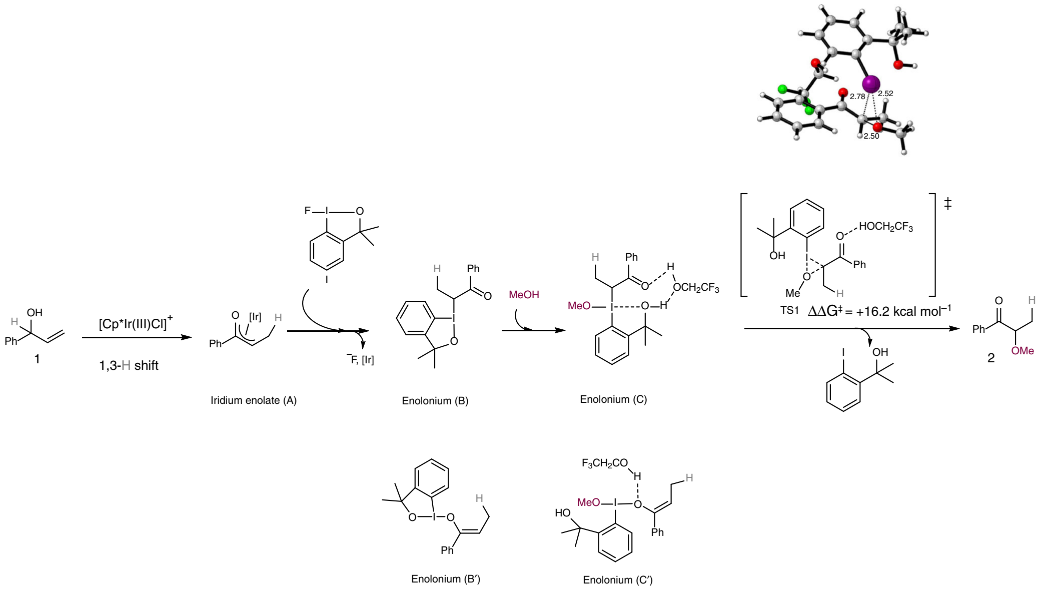
2.78
2.52
2.50
‡
HOCH2CF3
OH
Ph
O
Me
H
TS1 ΔΔG‡ = +16.2 kcal mol−1
OH
H
Ph
1
[Cp*Ir(III)Cl]+
1,3-H shift
O [Ir] H
Ph
Iridium enolate (A)
F—I—O
I
−F, [Ir]
H Ph
O
Enolonium (B)
MeOH
H Ph
O
H
OCH2CF3
MeO—I----O—H
Enolonium (C)
I OH
O H
Ph
OMe
2
H
O—I—O
Ph
Enolonium (B′)
F3CH2CO
H
MeO—I—O
HO
H
Ph
Enolonium (C′)

Fig. 5 Proposed intermolecular reaction mechanism. DFT calculations for the umpolung reaction of allylic alcohols with methanol. Values correspond to Gibbs free energies in kcal mol^{-1}

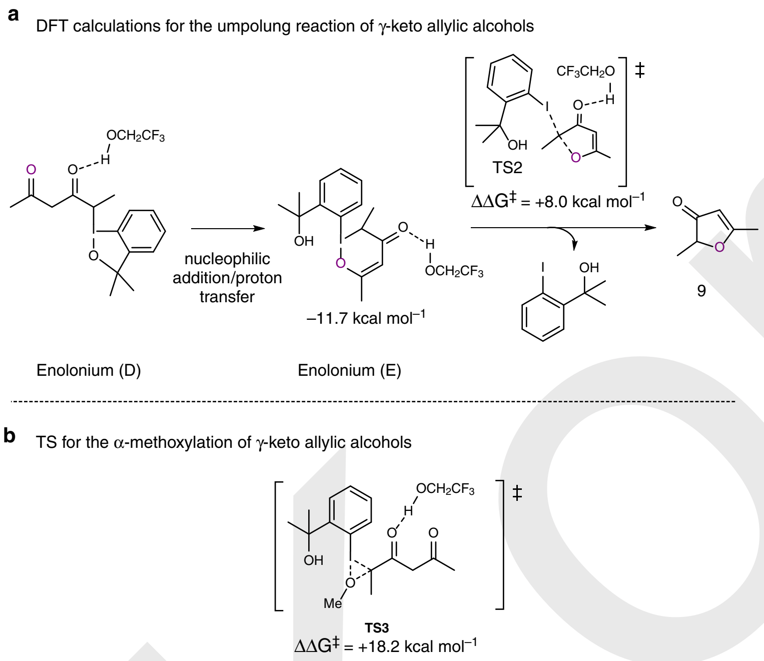
a DFT calculations for the umpolung reaction of γ-keto allylic alcohols

b TS for the α-methoxylation of γ-keto allylic alcohols

OCH2CF3
O
O---H
I
O
Enolonium (D)
nucleophilic
addition/proton
transfer
OH
I
O
O---H
OCH2CF3
−11.7 kcal mol−1
Enolonium (E)
CF3CH2O
I
O---H
OH
O
TS2
‡
ΔΔG‡ = +8.0 kcal mol−1
I OH
O
O
9
OCH2CF3
H
O
O
OH
I
O
Me
‡
TS3
ΔΔG‡ = +18.2 kcal mol−1

Fig. 6 Proposed intramolecular reaction mechanism. **a** DFT calculations for the umpolung reaction of γ-keto allylic alcohols. **b** TS for the α-methoxylation of γ-keto allylic alcohols

under catalytic conditions, with methanol. The catalytic enolate intermediate is formed by a 1,3-hydride shift mediated by an iridium catalyst. The two reacting species, the enolate and methanol, are both nucleophilic, so to allow them to react a polarity inversion must take place. This was achieved by carrying out the reaction in the presence of 1-fluoro-3,3-dimethyl-1,3-dihydro-$1\lambda^3$-benzo[*d*][1,2]iodaoxole. By this approach, α-methoxy ketones were formed in high yields as single constitutional isomers under very mild conditions. Importantly, and in contrast with other methods that require the use of electrophilic sources of oxygen, a simple alcohol species can be used as a nucleophile in this reaction. The reaction also works with the carbonyl oxygen of ketones or amides acting as nucleophiles in an intramolecular fashion, yielding highly functionalized 3(2*H*)-furanones. Thus, this approach offers a route to these heterocyclic compounds, which are important structural units in medicinal chemistry, starting from simple and readily available substrates. The mechanisms for the inter- and intramolecular reactions were studied computationally. We found that the C_α-OMe products were formed through a reductive elimination reaction (or ligand coupling) between the C-bound I(III)-enolate and methanol, and that the TFE additive activates the substrate through hydrogen bonding promoting the C−O bond formation. We also found that the intramolecular process that leads to the formation of furanones follows a similar mechanism.

Methods

General procedure for the catalytic reaction. The corresponding allylic alcohol (0.3 mmol, 1 equiv.) was dissolved in a mixture MeOH/TFE (3:1) (15 mL). KBF_4 (30 mg, 0.24 mmol, 80 mol%), 1-fluoro-3,3-dimethyl-1,3-dihydro-1-λ-3-benzo[*d*][1,2]iodaoxole (102 mg, 0.36 mmol, 1.2 equiv.), and $[Cp^*IrCl_2]_2$ (6 mg, 0.0075 mmol, 0.025 equiv.) were added and the mixture stirred at 35 °C during 2 h. After that, H_2O was added to dilute the reaction and the mixture was extracted with Et_2O (3 × 5 mL). The combined organic phases were dried with $MgSO_4$ and the solvent was evaporated under vacuum. The resulting crude was purified by column chromatography using petroleum ether/EtOAc (90:10) mixture as eluent.

DFT calculations. The calculations were carried out with the Gaussian 16 set of programs, using the M06 functional together with the 6-31G** basis sets for full structure optimization. IRC were done for both TS, where only one imaginary frequency was found and zero for the intermediate molecules. Then DEF2TZVPP in single point has been used with M06 for the energies. An implicit solvent model (IEFPCM, solvent = dimethyl formamide) was also used in all calculations (see the Supplementary Figs. 7 and 8, and Supplementary Data 1).

Data availability

The authors declare that all data supporting the findings of this report are available in the article or in their supplementary information files. This includes experimental procedures, compound characterization and full computational details. Date are also available upon request from the corresponding author.

Received: 10 June 2019; Accepted: 24 October 2019;
Published online: 20 November 2019

References

1. Seebach, D. Methods of reactivity umpolung. *Angew. Chem. Int. Ed.* **18**, 239–258 (1979).
2. Seebach, D. & Corey, E. J. Generation and synthetic applications of 2-lithio-1,3-dithianes. *J. Org. Chem.* **40**, 231–237 (1975).
3. Seebach, D. & Enders, D. Umpolung of amine reactivity. Nucleophilic α-(secondary amino)-alkylation via metalated nitrosamines. *Angew. Chem. Int. Ed.* **14**, 15–32 (1975).
4. Patra, A. et al. *N*-heterocyclic-carbene-catalyzed umpolung of imines. *Angew. Chem. Int. Ed.* **56**, 2730–2734 (2017).
5. Liu, J., Cao, C.-G., Sun, H.-B., Zhang, X. & Niu, D. Catalytic asymmetric umpolung allylation of imines. *J. Am. Chem. Soc.* **138**, 13103–13106 (2016).
6. Dickstein, J. S., Fennie, M. W., Norman, A. L., Paulose, B. J. & Kozlowski, M. C. Three component coupling of α-iminoesters via umpolung addition of organometals: synthesis of α,α-disubstituted α-amino acids. *J. Am. Chem. Soc.* **130**, 15794–15795 (2008).
7. Kaiser, D., Teskey, C. J., Adler, P. & Maulide, N. Chemoselective intermolecular cross-enolate-type coupling of amides. *J. Am. Chem. Soc.* **139**, 16040–16043 (2017).
8. De la Torre, A., Tona, V. & Maulide, N. Reversing polaruty: carbonyl α-aminations with nitrogen nucleophiles. *Angew. Chem. Int. Ed.* **56**, 12416–12423 (2017).
9. Streuff, J. et al. Mechanism of the tiiii-catalyzed acyloin-type umpolung: a catalyst-controlled radical reaction. *J. Am. Chem. Soc.* **137**, 14396–14405 (2015).
10. Leighty, M. W., Shen, B. & Johnston, J. N. Enantioselective synthesis of α-oxy amides via umpolung amide synthesis. *J. Am. Chem. Soc.* **134**, 15233–15236 (2012).
11. Marion, N., Díez-González, S. & Nolan, S. P. *N*-heterocyclic carbenes as organocatalysts. *Angew. Chem. Int. Ed.* **46**, 2988–3000 (2007).
12. Linghu, X., Potnick, J. R. & Johnson, J. S. Metallophosphites as umpolung catalysts: the enantioselective cross silyl benzoin reaction. *J. Am. Chem. Soc.* **126**, 3070–3071 (2004).
13. Burstein, C. & Glorius, F. Organocatalyzed conjugate umpolung of α,β-unsaturated aldehydes for the synthesis of γ-butyrolactones. *Angew. Chem. Int. Ed.* **43**, 6205–6208 (2004).
14. Miyata, O., Miyoshi, T. & Ueda, M. Umpolung reactions at the α-carbon position of carbonyl compounds. *Arkivoc* **2**, 60–81 (2013).
15. Dong, D.-Q., Hao, S.-H., Wang, Z.-L. & Chen, C. Hypervalent iodine: a powerful electrophile for asymmetric α-functionalization of carbonyl compounds. *Org. Biomol. Chem.* **12**, 4278–4289 (2014).
16. Zhdankin, V. V. & Stang, P. J. Chemistry of polyvalent iodine. *Chem. Rev.* **108**, 5299–5358 (2008).
17. Moriarty, R. M., Prakash, O., Duncan, M. P. & Vaid, R. K. Hypervalent iodine oxidation of silyl enol ethers under Lewis-acid conditions in methanol. A general route to α-methoxy ketones. *J. Org. Chem.* **52**, 150–153 (1987).
18. Arava, S. et al. Enolonium species-umpoled enolates. *Angew. Chem. Int. Ed.* **56**, 2599–2603 (2017).
19. Xu, Z., Chen, H., Wang, Z., Ying, A. & Zhang, L. One-pot synthesis of benzene-fused medium-ring ketones: gold catalysis-enabled enolate umpolung reactivity. *J. Am. Chem. Soc.* **138**, 5515–5518 (2016).
20. Wu, Y.-K., Dunbar, C. R., McDonald, R., Ferguson, M. J. & West, F. G. Experimental and computational studies on interrupted nazarov reactions: exploration of umpolung reactivity at the α-carbon of cyclopentanones. *J. Am. Chem. Soc.* **136**, 14903–14911 (2014).
21. Miyoshi, T., Miyakawa, T., Ueda, M. & Miyata, O. Nucleophilic α-arylation and α-alkylation of ketones by polarity inversion of N-alkoxyenamines: entry to the umpolung reaction at the α-carbon position of carbonyl compounds. *Angew. Chem. Int. Ed.* **50**, 928–931 (2011).
22. Wei, Y., Lin, S., Xue, H., Liang, F. & Zhao, B. Halonium-initiated C–O bond formation via umpolung of α-carbon to the carbonyl: efficient access to 5-amino-3(2*H*)-furanones. *Org. Lett.* **14**, 712–715 (2012).
23. Shneider, O. S., Pisarevsky, E., Fristrup, P. & Szpilman, A. M. Oxidative umpolung α-alkylation of ketones. *Org. Lett.* **17**, 282–285 (2015).
24. Mizar, P. & Wirth, T. Flexible stereoselective functionalizations of ketones through umpolung with hypervalent iodine reagents. *Angew. Chem. Int. Ed.* **53**, 5993–5997 (2014).
25. Yu, J., Tian, J. & Zhanga, C. Various α-oxygen functionalizations of β-dicarbonyl compounds mediated by the hypervalent iodine(III) reagent *p*-iodotoluene difluoride with different oxygen-containing nucleophiles. *Adv. Synth. Catal.* **352**, 531–546 (2010).
26. Hari, D. P., Caramenti, P. & Waser, J. Cyclic hypervalent iodine reagents: enabling tools for bond disconnection via reactivity umpolung. *Acc. Chem. Res.* **51**, 3212–3225 (2018).
27. Ilchenko, N. O., Hedberg, M. & Szabó, K. J. Fluorinative ring-opening of cyclopropanes by hypervalent iodine reagents. An efficient method for 1,3-oxyfluorination and 1,3-difluorination. *Chem. Sci.* **8**, 1056–1061 (2017).
28. Mai, B. K., Szabó, K. J. & Himo, F. Mechanisms of Rh-catalyzed oxyfluorination and oxytrifluoromethylation of diazocarbonyl compounds with hypervalent fluoroiodine. *ACS Catal.* **8**, 4483–4492 (2018).
29. Charpentier, J., Früh, N. & Togni, A. Electrophilic trifluoromethylation by use of hypervalent iodine reagents. *Chem. Rev.* **115**, 650–682 (2015).
30. Nagata, T., Matsubara, H., Kiyokawa, K. & Minakata, S. Catalytic activation of 1-cyano-3,3-dimethyl-3-(1*H*)-1,2-benziodoxole with $B(C_6F_5)_3$ enabling the electrophilic cyanation of silyl enol ethers. *Org. Lett.* **19**, 4672–4675 (2017).
31. Ochiai, M., Takeuchi, Y., Katayama, T., Sueda, T. & Miyamoto, K. Iodobenzene-catalyzed α-acetoxylation of ketones. In situ generation of hypervalent (diacyloxyiodo)benzenes using *m*-chloroperbenzoic acid. *J. Am. Chem. Soc.* **127**, 12244–12245 (2005).
32. García-Álvarez, R. et al. Ruthenium (II) arene complexes with asymmetrical guanidinate ligands: synthesis, characterization, and application in the base-

free catalytic isomerization of allylic alcohols. *Organometallics* **31**, 8301–8311 (2012).
33. Kechaou-Perrot, M. et al. Tethered η^5-oxocyclohexadienyl piano-stool ruthenium(II) complexes: a new class of catalyst? *Organometallics* **33**, 6294–6297 (2014).
34. Ahlsten, N. & Martín-Matute, B. Ir-catalysed formation of C-F bonds. From allylic alcohols to α-fluoroketones. *Chem. Commun.* **47**, 8331–8333 (2011).
35. Ahlsten, N., Bermejo Gómez, A. & Martín-Matute, B. Iridium-catalyzed 1,3-hydrogen shift/chlorination of allylic alcohols. *Angew. Chem. Int. Ed.* **52**, 6273–6276 (2013).
36. Bermejo Gómez, A., Erbing, E., Batuecas, M., Vázquez-Romero, A. & Martín-Matute, B. Iridium-catalyzed isomerization/bromination of allylic alcohols: synthesis of α-bromocarbonyl compounds. *Chem. Eur. J.* **20**, 10703–10709 (2014).
37. Vázquez-Romero, A., Bermejo Gómez, A. & Martín-Matute, B. Acid- and iridium-catalyzed tandem 1,3-transposition/3,1-hydrogen shift/chlorination of allylic alcohols. *ACS Catal.* **5**, 708–714 (2015).
38. Martinez-Erro, S. et al. Base-catalyzed stereospecific isomerization of electron-deficient allylic alcohols and ethers through ion-pairing. *J. Am. Chem. Soc.* **138**, 13408–13414 (2016).
39. Martinez-Erro, S., Bermejo Gómez, A., Vázquez-Romero, A., Erbing, E. & Martín-Matute, B. 2,2-Diiododimedone: a mild electrophilic iodinating agent for the selective synthesis of α-iodoketones from allylic alcohols. *Chem. Commun.* **53**, 9842–9845 (2017).
40. Sanz-Marco, A., Martinez-Erro, S. & Martín-Matute, B. Selective synthesis of unsymmetrical aliphatic acyloins through oxidation of iridium enolates. *Chem. Eur. J.* **45**, 11564–11567 (2018).
41. Sanz-Marco, A., Možina, S., Martinez-Erro, S., Iskra, J. & Martín-Matute, B. Synthesis of α-Iodoketones from allylic alcohols through aerobic oxidative iodination. *Adv. Synth. Catal.* **360**, 3884–3888 (2018).
42. Jiang, X., Chen, W. & Hartwig, J. F. Iridiium-catalyzed diastereoselective and enantioselective allylic substitutions with acyclic α-alkoxy ketones. *Angew. Chem. Int. Ed.* **55**, 5819–5823 (2016).
43. Hoyos, P., Sinisterra, J.-V., Molinari, F., Alcántara, A. R. & Domínguez de María, P. *Acc. Chem. Res.* **43**, 288–299 (2010).
44. Cinar, M. E. & Schmittel, M. One-pot domino aldol reaction of indium enolates affording 6-deoxy-α-D,L-altropyranose derivatives: synthesis, mechanism, and computational results. *J. Org. Chem.* **80**, 8175–8182 (2015).
45. Erbing, E. et al. General, simple, and chemoselective catalysts for the isomerization of allylic alcohols: the importance of the halide ligand. *Chem. Eur. J.* **22**, 15659–15663 (2016).
46. Li, Y. & Hale, K. J. Asymmetric total synthesis and formal total synthesis of the antitumor sesquiterpenoid (+)-eremantholide A. *Org. Lett.* **9**, 1267–1270 (2007).
47. Shamshina, J. L. & Snowden, T. S. Convergent synthesis of potent COX-2 inhibitor inotilone. *Tetrahedron Lett.* **48**, 3767–3770 (2007).
48. Hayashi, Y. et al. Asymmetric total synthesis of pseurotin A. *Org. Lett.* **5**, 2287–2290 (2003).
49. Han, Q. & Wiemer, D. F. Total synthesis of (+)-jatrophone. *J. Am. Chem. Soc.* **114**, 7692–7697 (1992).
50. Bartoszewicz, A., Jeżowska, M. M., Laymand, K., Möbus, J. & Martín-Matute, B. Synthesis of β-hydroxy and β-amino ketones from allylic alcohols catalyzed by η5-(Ph_5C_5)Ru$(CO)_2$Cl. *Eur. J. Inorg. Chem.* **2012**, 1517–1530 (2012).
51. Krug, C. & Hartwig, J. F. Reactions of an arylrhodium complex with aldehydes, imines, ketones, and alkynones. new classes of insertion reactions. *Organometallics* **23**, 4594–4607 (2004).
52. Geary, G. C., Hope, E. G., Singh, K. & Stuart, A. M. Preparation of iodonium ylides: probing the fluorination of 1,3-dicarbonyl compounds with a fluoroiodane. *RSC Adv.* **5**, 16501–16506 (2015).
53. Minhas, H. K., Riley, W. & Stuart, A. M. Activation of the hypervalent fluoroiodane reagent by hydrogen bonding to hexafluoroisopropano. *Org. Biomol. Chem.* **16**, 7170–7173 (2018).
54. Zhang, J., Szabó, K. J. & Himo, F. Metathesis mechanism of zinc-catalyzed fluorination of alkenes with hypervalent fluoroiodine. *ACS Catal.* **7**, 1093–1100 (2017).
55. Woerly, E. M., Banik, S. M. & Jacobsen, E. N. Enantioselective, catalytic fluorolactonization reactions with a nucleophilic fluoride source. *J. Am. Chem. Soc.* **138**, 13858–13861 (2016).
56. Mennie, K. M., Banik, S. M., Reichert, E. C. & Jacobsen, E. N. Catalytic diastereo- and enantioselective fluoroamination of alkenes. *J. Am. Chem. Soc.* **140**, 4797–4802 (2018).

Acknowledgements

This project was supported by the Swedish Research Council through Vetenskapsrådet and Formas, by the Knut and Alice Wallenberg Foundation (KAW 2016.0072), and by the Göran Gustafsson Foundation. A.S.-M. thanks Universitat de València, the Generalitat Valenciana, and the European Social Fund for a post-doctoral grant. We are also grateful to the European Funding Horizon 2020-MSCA (ITN-EJD CATMEC 14/06-721223). We also thank IZO-SGI SGIker of UPV/EHU for human and technical support. Open access funding provided by Stockholm University.

Author contributions

B.M.-M. and A.S.-M. conceived and designed the project. B.M.-M. directed the project. A.S.-M. and S.M.-E. carried out experiments and prepared the Supporting Information. E.G.-B. and M.P. carried out all the mechanistic calculations and contributed to the mechanistic understanding. They also prepared the corresponding Supporting Information. All the authors discussed the results, and all participated in writing the article.

Competing interests

The authors declare no competing interests.

Additional information

Supplementary Information accompanies this paper at https://doi.org/10.1038/s41467-019-13175-5.

Correspondence and requests for materials should be addressed to B.M.-M.

Peer review information *Nature Communications* thanks Jing-Ping Zhang and the other, anonymous, reviewer(s) for their contribution to the peer review of this work. Peer reviewer reports are available.

Reprints and permission information is available at http://www.nature.com/reprints

Publisher's note Springer Nature remains neutral with regard to jurisdictional claims in published maps and institutional affiliations.

Open Access This article is licensed under a Creative Commons Attribution 4.0 International License, which permits use, sharing, adaptation, distribution and reproduction in any medium or format, as long as you give appropriate credit to the original author(s) and the source, provide a link to the Creative Commons license, and indicate if changes were made. The images or other third party material in this article are included in the article's Creative Commons license, unless indicated otherwise in a credit line to the material. If material is not included in the article's Creative Commons license and your intended use is not permitted by statutory regulation or exceeds the permitted use, you will need to obtain permission directly from the copyright holder. To view a copy of this license, visit http://creativecommons.org/licenses/by/4.0/.

© The Author(s) 2019

Kor

Korre

IV

Korr

Korr

FULL PAPER DOI: 10.1002/adsc.202000566 Advanced Synthesis & Catalysis

Check for updates

Manganese-Catalyzed Multicomponent Synthesis of Tetrasubstituted Propargylamines: System Development and Theoretical Study

Stavros P. Neofotistos,[a] Nikolaos V. Tzouras,[a] Martin Pauze,[b]
Enrique Gómez-Bengoa,[b] and Georgios C. Vougioukalakis[a],*

[a] Department of Chemistry, Laboratory of Organic Chemistry
National and Kapodistrian University of Athens
Panepistimiopolis, 15771 Athens, Greece
Tel: +30-210-7274230
Fax: +30-210-7274761
E-mail: vougiouk@chem.uoa.gr
[b] Department of Organic Chemistry I, Faculty of Chemistry
University of the Basque Country
UPV/EHU, 20018 Donostia-San Sebastián, Spain

Manuscript received: May 12, 2020; Revised manuscript received: July 13, 2020;
Version of record online: August 4, 2020

This work is dedicated to Professor Robert H. Grubbs, on the occasion of the 50-year anniversary of his independent research.

Supporting information for this article is available on the WWW under https://doi.org/10.1002/adsc.202000566

Abstract: Herein, we report a catalytic system based on the earth-abundant manganese for the ketone, amine, alkyne (KA^2) reaction. The efficiency of manganese manifests at relatively high temperatures, combined with sustainable reaction conditions, and provides a tool for accessing propargylamines from structurally diverse starting materials, including synthetically relevant and bioactive molecules. Our efforts were also aimed at shedding light on the catalytic mode of action of manganese in this transformation, in order to explain its temperature-related behavior. The use of computational methods reveals mechanistic aspects of this reaction indicating important points regarding the reactivity of both manganese and ketones.

Keywords: manganese catalysis; ketone-amine-alkyne coupling; sustainability; multicomponent reactions; DFT calculations

Introduction

Propargylamines are a versatile family of organic compounds that have found numerous applications in the fields of organic synthesis and pharmaceutical chemistry.[1,2] The biological activity of various members of their family renders them inherently valuable in drug development, mostly against neurodegenerative diseases.[1–9] In addition, propargylic amines are useful building blocks in organic synthesis, providing access to diverse molecular architectures.[1,2] The unique structure of these compounds is based on the existence of an amine group in β-position to an alkyne moiety, which leads to diverse reactivity.[1] These characteristics make propargylamines susceptible to a variety of chemical transformations, thus fulfilling the conditions which have been established by the diversity-oriented synthesis strategy and natural product synthesis.[1,2,10–17] Moreover, through the integration of carbon dioxide or other small molecules, propargylamines can serve as intermediates or precursors for the synthesis of various heterocyclic compounds,[1] such as oxazolidinones,[18,19] same as their propargylic alcohol congeners.[20] Amongst others, propargylamines can be accessed in a facile manner through catalytic, multicomponent reaction protocols,[1,2,21–25] thus minimizing the required effort, time, and the generation of waste related to multistep processes.[26–33]

The development of various catalytic systems, based on sustainable and biorelevant transition

© 2020 Wiley-VCH GmbH

metals,[34] as well as the ever increasing interest related to atom- and step-economy arising from multicomponent synthesis combined with C–H activation,[35] allows the discovery of novel and green methodologies.[26–33] The A^3 coupling (aldehyde, amine, alkyne) is a well-known example of such a methodology.[2,36,37] Various sustainable and highly efficient catalytic protocols have been employed for the synthesis of trisubstituted propargylamines based on this multicomponent coupling.[36–45] Remarkably, not long after the initial discovery of this reaction, enantioselective versions were also developed, utilizing chiral ligands.[2b,46,47]

Ketimines exhibit lower reactivity than aldimines, a fact that stems from both their stereochemical and electronic features.[48,49] Nucleophilic addition to ketimines is in general challenging, although ketimines obtained from cyclohexanone are relatively reactive, due to the release of torsional strain.[50–52] Along these lines, employing ketones instead of aldehydes in the A^3 coupling remained a challenge until almost a decade ago. The synthesis of ketone-derived, tetrasubstituted propargylamines, through a catalytic, multicomponent coupling strategy, was attempted by several research teams, considering the great abundance of different natural products that possess α-tertiary amine moieties,[53] along with the inherent value of propargylamines and the scarcity of synthetic strategies leading to such molecular scaffolds.[54–57] An early related example was demonstrated by Ramón and co-workers in 2010, when the desired product was obtained in 38% yield after 7 days of reaction between piperidine, 3-pentanone, and phenylacetylene, catalyzed by $Cu(OH)_x$-Fe_3O_4 as the catalyst.[58] Nonetheless, the first breakthrough was made when the research group of Van der Eycken successfully prepared various tetrasubstituted propargylamines, derived from cyclohexanones, benzylamines and phenylacetylene, using a homogeneous, CuI-based and microwave-assisted catalytic system, under neat conditions. This discovery was made possible by taking advantage of the high reactivity of cyclohexanones, whilst they named the reaction "KA^2 coupling" (ketone, amine, alkyne – Scheme 1).[59] In a later work, the same research group utilized azoles instead of alkynes, along with secondary amines and cyclic ketones, under a similar, copper-catalyzed/microwave-irradiated protocol.[60] A catalytic system based on $AuBr_3$ in 4.0 mol% loading was also developed, using for the most part secondary amines, cyclohexanones, and phenylacetylene.[61] In a similar manner, a homogeneous *N*-heterocyclic carbene-Au(I)-based protocol was employed towards polysubstituted dihydropyrazoles *via* a three-component annulation of alkynes with *N, N′*-disubstituted hydrazines and aldehydes/ketones.[62] Larsen and co-workers developed additional efficient systems for the KA^2 coupling, based on $CuCl_2$ or $Cu(OTf)_2$.[63–65]

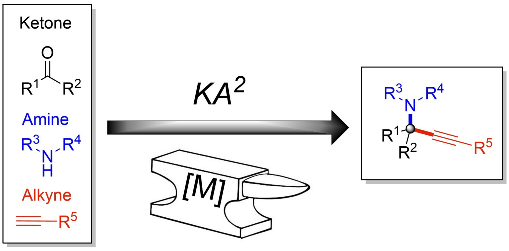

Previous works: *M= Cu(I), Cu(II), Au(III), Zn(II)*
This work: *M= Mn(II)*

Scheme 1. The metal-catalyzed KA^2 coupling reaction.

Further expansion of the scope of the reaction was achieved when $Ti(OEt)_4$ was employed as an additive, thereby allowing the integration of prochiral, linear ketones as coupling partners.[66] Likewise, a Cu(I) based system developed by Ma and co-workers was also very efficient for the KA^2 coupling of secondary amines, various ketones and terminal alkynes, in toluene, along with molecular sieves to assist with water removal.[67] The same research group was the first to report the successful integration of aromatic ketones, in the KA^2 coupling, which was mediated by a catalytic system based on $CuBr_2$, along with the use of $Ti(OEt)_4$ and sodium ascorbate.[68] Naturally, the increasing interest in this reaction and its potential has led to the development of a multitude of heterogeneous catalytic systems. Some leading examples include the use of Cu_2O nanoparticles on titania,[69] nano Cu_2O-ZnO,[70] Cu_2O/nano-$CuFe_2O_4$,[71] CuO/Fe_2O_3 nanoparticles,[72] Cu(II)-hydromagnesite,[73] polystyrene-supported, *N*-phenylpiperazine-$CuBr_2$, and highly active, polymer-supported bipyridine-$CuBr_2$,[74] Cu(II)@furfural imine-decorated Halloysite,[75] CuI on Amberlyst A-21,[76] as well as semi-heterogeneous, magnetically recoverable graphene oxide-supported $CuCl_2$.[77] Catalytic systems based on other metals have been also developed, such as Ag-doped nanomagnetic γ-Fe_2O_3@DA core-shell hollow spheres,[78] Fe_2O_3@SiO_2-IL/Ag hollow spheres,[79] and polystyrene-supported *N*-heterocyclic carbene-Au(III).[80]

More recently, our research group reported a robust catalytic system for the KA^2 reaction, introducing $Zn(OAc)_2$ as a reliable catalyst under neat conditions.[81] Additionally, we found that a catalytic system based on ZnI_2 can mediate the tandem formation of allenes from the *in situ* generated propargylamines in a one-pot procedure. This work highlighted that there is substantial reason to investigate new metals in this reaction, in order to gain more insight into its underlying principles, and, more importantly, that the choice of reaction conditions can lead to new and/or improved reactivity.

© 2020 Wiley-VCH GmbH

Manganese is a particularly attractive metal on account of its high natural abundance (the 3rd transition metal in the earth's crust after iron and titanium) and biocompatibility, which is particularly valuable for the pharmaceutical industry.[82] According to a recent report of the European Medicine Agency, manganese and copper are considered metals of low safety concern.[83] Therefore, manganese is a prominent candidate for the mediation of all kinds of chemical transformations.[82] In this regard, a plethora of manganese-based homogeneous catalytic systems have been developed,[82] successfully catalyzing the hydrosilylation of carbonylic compounds,[84,85] the electrochemical CO_2 reduction,[86–92] as well as the oxidation and allene epoxidation reactions.[93–99] A well-known example of manganese catalysis is the Katsuki reaction, which utilizes a Mn(I)-salen complex for the epoxidation of allenes.[98] Similarly, Mn(I)-based catalytic protocols utilizing porphyrin,[93,95,96] phthalocyanine,[97] or polyamine ligands,[100] have been reported. Mn-catalyzed C–H activation approaches have been also developed.[101–105] More specifically, Wang and co-workers introduced the first manganese-catalyzed aromatic C–H alkenylation with terminal alkynes.[102] Exploiting various pyridine derivatives as directing groups, they successfully accomplished the alkenylation of aromatic rings, mediated by a $MnBr(CO)_5$ complex and dicyclohexylamine as the base, at high chemo-, regio-, and stereo-selectivity. Interestingly, the same group proposed the formation of a σ-alkynyl intermediate in the catalytic cycle, based on Density Functional Theory (DFT) studies.[102] The formation of a Mn-acetylide was also proposed by Takai and co-workers as an intermediate.[106] Specifically, they reported that the mechanism for the hydantoin synthesis included an oxidative addition of a terminal alkyne to form an Mn-acetylide, followed by the insertion of an iso-cyanate into the manganese–carbon bond of the manganese acetylide.[106] Given that the formation of Mn-acetylides had been well established, a novel, $MnCl_2$-based protocol for the mediation of the A^3 coupling, along with a tandem intramolecular [3+2] dipolar cycloaddition, was reported by Lee and co-workers, introducing an efficient, one-pot strategy for the synthesis of propargylamines, as well as fused triazoles.[107]

To the best of our knowledge, manganese catalysis has not yet been tested in the KA^2 coupling. Inspired by the applications of sustainable metal catalysis in green organic transformations,[35,108–111] as well as our recent work on zinc catalysis,[81] we became interested in studying the potential of manganese catalysis in the KA^2 reaction. Our primary goal was the development of a highly-efficient, green, and user-friendly catalytic system based on a widely-available and cost-efficient manganese source, which could mediate the KA^2 coupling reaction of various challenging and synthetically intriguing substrates, under solvent-free conditions. Ideally, our KA^2 coupling protocol would be also viable under air, improving the sustainable aspects of this transformation even further. Finally, this provided an opportunity to study the reaction mechanism using computational tools for the first time, in order to further understand and more accurately pinpoint the reasons why ketone functionalization is significantly more challenging than that of aldehydes.

Results and Discussion

Based on our experience with the zinc-based catalytic protocol we have recently developed,[81] we chose cyclohexanone (**1a**), piperidine (**2a**) and phenylacetylene (**3a**) as model substrates for the optimization of the novel, manganese-based catalytic system. When $Mn(OAc)_2$ was employed in 20 mol% loading and the reaction was carried out under neat, inert conditions at 120 °C for 20 hours, propargylamine **4a** was obtained in 21% GC yield (Entry 1, Table 1). Despite this result, proving that manganese is able to mediate this reaction, a substantial amount of by-products were detected by GC/MS analysis.[20] Repetition of the reaction in toluene (1 M) at 120 °C, resulted in a 12% GC yield, which is considerably lower than the neat conditions (Entry 2, Table 1). This was a first indication that the reaction is favored under neat conditions. Then, we decided to proceed with the study of manganese halides. MnF_2 in 20 mol% loading under

Table 1. Metal sources screening and solvent tests.

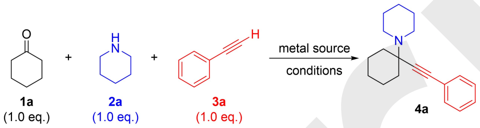

Entry	Metal source	mol%	Solvent	% GC yield[a] (isol. yield)[b]
1	$Mn(OAc)_2$	20	Neat & m. sieves	21
2	$Mn(OAc)_2$	20	Toluene (1 M)	12
3	MnF_2	20	Neat & m. sieves	52
4	MnF_2	20	Toluene (1 M)	8
5	$MnCl_2$	20	Neat & m. sieves	63 (58)
6	$MnCl_2$	20	Toluene (1 M)	18
7	$MnBr_2$	20	Neat & m. sieves	78 (74)
8	$MnBr_2$	20	Toluene (1 M)	45
9	MnI_2	20	Neat & m. sieves	55
10	MnI_2	20	Toluene (1 M)	79
11	–	–	Neat & m. sieves	Traces

All reactions were performed on a 2.0 mmol scale, running at 120 °C for 20 hours.

[a] Yield determined by GC/MS analysis, using *n*-octane as the internal standard.

[b] After column chromatography.

© 2020 Wiley-VCH GmbH

inert, neat conditions at 120 °C for 20 hours, resulted in a 52% yield (Entry 3, Table 1). When the same reaction was performed in toluene (1 M), the product was obtained with only 8% yield (Entry 4, Table 1). A significant increase in the reaction yield was observed, under neat conditions, at 120 °C using $MnCl_2$ as a catalyst, resulting in a 58% isolated yield (Entry 5, Table 1), suggesting that the counter ions of the manganese catalyst have a significant impact on the reaction. When the same reaction was performed in toluene (1 M), it resulted in an 18% GC yield (Entry 6, Table 1). When $MnBr_2$ was employed in 20 mol% loading at 120 °C, under neat, inert conditions, the desired product was obtained in 74% isolated yield (Entry 7, Table 1). Importantly, the formation of side products was also significantly reduced. The same reaction, when performed in toluene (1 M), resulted in the desired propargylamine **4a** in 45% GC yield (Entry 8, Table 1). When MnI_2 was used in 20 mol% loading at 120 °C, under neat, inert conditions, the desired product was obtained in 55% GC yield (Entry 9, Table 1). Besides being very difficult to handle because of its hydroscopic nature, MnI_2 is also characterized by reduced solubility in the reaction mixture. Therefore, the same reaction was performed in toluene, which efficiently dissolves MnI_2, affording propargylamine **4a** in 79% GC yield (Entry 10, Table 1). Furthermore, a blank test, using only molecular sieves, was performed, but, as anticipated, the product was not observed, as judged by GC-MS analysis (Entry 11, Table 1). Based on the above results, we decided that the optimal manganese source is $MnBr_2$, as it is easy to handle and it also affords very high product yields. The use of molecular sieves was deemed unnecessary, since their use only increased the complexity of the protocol (*vide infra*), while the use of solvent under these conditions negatively affects the reaction outcome. More importantly, the employment of solvent-free conditions is in line with the principles of green chemistry.

Then, we tested our protocol at various temperatures, using $MnBr_2$ at 20 mol% loading under an inert atmosphere and neat conditions for 20 hours. At 80 °C, the product was formed in 14% GC yield (Entry 1, Table 2). Performing the same reaction at 100 °C allowed the formation of propargylamine **4a** in 44% GC yield. When the reaction was repeated under the same conditions at 120 °C, it led to the formation of the desired product in 77% GC yield (Entry 3, Table 2). This result also suggested that the use of molecular sieves is not necessary, given that the results are practically the same with or without their presence (compare Entry 3, Table 2 with Entry 7, Table 1). When we performed the reaction employing $MnBr_2$ at 20 mol% loading under inert atmosphere and solvent-free conditions at 130 °C for 20 hours, the product was formed in 99% GC yield and 94% isolated yield (Entry 4, Table 2). Expanding our investigation, the same reaction was performed in the presence of molecular sieves, giving exactly the same results (Entry 5, Table 2), reaffirming the needlessness of molecular sieves.

Table 2. Optimization studies.

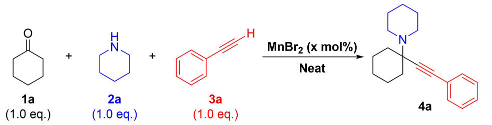

Entry	mol%	Temp. (°C)	Additive	% GC yield[a] (isol. yield)[b]
1	20	80	–	14
2	20	100	–	40
3	20	120	–	77
4	20	130	–	99 (94)
5	20	130	m. sieves	99
6	20	130	TEMPO (2eq)	98
7	20	130	–	99
8	10	130	–	98
9	5	130	–	98 (95)

All reactions were performed on a 2.0 mmol scale, with $MnBr_2$, under neat conditions for 20 hours.

[a] Yield determined by GC/MS analysis, using *n*-octane as the internal standard.

[b] After column chromatography.

We were also interested in shedding some light on the mechanism of the reaction. Besides carrying out a series of theoretical calculations (*vide infra*), we performed the transformation using $MnBr_2$, under the thus far optimal conditions (Entry 6, Table 2), by also adding 2.0 equivalents of (2,2,6,6-tetramethylpiperidin-1-yl)oxidanyl (TEMPO), a well-known free radical scavenger. Again, the product was formed in 98% GC yield. This suggests that the catalytic mechanism does not involve radical intermediates.

Finally, we investigated the impact of the catalyst loading on the reaction outcome (Entries 7–9, Table 2). To our surprise, the reaction can be very efficiently carried out even at 5 mol% $MnBr_2$ (Entry 9, Table 2) affording the desired product in 98% GC yield and 95% isolated yield. This very low catalyst loading, along with the solvent-free conditions, the sustainable nature of Mn, and the fact that this is a multicomponent reaction, render this protocol highly appealing and "green".

For the last part of our investigation we studied the progress of the reaction over time (Table 1, see Supporting Information). $MnBr_2$ was used at 5 mol% loading under an inert atmosphere at 130 °C and solvent-less conditions, while the reaction was repeated for different reaction times and analysed by GC/MS. Based on these results, we were able to construct a

© 2020 Wiley-VCH GmbH

reaction profile plot (Figure 1). The reaction reaches a yield plateau in 12 hours, proceeding to completion after 18 to 20 hours. Based on this result, we decided to run our substrate scope investigation studies that follow for 20 hours, given that some of the substrates we were planning to utilize are considered demanding coupling partners.

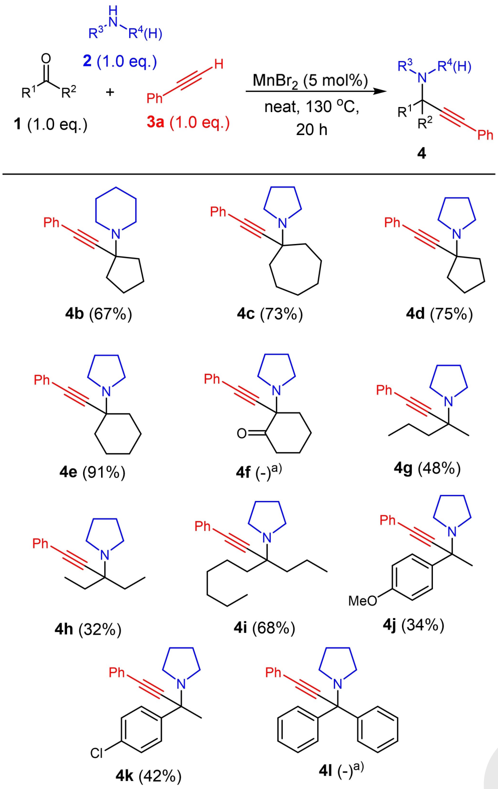

Scheme 2. The manganese-catalyzed KA^2 coupling: Scope of ketones. All reactions were performed on a 2.0 mmol scale and isolated yields are reported in parentheses. [a] The desired product was not observed by GC/MS analysis.

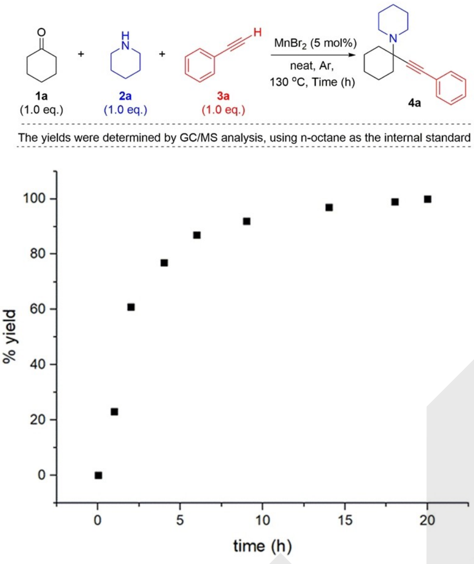

Figure 1. Kinetic profile of the reaction.

While investigating the scope of ketones (Scheme 2), phenylacetylene was used in combination with primarily pyrrolidine, as well as piperidine (Scheme 2). It was quickly determined that besides cyclohexanone a variety of different ketones can be successfully employed in this reaction under our protocol, with cyclopentanone and piperidine leading to propargylamine **4b** in 67% isolated yield. When cycloheptanone was used, propargylamine **4c** was obtained in 73% yield. Propargylamines **4d** or **4e** were obtained, in 75 or 91% isolated yield, respectively, when cyclopentanone or cyclohexanone were used along with pyrrolidine. The respective propargylamine **4f**, stemming from cyclohexane-1,2-dione, was not obtained. A drop in the yield was observed when linear ketones were employed. More specifically, 2-pentanone and 3-pentanone resulted in propargylamines **4g** and **4h** in 38% and 48% isolated yields, respectively. On the contrary, when 4-decanone was used, propargylamine **4i** was obtained in 68% isolated yield. The increased steric hindrance and the lack of torsional strain release during the acetylide attack on the *in-situ* formed ketiminium ion are most probably the reasons for this reactivity pattern.[50–52,64] Additionally, the lower boiling points of 2-pentanone and 3-pentanone may have a negative impact on the outcome of the reaction, which was not observed when 4-decanone was deployed. Surprisingly, our catalytic protocol was also able to successfully mediate the KA^2 coupling reaction of aromatic ketones. This result is of outmost importance, since, thus far, only one other example has been reported in the literature.[68] Specifically, we screened aromatic ketones bearing both electron-withdrawing (EWGs) and electron-donating groups (EDGs). When 4-methoxy-acetophenone was used, propargylamine **4j** was isolated in 34% isolated yield. Similarly, when 4-chloro-acetetophenone was employed, the respective propargylamine **4k** was obtained in 42% isolated yield. When benzophenone was utilized, propargylamine **4l** was not observed, which may be because of the increased steric hindrance imparted from the two phenyl moieties in the α-position of the carbonyl group.

To study the scope of alkynes (Scheme 3), cyclohexanone, along with piperidine or pyrrolidine, were coupled with various terminal alkynes, leading to the formation of the corresponding propargylamines. The presence of electron-donating groups (EDGs) on the aromatic ring of the aromatic terminal alkynes leads to the generation of propargylamines in high to excellent yields. Specifically, 3-ethynyl-toluene couples with cyclohexanone and piperidine to afford propargylamine **4 m** in 81% isolated yield. Similarly, when 4-ethynyl-toluene was employed along with pyrrolidine and cyclohexanone, propargylamine **4 n** was isolated in 87% yield. Propargylamine **4 o** was obtained in 70% isolated yield when *p*-methyl-phenylacetylene along piperidine and cyclohexanone were used. The coupling between 4-methoxy-2-methyl-phenylacetylene, piperidine and cyclohexanone led to the synthesis of **4 p** in 89% isolated yield. Moreover, propargylamine **4 q** was synthesized in 87% isolated yield using *p*-methoxy-phenylacetylene along with cyclohexanone and piperidine. We also became interested in the use of nornicotine, along with 2-methylbut-3-yn-2-ol and cyclohexanone, which allowed the synthesis of product **4 r** as a single diastereoisomer (see Supporting Information) in 81% isolated yield. Nornicotine is a natural, biologically-active molecule, bearing a pyridine moiety on the pyrrolidine heterocycle. Additionally, the pyrrolidine moiety is especially useful for derivatization of propargylic amines, taking into account their role as precursors to allenes.[112,113] Similarly, 2-methylbut-3-yn-2-ol is a useful handle for various applications,[114–119] providing access to terminal alkynes *via* a variety of deprotection techniques.[120,121] Alkynes bearing halide-containing moieties were also tested under our catalytic protocol. First, 4-chloro-ethynylbenzene was employed, along with pyrrolidine and cyclohexanone, leading to propargylamine **4 s** in 77% isolated yield. When piperidine was used instead of pyrrolidine, the desired propargylamine (**4 t**) was isolated in 64% yield. When 2-bromophenylacetylene was coupled with cyclohexanone and piperidine, the resulting propargylamine (**4 u**) was obtained in 57% isolated yield. This decrease in yield may stem from the increased steric hindrance, because of the presence of the bromine atom in the *ortho* position of the aromatic ring, obstructing the nucleophilic attack of the manganese acetylide. Additionally, upon using *p*-trifluomethyl-phenylacetylene, propargylamine **4 v** was observed by GC/MS analysis in low yields, but its isolation proved extremely difficult. This result suggests that strongly electron-withdrawing substituents reduce the ability of the corresponding acetylides to act as effective nucleophilic species. Furthermore, this observation agrees with the existing literature, in which the use of highly electron-deficient alkynes is rarely reported in similar studies, due to the decreased nucleophilicity of the respective acetylides.[68] Finally, 1-octyne was successfully employed, in combination with piperidine and cyclohexanone, affording propargylamine **4 w** in 70% isolated yield. Therefore, under these conditions, both simple and more elaborate aliphatic alkynes (e.g. 2-methylbut-3-yn-2-ol) can be derivatized.

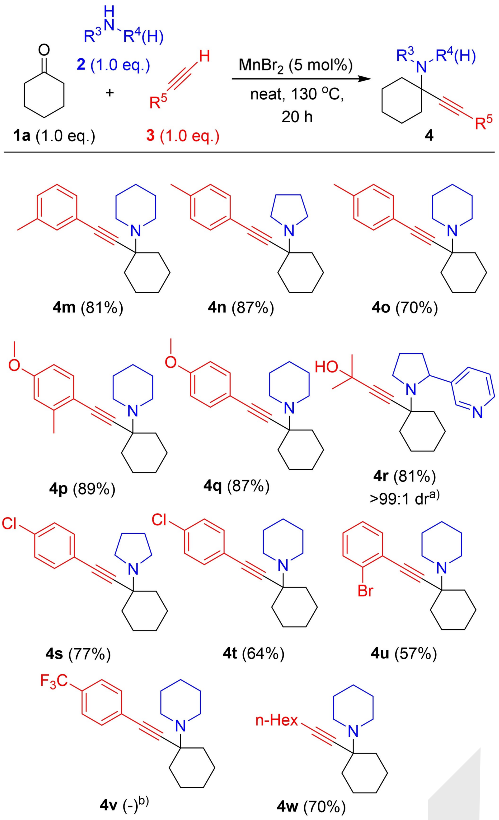

Scheme 3. The manganese-catalyzed KA^2 coupling: Scope of alkynes. All reactions were performed on a 2.0 mmol scale and isolated yields are reported in parentheses. a) The diastereomeric ratio was determined by ^{1}H-NMR analysis (see Supporting Information). b) This compound was detected by GC/MS analysis; however, it decomposed during column chromatography.

A wide variety of amines was also used, along with phenylacetylene and cyclohexanone (Scheme 4). As mentioned above, propargylamine **4 a** was obtained in 95% isolated yield during the optimization studies of our catalytic protocol. When morpholine was used, propargylamine **4 x** was obtained in 94% isolated yield,

© 2020 Wiley-VCH GmbH

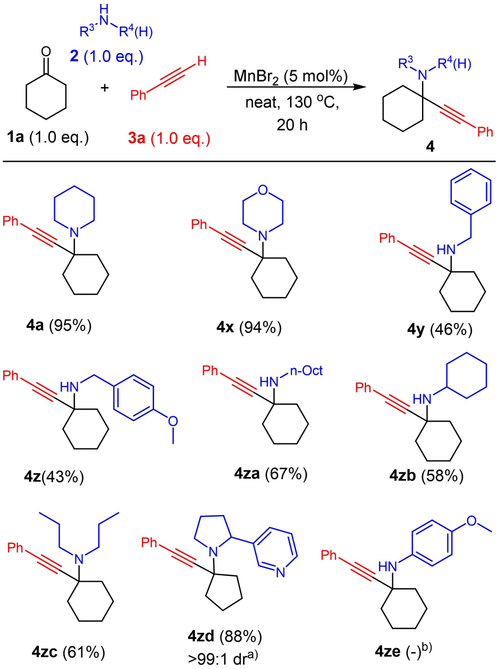

Scheme 4. The manganese-catalyzed KA^2 coupling: Scope of amines. All reactions were performed on a 2.0 mmol scale and isolated yields are reported in parentheses. a) The diastereomeric ratio was determined by ^{1}H-NMR analysis (see Supporting Information). b) The compound was detected by GC/MS analysis; however, it decomposes rapidly under ambient light. Despite our efforts, we could not isolate and characterize it.

while GC/MS analysis showed complete conversion. Benzylamine was also found to be a suitable coupling partner; propargylamine **4 y** was obtained in 46% isolated yield. This decreased yield may be attributed to the increased stability of the intermediate ketimine. Similarly, when *p*-methoxy-benzylamine was used, the resulting propargylamine **4 z** was isolated in 43% yield. We also tested the efficiency of our catalytic protocol on aliphatic amines. *N*-octylamine, along with cyclohexanone and phenylacetylene, furnished propargylamine **4 za** in 67% isolated yield. Along the same lines, utilization of cyclohexylamine led to the desired product (**4 zb**) in 58% yield. Upon using the secondary amine di-*n*-propylamine, the desired product **4 zc** was formed in 61% yield. Interestingly, the coupling between nornicotine, cyclopentanone and phenylacetylene led to the formation of the corresponding propargylamine (**4 zd**) as a single diastereoisomer in 88% isolated yield, without the need of purification *via* column chromatography, since crystallization of the product was achieved using a simple, green protocol (described in the experimental section), developed from our research group in previous studies.[81] Aromatic amines have not been successfully utilized in the KA^2 coupling reaction thus far. Indeed, although the product of the coupling reaction of *p*-methoxyaniline (**4 ze**) was observed by GC/MS analysis, it rapidly decomposes in light and, despite our efforts, could not be isolated.

We continued by testing our protocol under ambient conditions, performing the reaction under air. More specifically, we studied the coupling between morpholine, phenylacetylene and piperidine, which, under inert conditions, affords the synthesis of the desired product (**4 x**) in 94% yield. To our surprise, our protocol furnished product **4 x** in 89% isolated yield under air, after chromatographic purification. According to GC/MS analysis, the presence of air only slightly increased the formation of by-products. Additionally, we performed the synthesis of **4 x** on large scale under air, to evaluate the scalability of our protocol. Upon using 10 mmols of morpholine, along with equimolar amounts of cyclohexanone and phenylacetylene, the desired product was obtained in 93% isolated yield.

To gain some insight into the reaction mechanism, we carried out DFT calculations with the Gaussian 16 set of programs, using the B97-D functional for the structure optimizations, together with the 6-31G(d,p) basis sets for all the atoms. Experimentally, the reactions are run in neat conditions, and we used cyclohexanone in an implicit solvent model (IEFPCM) for the best description of the reaction medium during the energy refinements. We wanted to get information particularly about the role of the manganese salts during the process and also about the high temperatures needed in the reaction. As reagent models for the calculations, we used $MnBr_2$, cyclohexanone (**1 a**), piperidine (**2 a**) and phenylacetylene (**3 a**).

The first interesting data is that the manganese dibromide and its complexes with the substrates have lower energy in the quartet spin state than in the doublet for every computed structure (usually > 10 kcal/mol difference), showing that the metal contains three unpaired electrons in degenerate orbitals, along the entire reaction coordinate. Initially, the coordination of $MnBr_2$ to the triple bond in **I** increases the acidity of the alkyne, and activates it for the deprotonation by piperidine.[122] Upon proton abstraction, slippage of the metal fragment from the π-coordination to the terminal position produces the ate complex **II**, which is 4.2 kcal/mol higher in energy than **I** (Scheme 5a). Therefore, the reactive species **II** must be in a small concentration in the reaction medium. Then, the attack of the alkynyl-manganese **II** species to the iminium electrophile **III** presents an affordable activation energy (23.9 kcal/mol), in a

© 2020 Wiley-VCH GmbH

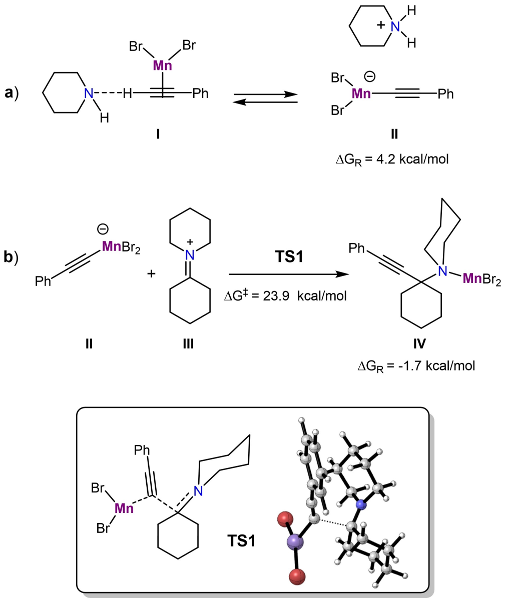

Scheme 5. a) Deprotonation equilibrium between $MnBr_2$-activated alkyne and alkynyl-Mn complex. b) C–C bond formation by nucleophilic attack of the alkyne to the iminium cation.

transition state (**TS1**, Scheme 5b) that does not present any interaction between the manganese and the iminium moiety. After the final product is formed, a stable complex **IV** was located, containing the expected N–Mn coordination. Taken both steps together (from **I** to **TS1**), the overall activation energy is 28.1 kcal/mol, which is in agreement with the high temperatures needed in the process. In other words, the nucleophilic attack of **II** to **III** could be moderately fast (23.9 kcal/mol), but is probably unfavourably affected by the small concentration of the nucleophile in the reaction medium. As detailed in the experimental section, $MnBr_2$ proved to be the most efficient catalyst, followed by MnI_2 and $MnCl_2$ (Table 1). Indeed, the activation energy of **TS1** in the presence of MnI_2 is higher (25.7 kcal/mol) than with $MnBr_2$. Meanwhile, $MnCl_2$ decreases the barrier to 22.8 kcal/mol, but its lower efficiency seems to be linked to a decreased coordination energy with the triple bond (> 4 kcal/mol worse than $MnBr_2$), inducing a lower concentration of **II** in the reaction medium.

Conclusion

A sustainable catalytic system based on manganese has been developed for the challenging KA_2 coupling. The efficiency of $MnBr_2$ is reflected on the low catalyst loading needed and the range of substrates that can be derivatized. DFT calculations show that the coordination of $MnBr_2$ activates the alkyne to facilitate its deprotonation by the amine, forming an anionic complex, which is nucleophilic enough to attack the iminium species. The moderate activation energy of the C–C bond forming process, together with the low concentration of the alkynyl-manganese bromide, make this step rate limiting, explaining the range of temperatures used experimentally. This result suggests that the reaction rate should increase, even at lower temperatures, if appropriate ligand design enables the stabilization of the generated acetylide species, in order for its concentration to be higher, and also enhances its nucleophilicity. Further investigation based on these observations is ongoing in our laboratories.

Experimental Section

General Reagent Information

All chemicals were purchased from commercial sources and were used as received, with the exception of cyclohexanone and piperidine, which were distilled before use. All metal sources were in anhydrous form and their purity grade was at least 98%. Toluene purification was carried out according to published procedures, and the solvent was distilled and stored under inert atmosphere prior to use. The reactions were set up in a fume hood and allowed to proceed under an atmosphere of argon, in Teflon seal screw-cap pressure tubes which were flame-dried prior to use. The course of the reactions was followed by thin layer chromatography (TLC), using aluminium sheets (0.2 mm) coated with silica gel 60 with fluorescence material absorbing at 254 nm (silica gel 60 F254) or by GC-MS analysis of aliquots. The purification of the products was carried out by flash column chromatography, using columns packed with silica gel 60 (230–400 mesh) and the corresponding eluting system.

Computational Methods

All reported structures were optimized at Density Functional Theory level by using the unrestricted B97-D[123] functional, which includes Grimme's dispersion, as implemented in Gaussian 16.[124] Optimizations were carried out with the 6-31G (d,p) basis set taking into account the doublet and quartet spin states for the Mn-containing species. The reported energy values correspond to Gibbs energies, including a solvent model (IEFPCM, cyclohexanone).[125] The critical stationary points were characterized by frequency calculations in order to verify that they have the right number of imaginary frequencies, and the intrinsic reaction coordinates (IRC)[126] were followed to verify the energy profiles connecting the key transition structures to the correct associated local minima.

General Analytical Information

^{1}H, ^{13}C and ^{19}F NMR spectra were measured on a Varian Mercury 200 MHz, or a Brucker Avance 400 MHz instrument, using $CDCl_3$ as the solvent and its residual solvent peak as a

© 2020 Wiley-VCH GmbH

reference. ^{1}H-NMR spectroscopic data are given in the following order: chemical shift, multiplicity (s, singlet, d, doublet, t, triplet, q, quartet, m, multiplet), the *J* coupling constant in Hertz (Hz), and the number of protons. The GC-MS spectra were recorded with a Shimandzu® GCMS-QP2010 Plus, Chromatograph Mass Spectrometer using a MEGA® (MEGA-5, F.T: 0.25 μm, I.D.: 0.25 mm, L: 30 m, Tmax: 350 °C, Column ID# 11475) column, using *n*-octane as the internal standard. HRMS spectra were recorded in a QTOF maxis Impact (Bruker®) spectrometer with Electron Spray Ionization (ESI).

General Procedure

Unless otherwise noted, the following procedure was used for all reactions: In a Teflon seal screw-cap pressure tube which had been flame-dried and was equipped with a stirring bar and a rubber septum was added 5 mol% $MnBr_2$ (21.5 mg, 0.1 mmol). Under an argon flow, 2.0 mmol of the amine were added and the mixture was stirred. Subsequently, 2.0 mmol of the corresponding alkyne were added and the mixture was stirred at room temperature and under an argon flow until the solid was either completely or partially dissolved. Briefly after the dissolution of the inorganic material, 2.0 mmol of the ketone were added and the rubber septum was replaced by a Teflon seal screw-cap under an argon flow. The reaction mixture was stirred in an oil bath, preheated at 130 °C, for 20 hours. After removal from the heating apparatus and cooling to room temperature, ethyl acetate was added (10 mL) and the mixture was stirred for 5 minutes in order to completely remove and dissolve the viscous mixture from the vessel's inner walls (this procedure was done twice, with 5 mL of solvent each time). The resulting mixture was filtered through a short silica gel plug in order to filter off inorganic materials, the filtrate was concentrated under vacuum and then loaded onto a silica gel column (if the compound was insoluble into the eluents' system, dry loading of the crude mixture was performed). Gradient column chromatography (usually of 15.0 cm length and 3.5 cm width and eluents' flow set at 2.0 cm/min) with ethyl acetate/petroleum ether provided the desired products. All products were characterized by ^{1}H NMR, $^{13}C\{^1H\}$ NMR, and HRMS, which were all in agreement with the assigned structures.

Modified Procedure for the Synthesis of 3-(1-(1-(Phenylethynyl)cyclopentyl)pyrrolidin-2-yl)pyridine (4 zd Single Diastereoisomer)

The general reaction setup was carried out. After cooling the reaction to room temperature, crystals started to form. Ethyl acetate was added (2x5 mL), the mixture was stirred rapidly until all viscous materials were removed from the reaction vessel and inorganic materials were filtered off by passing the mixture through a short silica gel plug. The yellow solution was allowed to cool overnight, and pale-yellow crystals precipitated. The solid was filtered on a frit, washed with cold ethyl acetate and dried under vacuum. The final product was obtained as yellow crystals in 88% yield (557 mg, 1.76 mmol). ^{1}H NMR (200 MHz, $CDCl_3$) δ 8.65–8.59 (s, 1H), 8.49–8.38 (d, *J* = 8.6 Hz, 1H), 7.82–7.69 (d, *J* = 12.8 Hz, 1H), 7.51–7.37 (m, 2H), 7.34–7.13 (m, 4H), 4.30–4.22 (dd, *J* = 7.4, 17.7 Hz, 1H), 3.28–3.16 (s, 1H), 3.12–2.92 (q, *J* = 16.8 Hz, 1H), 2.42–2.09 (p, *J* = 16.4 Hz, 2H), 2.05–1.42 (m, 10H, overlapping peaks). $^{13}C\{^1H\}$ NMR (50 MHz, $CDCl_3$) δ 149.2, 147.9, 143.9, 134.8, 132.0, 128.5, 128.0, 123.8, 123.3, 92.2, 84.1, 67.0, 62.5, 51.7, 40.9, 40.8, 36.7, 24.2, 23.3, 22.8. HRMS (ESI-TOF) m/z $[M+H]^+$ calcd for $C_{22}H_{25}N_2$ 317.2012; Found 317.2018.

Modified Procedure for the Synthesis of 4-(1-(Phenylethynyl)cyclohexyl)morpholine (4 x) under Air

A Teflon seal screw-cap pressure tube equipped with a stirring bar was charged with 5 mol% $MnBr_2$ (21.5 mg, 0.1 mmol). Under air, 2.0 mmol of morpholine (174 mg, 175 μL) were added and the mixture was stirred until the solid was partially dissolved. 2.0 mmol of phenylacetylene (204 mg, 220 μL) were added and the mixture was stirred at room temperature until the solid was completely dissolved. Afterwards, 2.0 mmol of cyclohexanone (196 mg, 207 μL) were added and the pressure tube was quickly sealed by a Teflon seal screw-cap. The reaction mixture was stirred in an oil bath in an oil bath, preheated at 130 °C, for 20 hours. After allowing the mixture to cool to room temperature, ethyl acetate was added and the mixture was stirred rapidly for 5 minutes. The crude product was filtered through a short silica gel plug using 5.0 mL of ethyl acetate. The mixture was concentrated under vacuum, and loaded atop a silica gel column. Eluting with mixtures of EtOAc:PE-1:30 and gradual change until 1:9 and then flashed with EtOAc afforded the sufficiently pure product as a yellow oil in 89% yield (480 mg, 1.78 mmol). ^{1}H NMR (200 MHz, $CDCl_3$) δ 7.52–7.37 (m, 2H), 7.31–7.23 (m, 3H), 3.81–3.70 (t, *J* = 4.4 Hz, 4H), 2.79–2.65 (t, *J* = 4.9 Hz, 4H), 2.07–1.95 (d, *J* = 12.2 Hz, 2H), 1.73–1.40 (m, 8H, overlapping peaks). $^{13}C\{^1H\}$ NMR (50 MHz, $CDCl_3$) δ 132.0, 128.5, 128.0, 123.6, 89.9, 86.7, 67.6, 59.0, 46.8, 35.6, 25.9, 22.9.[61]

Modified Procedure for the Synthesis of 4-(1-(Phenylethynyl)cyclohexyl)morpholine (4 x) on a Gram Scale under Air

A Teflon seal screw-cap pressure tube equipped with a stirring bar was charged with 5 mol% $MnBr_2$ (107.3 mg, 0.5 mmol). Under air, 10.0 mmol of morpholine (0.871 g, 0.875 mL) were added and the mixture was stirred. 10.0 mmol of phenylacetylene (1.02 g, 1.10 mL) were added and the mixture was stirred at room temperature until the solid was completely dissolved. Finally, 10.0 mmol of cyclohexanone (0.981 g, 1.04 mL) were added and the pressure tube was quickly sealed by a Teflon seal screw-cap. The reaction reaction mixture was stirred in an oil bath, preheated at 130 °C, for 20 hours. After allowing the mixture to cool to room temperature, ethyl acetate was added (2 × 10 mL) and the mixture was stirred rapidly for 5 minutes before being transferred to a round bottom flask. The mixture was concentrated under vacuum, and loaded atop a silica gel column. Eluting with mixtures EtOAc/PE-1:30 and gradual change until 1 : 9 and then flashed with EtOAc afforded the sufficiently pure product as a yellow oil in 93% yield (2.50 g, 9.30 mmol). ^{1}H NMR (200 MHz, $CDCl_3$) δ 7.52–7.37 (m, 2H), 7.31–7.23 (m, 3H), 3.81–3.70 (t, *J* = 4.4 Hz, 4H), 2.79–2.65 (t, *J* = 4.9 Hz, 4H), 2.07–1.95 (d, *J* = 12.2 Hz, 2H), 1.73–1.40 (m, 8H, overlapping peaks).[122]

© 2020 Wiley-VCH GmbH

Characterization Data for New Compounds

1-(1-(p–tolylethynyl)cyclohexyl)pyrrolidine (4n): Prepared according to the general procedure and obtained as pale yellow crystals in 87% yield (465 mg, 1.74 mmol). ^{1}H NMR (200 MHz, CDCl$_3$) δ 7.36–7.29 (d, J=8.1 Hz, 2H), 7.14–7.06 (d, J=8.1 Hz, 2H), 2.89 (d, J=6.0 Hz, 4H), 2.34 (s, 3H), 2.03 (t, J=5.2 Hz, 2H), 1.84 (p, J=3.3 Hz, 4H), 1.73–1.66 (t, 8H, overlapping peaks). ^{13}C{^{1}H} NMR (50 MHz, CDCl$_3$) δ 138.2, 131.9, 129.2, 120.4, 88.7, 87.0, 60.5, 47.5, 37.7, 25.7, 23.8, 23.3, 21.7. HRMS (ESI-TOF) m/z [M+H]$^+$ calcd for $C_{19}H_{26}N$ 268.2060; Found 268.2064.

2-methyl-4-(1-(2-(pyridin-3-yl)pyrrolidin-1-yl)cyclohexyl) but-3-yn-2-ol (**4r**, single diastereoisomer): Prepared according to the general procedure and obtained as pale yellow crystals in 81% yield (506 mg, 1.66 mmol) and >99:1 d.r. according to ^{1}H NMR. ^{1}H NMR (200 MHz, CDCl$_3$) δ 8.55 (s, 1H), 8.37 (d, J= 4.8 Hz, 1H), 7.71 (d, J=7.8 Hz, 1H), 7.16 (t, J=6.4 Hz, 1H), 4.21 (d, J=9.4 Hz, 1H), 3.41 (s, 1H), 3.12 (t, J=6.0 Hz, 1H), 2.81 (q, J=8.3 Hz, 1H), 2.15–1.93 (m, 1H), 1.93–1.74 (m, 2H), 1.80–1.60 (m, 3H), 1.55 (s, 6H), 1.49–1.32 (m, 5H), 1.34–1.15 (m, 2H), 1.10–0.83 (m, 3H). ^{13}C{^{1}H} NMR (50 MHz, CDCl$_3$) δ 148.2, 147.0, 145.3, 134.8, 123.2, 90.6, 82.7, 64.7, 60.3, 60.0, 49.8, 39.4, 38.2, 36.2, 32.5, 25.6, 23.8, 23.1, 23.0. HRMS (ESI-TOF) m/z [M+H]$^+$ calcd for $C_{20}H_{29}N_2O$ 313.2274 ; Found 313.2275.

1-(1-((4-chlorophenyl)ethynyl)cyclohexyl)pyrrolidine (4s): Prepared according to the general procedure and obtained as pale yellow crystals in 77% yield (440 mg, 1.53 mmol). ^{1}H NMR (200 MHz, CDCl$_3$) δ 7.40–7.25 (d, J=8.5 Hz, 2H), 7.22–7.14 (d, J=8.5 Hz, 2H), 2.76–2.67 (t, J=5.8 Hz, 4H), 2.00–1.88 (d, J=8.0 Hz, 2H), 1.81–1.38 (m, 12H, overlapping peaks). ^{13}C{^{1}H} NMR (50 MHz, CDCl$_3$) δ 133.8, 133.1, 128.6, 122.4, 91.9, 85.2, 59.5, 47.2, 38.0, 25.9, 23.7, 23.2. HRMS (ESI-TOF) m/z [M+H]$^+$ calcd for $C_{18}H_{23}ClN$ 288.1514; Found 288.1510.

1-(1-((4-chlorophenyl)ethynyl)cyclohexyl)piperidine (4t): Prepared according to the general procedure and obtained as pale yellow crystals in 64% yield (380 mg, 1.26 mmol). ^{1}H NMR (200 MHz, CDCl$_3$) δ 7.39–7.29 (d, J=8.7 Hz, 2H), 7.26–7.19 (d, J=8.7 Hz, 2H), 2.63 (t, J=5.0, 3.6 Hz, 4H), 2.03 (d, J=9.9 Hz, 2H), 1.53 (m, 14H, overlapping peaks). ^{13}C{^{1}H} NMR (50 MHz, CDCl$_3$) δ 133.8, 133.1, 128.7, 122.5, 92.1, 85.2, 59.5, 47.4, 35.9, 26.8, 25.9, 24.9, 23.3. HRMS (ESI-TOF) m/z [M+H]$^+$ calcd for $C_{19}H_{25}ClN$ 302.1670; Found 302.1670.

1-(phenylethynyl)-N, N-dipropylcyclohexan-1-amine (4zc): Prepared according to the general procedure and obtained as a pale - yellow oil in 61% yield (346 mg, 1.22 mmol). ^{1}H NMR (200 MHz, CDCl$_3$) δ 7.54–7.37 (m, 2H), 7.34–7.20 (m, 3H), 2.75–2.51 (t, J=7.8 Hz, 4H), 2.23–1.99 (d, J=11.2 Hz, 2H), 1.78–1.37 (m, 12H, overlapping peaks), 1.02–0.70 (t, J= 7.3 Hz, 6H). ^{13}C{^{1}H} NMR (50 MHz, CDCl$_3$) δ 131.8, 128.4, 127.7, 124.3, 93.3, 85.1, 59.8, 52.7, 37.5, 29.9, 26.0, 23.5, 23.3, 12.2. HRMS (ESI-TOF) m/z [M+H]$^+$ calcd for $C_{20}H_{30}N$ 284.2373; Found 284.2374.

Characterization Data for Known Compounds

1-(1-(phenylethynyl)cyclohexyl)piperidine (4a): Prepared according to the general procedure and obtained as a yellow oil in 97% yield (519 mg, 1.94 mmol). ^{1}H NMR (200 MHz, CDCl$_3$) δ 7.47–7.36 (m, 2H), 7.28–7.23 (m, 3H), 2.66 (s, 4H), 2.11–2.05 (m, 2H), 1.83–1.34 (m, 14H, overlapping peaks). ^{13}C{^{1}H} NMR (50 MHz, CDCl$_3$) δ 131.9, 128.4, 127.8, 124.0, 91.1, 86.3, 59.5, 47.4, 36.0, 26.9, 26.0, 25.0, 23.3.[63,70,76]

1-(1-(phenylethynyl)cyclopentyl)piperidine (4b): Prepared according to the general procedure and obtained as a yellow oil in 67% yield (339 mg, 1.34 mmol). ^{1}H NMR (200 MHz, CDCl$_3$) δ 7.41 (dd, J=6.5, 3.2 Hz, 2H), 7.31–7.25 (m, 3H), 2.65–2.62 (m, 4H), 2.13–2.10 (m, 2H), 1.87–1.44 (m, 12H, overlapping peaks). ^{13}C{^{1}H} NMR (50 MHz, CDCl$_3$) δ 131.9, 128.4, 127.8, 124.0, 91.6, 85.4, 67.7, 50.5, 40.1, 26.4, 24.7, 23.6.[70]

1-(1-(phenylethynyl)cycloheptyl)pyrrolidine (4c): Prepared according to the general procedure and obtained as a yellow oil in 73% yield (390 mg, 1.46 mmol). ^{1}H NMR (200 MHz, CDCl$_3$) δ 7.42 (dd, J=6.6, 3.1 Hz, 2H), 7.28 (dd, J=6.6, 2.7 Hz, 3H), 2.79 (t, J=6.0 Hz, 4H), 2.10–1.83 (m, 4H, overlapping peaks), 1.78 (p, J=3.2 Hz, 4H), 1.71–1.46 (m, 8H, overlapping peaks). ^{13}C{^{1}H} NMR (50 MHz, CDCl$_3$) δ 132.0, 128.4, 128.0, 123.7, 91.4, 85.3, 63.3, 48.2, 40.0, 28.2, 24.0, 22.4.[70]

1-(1-(phenylethynyl)cyclopentyl)pyrrolidine (4d): Prepared according to the general procedure and obtained as an orange/yellow oil in 75% yield (359 mg, 1.50 mmol). ^{1}H NMR (200 MHz, CDCl$_3$) δ 7.48–7.35 (m, 2H), 7.33–7.17 (m, 3H), 2.88–2.61 (t, J=6.7 Hz, 4H), 2.21–1.98 (m, 2H), 1.93–1.64 (m, 10H, overlapping peaks). ^{13}C{^{1}H} NMR (50 MHz, CDCl$_3$) δ 131.9, 128.4, 127.9, 123.9, 91.4, 85.1, 65.9, 49.5, 40.7, 23.9, 23.7.[70]

1-(1-(phenylethynyl)cyclohexyl)pyrrolidine (4e): Prepared according to the general procedure and obtained as an orange/yellow oil in 91% yield (461 mg, 1.82 mmol). ^{1}H NMR (200 MHz, CDCl$_3$) δ 7.44 (dd, J=6.7, 3.1 Hz, 2H), 7.30 (m, 3H), 2.82 (t, J=5.9 Hz, 4H), 2.13–1.94 (m, 2H), 1.91–1.41 (m, 12H, overlapping peaks). ^{13}C{^{1}H} NMR (50 MHz, CDCl$_3$) δ 131.7, 128.1, 127.6, 123.6, 90.3, 86.1, 59.3, 47.0, 37.8, 25.7, 23.5, 23.0.[76]

1-(3-methyl-1-phenylhex-1-yn-3-yl)pyrrolidine (4g): Prepared according to the general procedure and obtained as an orange/brown oil in 48% yield (232 mg, 0.96 mmol). ^{1}H NMR (200 MHz, CDCl$_3$) δ 7.45–7.36 (m, 2H), 7.28–7.25 (m, 3H), 2.79 (t, J=5.4 Hz, 4H), 1.85–1.74 (m, 4H), 1.73–1.47 (m, 4H), 1.43 (s, 3H), 0.95 (t, J=7.1 Hz, 3H). ^{13}C{^{1}H} NMR (50 MHz, CDCl$_3$) δ 132.0, 128.4, 127.9, 123.8, 91.5, 84.7, 58.3, 48.0, 44.0, 26.1, 23.9, 18.0, 14.8.[76]

1-(3-ethyl-1-phenylpent-1-yn-3-yl)pyrrolidine (4h): Prepared according to the general procedure and obtained as a yellow oil in 32% yield (154 mg, 0.64 mmol). ^{1}H NMR (200 MHz, CDCl$_3$) δ 7.41 (dd, J=6.7, 3.1 Hz, 2H), 7.32–7.23 (m, 3H), 2.78 (s, 4H), 1.88–1.66 (m, 8H, overlapping peaks), 0.96 (t, J= 7.4 Hz, 6H). ^{13}C{^{1}H} NMR (50 MHz, CDCl$_3$) δ 131.9, 128.3, 127.7, 123.8, 91.5, 85.0, 62.2, 47.6, 29.0, 23.7, 8.3.[81]

© 2020 Wiley-VCH GmbH

1-(4-(phenylethynyl)decan-4-yl)pyrrolidine (4 i): Prepared according to the general procedure and obtained as a yellow oil in 68% yield (424 mg, 1.36 mmol). ^{1}H NMR (200 MHz, CDCl$_3$) δ 7.41 (dd, $J=6.6$, 3.1 Hz, 2H), 7.32–7.24 (m, 3H), 2.76 (s, 4H), 1.88–1.58 (m, 8H, overlapping peaks), 1.51–1.18 (m, 10H), 1.00–0.77 (m, 6H). ^{13}C{^{1}H} NMR (50 MHz, CDCl$_3$) δ 131.7, 128.2, 127.6, 123.7, 91.6, 84.7, 61.3, 47.5, 39.4, 37.1, 31.9, 29.8, 23.6, 22.8, 17.2, 14.6, 14.2.[81]

1-(2-(4-methoxyphenyl)-4-phenylbut-3-yn-2-yl)pyrrolidine (4 j): Prepared according to the general procedure and obtained as a yellow oil in 34% yield (208 mg, 0.68 mmol). ^{1}H NMR (200 MHz, CDCl$_3$) δ 7.76–7.63 (d, $J=8.7$ Hz, 2H), 7.59–7.46 (dd, $J=2.7$, 6.1 Hz, 2H), 7.41–7.29 (m, 3H), 6.95–6.83 (d, $J=8.7$ Hz, 2H), 3.91–3.76 (s, 3H), 2.83–2.69 (m, 2H), 2.69–2.54 (m, 2H), 1.91–1.75 (m, 4H), 1.78–1.69 (s, 3H). ^{13}C{^{1}H} NMR (50 MHz, CDCl$_3$) δ 158.9, 138.2, 132.1, 128.6, 128.2, 127.8, 123.7, 113.6, 89.9, 87.4, 62.3, 55.5, 48.7, 32.6, 24.1.[68]

1-(2-(4-chlorophenyl)-4-phenylbut-3-yn-2-yl)pyrrolidine (4 k): Prepared according to the general procedure and obtained as a yellow oil in in 42% yield (260 mg, 0.84 mmol). ^{1}H NMR (200 MHz, CDCl$_3$) δ 7.87–7.71 (d, $J=8.3$ Hz, 2H), 7.66–7.53 (m, 2H), 7.47–7.30 (m, 5H, overlapping peaks), 2.87–2.75 (m, 2H), 2.72–2.59 (m, 2H), 1.91–1.79 (m, 4H), 1.82–1.70 (s, 3H). ^{13}C{^{1}H} NMR (50 MHz, CDCl$_3$) δ 144.7, 133.0, 132.2, 128.6, 128.5, 128.4, 128.2, 123.5, 89.1, 87.8, 62.5, 48.7, 32.8, 24.2.[68]

1-(1-(*m*–tolylethynyl)cyclohexyl)piperidine (4 m): Prepared according to the general procedure and obtained as a yellow oil in 81% yield (456 mg, 1.64 mmol). ^{1}H NMR (200 MHz, CDCl$_3$) δ 7.25–7.03 (m, 4H), 2.77–2.61 (t, $J=3.0$, 3.9 Hz, 4H), 2.36–2.30 (s, 3H), 2.15–2.03 (d, $J=12.1$ Hz, 2H), 1.85–1.34 (m, 14H, overlapping peaks). ^{13}C{^{1}H} NMR (50 MHz, CDCl$_3$) δ 137.9, 132.3, 128.8, 128.6, 128.1, 123.6, 90.3, 86.4, 59.5, 47.2, 35.8, 26.6, 25.8, 24.8, 23.2, 21.3.[81]

1-(1-(*p*–tolylethynyl)cyclohexyl)piperidine (4 o): Prepared according to the general procedure and obtained as a yellow oil in 70% yield (394 mg, 1.40 mmol). ^{1}H NMR (200 MHz, CDCl$_3$) δ 7.33 (d, $J=6.5$ Hz, 2H), 7.09 (d, $J=6.5$ Hz, 2H), 2.69 (s, 4H), 2.33 (s, 3H), 2.14–2.07 (m, 2H), 1.73–1.44 (m, 14H, overlapping peaks). ^{13}C{^{1}H} NMR (50 MHz, CDCl$_3$) δ 137.9, 131.8, 129.2, 120.8, 90.1, 86.4, 59.9, 47.3, 35.9, 26.6, 25.9, 24.9, 23.4, 21.6.[70]

1-(1-((4-methoxy-2-methylphenyl)ethynyl)cyclohexyl)piperidine (4 p): Prepared according to the general procedure and obtained as a yellow crystals in 89% yield (554 mg, 1.78 mmol). ^{1}H NMR (200 MHz, CDCl$_3$) δ 7.34 (d, $J=8.4$ Hz, 1H), 6.73 (s, 1H), 6.66 (d, $J=8.5$ Hz, 1H), 3.77 (s, 3H), 2.73–2.63 (m, 4H), 2.42 (s, 3H), 2.11 (d, $J=11.5$ Hz, 2H), 1.75–1.52 (m, 10H, overlapping peaks), 1.55–1.37 (m, 4H, overlapping peaks). ^{13}C{^{1}H} NMR (50 MHz, CDCl$_3$) δ 159.1, 141.5, 133.3, 116.0, 115.0, 111.1, 92.9, 84.8, 59.7, 55.3, 47.2, 36.0, 26.6, 25.8, 24.8, 23.3, 21.5.[81]

1-(1-((4-methoxyphenyl)ethynyl)cyclohexyl)piperidine (4 q): Prepared according to the general procedure and obtained as yellow crystals in 87% yield (517 mg, 1.74 mmol). ^{1}H NMR (200 MHz, CDCl$_3$) δ 7.48–7.22 (d, $J=8.9$ Hz, 2H), 6.92–6.70 (d, $J=8.9$ Hz, 2H), 3.98–3.47 (s, 3H), 2.68–2.62 (t, $J=5.3$ Hz, 4H), 2.31–1.91 (d, $J=12.7$ Hz, 2H), 1.80–1.37 (m, 14H, overlapping peaks). ^{13}C{^{1}H} NMR (50 MHz, CDCl$_3$) δ 159.3, 133.2, 116.2, 114.0, 89.3, 86.0, 59.4, 55.4, 47.3, 36.1, 26.9, 26.0, 25.0, 23.3.[127]

1-(1-((2-bromophenyl)ethynyl)cyclohexyl)piperidine (4 u): Prepared according to the general procedure and obtained as an orange oil in 57% yield (395 mg, 1.14 mmol). ^{1}H NMR (200 MHz, CDCl$_3$) δ 7.67–7.37 (m, 2H, overlapping peaks), 7.29–7.06 (m, 2H, overlapping peaks), 2.83–2.64 (t, $J=5.5$ Hz, 4H), 2.25–2.09 (d, $J=11.6$ Hz, 2H), 1.89–1.35 (m, 14H, overlapping peaks). ^{13}C{^{1}H}NMR (50 MHz, CDCl$_3$) δ 133.7, 132.5, 129.0, 127.1, 126.0, 125.7, 96.1, 85.0, 59.9, 47.4, 35.9, 26.8, 25.9, 25.0, 23.4.[81]

1-(1-(oct-1-yn-1-yl)cyclohexyl)piperidine (4 w): Prepared according to the general procedure and obtained as a yellow oil in 70% yield (386 mg, 1.40 mmol). ^{1}H NMR (200 MHz, CDCl$_3$) δ ^{1}H NMR (200 MHz, CDCl$_3$) δ 2.77–2.65 (m, 4H), 2.21 (t, $J=6.7$ Hz, 2H), 1.87 (d, $J=11.2$ Hz, 2H), 1.78–1.70 (m, 4H), 1.63–1.24 (m, 17H), 0.95–0.79 (m, 4H). ^{13}C{^{1}H} NMR (50 MHz, CDCl$_3$) δ ^{13}C NMR (50 MHz, CDCl$_3$) δ 86.1, 80.1, 59.2, 47.0, 38.1, 31.5, 29.4, 28.6, 25.9, 23.6, 23.2, 22.7, 18.8, 14.2.[63,64,76]

***N*-benzyl-1-(phenylethynyl)cyclohexanamine (4 y)**: Prepared according to the general procedure and obtained as a yellow oil in 46% yield (266 mg, 0.92 mmol). ^{1}H NMR (200 MHz, CDCl$_3$) δ 7.56–7.16 (m, 10H, overlapping peaks), 3.97 (s, 2H), 2.01–1.95 (m, 2H), 1.77–1.41 (m, 8H, overlapping peaks). ^{13}C{^{1}H} NMR (50 MHz, CDCl$_3$) δ 141.1, 132.0, 128.9, 128.4, 128.2, 127.9, 127.0, 124.0, 90.7, 86.4, 59.6, 47.3, 38.1, 26.0, 23.8.[59]

***N*-(4-methoxybenzyl)-1-(phenylethynyl)cyclohexanamine (4 z)**: Prepared according to the general procedure and obtained as an orange oil in 43% yield (275 mg, 0.86 mmol). ^{1}H NMR (200 MHz, CDCl$_3$) δ 7.53–7.40 (m, 2H), 7.36–7.27 (m, 5H, overlapping peaks), 6.86 (d, $J=8.7$ Hz, 2H), 3.91 (s, 2H), 3.79 (s, 3H), 2.00–1.94 (m, 2H), 1.75–1.39 (m, 8H, overlapping peaks). ^{13}C{^{1}H} NMR (50 MHz, CDCl$_3$) δ 158.9, 133.3, 132.0, 130.0, 128.6, 128.1, 124.0, 114.1, 93.9, 85.1, 55.6, 55.5, 47.7, 38.5, 26.2, 23.3.[59]

***N*-octyl-1-(phenylethynyl)cyclohexanamine (4 za)**: Prepared according to the general procedure and obtained as a yellow oil in 67% yield (417 mg, 1.34 mmol). ^{1}H NMR (200 MHz, CDCl$_3$) δ 7.42 (dd, $J=6.7$, 3.1 Hz, 2H), 7.33–7.23 (m, 3H), 2.79 (t, $J=7.1$ Hz, 2H), 1.94 (d, $J=11.6$ Hz, 2H), 1.74–1.07 (m, 20H, overlapping peaks), 0.88 (dd, $J=9.7$, 6.6 Hz, 3H). ^{13}C{^{1}H} NMR (50 MHz, CDCl$_3$) δ 131.6, 128.1, 127.7, 123.6, 93.3, 84.6, 55.2, 43.2, 38.1, 31.8, 30.5, 29.5, 29.3, 27.5, 25.9, 23.1, 22.7, 14.1.[81]

***N*-cyclohexyl-1-(phenylethynyl)cyclohexan-1-amine (4 zb)**: Prepared according to the general procedure and obtained as a yellowish oil in 58% yield (326 mg, 1.16 mmol). ^{1}H NMR (200 MHz, CDCl$_3$) δ 7.46–7.35 (m, 2H), 7.33–7.23 (m, 3H), 2.98–2.71 (dt, $J=6.6$, 10.2 Hz, 1H), 2.04–1.84 (d, $J=10.2$ Hz, 4H), 1.79–1.49 (m, 6H), 1.50–1.01 (m, 10H, overlapping peaks). ^{13}C{^{1}H} NMR (50 MHz, CDCl$_3$) δ 131.7, 128.5, 127.9, 124.1, 94.6, 84.1, 55.4, 52.8, 39.5, 36.8, 26.0, 26.0, 26.0, 23.4.[128]

© 2020 Wiley-VCH GmbH

Acknowledgements

This work was supported by the Hellenic Foundation for Research and Innovation (H.F.R.I.) under the "First Call for H.F.R.I. Research Projects to support Faculty members and Researchers and the procurement of high-cost research equipment grant" (Project Number: 16-Acronym: SUSTAIN), as well as by European Funding: Horizon 2020-MSCA (ITN-EJD CATMEC 14/06-721223). The contribution of COST Action CA15106 (C–H Activation in Organic Synthesis - CHAOS) is also gratefully acknowledged. Moreover, we are thankful for the human and technical support provided by the IZO-SGI SGIker of UPV/EHU. Mr. Savvas G. Chalkidis is gratefully acknowledged for the synthesis and characterization of compound ***4w****.*

References

[1] K. Lauder, A. Toscani, N. Scalacci, D. Castagnolo, *Chem. Rev.* **2017**, *117*, 14091–14200.

[2] a) V. A. Peshkov, O. P. Pereshivko, E. V. Van der Eycken, *Chem. Soc. Rev.* **2012**, *41*, 3790–3807; b) B. V. Rokade, J. Barker, P. J. Guiry, *Chem. Soc. Rev.*, **2019**, *48*, 4766–4790.

[3] J. W. Langston, I. Irwin, E. B. Langston, L. S. Forno, *Science* **1984**, *225*, 1480–1482.

[4] J. J. Chen, D. M. Swope, *J. Clin. Pharmacol.* **2005**, *45*, 878–894.

[5] I. Bolea, A. Gella, M. Unzeta, *J. Neural Transm.* **2013**, *120*, 893–902.

[6] F. T. Zindo, J. Joubert, S. F. Malan, *Future Med. Chem.* **2015**, *7*, 609–629.

[7] M. Baranyi, P. F. Porceddu, F. Gölöncsér, S. Kulcsár, L. Otrokocsi, Á. Kittel, A. Pinna, L. Frau, P. B. Huleatt, M.-L. Khoo, C. L. L. Chai, P. Dunkel, P. Mátyus, M. Morelli, B. Sperlágh, *Mol. Neurodegener.* **2016**, *11*, 1–21.

[8] J. Marco-Contelles, M. Unzeta, I. Bolea, G. Esteban, R. R. Ramsay, A. Romero, R. Martínez-Murillo, M. C. Carreiras, L. Ismaili, *Front. Neurosci.* **2016**, *10*, 294.

[9] A. Albreht, I. Vovk, J. Mavri, J. Marco-Contelles, R. R. Ramsay, *Front. Chem.* **2018**, *6*, 169.

[10] D. S. Ermolat'ev, J. B. Bariwal, H. P. L. Steenackers, S. C. J. De Keersmaecker, E. V. Van der Eycken, *Angew. Chem. Int. Ed.* **2010**, *49*, 9465–9468; *Angew. Chem.* **2010**, *122*, 9655–9658.

[11] N. Sharma, U. K. Sharma, N. M. Mishra, E. V. Van der Eycken, *Adv. Synth. Catal.* **2014**, *356*, 1029–1037.

[12] F. Nie, D. L. Kunciw, D. Wilcke, J. Stokes, W. R. J. D. Galloway, S. Bartlett, H. F. Sore, D. R. Spring, *Angew. Chem. Int. Ed.* **2016**, *55*, 11139–11143; *Angew. Chem.* **2016**, *128*, 11305–11309.14.

[13] B. Jiang, M. Xu, *Angew. Chem. Int. Ed.* **2004**, *43*, 2543–2646; *Angew. Chem.* **2004**, *116*, 2597–2600.

[14] J. J. Fleming, J. Du Bois, *J. Am. Chem. Soc.* **2006**, *128*, 3926–3927.

[15] V. K.-Y. Lo, Y. Liu, M.-K. Wong, C.-M. Che, *Org. Lett.*, **2006**, *8*, 1529–1532.

[16] S. Arshadi, E. Vessally, L. Edjlali, R. Hosseinzadeh-Khanmiri, E. Ghorbani-Kalhor, *Beilstein J. Org. Chem.*, **2017**, *13*, 625–638.

[17] X.-B. Zhao, W. Ha, K. Jiang, J. Chen, J.-L. Yang, Y.-P. Shi, *Green Chem.*, **2017**, *19*, 1399–1406.

[18] W.-J. Yoo, C.-J. Li, *Adv. Synth. Catal.* **2008**, ***350***, 1503–1506.

[19] X. Liu, M. Wang, S. Wang, Q. Wang, L. He, *ChemSusChem* **2016**, *10*, 1210–1216.

[20] Y. Yuan, Y. Xie, D. Song, C. Zeng, S. Chaemchuen, C. Chen, F. Verpoort, *Appl. Organomet. Chem.* **2017**, *31*, e3867.

[21] B. B. Touré, D. G. Hall, *Chem. Rev.* **2009**, *109*, 4439–4486.

[22] B. Ganem, *Acc. Chem. Res.* **2009**, *42*, 463–472.

[23] A. Dömling, W. Wang, K. Wang, *Chem. Rev.* **2012**, *112*, 3083–3135.

[24] C. Chen, P. Liu, J. Tang, G. Deng, X. Zeng, *Org. Lett.* **2017**, *19*, 2474–2477.

[25] R. Afshari, A. Shaabani, *ACS Comb. Sci.* **2018**, *20*, 499–528.

[26] B. M. Trost, *Science* **1991**, *254*, 1471–1476.

[27] R. Noyori, *Chem. Commun.* **2005**, 1807–1811.

[28] R. A. Sheldon, *Green Chem.* **2005**, *7*, 267–268.

[29] C.-J. Li, B. M. Trost, *Proc. Natl. Acad. Sci. USA*, **2008**, *105*, 13197–13202.

[30] P. G. Jessop, *Green Chem.* **2011**, *13*, 1391–1398.

[31] R. A. Sheldon, *Chem. Soc. Rev.* **2012**, *41*, 1437–1451.

[32] R. A. Sheldon, *Green Chem.* **2017**, *19*, 18–43.

[33] R. A. Sheldon, *Chem. Commun.* **2008**, 3352–3365.

[34] M. S. Holzwarth, B. Plietker, *ChemCatChem* **2013**, *5*, 1650–1679.

[35] N. V. Tzouras, I. K. Stamatopoulos, A. T. Papastavrou, A. A. Liori, G. C. Vougioukalakis, *Coord. Chem. Rev.* **2017**, *343*, 25–138.

[36] L. Zani, C. Bolm, *Chem. Commun.* **2006**, 4263–4275.

[37] C. Wei, Z. Li, C.-J. Li, *Synlett* **2004**, 1472–1483.

[38] M. Kidwai, V. Bansal, A. Kumar, S. Mozumdar, *Green Chem.* **2007**, *9*, 742–745.

[39] T. Zeng, W.-W. Chen, C. Cirtiu, A. Moores, G. Song, C.-J. Li, *Green Chem.* **2010**, *12*, 570–573.

[40] C. Wei, Z. Li, C. J. Li, *Org. Lett.* **2003**, *23*, 4473–4475.

[41] C. M. Wei, C. J. Li, *J. Am. Chem. Soc.* **2003**, *125*, 9584–9585.

[42] C.-J. Li, C. Wei, *Chem. Commun.* **2002**, 268–269.

[43] S. Sakaguchi, T. Kubo, Y. Ishii, *Angew. Chem. Int. Ed.* **2001**, *40*, 2534–2536; *Angew. Chem.* **2001**, *113*, 2602–2604.

[44] A. B. Dyatkin, R. A. Rivero, *Tetrahedron Lett.* **1998**, *39*, 3647–3650.

[45] W. J. Yoo, L. Zhao, C.-J. Li, *Aldrichimica Acta* **2011**, *44*, 43–52.

[46] C. Wei, C.-J. Li, *J. Am. Chem. Soc.* **2002**, *124*, 5638–5639.

[47] N. Gommermann, C. Koradin, K. Polborn, P. Knochel, *Angew. Chem. Int. Ed.* **2003**, *42*, 5763–5766; *Angew. Chem.* **2003**, *115*, 5941–5944.

© 2020 Wiley-VCH GmbH

[48] W. Zhuang, S. Saaby, K. A. Jørgensen, *Angew. Chem. Int. Ed.* **2004**, *43*, 4476–4478; *Angew. Chem.* **2004**, *116*, 4576–4578.

[49] R. Wada, T. Shibuguchi, S. Makino, K. Oisaki, M. Kanai, M. Shibasaki, *J. Am. Chem. Soc.* **2006**, *128*, 7687–7691.

[50] H. C. Brown, J. Muzzio, *J. Am. Chem. Soc.* **1966**, *88*, 2811–2822.

[51] M. Cherest, H. Felkin, N. Prudent, *Tetrahedron Lett.* **1968**, 2199–2204.

[52] M. Cherest, H. Felkin, *Tetrahedron Lett.* **1968**, 2205–2208.

[53] A. Hager, N. Vrielink, D. Hager, J. Lefranc, D. Trauner, *Nat. Prod. Rep.* **2016**, *33*, 491–522.

[54] M. Biyikal, M. Porta, P. Roesky, S. Blechert, *Adv. Synth. Catal.* **2010**, *352*, 1870–1875.

[55] C. J. Pierce, H. Yoo, C. H. Larsen, *Adv. Synth. Catal.* **2013**, *355*, 3586–3590.

[56] Z. Palchak, D. Lussier, C. Pierce, H. Yoo, C. H. Larsen, *Adv. Synth. Catal.* **2015**, *357*, 539–548.

[57] M. Periasamy, P. O. Reddy, I. Satyanarayana, L. Mohan, A. Edukondalu, *J. Org. Chem.* **2016**, *81*, 987–999.

[58] M. J. Aliaga, D. J. Ramón, M. Yus, *Org. Biomol. Chem.* **2010**, *8*, 43–46.

[59] O. P. Pereshivko, V. A. Peshkov, E. V. Van der Eycken, *Org. Lett.* **2010**, *12*, 2638–2641.

[60] D. D. Vachhani, A. Sharma, E. V. Van der Eycken, *Angew. Chem. Int. Ed.* **2013**, *52*, 2547–2550; *Angew. Chem.* **2013**, *125*, 2607–2610.

[61] M. Cheng, Q. Zhang, X.-Y. Hu, B.-G. Li, J.-X. Ji, A. C. Chan, *Adv. Synth. Catal.* **2011**, *353*, 1274–1278.

[62] Y. Suzuki, S. Naoe, S. Oishi, N. Fujii, H. Ohno, *Org. Lett.* **2011**, *14*, 326–329.

[63] C. J. Pierce, C. H. Larsen, *Green Chem.* **2012**, *14*, 2672–2676.

[64] Z. L. Palchak, D. J. Lussier, C. J. Pierce, C. H. Larsen, *Green Chem.* **2015**, *17*, 1802–1810.

[65] C. E. Meyet, C. J. Pierce, C. H. Larsen, *Org. Lett.* **2012**, *14*, 964–967.

[66] C. J. Pierce, M. Nguyen C H Larsen, *Angew. Chem.* **2012**, *124*, 12455–12458; *Angew. Chem. Int. Ed.* **2012**, *51*, 12289–12292.

[67] X. Tang, J. Kuang, S. Ma, *Chem. Commun.* **2013**, *49*, 8976.

[68] Y. Cai, X. Tang, S. Ma, *Chem. Eur. J.* **2016**, *22*, 2266–2269.

[69] M. J. Albaladejo, F. Alonso, Y. Moglie, M. Yus, *Eur. J. Org. Chem.* **2012**, *2012*, 3093–3104.

[70] M. Hosseini-Sarvari, F. Moeini, *New J. Chem.* **2014**, *38*, 624–635.

[71] F. Nemati, A. Elhampour, H. Farrokhi, M. Bagheri Natanzi, *Catal. Commun.* **2015**, *66*, 15–20.

[72] C. Rajesh, U. Gulati, D. S. Rawat, *ACS Sustainable Chem. Eng.* **2016**, *4*, 3409–3419.

[73] U. Gulati, U. Chinna Rajesh, D. S. Rawat, *Tetrahedron Lett.* **2016**, *57*, 4468–4472.

[74] a) P. C. Perumgani, S. Keesara, S. Parvathaneni, M. R. Mandapati, *N. J. Chem.* **2016**, *40*, 5113–5120; b) S. Yan, S. Pan, T. Osako, Y. Uozumi, *ACS Sustainable Chem. Eng.* **2019**, *7*, 9097–9102.

[75] S. Sadjadi, T. Hosseinnejad, M. Malmir, M. M. Heravi, *N. J. Chem.* **2017**, *41*, 13935–13951.

[76] G. Bosica, R. Abdilla, *J. Mol. Catal. A* **2017**, *426*, 542–549.

[77] X. Xiong, H. Chen, X. Liao, S. Lai, L. Gao, *ChemistrySelect* **2018**, *3*, 8819–8825.

[78] A. Elhampour, M. Malmir, E. Kowsari, F. Boorboor ajdari, F. Nemati, *RSC Adv.* **2016**, *6*, 96623–96634.

[79] S. Sadjadi, M. M. Heravi, M. Malmir, *Appl. Organomet. Chem.* **2017**, *32*, e4029.

[80] J. Cao, P. Li, G. Xu, M. Tao, N. Ma, W. Zhang, *Chem. Eng. J.* **2018**, *349*, 456–465.

[81] N. V. Tzouras, S. P. Neofotistos, G. C. Vougioukalakis, *ACS Omega* **2019**, *4*, 10279–10292.

[82] D. A. Valyaev, G. Lavigne, N. Lugan, *Coord. Chem. Rev.* **2016**, *308*, 191–235.

[83] European Medicies Agency. Guideline on the specification limits for residues of metal catalysts or metal reagents. In *Commitee for medicinal products for human use*; 2008; pp 6–7.

[84] T. K. Mukhopadhyay, M. Flores, T. L. Groy, R. J. Trovitch, *J. Am. Chem. Soc.* **2014**, *136*, 882–885.

[85] J. Zheng, S. Chevance, C. Darcela, J. Sortaisa, *Chem. Commun.* **2013**, *49*, 10010–10112.

[86] M. Bourrez, F. Molton, S. Chardon-Noblat, A. Deronzier, *Angew. Chem. Int. Ed.* **2011**, *50*, 9903–9906; *Angew. Chem.* **2011**, *123*, 10077–10080.

[87] J. M. Smieja, M. D. Sampson, K. A. Grice, E. E. Benson, E. J. D. Froehlich, C. P. Kubiak, *Inorg. Chem.* **2013**, *52*, 2484–2491.

[88] J. Agarwal, T. W. Shaw, C. J. Stanton, G. F. Majetich, A. B. Bocarsly, H. F. Schaefer, *Angew. Chem. Int. Ed.* **2014**, *53*, 5152–5155; *Angew. Chem.* **2014**, *126*, 5252–5255.

[89] M. D. Sampson, A. D. Nguyen, K. A. Grice, C. E. Moore, C. E. A. L. Rheingold, C. P. Kubiak, *J. Am. Chem. Soc.* **2015**, *137*, 3718–3718.

[90] F. Franco, C. Cometto, F. Ferrero Vallana, F. Sordello, E. Priola, C. Minero, C. Nervi, R. Gobetto, *Chem. Commun.* **2014**, *50*, 14670–14673.

[91] H. Takeda, H. Koizumi, K. Okamoto, O. Ishitani, *Chem. Commun.* **2014**, *50*, 1491–1493.

[92] J. J. Walsh, G. Neri, C. L. Smith, A. J. Cowan, *Chem. Commun.* **2014**, *50*, 12698–12701.

[93] B. Meunier, *Chem. Rev.* **1992**, *92*, 1411–1456.

[94] J. Luo, S. Preciado, S. O. Araromi, I. Larrosa, *Chem. Asian J.* **2016**, *11*, 347–350.

[95] C.-M. Che, V. K.-Y. Lo, C.-Y. Zhou, J.-S. Huang, *Chem. Soc. Rev.* **2011**, *40*, 1950–1975.

[96] H. Lu, X. P. Zhang, *Chem. Soc. Rev.* **2011**, *40*, 1899–1909.

[97] A. B. Sorokin, *Chem. Rev.* **2013**, *113*, 8152–8191.

[98] T. Katsuki, *Coord. Chem. Rev.* **1995**, *140*, 189–214.

[99] E. M. McGarrigle, D. G. Gilheany, *Chem. Rev.* **2005**, *105*, 1563–1602.

Korr

© 2020 Wiley-VCH GmbH

[100] P. Saisaha, J. W. De Boer, W. R. Browne, *Chem. Soc. Rev.* **2013**, *42*, 2059–2074.
[101] Y. Kuninobu, Y. Nishina, T. Takeuchi, K. Takai, *Angew. Chem. Int. Ed.* **2007**, *46*, 6518–6520; *Angew. Chem.* **2007**, *119*, 6638–6640.
[102] B. Zhou, H. Chen, C. Wang, *J. Am. Chem. Soc.* **2013**, *135*, 1264–1267.
[103] R. He, Z. T. Huang, Q. Y. Zheng, C. Wang, *Angew. Chem. Int. Ed.* **2014**, *53*, 4950–4953; *Angew. Chem.* **2014**, *126*, 5050–5053.
[104] B. Zhou, P. Ma, H. Chen, C. Wang, *Chem. Commun.* **2014**, *50*, 14558–14561.
[105] W. Liu, D. Zell, M. John, L. Ackermann, *Angew. Chem. Int. Ed.* **2015**, *54*, 4092–4096; *Angew. Chem.* **2015**, *127*, 4165–4169.
[106] Y. Kuninobu, K. Kikuchi, K. Takai, *Chem. Lett.* **2008**, *37*, 740–741.
[107] S. N. Afraj, C. Chen, G. H. Lee, *RSC Adv.* **2014**, *4*, 26301–26308.
[108] E. Voutyritsa, I. Triandafillidi, N. V. Tzouras, N. F. Nikitas, E. K. Pefkianakis, G. C. Vougioukalakis, C. G. Kokotos, *Molecules* **2019**, *24*, 1644.
[109] A. T. Papastavrou, M. Pauze, E. Gómez-Bengoa, G. C. Vougioukalakis, *ChemCatChem* **2019**, *11*, 5379–5386.
[110] A. A. Liori, I. K. Stamatopoulos, A. T. Papastavrou, A. Pinaka, G. C. Vougioukalakis, *Eur. J. Org. Chem.* **2018**, *2018*, 6134–6139.
[111] A. Pinaka, G. C. Vougioukalakis, *Coord. Chem. Rev.* **2015**, *288*, 69–97.
[112] X. Tang, C. Zhu, T. Cao, J. Kuang, W. Lin, S. Ni, J. Zhang, S. Ma, *Nat. Commun.* **2013**, *4*, 2450.
[113] J. Kuang, X. Tang, S. Ma, *Org. Chem. Front.* **2015**, *2*, 470–475.
[114] J. H. Park, D. H. Lee, H. Kong, M. J. Park, M. I. H. Jung, C. E. Park, H. K. Shim, *Org. Electron.* **2010**, *11*, 820–830.
[115] A. C. Grimsdale, K. L. Chan, R. E. Martin, P. G. Jokisz, A. B. Holmes, *Chem. Rev.* **2009**, *40*, 897–1091.
[116] G. Mao, A. Orita, L. Fenenko, M. Yahiro, C. Adachi, J. Otera, *Mater. Chem. Phys.* **2009**, *115*, 378–384.
[117] X. Cheng, A. Heyen, W. Ver Mamdouh, H. Uji-i, F. De Schryver, S. Höger, S. De Feyter, *Langmuir* **2007**, *23*, 1281–1286.
[118] K. Königsberger, G. P. Chen, R. R. Wu, M. J. Girgis, K. Prasad, O. Repič, T. J. Blacklock, *Org. Process Res. Dev.* **2003**, *7*, 733–742.
[119] A. Caporale, S. Tartaggia, A. Castellin, O. De Lucchi, *Beilstein J. Org. Chem.* **2014**, *10*, 384–393.
[120] J. Li, P. Huang, *Beilstein J. Org. Chem.* **2011**, *7*, 426–431.
[121] T. A. Gschneidtner, K. Moth-Poulsen, *Tetrahedron Lett.* **2013**, *54*, 5426–5429.
[122] Even if just 1 equiv. of piperidine is employed, which is fully involved in iminium formation, the three species: piperidine, piperidinium, and **II**, must be in equilibrium, maintaining some free base in the reaction medium. Also, the final product can act as a basic tertiary amine for deprotonation.
[123] S. Grimme, *J. Comb. Chem.* **2006**, *27*, 1787–1799.
[124] Gaussian 16, Revision A.03; M. J. Frisch, G. W. Trucks, H. B. Schlegel, G. E. Scuseria, M. A. Robb, J. R. Cheeseman, G. Scalmani, V. Barone, B. Mennucci, G. A. Petersson, H. Nakatsuji, M. Caricato, X. Li, H. P. Hratchian, A. F. Izmaylov, J. Bloino, G. Zheng, J. L. Sonnenberg, M. Hada, M. Ehara, K. Toyota, R. Fukuda, J. Hasegawa, M. Ishida, T. Nakajima, Y. Honda, O. Kitao, H. Nakai, T. Vreven, J. A. Montgomery, Jr., J. E. Peralta, F. Ogliaro, M. Bearpark, J. J. Heyd, E. Brothers, K. N. Kudin, V. N. Staroverov, T. Keith, R. Kobayashi, J. Normand, K. Raghavachari, A. Rendell, J. C. Burant, S. S. Iyengar, J. Tomasi, M. Cossi, N. Rega, J. M. Millam, M. Klene, J. E. Knox, J. B. Cross, V. Bakken, C. Adamo, J. Jaramillo, R. Gomperts, R. E. Stratmann, O. Yazyev, A. J. Austin, R. Cammi, C. Pomelli, J. W. Ochterski, R. L. Martin, K. Morokuma, V. G. Zakrzewski, G. A. Voth, P. Salvador, J. J. Dannenberg, S. Dapprich, A. D. Daniels, O. Farkas, J. B. Foresman, J. V. Ortiz, J. Cioslowski, and D. J. Fox, Gaussian, Inc., Wallingford CT, **2016**.
[125] a) E. Cancès, B. Mennucci, J. Tomasi, *J. Chem. Phys.* **1997**, *107*, 3032–3047; b) M. Cossi, V. Barone, B. Mennucci, J. Tomasi, *Chem. Phys. Lett.* **1998**, *286*, 253–260; c) J. Tomasi, B. Mennucci, E. Cancès, *J. Mol. Struct.*, **1999**, *464*, 211–226.
[126] C. Gonzalez, H. B. Schlegel, *J. Phys. Chem.* **1990**, *94*, 5523–5527.
[127] A. P. Shah, A. S. Sharma, S. Jain, N. G. Shimpi, *N. J. Chem.* **2018**, *42*, 8724–8737.
[128] T. Sugiishi, H. Nakamura, *J. Am. Chem. Soc.* **2012**, *134*, 2504–2507.

© 2020 Wiley-VCH GmbH